

Diakoptic Assessment of Power System Voltage Variations and Applications in Weak Grids Introduced By Wind Energy – The Nigerian Power System in Perspective

by

Flourish A. Olobaniyi

A thesis submitted to the University of the West of England, Bristol in partial
fulfillment of the requirements for the degree of

Doctor of Philosophy

Department of Engineering Design and Mathematics
Faculty of Environment and Technology
University of the West of England, Bristol

May, 2015

ABSTRACT

The electrical power system is a large interconnected system made up of electrical components to generate, transport and utilize electrical power. The size and complexity of the power system have increased significantly in recent years due to the introduction of wind energy and other renewable energy sources. Hence there is an urgent need to search for new or improved analytical tools for the system performance evaluation and assessment. Load flow analysis is the most important method of assessing the steady-state behaviour of all the components of the power network.

The common approach in load flow analysis is to study the network as one-piece and this can take a long time for a very large system. An alternative solution is to reduce the size of the network by tearing apart a large system into small subnetworks, thus a cluster of computers can be supplemented to speed-up the process. Then the system can be solved as separate entities after which their solutions are connected together by mathematical modelling in order to obtain the solution of the original system as if it was solved as one-piece. This method in its original conception is known as diakoptics which, though was conceived for power systems analysis, is now widely viewed as a mathematical method rather than a power systems analysis tool.

The work presented in this thesis proposes two novel diakoptic tools for the power system analysis; i.e. the branch voltage multiplier technique (BVMT) and slack bus voltage updating diakoptics (SVUD). Various research works so far have shown that the key factor is in the process of obtaining the *fundamental equations of diakoptics* and the *final equation of solution*. The BVMT is a variant of the original diakoptic algorithm mainly by the process of obtaining the diakoptic equations of solution which can reduce the number of solution steps and simplify the method considerably. The resultant algorithm is easier to apply and also more effective in load flow analysis by current injection methods where the relationship is linear. The common practice in present load flow analyses is by power injection which yields nonlinear equations. The BVMT technique has been extended by applying various transformations which make it suitable for nonlinear solutions. This yields the SVUD load flow method that incorporates the classical Gauss-Seidel method. The analysis

tools produced have been validated by applying to sample systems including IEEE benchmark systems.

In one-piece load flow analysis, the usual practice is to choose one slack bus whose voltage remains unchanged throughout the iterative process. In diakoptic analysis, the systems to be analysed are more than one after tearing, so the subnetworks without the original slack bus will require temporary slack buses during the load flow analysis. During iteration, the voltages of these temporary slack buses would also remain unchanged; the SVUD method ensures that their voltages vary to reflect the state they would have been in one-piece solutions. This is achieved by updating the voltages during iteration using given and computed parameters which, in this case, are the complex powers. This has resulted in the improvement of the convergence characteristics of the traditional Gauss-Seidel method. For example, in the analysis of the IEEE 30-bus network, the number of iterations in one-piece Gauss-Seidel solution was 202 while with the SVUD, the numbers of iterations were 17 when cut into two subnetworks, and 13 when cut into three subnetworks. The SVUD also removes some common problems associated with temporary slack buses. This is demonstrated in the analysis of the 14-bus system using the one-piece Gauss-Seidel, SVUD and diakoptics with the temporary slack bus voltage remaining unchanged during iteration. The one-piece method converged after 106 iterations and the SVUD converged after 5 iterations. The diakoptic analysis with constant temporary slack-bus voltage converged after 146 iterations and erroneous results were obtained.

The SVUD analysis of the Nigeria 330kV power transmission network without wind power electricity shows a voltage profile with some violations at a number of buses. The analysis with wind power electricity shows voltage rises, especially at buses close to the point of common coupling. This is a generally accepted effect of electricity from wind on an existing power system. In the Nigeria case, the conventional generation capacity is far below what is required and so the voltage profile is seen to improve because the wind farm constitutes an extra generating capacity. For example, at rated wind power, the voltage magnitudes show rises of 0.12% at bus 31 and 0.15% at bus 32. Increase of wind power to 4.1018 pu shows rises of 3.9% at bus 31 and 4.5% at bus 32.

ACKNOWLEDGEMENTS

I am grateful to God for His help and strength; without Him I would not have been able to start the programme in the first place. He gave me the opportunity and saw me through the programme.

Firstly, my appreciation goes to my supervisors, Professor Yufeng Yao and Dr. Sabir Ghauri for their guidance, support and encouragement during the research project.

I would also like to acknowledge the contributions of Dr Hassan Nouri and the support of colleagues in the Electrical Power Group who were always willing to share knowledge and research materials, especially at the early stage of this work. I would also like to thank Professor Paul Olomolaiye and Dr. Alistair Clark for their advice and help especially during the challenging times in the course of this programme. I deeply appreciate the support of brethren in the church, especially Pastor and Mrs Kasali for their prayers.

I deeply appreciate the Federal Government of Nigeria for awarding me a grant under ETF 2009/2010 AST&D intervention for University of Lagos (UNILAG), through the Education Trust Fund (ETF), now Tertiary Education Trust Fund (TETFund). The fund provided the finance that enabled me pay my fees and meet other needs. Consequently, I could focus on the PhD research.

I also appreciate the University of Lagos management for granting me a study leave so that I could leave for the PhD programme and partly provided the finance I required by paying my salaries. I acknowledge especially, Professor (Mrs) C. I. Igwilo, who was the Director of Academic Planning, for her role in making sure that the ETF grant was released in time.

My special gratitude goes to my family for their support which is still ongoing, especially, Mrs N. I. Ojdiran and my daughter for various forms of support that helped me to remain focussed. Finally, I am very grateful to my husband Sam, for his love, patience, advice, sacrifices, finances and much more. His support motivated and helped me to concentrate on the work.

DEDICATION

This thesis is dedicated to the Almighty God, the Lord Jesus Christ, and the Holy Spirit, my great teacher.

STATEMENT OF OBJECTIVES

This research set out to contribute to the knowledge of developing less tasking but effective computational tools or methods for the analysis of power systems for which the growth in size and complexity seems to be unending. Diakoptics presents a method of reducing the size of a system to be analysed so the main objectives are to find the most suitable method that can be used with the traditional diakoptics in order to produce a new diakoptic algorithm that is more user-friendly. With the new tool, voltage change (ΔV) in a weak grid could be determined when wind energy is integrated into it.

All the work in this thesis was performed by the author except the MATLAB codes in their original states before adapting them to suit my algorithms, and the assistance from Adam Chapman in the initial computer programme for the execution of the SVUD. Because I understand the intricacies of the SVUD tool better, the final modifications to make the programme suit its purpose were done by me.

ABBREVIATIONS

BDM	Bordered Block Matrix
BBDM	Bordered block diagonal matrix
PCC	Point of Common Coupling
PSCAD	Power System Computer-Aided Design
SCR	Short circuit ratio
WT	Wind Turbine
CPU	Central Processing Unit
pu	per unit
G-S	Gauss-Seidel
N-R	Newton-Raphson
FDLF	Fast Decoupled Load Flow
BVMT	Branch voltage multiplier technique
SVUD	Slack voltage updating diakoptics
DC	Direct current
AC	Alternating current
SN	Subnetwork number

GLOSSARY

Terminating or boundary buses	Buses to which removed branches were originally connected
Subnetwork or subsystem	One of the smaller networks or systems obtained when the original whole network is torn into parts.
Subnet	Shortened form of subnetwork which is also referred to as subsystem
Removed branches	Branches, which when removed will tear the network into subnetworks without coupling between subnetworks
One-piece	Whole network solved without tearing
Tear	Remove branches of the original network to form subnetworks

LIST OF SYMBOLS

Units Symbols

A	Ampere
V	Volt
Ω	Ohm
S	Siemen
pu	per unit
kW	kilowatt
kVA	kilovoltampere
MVA	megavoltampere
kVAr	kilovoltampere reactive
$^{\circ}$	degree

General Symbols

ΔV	Voltage variation/change (V or pu)
$\cos \phi$	Power factor
I	Current (A or pu)
P	Real or Active power (kW or pu)
S_w	Electrical power from wind (kVA or pu)
S_k	Short-Circuit capacity (kVA or pu)
Q	Reactive power (kVAr or pu)

w	Real power loss (kW or pu)
S	Apparent power (kVA or pu)
s	Slip
V	Voltage (V or pu)
V_{PCC}	Voltage at point of common coupling (V or pu)
R	Resistance (Ω or pu)
X	Reactance (Ω or pu)
X_{PFC}	Power factor correction capacitance (Ω or pu)
Y	Admittance (S or pu)
Z	Impedance (Ω or pu)
δ	Power angle or load angle.
ψ	Impedance angle
ϕ	Power factor angle
Z	Impedance matrix (Ω or pu)
Y	Admittance matrix (Ω or pu)
Y_d	Diagonal admittance matrix of a torn network (Ω or pu)
I	Current vector (A or pu)
V	Voltage vector (V or pu)
Y_m	Admittance matrix of m^{th} subnet (pu)
V_{m0}	Voltage vector of m^{th} subnet (pu)
V_m	Updated voltage vector of m^{th} subnet (pu)

\mathbf{L}_m	Matrix that shows the relationship between nodes in subnet M and all removed branches
\mathbf{L}_m^t	Transpose of \mathbf{L}_m
\mathbf{Z}_b	Impedance matrix of network of removed branches
\mathbf{e}_b	Branch voltage vector
A, B, C, \dots	Subnetworks labels
\mathbf{Y}_A	Admittance matrix of subnetwork A
\mathbf{V}_{0A}	Vector of node voltages in subnetwork A
\mathbf{I}_A	Vector of injected currents in subnetwork A
\mathbf{V}_{A2}	Voltage at node 2 to of subnetwork A
\mathbf{L}_A	Matrix that captures which nodes in subsystem A were connected to removed branches, and the direction of current flow from that specific node.
<i>(Definitions for subnet A also apply to other subnetworks. For example, for subnetwork B, the subscripts A will be replaced by B, etc.)</i>	
i_b	Branch current vector (e.g. i_{b1} = current in branch b_1)
\mathbf{Z}_b	Impedance matrix of branch equations
y_1	Independent variable representing either nodal voltage or branch current
v_j	Element of the vector y_1 ,
v_m	Element of y_2
i_f	Additional variable (current) due to tearing of a network in large change sensitivity
F	State of a switch in large change sensitivity i.e. open, $F=0$, or closed, $F=1$

Δy^k	An $s \times 1$ vector of the incremental changes in the k^{th} iteration and
s	Number of switches in a network for tearing

Symbols in Traditional Diakoptics

I	Currents or current sources (A or pu)
I^*	Hypothetical current vector (A or pu)
I_A	Vector of currents in subnet A (A or pu)
I_B	Vector of currents in subnet B (A or pu)
i_b	Vector of cut branches currents (A or pu)
e^*, i^*, Y^*	Quantities due to subdivisions
e_b^*	Vector of hypothetical voltages (V or pu)
Y	Admittance or admittance matrix (S or pu)
Z	Impedance or impedance matrix (Ω or pu)
Z_b	Diagonal impedance matrix of removed branches
C, K, L	Connection matrices
τ	Unit matrix
μ	Real part of corrective voltage (pu)
λ	Imaginary part of corrective voltage (pu)
ν	Complex corrective voltage (pu)
ℓ	Removed link quantity
t	Superscript indicating transpose

Contents

ABSTRACT.....	ii
ACKNOWLEDGEMENTS	iv
DEDICATION.....	v
STATEMENT OF OBJECTIVES	vi
ABBREVIATIONS	vii
GLOSSARY	viii
LIST OF SYMBOLS	ix
LIST OF FIGURES	xx
LIST OF TABLES	xxv
1 GENERALTRODUCTION.....	1
1.1 Introduction.....	1
1.2 Potentials of Diakoptics in Modern Power System Analysis	3
1.2.1 Benefits of Diakoptic Analysis.....	4
1.2.2 Applications of Diakoptics	6
1.3 Research Context	8
1.4 Thesis Aims and Objectives.....	9
1.4.1 Aim of the Research	10
1.4.2 Research Objectives.....	10
1.5 Research Questions	11
1.6 Thesis Contribution.....	11
1.7 Thesis Organization	12
2 BACKGROUND TO THE STUDY.....	13
2.1 Introduction.....	13
2.2 The Concept of Diakoptics	13
2.2.1 Tearing in Diakoptics	14

2.2.2	Analysis Procedure	15
2.3	Forming Connection Matrices	18
2.4	Survey of Different Diakoptic Methods	20
2.4.1	One-Piece Nodal analysis	21
2.4.2	Diakoptic Methods.....	21
2.4.3	Impedance Matrix Method Load flow	27
2.4.4	Large Change Sensitivity.....	30
2.4.5	The Multi-Area Thevenin Equivalent (MATE) Concept	36
2.4.6	Deductions	39
2.5	Advantages of Diakoptics in Multicomputer Configuration	39
2.6	Influence of Wind energy on Weak Grids	40
2.6.1	Steady-state Voltage level	40
2.6.2	Change in voltage Level	42
2.6.3	Reactive power effects.....	43
2.7	Per Unit System	43
2.7.1	Basic Procedure in Per Unit System.....	45
2.7.2	Selecting Base Values.....	45
2.7.3	Three-Phase System.....	46
2.7.4	Single Phase System	46
2.7.5	Change of Base	47
2.7.6	Advantages of the per unit system.....	48
2.8	Important Considerations for Wind Integration.....	48
2.8.1	Strength of Grid	48
2.8.2	Point of Common Coupling or Connection	49
2.8.3	Short-Circuit level	50

2.8.4	Impedance angle (ψ).....	50
2.9	Weak Grid.....	50
2.10	Voltage Variation Due to Wind Integration.....	51
2.10.1	Determination of Voltage Variation and Short-circuit ratio in a Weak Grid	
	52	
2.10.2	Reactive power control.....	54
2.11	Voltage Variation in a Strong Grid.....	55
2.12	Load Flow Analysis	55
2.12.1	Power System Basics	56
2.12.2	Types of Buses	57
2.12.3	Power Flow Equations	58
2.12.4	Direct methods and Iterative methods in Load Flow solutions.....	60
2.12.5	Diakoptics in Load Flow Analysis	60
2.12.6	Diakoptics in Impedance Matrix Load Flow.....	61
2.12.7	Piecewise Load Flow by Admittance Matrix Method	62
2.12.8	Diakoptics and Large Change Sensitivity Method.....	63
2.13	Proposed Method	65
2.14	Summary	67
3	NOVEL ANALYSIS METHODS: the Bvmt AND the Svud method of LOAD	
	FLOW	68
3.1	Introduction.....	68
3.2	The Foundational Principle of BVM and SVUD Methods.....	68
3.2.1	Basic Solution Steps of the BVMT and the SVUD.....	69
3.3	Choosing Method of Tearing for BVMT and SVUD	72
3.3.1	Methods of Tearing.....	72
3.4	Formulation of the BVMT Equations for Solution.....	77

3.4.1	Obtaining Complete Solution of the Subnetworks Separately	81
3.5	Slack Bus Voltage-Updating Diakoptic (SVUD) Load Flow	85
3.5.1	Subnetworks	87
3.5.2	Load Flow Studies	87
3.5.3	Modelling Voltages of Subnetworks	93
3.5.4	Updating Algorithm for Temporary Slack Bus Voltage.....	97
3.6	Flow Charts for Slack Bus Voltage-Updating Diakoptics (SVUD) Load Flow	104
3.6.1	Flow Chart for Sequential Computing.....	105
3.6.2	Flow Chart for Parallel Computing	105
3.7	Process of Modifying Node Voltages and Updating Slack Bus Voltage.....	111
3.7.1	Modifying Node Voltages at iteration k	112
3.7.2	Updating Temporary Slack Bus Voltage.....	113
3.8	Summary	116
4	IMPLEMENTATION OF The BVMT AND THE SVUD LOAD FLOW METHOD	117
4.1	Introduction.....	117
4.2	Layout of Implementation of Algorithms	117
4.3	Network Tearing Algorithm	119
4.3.1	Automatic Network Splitting.....	119
4.3.2	Forming Adjacency Matrix.....	127
4.3.3	Algorithm for Automatic Assessment of Cut Configurations	127
4.3.4	Subnetwork Sizing.....	134
4.3.5	Automatic versus Manual Tearing of Network	135
4.3.6	Tearing Times of Test Systems	135
4.4	Implementation of the Branch Voltage Modifier Technique.....	137
4.4.1	Application of BVMT to Linear System	137

4.4.2	Application of BVMT to Nonlinear system with Current Injections	145
4.5	Implementation of Slack Bus Voltage-updating Diakoptic (SVUD) Load Flow	150
4.5.1	Summary of Application of SVUD to Test Systems	151
4.5.2	Solution Procedure Slack Bus Voltage-Updating Load Flow	152
4.6	Application of the SVUD Load Flow to IEEE Test Systems	156
4.6.1	Application of SVUD to IEEE 14-Bus Test System	157
4.6.2	SVUD Analysis of IEEE 30-Bus Network	164
4.7	Comparison of SVUD with One-piece Gauss-Seidel Load Flow.....	175
4.8	Convergence Characteristics of SVUD Load Flow	176
4.8.1	SVUD and Effect of the Iterative Procedure	178
4.9	Summary	179
5	The Nigeria Electrical Power System Analysis.....	181
5.1	Introduction.....	181
5.2	Snapshot of the Nigeria Electrical Power System	182
5.2.1	Nigeria Grid Codes for Transmission the System	186
5.2.2	Overview of the SVUD Load Flow Method.....	186
5.3	Analysis of the of the Nigeria 330kV transmission network	187
5.3.1	Application of SVUD the 330kV Transmission Network.....	188
5.3.2	Considerations for Choosing Lines of Cut	194
5.4	The Split Network Characteristics	196
5.5	Comparison of Results of One-piece Solutions with SVUD Load Flow.....	197
5.6	Voltage profile of the system.....	201
5.7	Summary	201
6	ANALYSIS OF NIGERIA 330KV NETWORK INTEGRATED WITH WIND ENERGY	203

6.1	Introduction.....	203
6.2	Choice of Wind Power for Electricity Generation.....	204
6.3	Wind Energy Prospects in Nigeria.....	206
6.4	The Nigeria Wind Farm Project.....	207
6.5	Investigation of Effects Wind Energy Integration	209
	6.5.1 PSCAD analysis of integration of wind energy.....	210
6.6	SVUD Analysis of the Nigeria 330kV Network Integrated with wind Power .	217
	6.6.1 Grid Impedance and Short Circuit Ratio of the Network	217
	6.6.2 Determination of the grid impedance	217
	6.6.3 Short circuit ratio	219
6.7	SVUD Assessment of Voltage Variation Introduced by Wind Energy in the 330kV Network.....	220
6.8	Effect of Injecting Reactive Power on Voltage Change	225
6.9	Effect of Increased Wind Power on the Voltage Level	230
6.10	Analysis of the Stronger Grid	231
6.11	Characterization of wind turbines	232
6.12	Options to Enable More Wind Power in a Weak Grid	233
6.13	Other Strategies for Increasing Wind Energy in the Grid and Application to Nigeria.....	234
	6.13.1 Getting Organized	234
	6.13.2 Combining Wind Farm and Solar Energy.....	235
	6.13.3 Application of Supernode to Nigeria power system	235
6.14	Summary	238
7	CONCLUSIONS AND RECOMMENDATIONS	240
7.1	Introduction.....	240
7.2	Contributions.....	241

7.3	Recommendations and Further Work	245
7.4	Summary	258
	REFERENCES.....	250
APPENDIX A	LOAD FLOW PROGRAMS	269
APPENDIX B	PROGRAMMES FOR DIRECT COMPUTATION OF ADMITTANCE MATRICES	276
APPENDIX C	PROGRAMMES FOR DIRECT COMPUTATION OF IMPEDANCE MATRICES	278
APPENDIX D	WIND ENERGY AND THE GRID.....	284
D.1.1	Power Available for Extraction	284
D.2.1	Fixed-speed wind turbine.....	286
D.2.2	Variable-speed wind turbines	288
APPENDIX E	CODE FOR SVUD LOAD FLOW ANALYSIS.....	307
APPENDIX F	PUBLICATION.....	327

LIST OF FIGURES

Figure 1.1 Human body model for EMC study using diakoptics [11].....	6
Figure 2.1 A network of two areas connected by a line.....	16
Figure 2.2 Branches with injected currents.....	16
Figure 2.3 Addition of voltage source	17
Figure 2.4. A generic network	19
Figure 2.5. Original network 5-node network to be analysed.....	20
Figure 2.6. Original network showing line of tear	22
Figure 2.7. The 5-node network decomposed into two subnetworks	24
Figure 2.8. Intersection network of the 5-node network.....	24
Figure 2.9. Matrix formation in impedance matrix diakoptics	28
Figure 2.10. Impedance matrix for Figure 2.5 showing relation of subnetworks to each other	28
Figure 2.11. A large nonlinear network	31
Figure 2.12 Effect of ideal switch.....	32
Figure 2.13. Multicomputer configurations for diakoptics	40
Figure 2.14 Voltage Profile of a feeder without wind	41
Figure 2.15 Voltage profile of a feeder with wind energy.....	41
Figure 2.16. Grid connection of a wind farm.....	52
Figure 2.17 Typical power system.....	56
Figure 2.18 Block diagram of the simple power system	57
Figure 2.19. Typical BBD matrix typical for diakoptic analysis	66
Figure 3.1. Schematic diagram of basic diakoptic steps and one-piece solution.....	71
Figure 3.2. An 8-bus system	72
Figure 3.3. Branch tearing –original network with proposed line of tear.....	73

Figure 3.4. Nodes to be removed or cut.....	75
Figure 3.5. Chosen branches showing overlap of the nodes.....	76
Figure 3.6. An N-bus network	86
Figure 3.7. The n-bus network torn into two (a) Subnetworks (b) removed branches ...	87
Figure 3.8. Six-bus network.....	90
Figure 3.9. Parallel computing arrangement for two subnetworks.....	106
Figure 3.10. Flow chart for sequential implementation of SVUD load flow	107
Figure 3.11. Flow chart for parallel implementation of SVUD load flow.....	109
Figure 3.12 Network of Figure.3.8 torn into two.....	111
Figure 4.1. Implementation structure of devised methods.....	118
Figure 4.2. Network architecture of Figure 3.8	119
Figure 4.3. Algorithm for identifying line numbers and connections.....	120
Figure 4.4. Graph of network of Figure 4.2.....	121
Figure 4.5. Code for finding possible combinations e [159]	121
Figure 4.6. Subnetworks formed by removing cut combinations	124
Figure 4.7. Code for new adjacency matrix after a link is removed.....	129
Figure 4.8. Code for analysing the new matrix D	129
Figure 4.9 Reversed order of Figure 4.7	130
Figure 4.10. Reversed row and column code of Figure 4.10.....	131
Figure 4.11. Code that identifies the nodes in each subnet.....	132
Figure 4.12. Computer representation of Figure 3.8 before cutting	133
Figure 4.13. Network successfully split into two distinct subnetworks	133
Figure 4.14. Cut network representation of Figure 4.5 (cut lines = 4, 5)	134
Figure 4.15. Another cut configuration for successful tearing into two distinct subnetworks (cut lines = 1, 2, 6)	134

Figure 4.16. A 22-node Network	138
Figure 4.17. Network of Figure 4.1 decomposed into six subnetworks	139
Figure 4.18. Removed branches of Figure 4.1	140
Figure 4.19. Full block diagonal matrix of the subnetworks admittances	143
Figure 4.20. Power system with two generating stations [106].....	146
Figure 4.21. System torn into two.....	146
Figure 4.22. Network of current sources and per unit admittances [106] (AB = line of tear)	147
Figure 4.23. Network of current sources and per unit admittances [106] (AB = line of tear)	147
Figure 4.24 Procedure for analysis of test systems.....	152
Figure 4.25 Plot of voltage magnitudes of one-piece load flow and SVUD method	155
Figure 4.26. Plot of voltage angles of One-piece and SVUD solutions	156
Figure 4.27. IEEE 14-bus test system [107]	158
Figure 4.28. Network map 14-bus system showing bus numbers	1616
Figure 4.29. IEEE 14-bus test system showing cut= lines 10, 18, 20.....	162
Figure 4.30 Computer output of the 14-bus network with cut =10, 18, 20	163
Figure 4.31. IEEE 30-bus test system [107]	165
Figure 4.32. Network map of 30-bus test system before tearing.....	169
Figure 4.33. Network map of Figure 4.28 with cut lines = 12, 14, 15, 36.....	170
Figure 4.34. Convergence characteristics for cuts = 6,7,9,19,23,29,31,36.....	171
Figure 4.35. Convergence characteristics for cuts = 10,12,14,15,31,32,41	171
Figure 4.36. Network map for the 30-bus network for cuts = 6, 7, 9, 19, 23, 29, 31, 36.....	172
Figure 4.37. Network map for 30-bus cuts = 10,12,14,15,31,32,41	173

Figure 4.38. Convergence properties of 14-bus network for cut lines =10, 18, 20	177
Figure 4.39. Oscillatory convergence of 30-bus for the cut lines 12,14,15,36.....	178
Figure 4.40. Divergence characteristic of Nigeria network with cut lines 13, 19	178
Figure 5.1. Schematic of Nigeria power System operation before deregulation	183
Figure 5.2. Structure of Nigeria Power System Control Centre [117].....	184
Figure 5.3. Map of Nigeria 330kV transmission network	185
Figure 5.4. Computer arrangement of Nigeria 330kVsystem buses.....	189
Figure 5.5. Nigeria 330kV transmission network.....	190
Figure 5.6. Subnetworks of Nigeria 330kV transmission network.....	193
Figure 5.7. Subnet B of 330kV network showing long lines lengths.	194
Figure 5.8. Nigeria 33-kV network map showing removed line	196
Figure 5.9. Voltage profile of 330kV network by SVUD.....	200
Figure 5.10. Voltage profile 330kV network showing subnetworks	200
Figure 6.1. Wind farm layout.....	206
Figure 6.2. Nigeria with lines of equal wind speeds [135]	207
Figure 6.3. Section of map of Nigeria showing Katsina State - Location of the wind farm	208
Figure 6.4. Electrical layout of the Katsina wind farm [137]	209
Figure 6.5 Four-bus test system for PSCAD simulation of wind integration.....	210
Figure 6.6. Voltages at the four buses.....	211
Figure 6.7 Frequencies at the four buses during simulation (a) actual representation of system frequency (b) Average value.....	213
Figure 6.8. Thevenin equivalent at Kano	218
Figure 6.9. Voltage profiles without wind and with rated wind power	221
Figure 6.10. Voltage profiles for rated wind power at different buses	224

Figure 6.11. Induction generator connected to power system	226
Figure 6.12. Wind integration without and with reactive power compensation at bus 30.....	227
Figure 6.13. Increased levels of wind power at the PCC	230
Figure 6.14. Voltage profile of strengthened grid.....	231
Figure 6.15. Voltage profile of strengthened grid with wind power ($P = 10.1018\text{MW}$)	232
Figure 6.16. Supernode concept for wind farms.....	236
Figure 6.17. Application of supernode concept proposed for the Nigerian System Nigeria System.....	237
Figure D.1. Power curve of a wind turbine.....	293
Figure D.2. Wind turbine configurations.....	299
Figure D.3. Approximate equivalent circuit of the induction.....	301
Figure D.4. Wind turbine generator coupling to grid	303
Figure D.5. Equivalent circuit of induction machine connected to power.....	304
Figure D.6. Effect of system reactance and voltage on pull-out torque.....	305

LIST OF TABLES

Table 2.1	Connection matrices of all subnetworks	19
Table 2.2	Results on node voltages obtained from different diakoptic methods	39
Table 2.3	Types of buses	57
Table 3.1	Bus numbers in original network and subnetworks	114
Table 4.1	Line numbers and bus numbers for network	120
Table 4.2	Combinations of possible lines to cut in 6-node network	122
Table 4.3	Configurations that can successfully split network into two subnetworks	123
Table 4.4	Configurations that can successfully split network into three subnetworks ..	123
Table 4.5	The adjacency matrix	127
Table 4.6	Computation time for automatic tearing	136
Table 4.7	Matrices of subnetworks from the torn network	141
Table 4.8	Matrix for one-piece solution	142
Table 4.9	Node Voltages in pu for One-Piece Solution and BVMT	145
Table 4.10	Data for	148
Table 4.11	Results for	150
Table 4.12	Bus data of the network of Figure 3.8	152
Table 4.13	Line data of the network	153
Table 4.14	Result of load flow on full network	153
Table 4.15	Line data of torn network with buses reordered	153
Table 4.16	Results of each iteration and update	154
Table 4.17	Comparison of results	155
Table 4.18	Comparison of results (magnitudes and angles)	155
Table 4.19	Bus data of the IEEE 14-bus system [108]	159
Table 4.20	Line data of the IEEE 14-bus system [108]	160

Table 4.21 Computer output of network line and bus numbers.....	161
Table 4.22 Results of 14 bus network using different solution methods.....	163
Table 4.23 Voltage magnitudes of 14-bus solution in per unit.....	164
Table 4.24 Bus data of the IEEE 30-bus system [99] [100]	166
Table 4.25 Line data of the IEEE 30-bus system.....	167
Table 4.26 Line and node numbers of the 30-bus.....	168
Table 4.27 Results for 30-bus system	174
Table 4.28 Comparison of number of iterations for different networks	175
Table 4.29 Voltage mean Square errors (VMSE) between SVUD and one-piece G-S .	176
Table 5.1 Voltage Control Ranges of Nigeria Transmission system.....	186
Table 5.2 Bus data of the Nigerian 330kV network	191
Table 5.3 Line data of the Nigerian 330kV network	192
Table 5.4 Bus data in subnet <i>A</i> of Nigeria network.....	195
Table 5.5 Bus data in subnet <i>B</i> of Nigeria network.....	195
Table 5.6 Results of different methods of analysis.....	198
Table 5.7 SVUD Results separated into subnetworks	199
Table 5.8 Voltage mean square error (VSME) in comparison with G-S one-piece	199
Table 6.1 Cost Comparison of Renewable Electricity Technologies [134].....	205
Table 6.2 Electrical efficiencies of electricity generation [135].....	205
Table 6.3 Steady-state voltage levels measured at the four buses	212
Table 6.4 Changes in voltage levels	213
Table 6.5 Frequencies measured at the four buses	214
Table 6.6 Effect of integrating rated wind power at different buses	222
Table 6.7 VMSE for wind integration at different PCC's	224
Table 6.8 Increased levels of wind power	228

Table 6.9 Increased levels of wind power229

1 GENERAL INTRODUCTION

1.1 Introduction

The electrical power system is about the largest man-made system and its size coupled with the heterogeneous nature of its components makes its analysis very tasking. This raises the need for new analysis tools that will reduce the burden of computation. Furthermore, the need to decarbonize electricity generation has moved the electrical power world towards renewable energy generation, especially wind energy which has characteristics that are different from the conventional energy sources. The attempt to incorporate the characteristics of wind energy into the existing system increases the analyses required for effective planning and operation of power systems. This work is therefore a contribution to analysis methods for effective assessment of the system.

The major challenge introduced by wind energy is linked to the variable nature of wind which impacts on the characteristics of wind power generators. Induction and synchronous machines are used as generators in wind farms, though the former are more common especially the doubly-fed induction generator (DFIG). The main advantages of the induction generator are its robust brushless construction and the fact that it does not require a separate DC excitation. It is therefore free from these disadvantages of DC and synchronous generators; consequently its cost and maintenance are lower, and its transient characteristics are better [1]. In modified forms, both synchronous and induction generators are used in fixed-speed and variable speed wind turbine configurations. Wind turbine configurations are briefly explained in appendix D.

The characteristics of the induction generator which impact on the power system are [2]:

- Higher energy losses in the rotor due to the damping action.

- It draws the reactive power it requires for excitation from the grid or local capacitors. Local capacitors also pose the threat of self-excitation in the event of disconnection from the grid.
- There is no direct control of the terminal voltage.
- It cannot sustain three phase fault currents on the network.
- The large generators have instability issues.

The main wind energy integration issues are therefore, how to maintain the voltage level within acceptable limits and how to balance the power of the system. In order to maintain the service quality offered to consumers, the characteristics of wind power must be successfully incorporated into the existing system. This imposes extra burden on power system planning and operation.

An effective way of dealing with large-scale electrical networks is to analyse the system in parts and still obtain the same results as if it was analysed as a whole piece. Connection of new generating sources to an existing grid requires clear understanding of all the component parts that would be involved. Technically, successful integration of wind energy to the grid depends on electrical power system characteristics, wind turbine technology, grid connection requirements and simulation tools or method of analysis. Generally, one-piece solutions are employed in power systems analysis and load flow analysis is generally employed.

Load flow or power flow analysis is a very important computation in power system analysis where the steady-state operation of a system is determined. Through load flow analysis, proper planning and control of an existing system can be done and requirements for future expansion like increase in generation or transmission capacity can also be determined. Contingencies can be predicted and level of reactive power for maintaining acceptable voltage level can be determined.

For very large systems, conducting load flow analysis can take several hours to run on a single computer. Reducing the size of the system to be analysed or the volume of data to be handled by a computer or analyst per time to manageable sizes can improve the quality of load flow analysis results and reduce the burden on engineers and grid managers. One way of doing this is by tearing the system into subsystems by a

method known as diakoptics. It has been shown that torn networks can be solved while the whole network could not be solved as a piece with the same analysis program because the whole was network was more than the required limit of complexity for the program

1.2 Potentials of Diakoptics in Modern Power System Analysis

Diakoptics was conceived by Gabriel Kron in the 1950's [3] and furthered by his close follower, Happ [4-6]. Since then there have been several formulations and extensions of the concept; a lot of literature is available and can easily be accessed. Diakoptics combines a pair of information namely, *equations+graph* (or *matrices+graph*), associated with a given physical or economic system [7]. Diakoptics was coined from two Greek words, *dia* which could be taken to mean system, and *kopto* which means tear or cut [8]. Diakoptics was criticised for being presented in technically complex language that was difficult for an average engineer to understand. The fact that a system is torn into smaller systems is clear, but the transformations to yield the solution of the original network were the main concern [5]. This may have delayed its full acceptance, and therefore its full potentials in power system analysis were not immediately evident. This difficulty still persists but research is ongoing to utilize its benefits and this work is part of that effort.

In diakoptics, a network is split into subnetworks based on the topology of the network. Each subnetwork is analysed or solved separately as if other subnetworks are non-existent. The solutions of the subnetworks are then combined and modelled to provide a solution to the whole subnetwork as if it was solved as a piece, giving a high degree of accuracy. Kron called the tearing process '*a topological science on its own right*' [8]. In other words, there are important factors to consider when tearing a system and this is based on the nature of the problem. So the engineer needs to pick the point(s) of tear carefully. Also, there is usually a need to solve an additional system. The equations of solutions required are usually the mesh or nodal equations or special combinations of them.

When a system (but not its equations or matrices) is split wide open, a set of hitherto hidden unknowns arise at the points of split. Reason for tearing a network and not the set of equations is explained in Section 2.2. Similarly, when isolated systems are interconnected to form a new system, *hitherto non-existing forces* are created at the points of connection. That means diakoptics goes beyond tearing; it can also be used to interconnect isolated systems. Diakoptics mainly uses these new variables or unknowns to simplify the solution [7].

It may be argued that diakoptics is no longer necessary since present computers are faster. But speed was only a by-product of the main intention - the facilitation of large system analysis. The method allows the most complex network problems to be solved in a detailed and orderly manner [9]. No doubt, modern computers are much faster than the computers when diakoptics was conceived, yet their speeds and storages in most instances, cannot cope with the rapid increase in size and complexity of power systems. Presently, computers that can handle very large power systems as a piece are not readily available. In fact, the computers available to most researchers and engineers cannot handle many power system problems as a piece. The computers have insufficient memory and are generally slow. In this regard diakoptics is a good tool with which to augment computation cost by employing cheaper computers in parallel combinations. The volume of research involving diakoptics in many fields attests to its potential and benefits.

1.2.1 *Benefits of Diakoptic Analysis*

Diakoptics is a well-developed theory and some of the inherent benefits deduced from [5, 6, 9-16] are summarized below.

- a) It can be applied in many fields.
- b) It is based on established mathematical procedures.
- c) It can be used in computations involving symmetrical and non-symmetrical matrices.
- d) Original qualities of subnetworks are preserved which is very difficult to achieve with Sparsity techniques that also involve matrix reduction. This advantage is very important in computer aided analysis.

- e) Though the same challenge encountered with an original network is encountered when the system is torn, it is less complex and reduced in significance.
- f) It requires less computer memory and the level of accuracy is quite high. It is easy to apply and could give a better cost/benefit ratio in electromagnetic compatibility problems.
- g) Matrices handled per time during computation are smaller. Matrix partitioning also reduces matrices but much less time is required in in diakoptics.
- h) Diakoptics uses more information about a system to be analysed or solved than conventional methods, where only the equations or matrices available about a system are utilized. The tearing apart or interconnection of systems automatically introduces some extra linear variables that are used to simplify the process of solution of a system.
- i) It saves time in computer analysis which is a quality often desired. The saving in time is analysed briefly below:

A first step in power systems analysis is forming the immittance matrix and in most cases, inverting the matrix is required and involves floating point operations. Elimination methods such as, Gaussian elimination, are often used for inversion of matrices. For a network of say, N nodes, the immittance is an $N \times N$ matrix. For a large N , the number operations required to invert the $(N \times N)$ matrix is N^3 and since floating point operations are the dominant operations, they are proportional to computation time [17]. Let the time required to invert an $(N \times N)$ matrix be T , then,

$$T = kN^3 \quad (1.1)$$

If the network is divided into s parts, then each subdivision matrix will be an $N/s \times N/s$ matrix. The total time, T_d , required to solve the system diakoptically will be of the order

$$T_d = 2ks \left(\frac{N}{s} \right)^3 = \frac{T}{\left(\frac{1}{2} s^2 \right)} \quad (1.2)$$

A safety factor of 2 has been included to account for the additional labour required for the division into subsystems and the inversion of the tie impedance matrix, and for

the computation of various additional products [17, 18] shows that even a division into two or three parts will yield an appreciable reduction in labour especially in data handling.

1.2.2 *Applications of Diakoptics*

The original intent of Gabriel Kron was to solve electrical power system problems in a less tasking manner with desired accuracy [3, 4] but it has become a versatile tool unconnected with specific applications. It has been extended and/or combined with other methods by a number of researchers to achieve great results.

1.2.2.1 Diakoptics in other fields

The versatility of diakoptics is demonstrated in the interesting application to the analysis of electromagnetic compatibility (EMC) effects on the human body [11].

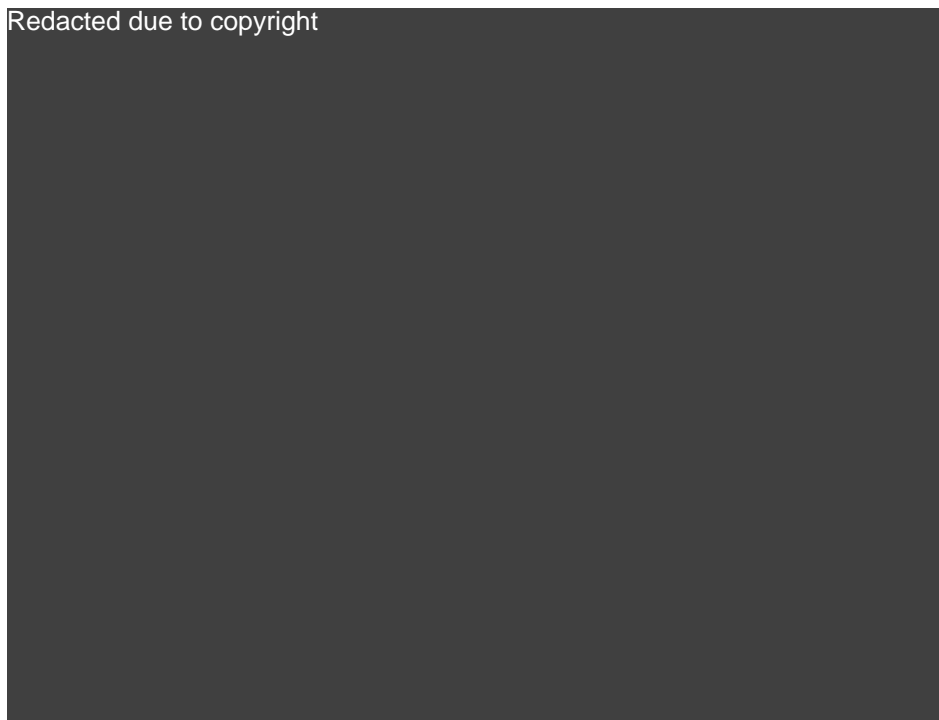


Figure 1.1 Human body model for EMC study using diakoptics [11]

The human body is “torn” into spheroids that correspond to easily identifiable parts of the anatomy as shown in Figure 2.1. Each spheroid is then represented by electrical parameters - resistance, inductance and capacitance and analysed for response to

extremely low frequency (ELF) electric field exposure and electrostatic discharge (ESD). The diakoptic approach in this analysis is reported to require less computation time and computer memory compared to one-piece approaches. Detailed analysis is given in the reference [11].

Other applications not involving electrical power systems analysis include:

- Mechanical engineering [19].
- Communications engineering involving analysis of antennas [20]
- Railway for solution of DC network equations [21]
- Mathematics and computer science for solution of large eigenvalue problems and topological network theory for connecting matroids [22-24].
- Microwave analysis for electromagnetic simulation to obtain the response of circuits [25-27].
- For reduction of computational load in computer modelling of water distribution systems [28].
- In civil and structural engineering for modelling of beam structures [29] and global structures which are divided into substructures based on set criteria. Identical substructures increase the efficiency of the method [30].
- Formulation of special diakoptic algorithm for general application to various fields of engineering [31].

1.2.2.2 Applications of diakoptics in electrical power systems analysis

Literatures abound on application of diakoptics to power systems analysis, which is where diakoptics originated from as explained above. A few of them are:

- Fault studies in electrical network and in large transformers [16, 32].
- Transient stability analysis [9, 33]
- Compensation methods for simulation of branch outages [34].
- State estimation for monitoring and controlling power systems [35-37]
- Load flow analysis [38-43]

1.3 Research Context

The challenges of integration of wind farms into grids are more pronounced in weak grids. A weak grid is defined as *a network or part of a network where fault levels are low; that is, the Thevenin or source impedance is high* [44]. This implies that the node voltages would be sensitive to the flow of active and/or reactive power flow. The issues related to a weak grid coupled to a wind farm are voltage quality issues, namely, steady-state voltage level, voltage fluctuations and possible distortion of the voltage waveform due power electronic devices used in the wind turbine generators. The most important factor is the steady-state voltage level and informs the design criteria for connection of wind turbines to the grid [45]. Fluctuations in the voltage may, in extreme conditions, trigger a voltage collapse, as voltage drop causes increased reactive power consumption, which feeds back as an increased voltage drop [46, 47].

Power system analysis is fundamental in making sure that wind farms fulfil the purpose of being a contributing generation in the delivery of quality power to consumers. Modern power systems analyses are based on digital computers; hence, establishment of suitable mathematical models that effectively describe the physical processes is the key element in successful analysis. Stiff and weak grids have been modelled mathematically for steady-state voltage variation, ΔV , to determine the state of a grid for operation and planning purposes.

There have been attempts to apply diakoptics to load flow analysis but in most cases complexity is increased, and the same number of iterations as the full network solution is obtained as in [42]. Also, current injection which involves linear load flow equations is applied. Therefore, research into easier ways of incorporating diakoptics into the commonly used methods which is based on nonlinear equations derived by power injection is desirable. Moreover, the performance of personal computers (PC) has increased tremendously in the past two decades and prices are reasonably cheap; these can be utilized in parallel combinations to run load flow of large networks instead of one supercomputer.

In view of the above, a literature review on diakoptics or piecewise load flow methods applied to electrical networks will be presented. An overview of wind

energy integration to grids will be given. Lastly, the main reason for the present work will be introduced, followed by the main achievements resulting from this research project.

1.4 Thesis Aims and Objectives

This thesis is predicated on three elements. The main one is the need for less complicated ways to analyse the ever enlarging and complex power systems which is reflected in the volume of literature that deals with the issue. Secondly, wind energy which is currently the hub of renewable energy in the world and its integration increases the size and complexity of the system. Thirdly, in an attempt to simplify the procedure required for circuit formulation and computation in power system analysis, diakoptics is chosen as the foundational analysis method because of its advantages, some of which are outlined in section 1.2.

With all the desirable qualities of diakoptics, the question that comes to mind is, ‘Why is diakoptics not a universal tool for the study of large and complex power systems?’ Two main reasons could be identified from review of extant literature. The first one is the difficulty of formulating the diakoptics solutions which made its appreciation restricted to a few experts of the technique [15, 37, 48, 49] and the favourable outcome of Sparsity Techniques [10] which was introduced about the period diakoptics was making a headway as an analysis tool [13, 39, 50].

Diakoptics and Sparsity techniques take advantage of the sparsity of the power system matrix but according to the literature [10], the superiority of diakoptics comes to the fore in real time solutions, especially in multicomputer solutions. Maintaining the identity of subsystems in solutions involving matrix reduction is an uphill task with sparsity techniques but diakoptics does this easily. Preserving the identity of subsystems allows, among others, the pre-determination of inverses of matrices for subnetworks which topology remain the same before inserting them in the simulation loop. This is also, important in latency exploitation in certain types of solutions like electromagnetic transient program (EMTP). Latency exploitation is defined as the ability to solve a network with different discretization step sizes of its component parts [10].

In view of the above, the major aim and objectives of this research are outlined as:

1.4.1 *Aim of the Research*

The main aim of this research is to create new and ‘user-friendly’ diakoptics with a view to making it a universal tool in the analysis of large-scale power systems including wind integrated systems.

1.4.2 *Research Objectives*

The aim would be achieved through the following objectives:

1. To critically review literature on diakoptics with emphasis on those relating to electrical power systems analysis.
2. To critically study the technicalities of selected diakoptic methods in extant literature and perform calculations on a selected network using methods proposed in the literature for comparison in order to appreciate the challenges of the different approaches.
3. To conduct literature review on wind integration to find out the method of analysis most suitable for assessing the effect of wind power integration into weak grids.
4. To carry out rigorous mathematical formulations and calculations with a view to producing novel diakoptic methods that would be ‘attractive’, especially in their final states, to power systems analysts.
5. To develop a computer programme that will execute the new load flow method for easy analysis of networks by just plugging in the network data and following the instructions.
6. The new method will then be applied to sample networks including IEEE benchmark networks and results will be compared with those of one-piece methods for validation and in order to highlight the desirable qualities of the new method.

7. The Nigeria electrical network, with and without wind energy, will be analysed using the new load flow tool to determine its ability to cope with high wind power in its present state and make recommendations.

1.5 Research Questions

Based on the aim and objectives stated above, the main questions that this research set out to answer are laid out as follows:

- Traditionally, centralized analyses of large-scale power systems are generally employed which involves a lot of labour and computer storage due to their size and complexity. Can diakoptics in a simpler form reduce the labour of analysing large systems by reducing the volume of data to handle per time and through sharing of tasks?
- From the engineering point of view, the successful integration of wind energy into the grid involves four main factors, namely, electrical power system characteristics, wind turbine technology, grid connection requirements, and simulation tools. How may a new load flow analysis tool improve existing load flow tools?
- Most diakoptic methods reported in literature are based on linear analyses. The few methods which involve nonlinear load flow analysis tend to make the diakoptic solution more complex. Is it possible to develop a new algorithm that would make diakoptic load flow more ‘user-friendly’?
- How may the developed algorithm aid the assessment of effect of wind power on the steady-state voltage change of weak grids including the Nigerian power system?

1.6 Thesis Contribution

The main contributions of this thesis are:

- Introduction of a simpler method of deriving the diakoptic equations of solution, and the resultant branch voltage multiplier technique (BVMT) suitable for linear analysis;
- Development of a novel load flow analysis tool - the slack bus voltage update diakoptics (SVUD);
- Improvement of the convergence characteristics of the classical Gauss-Seidel load flow method in the new algorithm;
- Implementation of the SVUD load flow on the Nigerian system for determination of its state based on the voltage profile;
- Verification of the suitability of Nigeria network for wind energy integration using the SVUD analysis, and recommending suitable procedures for increased wind integration.

1.7 Thesis Organization

Subsequent chapters of the thesis start by surveying the literature that establishes the background of the research in chapter 2. Chapter 3 describes the methodology for obtaining the proposed branch voltage modifier algorithm (BVMT) and the slack voltage update diakoptics (SVUD) for linear and nonlinear analyses, respectively. In chapter 4, the proposed algorithms are applied to networks and their validity is proved by comparing the results with those of traditional one-piece solutions. Their desirable qualities compared to other methods are highlighted in the analysis. The determination of the voltage profile of the Nigeria 330kV transmission network by applying the SVUD is presented in Chapter 5. Extension of the SVUD to the analysis of Nigeria system integrated with wind power is explained in Chapter 6. Finally, in Chapter 7, the main conclusions are summarized in the contributions to the field, recommendations for future work and possible measures for the improvement of the Nigeria transmission system are also presented.

2 BACKGROUND TO THE STUDY

2.1 Introduction

The background to this research is the tremendous growth of electricity generation from wind energy and finding new or improved analysis approaches to the solution network analysis problems in line with the growth and accompanying complexities. Many power system problems especially load flow require the consideration of the whole network which can be difficult in many cases. The need for tools to easily and effectively analyse the power system can be summarized in the following words: *“Grids and grid managers are becoming more stressed due to increasing congestion, regulatory compliance requirements, changing generation mix, increasing interconnection complexity, increasing transmission asset utilization and aged assets”* [51].

The special feature of this work is the development and application of mathematical models based on a concept developed by Gabriel Kron known as diakoptics; a concept that creates smaller networks from the original system. In other words, attempts will be made to develop new mathematical models that will make diakoptics more ‘user-friendly or more efficient’ in the form of the diakoptic algorithm. Diakoptics is a tool which can reduce the complexity and burden of computation in power system analysis and from a computational point of view reduces the dimensions of matrices. Partitioning of matrices is often used for this same purpose but the savings in number of computations in the case of diakoptics is quite large [6, 7].

2.2 The Concept of Diakoptics

In diakoptics, a system is torn into a desired number of subsystems. The individual subsystems are solved separately, after which the solutions are combined and modified to yield the complete solution as if the system was not torn apart but solved

as one piece. [3, 5, 6, 13, 17] The torn parts are compensated for by introducing hypothetical currents at the points of tear. There is no official method of choosing the best set of tearing branches or nodes; the engineer needs to pick the point(s) of tear by heuristic methods. Though this conclusion was reached in the early years of diakoptics [52-54], the search for literature to show that this situation has changed has not yielded such result. There are different suggestions by different researchers, for example, it is suggested in [55] that lines of tear should not include one that was originally linked to a *dispatchable source*.

When a network is torn into independent parts, a new set of variables arises due to tearing. Similarly, when networks that were originally separate are interconnected to form a larger network, new variables are created due to interconnection. Diakoptics mainly employs these extra variables to simplify the solution of the system [7]. In its original formulation, a system or its graph has to be split and not its equations or matrices because physical models easily supply these extra variables by inspection. Matrix partitioning, for example, does not introduce extra variables [7].

2.2.1 *Tearing in Diakoptics*

2.2.1.1 Network tearing or Equations Tearing

In diakoptics, a system or network model is often required for tearing in order to take full advantage of the method. The choice for tearing the network instead of equations is because the former gives rise to extra variables that simplify the solution. The new unknown variables released when a system is torn, increases the total number of unknowns in the equations to be solved. Though this may seem like a disadvantage, they actually simplify the solution of the main unknowns. According to the literature [7], these extra unknowns are likened to Lagrangian multipliers but diakoptics unknowns form linear relationships with the other unknowns. Physical models readily supply these extra unknowns by inspection when torn. Equations, by implication, contain these extra unknowns but tearing the equations, for example in matrix partitioning, does not introduce any extra unknowns. It is possible to partition a set of equations or matrix in such a way that more variables are introduced but it is a laborious process that is not necessary when there is an easier alternative.

Admittance matrix tearing is engaged in [56] with partial inverse which is useful when a small part of a system needs to be analysed. Tearing of equations is proposed in [57] but it is also noted as a difficult process. Apart from this, the authors still needed some form of physical system to effectively tear the equations as proposed by Kron in [7] that a physical system is required in diakoptics either in form of a network or graph.

2.2.1.2 Network tearing considerations

A number of factors determine the points of tear and the number of subnetworks derived. The points of tear should be such that there is no mutual coupling between the subnetworks though this is not absolutely necessary because electrical isolation is sufficient for the method of tearing.

The topological features of a network play an important role in determining the points for tearing. In the case of electrical power networks, the subnetworks often occur naturally like boundaries between power companies. For example, the transmission lines spanning a whole country may be subdivided according to state boundaries. Subdivision of the states' network will depend on the computer capability [3] or other technical considerations like the number of generators connected to proposed boundary nodes. Choosing branches between load buses are particularly advantageous as shown in chapter 4. In branch tearing, the removed branches must not form a closed loop and must not contain nodes that are not in the remaining network. Ideal branches to remove are those that will yield subnetworks with sufficiently large meshes or nodes [13].

2.2.2 Analysis Procedure

Splitting a network into pieces is a procedure that is easily understood, but transforming solutions of individual subnetworks to yield the solution of the original network is the challenging aspect of diakoptics. The following summarises the basic principle of transforming individual solutions.

In steady-state analysis of a network, the system of linear equations generally expressed mathematically as $Ax = b$ is given in electrical power system as:

$$\mathbf{I} = \mathbf{YV} \quad (2.1)$$

where \mathbf{Y} is the admittance matrix and \mathbf{I} is the injected current vector and \mathbf{V} is the vector of node voltages to be determined. Consider a network represented by Figure 2.1 where branches m and n when removed would tear the network into two independent subnetworks. Buses m and n are therefore known as boundary buses.

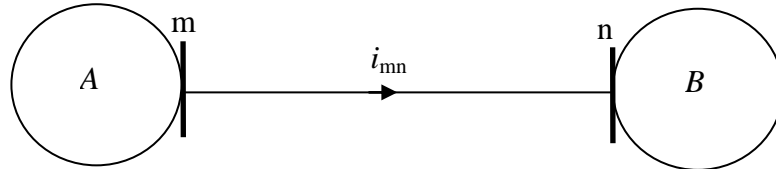


Figure 2.1 A network of two areas connected by a line

Hypothetical currents

When the branches are removed, the current i_{mn} would no longer flow. To account for this missing current, unknown currents, $-i_m^* = i_n^* = i_{mn}$, are injected into the boundary nodes as shown in Figure 2.2. This is represented in matrix form in (2.2) and concise form in (2.3).



Figure 2.2 Branches with injected currents

$$\begin{bmatrix} i_m^* \\ i_n^* \end{bmatrix} = \begin{bmatrix} -1 \\ 1 \end{bmatrix} [i_{mn}] \quad (2.2)$$

$$\mathbf{i}^* = \mathbf{Li} \quad (2.3)$$

Hypothetical voltage sources

The unknown currents, i^* , that have been introduced create unbalance in the system

To balance the system [58], hypothetical voltage source e_{mn}^* is introduced into the removed branches as shown in Figure 2.3.

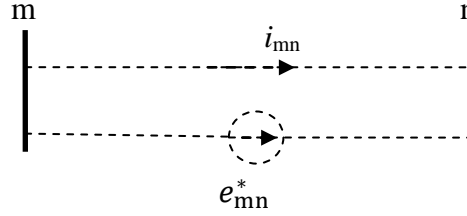


Figure 2.3 Addition of voltage source

The new voltage, e_{mn}^* , described in terms of the node voltages is given in (2.4) equation and written in matrix form as equation (2.5) and the concise form is equation (2.6).

$$e_{mn}^* = V_m - V_n \quad (2.4)$$

$$e_{mn}^* = [1 \quad -1] \begin{bmatrix} V_m \\ V_n \end{bmatrix} \quad (2.5)$$

$$\mathbf{e}_{mn}^* = \mathbf{K}\mathbf{V}_m \quad (2.6)$$

The connection matrices are \mathbf{L} and \mathbf{K} in (2.3) and (2.7). The connection matrices can be formed by inspection as explained in section 2.3. The relationship between the connection matrices can be seen in (2.2) and (2.5) and is stated as

$$\mathbf{K} = -\mathbf{L}^t \quad (2.7)$$

This completes the second part towards the realization of diakoptics *equation of solution*. The relationship between the two connection matrices saves computer storage requirements [58]. The next part is the determination of impedance matrix of the removed branches.

Branch Impedance Matrix

Let the impedance of the removed branches be Z_{mn} , then $i_{mn} = (V_m - V_n)/Z_{mn}$ which

can be written in matrix form as:

$$\mathbf{Zi} = \mathbf{e}^* \quad (2.8)$$

Combining the Equations

The removal of branch mn creates two subnetworks A and B , resulting in (2.2). The combined equations in the first three steps yield equation (2.9) for the complete network.

$$\begin{bmatrix} \mathbf{Y}_A & 0 & 0 \\ 0 & \mathbf{Y}_B & 0 \\ 0 & 0 & \mathbf{Z} \end{bmatrix} \begin{bmatrix} \mathbf{V}_A \\ \mathbf{V}_B \\ \mathbf{i} \end{bmatrix} = \begin{bmatrix} \mathbf{i}_m + \mathbf{i}_m^* \\ \mathbf{i}_n + \mathbf{i}_n^* \\ \mathbf{e}_{mn}^* \end{bmatrix} \quad (2.9)$$

Further analysis is given in section 2.3.2 where the equations of solution are applied for nodal analysis of a sample network before substituting numerical values.

2.3 Forming Connection Matrices

Connection matrices play a very important role in diakoptic analysis and indicate the relationship between the subnetworks. The procedure for forming the connection matrix is described in this section. Figure 2.4 is a generic network to be torn into subnetworks A , B , C , and D by removing lines b_1 , b_2 , b_3 , b_4 , and b_5 . The arrows indicate current directions and can be chosen arbitrarily if the directions are not known, but any chosen direction must be followed in forming the matrices.

In any typical connection matrix, the number of rows is equal to the number of buses or nodes in the subnetwork and the number of columns is equal to the number of tearing branches. The numbers of columns in all subnetworks' connection matrices are equal but the rows depend on the number of buses. They contain only +1, -1 and 0. If a node was connected to a removed branch and the current direction is out of the node, the entry in the connection matrix is +1 and if the flow is into the node, the entry is -1. The signs (+ and -) indicate the direction of current flow in the removed lines or branches.

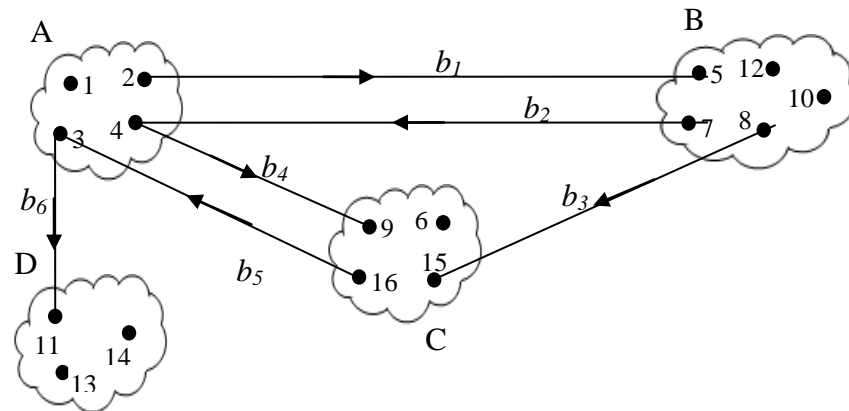


Figure 2.4. A generic network

Table 2.1 Connection matrices of all subnetworks

SUBNETWORKS	Node no.	b_1	b_2	b_3	b_4	b_5	b_6
A	1	0	0	0	0	0	0
	2	1	0	0	0	0	0
	3	0	0	0	0	-1	1
	4	0	-1	0	1	0	0
B	5	-1	0	0	0	0	0
	7	0	1	0	0	0	0
	8	0	0	1	0	0	0
	10	0	0	0	0	0	0
	12	0	0	0	0	0	0
C	6	0	0	0	0	0	0
	9	0	0	0	-1	0	0
	15	0	0	-1	0	0	0
	16	0	0	0	0	1	0
D	11	0	0	0	0	0	-1
	13	0	0	0	0	0	0
	14	0	0	0	0	0	0

If a node was not connected to a removed branch, the entry in the connection matrix is 0. If the number of subnetworks is four, the connection matrices will be four. If N_b branches were removed and the consequent subnetworks formed have N_1 and N_2 nodes, the connection matrices formed will be of dimension $(N_1 \times N_b)$ and $(N_2 \times N_b)$ respectively. The resulting connection matrices are shown in Table 2.1; for an element L_{ir} , the connection matrix is defined as

$$L_{ir} = \begin{cases} +1, & \text{if the branch } r \text{ is directed away from node } i \\ -1, & \text{if the branch } r \text{ is directed towards node } i \\ 0, & \text{if node } i \text{ does not include branch } r \end{cases}$$

2.4 Survey of Different Diakoptic Methods

Some literature of particular interest were reviewed and the methods proposed were applied to the linear network of Figure 2.4 adapted from [13] for simplicity. The network is first solved using one-piece nodal analysis and classical diakoptic method before applying other methods for comparison of results. The results of the different methods are shown in Table 2.2. Apart from large change sensitivity which gave slightly different results, all the methods gave the same node voltages as the one-piece solution. All computations were done with MATLAB. Large Change Sensitivity and Impedance Matrix load flow are also applicable to nonlinear networks.

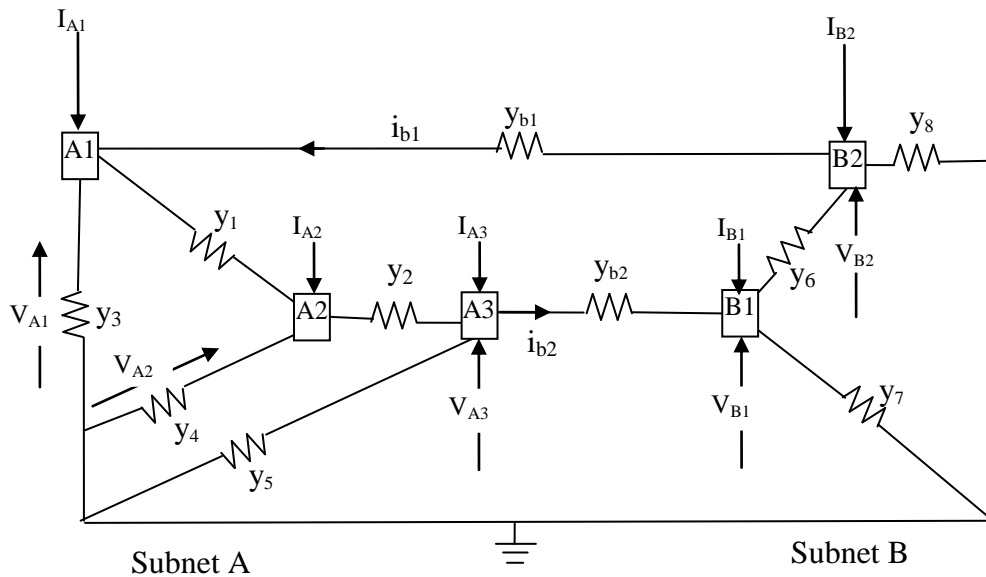


Figure 2.5. Original network 5-node network to be analysed

The values of the admittances are 1siemen each; currents injected at the nodes are 1ampere each. The voltages in volts are the unknown values to be computed.

2.4.1 One-Piece Nodal analysis

In the one-piece analysis the network is not torn. The admittance matrix of the original network, \mathbf{Y} , is given in (2.10) which corresponds to (2.1). The voltage vector to be determined, \mathbf{V}_a , and vector of currents, \mathbf{I} , injected at the nodes are given in equations (2.11) - (2.13). Numerical values are substituted in (2.10) and the node voltages are computed as $\mathbf{V} = \mathbf{Y}^{-1}\mathbf{I}$ shown in (2.14) where the full admittance matrix is inverted. The results are shown in column one of Table 2.2.

$$\begin{bmatrix} (y_1 + y_3 + y_{b1}) & -y_1 & 0 & 0 & -y_{b1} \\ -y_1 & (y_1 + y_2 + y_4) & -y_2 & 0 & 0 \\ 0 & -y_2 & (y_2 + y_5 + y_{b2}) & -y_{b2} & 0 \\ 0 & 0 & -y_{b2} & (y_6 + y_7 + y_{b2}) & -y_6 \\ -y_{b1} & 0 & 0 & -y_6 & (y_6 + y_8 + y_{b1}) \end{bmatrix} \times \begin{bmatrix} V_{A1} \\ V_{A2} \\ V_{A3} \\ V_{B1} \\ V_{B2} \end{bmatrix} = \begin{bmatrix} I_{A1} \\ I_{A2} \\ I_{A3} \\ I_{B1} \\ I_{B2} \end{bmatrix} \quad (2.10)$$

$$\mathbf{Y} = \begin{bmatrix} 3 & -1 & 0 & 0 & -1 \\ -1 & 3 & -1 & 0 & 0 \\ 0 & -1 & 3 & -1 & 0 \\ 0 & 0 & -1 & 3 & -1 \\ -1 & 0 & 0 & -1 & 3 \end{bmatrix} \quad (2.11)$$

$$\mathbf{V}_a = \begin{bmatrix} V_{A1} \\ V_{A2} \\ V_{A3} \\ V_{B1} \\ V_{B2} \end{bmatrix} \quad (2.12)$$

$$\mathbf{I} = \begin{bmatrix} I_{A1} \\ I_{A2} \\ I_{A3} \\ I_{B1} \\ I_{B2} \end{bmatrix} = \begin{bmatrix} 1 \\ 0 \\ 1 \\ 0 \\ 1 \end{bmatrix} \quad (2.13)$$

$$\mathbf{V}_a = \begin{bmatrix} V_{A1} \\ V_{A2} \\ V_{A3} \\ V_{B1} \\ V_{B2} \end{bmatrix} = \begin{bmatrix} 3 & -1 & 0 & 0 & -1 \\ -1 & 3 & -1 & 0 & 0 \\ 0 & -1 & 3 & -1 & 0 \\ 0 & 0 & -1 & 3 & -1 \\ -1 & 0 & 0 & -1 & 3 \end{bmatrix}^{-1} \begin{bmatrix} 1 \\ 0 \\ 1 \\ 0 \\ 1 \end{bmatrix} \quad (2.14)$$

2.4.2 Diakoptic Methods

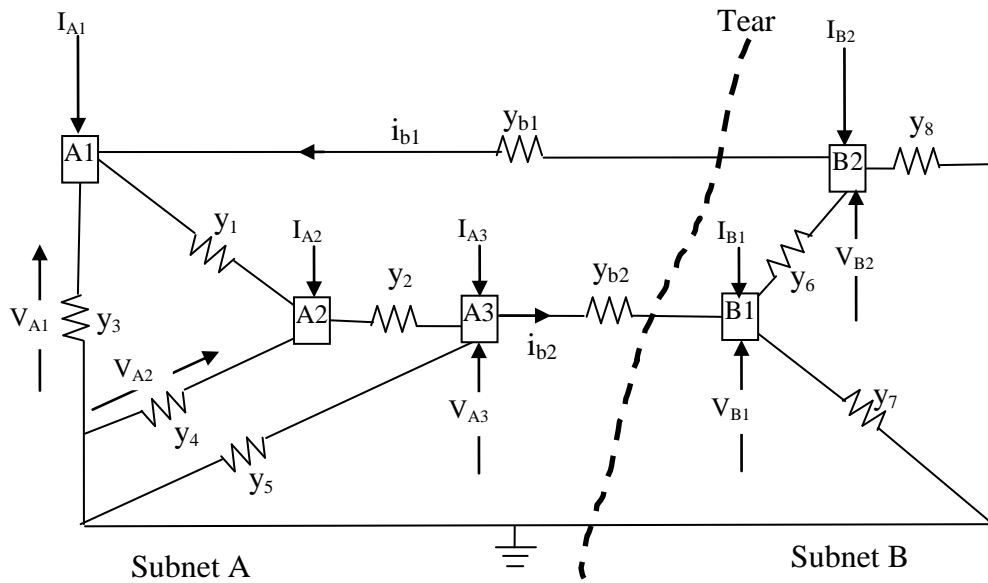


Figure 2.6. Original network showing line of tear

In the application of diakoptic methods the network of Figure 2.5 has been torn into the two subnetworks of along the line of tear shown in Figure 2.7. In real network analysis the network is torn theoretically. In the analysis of the torn network the equations (2.15) to (2.26) are used in all the methods with the symbols shown.

$$\mathbf{Y}_A = \begin{bmatrix} 2 & -1 & 0 \\ -1 & 3 & -1 \\ 0 & -1 & 2 \end{bmatrix} \quad (2.15)$$

$$\mathbf{Y}_B = \begin{bmatrix} 2 & -1 \\ -1 & 2 \end{bmatrix} \quad (2.16)$$

$$\mathbf{I}_A = \begin{bmatrix} 1 \\ 0 \\ 1 \end{bmatrix} \quad (2.17)$$

$$\mathbf{I}_B = \begin{bmatrix} 0 \\ 1 \end{bmatrix} \quad (2.18)$$

$$\mathbf{Z}_b = \begin{bmatrix} 1 & \cdot \\ \cdot & 1 \end{bmatrix} \quad (2.19)$$

$$\mathbf{L}_A = \begin{bmatrix} 1 & 0 \\ 0 & 0 \\ 0 & 1 \end{bmatrix} \quad (2.20)$$

$$\mathbf{L}_B = \begin{bmatrix} 0 & -1 \\ -1 & 0 \end{bmatrix} \quad (2.21)$$

2.4.2.1 Classical diakoptics

The diakoptic analysis reviewed in this section can be found in [13] where a detailed derivation of the equations is given. The classical diakoptics is explained briefly in section 2.2 and can be related to the following application to Figure 2.5.

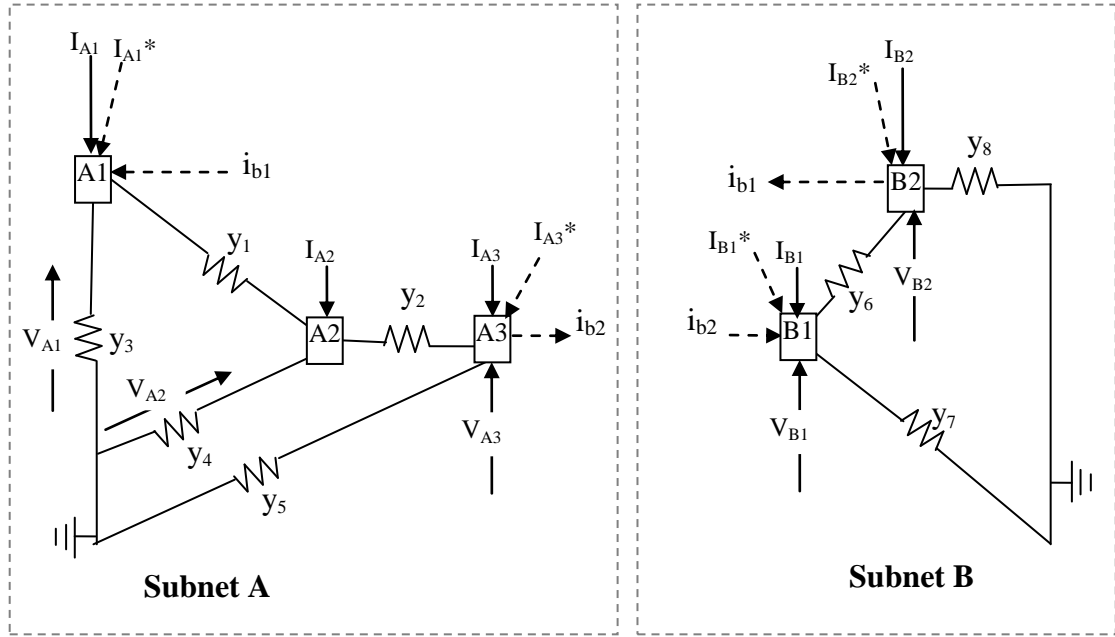


Figure 2.7. The 5-node network decomposed into two subnetworks

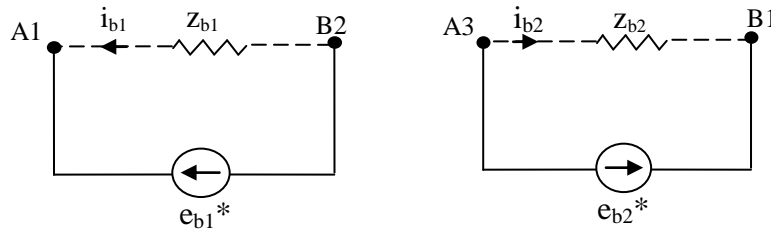


Figure 2.8. Intersection network of the 5-node network

Intersection Network Equations

The relationship between the hypothetical currents, I^* and the assumed branch currents i_b in all detached branches are expressed as

$$\begin{bmatrix} I_{A1}^* \\ I_{A2}^* \\ I_{A3}^* \\ I_{B1}^* \\ I_{B2}^* \end{bmatrix} = \begin{bmatrix} 1 & 0 \\ 0 & 0 \\ 0 & -1 \\ 0 & 1 \\ -1 & 0 \end{bmatrix} \begin{bmatrix} i_{b1} \\ i_{b2} \end{bmatrix} \text{ or } \mathbf{I}^* = \mathbf{L}_{mb} \mathbf{i}_b \quad (2.22)$$

The hypothetical voltage sources, e_b^* , expressed in terms of nodal voltages V_m in equation (2.23) where K_{bm} is the same as $-L_{bm}^t$ in equation (2.22), therefore (2.23) can be rewritten as (2.24).

$$\begin{bmatrix} e_{b1}^* \\ e_{b2}^* \end{bmatrix} = \begin{bmatrix} -1 & \cdot & \cdot & \cdot & 1 \\ \cdot & \cdot & 1 & -1 & \cdot \end{bmatrix} \begin{bmatrix} V_{A1} \\ V_{A2} \\ V_{A3} \\ V_{B1} \\ V_{B2} \end{bmatrix} \quad \text{or} \quad \mathbf{e}_b^* = \mathbf{K}_{bm} \mathbf{V}_m \quad (2.23)$$

Therefore,

$$\mathbf{e}_b^* = -\mathbf{L}_{bm}^t \mathbf{V}_m \quad (2.24)$$

The equations relating the voltages and currents of the removed branches are:

$$\begin{bmatrix} z_{b1} & \cdot \\ \cdot & z_{b2} \end{bmatrix} \begin{bmatrix} i_{b1} \\ i_{b2} \end{bmatrix} = \begin{bmatrix} e_{b1}^* \\ e_{b2}^* \end{bmatrix} \quad \text{or} \quad \mathbf{Z}_b \mathbf{i}_b = \mathbf{e}_b^* \quad (2.25)$$

Equations of Subnetworks

The subnetworks are described by the nodal voltage equations for subnetworks A and B in equations (2.26) and (2.27).

$$\begin{bmatrix} (y_1 - y_3) & -y_1 & 0 \\ -y_1 & (y_1 + y_2 + y_4) & -y_2 \\ 0 & -y_2 & (y_2 + y_5) \end{bmatrix} \begin{bmatrix} V_{A1} \\ V_{A2} \\ V_{A3} \end{bmatrix} = \begin{bmatrix} I_{A1} + i_{A1}^* \\ I_{A2} + i_{A2}^* \\ I_{A3} + i_{A3}^* \end{bmatrix} \quad (2.26)$$

or

$$\mathbf{Y}_A \mathbf{V}_A = \mathbf{I}_A + \mathbf{i}_A^*$$

and

$$\begin{bmatrix} (y_6 + y_7) & -y_6 \\ -y_6 & (y_6 + y_8) \end{bmatrix} \begin{bmatrix} V_{B1} \\ V_{B2} \end{bmatrix} = \begin{bmatrix} I_{B1} + i_{B1}^* \\ I_{B2} + i_{B2}^* \end{bmatrix} \quad (2.27)$$

or

$$\mathbf{Y}_B \mathbf{V}_B = \mathbf{I}_B + \mathbf{i}_B$$

Combining (2.26) and (2.27) gives the compound form as

$$\begin{bmatrix} \mathbf{Y}_A & \cdot \\ \cdot & \mathbf{Y}_B \end{bmatrix} \begin{bmatrix} \mathbf{V}_A \\ \mathbf{V}_B \end{bmatrix} = \begin{bmatrix} \mathbf{I}_A + \mathbf{i}_A^* \\ \mathbf{I}_B + \mathbf{i}_B^* \end{bmatrix} \quad \text{or} \quad \mathbf{Y}_m \mathbf{V}_m = \mathbf{I}_m + \mathbf{i}_m^* \quad (2.28)$$

\mathbf{Y}_m is a block diagonal matrix (BDM) comprising submatrices \mathbf{Y}_A and \mathbf{Y}_B . The corresponding, \mathbf{Y} , of the original network in **Error! Reference source not found.** is of the same order but is not a BDM. Analysis of equations (2.24) to (2.27) yields (2.29) and (2.30) which are the *fundamental equations of diakoptics*.

$$\mathbf{Z}_b \mathbf{i}_b = -\mathbf{L}_{bm}^t \mathbf{V}_m \quad (2.29)$$

$$\mathbf{Y}_m \mathbf{V}_m = \mathbf{I}_m + \mathbf{L}_{mb} \mathbf{i}_b \quad (2.30)$$

By eliminating \mathbf{i}_b in equations (2.29) and (2.30), *the final equation of solution* is obtained as (2.31) which eliminates the need to invert the full true matrix, \mathbf{Y} , of the original network thereby saving storage space and computation time.

$$\mathbf{V}_m = \mathbf{Y}_m^{-1} \mathbf{I}_m - \mathbf{Y}_m^{-1} \mathbf{C}_{mb} \mathbf{Z}_b^{-1} \mathbf{C}_{bm}^t \mathbf{Y}_m^{-1} \mathbf{I}_m \quad (2.31)$$

Equation (2.31) gives the complete solution of the full network instead of solution of separate subnetworks. Also, it can be seen that the block diagonal matrix for the two subnetworks is inverted as a piece. In separate solutions, computation of branch current \mathbf{i}_b is crucial for obtaining the solution of the original network. Rigorous derivation of the *fundamental equations of diakoptics* and *equation of solution* are given in [13]. Inserting numerical values in the nodal voltage equations which describe subnetworks in Figure 2.7 gives:

$$\begin{bmatrix} 2 & -1 & 0 \\ -1 & 3 & -1 \\ 0 & -1 & 2 \end{bmatrix} \begin{bmatrix} V_{A1} \\ V_{A2} \\ V_{A3} \end{bmatrix} = \begin{bmatrix} 1 \\ 0 \\ 1 \end{bmatrix} \quad (2.32)$$

and

$$\begin{bmatrix} 2 & -1 \\ -1 & 2 \end{bmatrix} \begin{bmatrix} V_{B1} \\ V_{B2} \end{bmatrix} = \begin{bmatrix} 0 \\ 1 \end{bmatrix} \quad (2.33)$$

Combining (2.32) and (2.33) as in (2.28) the compound form of the subnetworks equations is obtained in (2.34).

$$= \begin{bmatrix} 2 & -1 & 0 & 0 & 0 \\ -1 & 3 & -1 & 0 & 0 \\ 0 & -1 & 2 & 0 & 0 \\ 0 & 0 & 0 & 2 & -1 \\ 0 & 0 & 0 & -1 & 2 \end{bmatrix} \begin{bmatrix} V_{A1} \\ V_{A2} \\ V_{A3} \\ V_{B1} \\ V_{B2} \end{bmatrix} = \begin{bmatrix} 1 \\ 0 \\ 1 \\ 0 \\ 1 \end{bmatrix} \quad (2.34)$$

Numerical values are substituted in (2.25) gives $Z_b i_b = e_b^*$

$$Z_b i_b = e_b^*, \text{ that is, } \begin{bmatrix} 1 & 0 \\ 0 & 1 \end{bmatrix} \begin{bmatrix} i_{b1} \\ i_{b2} \end{bmatrix} = \begin{bmatrix} e_{b1}^* \\ e_{b2}^* \end{bmatrix} \quad (2.35)$$

The individual matrices are substituted in the diakoptics *final equation of solution* given in (2.31) and computed to obtain the results in column 2 of Table 2.1

2.4.3 Impedance Matrix Method Load flow

The method proposed by Andretich et al [5, 38, 39, 43] is summarized before application to the sample network. For an N-bus network, the matrix for the solution of the original network is a bordered block diagonal (BBD) or arrow head matrix shown in Figure 2.8. The impedance matrices of the individual zones or subnetworks which can be built separately are $Z_A, Z_B, Z_C, \dots, Z_N$ and form the block diagonal matrix, Z_1 . Each of these submatrices is full, symmetric and complex. Each column of a subnetwork Z_1 matrix corresponds to a bus in that subnetwork. The elements of Z_2 are selected from Z_1 and are sparse. The Z_4 intersection matrix which is the backbone of diakoptics is the means by which effects are transmitted from one zone to another. The Z_4 is constructed from rows of Z_2 sub-matrices and is also symmetric, complex, and non-sparse.

The method of forming the matrices in Figure 2.8 for the network of Figure 2.5 is illustrated in Figure 2.9. Where z_A and z_B represent elements of impedance matrices of subnet A and subnet B , respectively. The cumbersome steps in forming the solution matrix is removed by using admittance matrices and connection matrices in other methods. The method of solution is illustrated in the following steps with actual values of the network. The admittance matrices of the subnetworks in (2.25) are inverted to yield the impedance matrix in (2.37). The complete equation for computation of node voltages is stated by (2.36). Numerical values substituted are given in (2.37).

V_{A1}	=	Z_{A11}	Z_{A12}	Z_{A13}	·	·	Z_{A11-0}^*	Z_{A13-0}	I_{A1}
V_{A2}		Z_{A21}	Z_{A22}	Z_{A23}	·	·	Z_{A21-0}	Z_{A23-0}	I_{A2}
V_{A3}		Z_{A31}	Z_{A32}	Z_{A33}	·	·	Z_{A31-0}	Z_{A33-0}	I_{A3}
V_{B1}		·	·	·	Z_{B11}	Z_{B12}	$0-Z_{B12}$	$0-Z_{B11}$	I_{B1}
V_{B2}		·	·	·	Z_{B21}	Z_{B22}	$0-Z_{B22}^*$	$0-Z_{B21}$	I_{B2}
e_{b1}^*		Z_{A11-0}	Z_{A21-0}	Z_{A31-0}	$0-Z_{B12}$	$0-Z_{B22}$	$(Z_{A11-0})-$ $(0-Z_{B22})$ $+Z_{b1}$	$(Z_{A13-0})-$ $(0-Z_{B21})$	i_{b1}
e_{b2}^*		Z_{A13-0}	Z_{A23-0}	Z_{A33-0}	$0-Z_{B11}$	$0-Z_{B21}$	$(Z_{A31-0})-$ $(0-Z_{B12})$	$(Z_{A33-0})-$ $(0-Z_{B11})$ $+Z_{b2}$	i_{b2}

(2.36)

	=	A1 cut1	A2	A3 cut2	B1 cut2	B2 cut1	$b_1=A_1B_2$	$b_2=A_3B_1$	I_T
V_{A1}		0.6250	0.2500	0.1250	·	·	0.625	0.1250	1
V_{A2}		0.2500	0.5000	0.2500	·	·	0.25	0.2500	0
V_{A3}		0.1250	0.2500	0.6250	·	·	0.125	0.6250	1
V_{B1}		·	·	·	0.6667	0.3333	-0.3333	-0.6667	0
V_{B2}		·	·	·	0.3333	0.6667	-0.6667	-0.3333	1
e_{b1}^*		0.6250	0.2500	0.1250	-0.3333	-0.6667	1.2917	0.4583	i_{b1}
e_{b2}^*		0.1250	0.2500	0.6250	-0.6667	-0.3333	0.4583	1.2917	i_{b2}

(2.37)

The cut bus voltages, E_{T0} , without link currents are computed using (2.38)

$$\mathbf{E}_{T0} = \mathbf{Z}_T \mathbf{I}_T \tag{2.38}$$

The vector of differences of voltages, \mathbf{E}_{L0} , across torn subnetworks and the cut branch currents, \mathbf{i}_b are computed using (2.39) and (2.40) respectively.

$$\mathbf{E}_{L0} = \mathbf{Z}_3 \mathbf{I}_T \quad (2.39)$$

$$\mathbf{i}_b = \mathbf{Y}_4 \mathbf{E}_{L0} \quad (2.40)$$

$$\mathbf{I}'_T = -\mathbf{i}_b \quad (2.41)$$

$$\mathbf{E}_{T1} = \mathbf{Z}_2 \mathbf{I}'_T \quad (2.42)$$

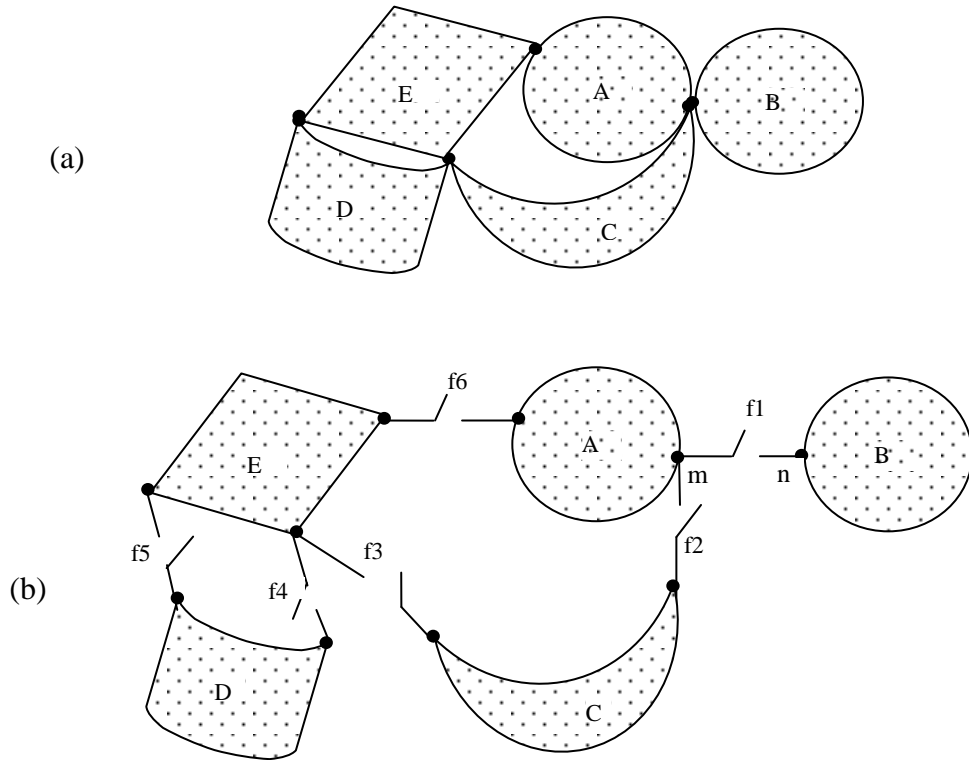
$$\mathbf{E}_T = \mathbf{E}_{T0} + \mathbf{E}_{T1} \quad (2.43)$$

Equation (2.43) computes the required node voltages for the complete network and the results are shown in column 3 of Table 2.2.

2.4.4 *Large Change Sensitivity*

Large change sensitivity (LCS) is a sensitivity analysis for determination of a system response when the parameters are subject to changes that are not necessarily small [59]. When a network is torn, there is a change in the parameters of the original network. Through LCS, the influence of tearing, which is the disturbance in this case, on the original network can be employed in the transformation of solutions of subnetworks into the solution of the original network [15].

The diakoptic algorithm presented in [9, 15] is summarized in this section. The algorithm is based on large change sensitivity (LCS) and is applicable to linear and nonlinear systems. Figure 2.11a represents a large nonlinear network. The network is torn by cutting buses instead of lines. Ideal switches, f1–f6, are inserted at the points of tear. This is equivalent to connecting a bus to itself by a line of zero impedance [38]. When the switches are closed the network is as if it is not torn; when the switches are open the network is torn into pieces as shown in Figure 2.11b. The resultant equations can be solved separately which is ideal for parallel computing. Each subnetwork in Figure 2.11b is assumed to contain a common reference node which for simplicity can be described by the nonlinear vector equation in (2.44).



(a) Original network (b) Network torn with ideal switches

Figure 2.11. A large nonlinear network

$$g_l y_l = 0 \quad l = 1, 2, 3, \dots, M \quad (2.44)$$

where y_l are independent variables representing nodal voltages in this case. It may also represent branch currents in some analysis. Both vectors g_l and y_l have the same dimension N_l . N represents the number of nodes or meshes in the network, l is the particular subnetwork considered, that is, the network identifier, and M is the total number of subnetworks which, for the system in Figure 2.11, is five.

Considering subnetworks A and B in Figure 2.11 connected by an ideal switch, f , Figure 2.10 then represents the subnetworks originally connected by a common bus. In this case it is node tearing instead of branch tearing. When the switch is closed the network is one piece and when it is open, the network splits into two at the nodes. If the voltage at node m is V_m , and the voltage at n is V_n , then the equation at the boundary buses can be represented by (2.45).

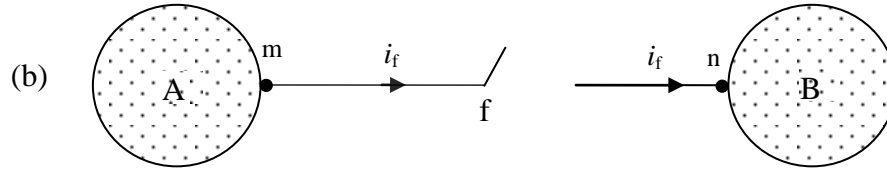


Figure 2.12 Effect of ideal switch

$$(e_{mA} - e_{nB})F + (F-1)i_f = 0 \quad (2.45)$$

where e_m is an element of the vector y_1 , e_n is an element of y_2 and i_f is an additional variable due to the opening of switch.

When the switch is open the value of F is 0 and when the switch is closed F is 1. All switches are assumed to operate simultaneously, thus F is a scalar representing the state of all switches. If s is the number of switches used for interconnection then there will be s such equations in (2.45). The system of nonlinear equations for the interconnected network $g(y) = 0$ is solved through the Newton-Raphson iterative process based on:

$$\frac{\partial g(y)}{\partial y} \Delta y = -g(y) \quad (2.46)$$

where Δy is an $s \times 1$ vector of the incremental changes when applied in iterative solution. The Jacobian of the system equation has the following form:

$$\frac{\partial g(y)}{\partial y} = \left[\begin{array}{cccc|c} \frac{\partial g_1}{\partial y_1} & & & & \lambda_1 \\ & \frac{\partial g_2}{\partial y_2} & & & \lambda_2 \\ & & \ddots & & \vdots \\ & & & \frac{\partial g_s}{\partial y_s} & \lambda_s \\ \hline F_1 & F_2 & \cdots & F_s & (F-1)\tau \end{array} \right] \quad (2.47)$$

where

$$\mathbf{y} = \begin{bmatrix} y_1 \\ y_2 \\ \vdots \\ y_s \\ i_f \end{bmatrix}, \quad (2.48a)$$

$$\mathbf{g}(\mathbf{y}) = \begin{bmatrix} g_1(y_1) + \lambda_1 i_f \\ g_2(y_2) + \lambda_2 i_f \\ \vdots \\ g_s(y_s) + \lambda_s i_f \\ \sum_{i=1}^s F \lambda_i^T y_i + (F-1)\tau i_f \end{bmatrix} \quad (2.48b)$$

$$\mathbf{i}_f = \begin{bmatrix} i_1 \\ i_2 \\ \vdots \\ i_t \end{bmatrix} \quad (2.48c)$$

The element c_{mf} of the incidence matrix λ_i is as follows:

$$c_{mf} = \begin{cases} 1 & \text{if } i_f \text{ is directed out of the node } m \\ -1 & \text{if } i_f \text{ is directed into node } m \\ 0 & \text{if } i_f \text{ is not flowing in or out of node } m \end{cases}$$

When the switches are all open, $F=0$, equation (2.46) can be represented by (2.49).

$$\mathbf{T}_0 \mathbf{X}_0 = \mathbf{W}_0 \quad (2.49)$$

where

$$\mathbf{T}_0 = \frac{\partial \mathbf{g}(\mathbf{y}^k)}{\partial \mathbf{y}} \Big|_{F=0} = \begin{bmatrix} \frac{\partial g_1}{\partial y_1} & & & & \lambda_1 \\ & \frac{\partial g_2}{\partial y_2} & & & \lambda_2 \\ & & \ddots & & \vdots \\ & & & \frac{\partial g_s}{\partial y_s} & \lambda_s \\ & & & & -\tau \end{bmatrix} \quad (2.50)$$

and

$$\mathbf{X}_0 = \Delta \mathbf{y}^k \Big|_{F=0} \quad (2.51)$$

$$\mathbf{W}_0 = -\mathbf{g}(\mathbf{y}^k) \Big|_{F=0}$$

$$\mathbf{T}_0^{-1} = \begin{bmatrix} \left(\frac{\partial \mathbf{g}_1}{\partial \mathbf{y}_1}\right)^{-1} & & & \left(\frac{\partial \mathbf{g}_1}{\partial \mathbf{y}_1}\right)^{-1} \lambda_1 \\ & \left(\frac{\partial \mathbf{g}_2}{\partial \mathbf{y}_2}\right)^{-1} & & \left(\frac{\partial \mathbf{g}_2}{\partial \mathbf{y}_2}\right)^{-1} \lambda_2 \\ & & \ddots & \vdots \\ & & & \left(\frac{\partial \mathbf{g}_s}{\partial \mathbf{y}_s}\right)^{-1} \lambda_s \\ & & & & -\tau \end{bmatrix} \quad (2.52)$$

When the switches are closed, equation (2.46) is defined in (2.53). This is the solution of subnetworks transformation to solution of the original network.

$$\mathbf{TX} = \mathbf{W} \quad (2.53)$$

where

$$\mathbf{T} = \frac{\partial \mathbf{g}(\mathbf{y}^k)}{\partial \mathbf{y}} \Big|_{F=1} = \begin{bmatrix} \frac{\partial \mathbf{g}_1}{\partial \mathbf{y}_1} & & & \lambda_1 \\ & \frac{\partial \mathbf{g}_2}{\partial \mathbf{y}_2} & & \lambda_2 \\ & & \ddots & \vdots \\ & & & \frac{\partial \mathbf{g}_s}{\partial \mathbf{y}_s} \lambda_s \\ \lambda_1^t & \lambda_2^t & \dots & \lambda_s^t & . \end{bmatrix} \quad (2.54)$$

and

$$\mathbf{X} = \Delta \mathbf{y}^k \Big|_{F=1} \quad \mathbf{W} = -\mathbf{g}(\mathbf{y}^k) \Big|_{F=1} \quad (2.55)$$

By applying LCS, the solution vector can be updated as:

$$\mathbf{X} = \mathbf{X}_0 - \mathbf{T}_0^{-1} \mathbf{Uz} \quad (2.56)$$

\mathbf{z} is of dimension $s \times 1$ where s is the number of switches and \mathbf{z} can be obtained from:

$$(\boldsymbol{\tau} - \mathbf{H}^T \mathbf{T}_0^{-1} \mathbf{U}) \mathbf{z} = \mathbf{H}^T \mathbf{X}_0 \quad (2.57)$$

\mathbf{U} and \mathbf{H} define the positions of switches and given by

$$\mathbf{U} = \begin{bmatrix} 0 \\ 0 \\ \vdots \\ 0 \\ \tau \end{bmatrix} \quad (2.58a)$$

$$\mathbf{H} = \begin{bmatrix} \lambda_1 \\ \lambda_2 \\ \vdots \\ \lambda_s \\ \tau \end{bmatrix} \quad (2.58b)$$

From (2.56), the solution of the original network is obtained as:

$$\mathbf{X} = \begin{bmatrix} \mathbf{X}_1 \\ \mathbf{X}_2 \\ \vdots \\ \mathbf{X}_s \\ \mathbf{X}_{s+1} \end{bmatrix} = \begin{bmatrix} \mathbf{X}_{10} \\ \mathbf{X}_{20} \\ \vdots \\ \mathbf{X}_{s0} \\ 0 \end{bmatrix} - \begin{bmatrix} \left(\frac{\partial \mathbf{g}_1}{\partial \mathbf{y}_1} \right)^{-1} \lambda_1 \\ \left(\frac{\partial \mathbf{g}_2}{\partial \mathbf{y}_2} \right)^{-1} \lambda_2 \\ \vdots \\ \left(\frac{\partial \mathbf{g}_s}{\partial \mathbf{y}_s} \right)^{-1} \lambda_s \\ -\tau \end{bmatrix} \mathbf{z} \quad (2.59)$$

Translating equations (2.47), (2.52) and (2.59) for the solution of the sample network as used in [9, 42] gives equation (2.60), (2.61) and (2.62) respectively.

$$\begin{bmatrix} \mathbf{Y}_A & & \mathbf{L}_A \\ & \mathbf{Y}_B & \mathbf{L}_B \\ \mathbf{F.L}_A^t & \mathbf{F.L}_B^t & (\mathbf{F}-\mathbf{1}).\boldsymbol{\tau} \end{bmatrix} \begin{bmatrix} \mathbf{V}_A \\ \mathbf{V}_B \\ \mathbf{i}_f \end{bmatrix} = \begin{bmatrix} \mathbf{I}_A \\ \mathbf{I}_B \\ 0 \end{bmatrix} \quad (2.60)$$

Equation (2.60) represents the network solution, where τ is an identity matrix whose dimensions are equal to the number of switches or cut nodes, s , and F is the state of the switch, that is, whether off or on. In the sample network of Figure 2.5, the subnetworks are connected at two points, so the last row of (2.60) will be two matrices with two rows each. The connection matrices L_A and L_B have dimensions $N_A \times s$ and $N_B \times s$, where N_A and N_B are the total number of nodes in subnet A and subnet B.

$$\begin{bmatrix} \mathbf{V}_{A0} \\ \mathbf{V}_{B0} \\ \mathbf{i}_f \end{bmatrix} = \begin{bmatrix} \mathbf{Y}_A^{-1} & \mathbf{Y}_A^{-1}\mathbf{L}_A \\ & \mathbf{Y}_B^{-1} & \mathbf{Y}_B^{-1}\mathbf{L}_B \\ 0 & & -\tau \end{bmatrix} \begin{bmatrix} \mathbf{I}_A \\ \mathbf{I}_B \\ 0 \end{bmatrix} \quad (2.61)$$

$$\begin{bmatrix} \mathbf{V}_A \\ \mathbf{V}_B \\ \mathbf{i}_f \end{bmatrix} = \begin{bmatrix} \mathbf{V}_{A0} \\ \mathbf{V}_{B0} \\ \mathbf{0} \end{bmatrix} = \begin{bmatrix} \mathbf{Y}_A^{-1} & \mathbf{Y}_A^{-1}\mathbf{L}_A \\ & \mathbf{Y}_B^{-1} & \mathbf{Y}_B^{-1}\mathbf{L}_B \\ \mathbf{L}_A^t & \mathbf{L}_B^t & -\tau \end{bmatrix} \times \begin{bmatrix} \mathbf{0} \\ \mathbf{0} \\ \tau \end{bmatrix} \mathbf{i}_f \quad (2.62)$$

where

$$\mathbf{i}_f = (\mathbf{L}_A^t \mathbf{Y}_A^{-1} \mathbf{L}_A + \mathbf{L}_B^t \mathbf{Y}_B^{-1} \mathbf{L}_B)^{-1} \mathbf{H}^t \mathbf{V}_0 \quad (2.63)$$

$$\mathbf{H}^t = [\mathbf{L}_A^t \quad \mathbf{L}_B^t \quad \tau] \quad (2.64)$$

Equation (2.62) in iterative solution is given in (2.65).

$$\begin{bmatrix} \mathbf{V}_A^k \\ \mathbf{V}_B^k \\ \mathbf{i}_f^k \end{bmatrix} = \begin{bmatrix} \mathbf{V}_{A0}^k \\ \mathbf{V}_{B0}^k \\ \mathbf{0} \end{bmatrix} = \begin{bmatrix} \mathbf{Y}_A^{-1} & \mathbf{Y}_A^{-1}\mathbf{L}_A \\ & \mathbf{Y}_B^{-1} & \mathbf{Y}_B^{-1}\mathbf{L}_B \\ \mathbf{L}_A^t & \mathbf{L}_B^t & -\tau \end{bmatrix} \times \begin{bmatrix} \mathbf{0} \\ \mathbf{0} \\ \tau \end{bmatrix} \mathbf{i}_f^k \quad (2.65)$$

Numerical values for the network of Figure 2.2 were substituted and computed, yielding the results in column 5 of Table 2.2.

2.4.5 *The Multi-Area Thevenin Equivalent (MATE) Concept*

The MATE concept is an extension of the traditional multinode Thevenin which states that, if only N visible nodes from an internal linear system are needed to connect to an external subsystem, then the internal linear system can be represented

by a Thevenin source voltage vector $[\mathbf{E}_{\text{TH}}]_{N1}$ and a Thevenin impedance matrix $[\mathbf{Z}_{\text{TH}}]_{NN}$ with reference to the external system [60, 61]. The solution of this reduced system, voltages and currents in the full internal linear system are then updated by injecting current sources equal to the currents that flow in the links connecting the internal and external systems. MATE allows for the solution of arbitrary number of $[\mathbf{E}_{\text{TH}}]$, $[\mathbf{Z}_{\text{TH}}]$ subsystems. The concise form of the resulting algorithm for a two-subnetwork tearing is given in (2.66). It can be noted that the application is on linear systems.

$$\begin{bmatrix} \mathbf{V}_A \\ \mathbf{V}_B \\ \mathbf{i}_\ell \end{bmatrix} = \begin{bmatrix} \mathbf{Y}_A & & \mathbf{L}_A \\ & \mathbf{Y}_B & \mathbf{L}_B \\ \mathbf{L}_A^t & \mathbf{L}_A^t & -\mathbf{Z}_{\ell 0} \end{bmatrix}^{-1} \begin{bmatrix} \mathbf{I}_A \\ \mathbf{I}_B \\ \mathbf{0} \end{bmatrix} \quad (2.66)$$

The matrices in (2.66) are manipulated in a series of steps that reduce them to Thevenin equivalents; details can be found in [60, 61]. The final equation of solution is obtained as

$$\begin{bmatrix} \mathbf{V}_A \\ \mathbf{V}_B \\ \mathbf{i}_\ell \end{bmatrix} = \begin{bmatrix} \mathbf{Y}_A & & \mathbf{L}_A \\ & \mathbf{Y}_B & \mathbf{L}_B \\ \mathbf{0} & \mathbf{0} & \mathbf{Z}_\ell \end{bmatrix}^{-1} \begin{bmatrix} \mathbf{I}_A \\ \mathbf{I}_B \\ \mathbf{e}_\ell \end{bmatrix} \quad (2.67)$$

where \mathbf{i}_ℓ is the link current vector (e.g. $i_{\ell 1}$ = current in link branch ℓ_1 ($i_\ell = i_b$) in classical diakoptics) and $\mathbf{Z}_{\ell 0}$ is the diagonal impedance matrix of the links' branch equations, which is equivalent to \mathbf{Z}_b in classical diakoptics. Other symbols have the same meanings as above. Expansion of \mathbf{Z}_ℓ in (2.67) gives:

$$\begin{bmatrix} \mathbf{V}_A \\ \mathbf{V}_B \\ \mathbf{i}_{\ell 1} \\ \mathbf{i}_{\ell 2} \end{bmatrix} = \begin{bmatrix} \mathbf{Y}_A & & \mathbf{L}_A & \\ & \mathbf{Y}_B & \mathbf{L}_B & \\ 0 & 0 & z_{\ell 11} & z_{\ell 12} \\ 0 & 0 & z_{\ell 21} & z_{\ell 22} \end{bmatrix}^{-1} \begin{bmatrix} \mathbf{I}_A \\ \mathbf{I}_B \\ \mathbf{e}_{\ell 1} \\ \mathbf{e}_{\ell 2} \end{bmatrix} \quad (2.68)$$

Other variables are defined in equations (2.69) – (2.72).

$$\mathbf{Z}_\ell = \mathbf{L}_A^t \mathbf{Y}_A^{-1} \mathbf{L}_A + \mathbf{L}_B^t \mathbf{Y}_B^{-1} \mathbf{L}_B + \mathbf{Z}_{\ell 0} \quad (2.69)$$

$$\mathbf{e}_\ell = \mathbf{Y}_A^t \mathbf{e}_A + \mathbf{Y}_B^t \mathbf{e}_B \quad (2.70)$$

$$\mathbf{e}_A = \mathbf{Y}_A^{-1} \mathbf{I}_A \quad (2.71a)$$

$$\mathbf{e}_B = \mathbf{Y}_B^{-1} \mathbf{I}_B \quad (2.71b)$$

$$\mathbf{i}_\ell = \mathbf{Z}_\ell^{-1} \mathbf{e}_\ell \quad (2.72)$$

Equations of the subnetworks are modified by the link currents, \mathbf{i}_ℓ , that is,

$$\mathbf{i}^A = \mathbf{I}_A - \mathbf{L}_A \mathbf{i}_\ell \quad (2.73a)$$

$$\mathbf{i}^B = \mathbf{I}_B - \mathbf{L}_B \mathbf{i}_\ell \quad (2.73b)$$

The complete solution for nodal voltages for each subnetwork is given in equations (2.74) which give the solution of the original network.

$$\mathbf{V}_A = \mathbf{Y}_A^{-1} \mathbf{i}_A \quad (2.74a)$$

$$\mathbf{V}_B = \mathbf{Y}_B^{-1} \mathbf{i}_B \quad (2.74b)$$

Substituting numerical values in (2.68) gives (2.75). The impedance matrix, \mathbf{Z}_ℓ , and voltage vector, \mathbf{e}_ℓ , in (2.75) are computed using (2.69) and (2.70). The results are shown in column 3 of Table 2.2.

v_{A1}	2	-1	0		1	0	1	(2.75)	
v_{A2}	-1	3	-1		0	0	0		
v_{A3}	0	-1	2		0	1	1		
v_{B1}				2	-1	0	-1		0
v_{B2}				-1	2	-1	0		1
$i_{\ell 1}$	0	0	0	0	0	2.2917	0.4583		0.0833
$i_{\ell 2}$	0	0	0	0	0	0.4583	2.2917	0.4167	
				↓		↓			
				\mathbf{Z}_ℓ		\mathbf{e}_ℓ			

Table 2.2 Results of node voltages obtained from different diakoptic methods

Nodes	One-Piece Nodal analysis (V)	Classical diakoptics (V)	Impedance matrix load flow (V)	Large Change Sensitivity (V)	Multiarea Thevenin equivalents (V)
VA1	0.7273	0.7273	0.7273	0.7429	0.7273
VA2	0.4545	0.4545	0.4546	0.4286	0.4545
VA3	0.6364	0.6364	0.6364	0.5428	0.6364
VB1	0.4545	0.4545	0.4545	0.5429	0.4545
VB2	0.7272	0.7272	0.7273	0.7428	0.7273

2.4.6 *Deductions*

The results obtained in for the linear network tend to agree with the conclusions by Sasson in [5] that Diakoptics being an algebraic process is most effective in linear problems and can be applied to nonlinear problems if the problem is broken into a sequence of linear problems. This is evident especially in the Multi-area Thevenin equivalent (MATE) method.

2.5 **Advantages of Diakoptics in Multicomputer Configuration**

An important benefit of diakoptics is that multicomputer configurations [62] also known as parallel computing can be exploited for speed, *information security, processing power and real-time constraints with minimum investments* in the power network [16]. This ‘division of labour’ will greatly reduce the burden at the centre. Each computer in Figure 2.13 handles a subnet which may be an area in a network. The subnetworks can also be regional power networks located far apart. The coordinating CPU may be the control centre where analysis of all other utilities are coordinated or an extra computer to modify the solutions of the subnetworks to give the solution of the complete network. The computers can be physically next to each other or kilometres apart.

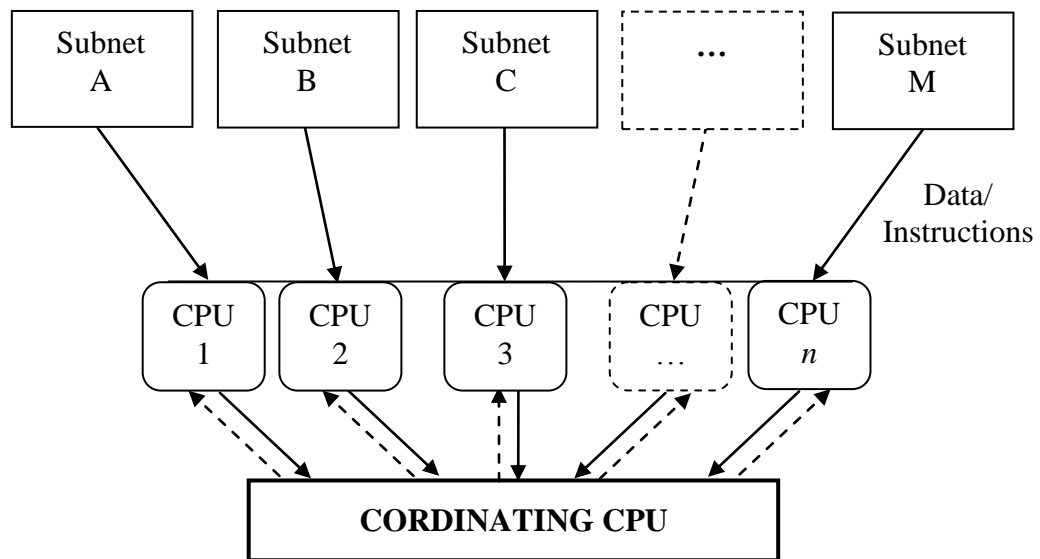


Figure 2.13. Multicomputer configurations for diakoptics

2.6 Influence of Wind energy on Weak Grids

The influence of wind energy on the steady-state voltage of the grid is summarized below. It is recommended that the change in voltage at point of common coupling (PCC) of wind generation should not exceed 2%; this is adopted in Germany. This is part of the recommendations for connection of wind to the grid [63, 64].

2.6.1 *Steady-state Voltage level*

As already stated in section 1.3, the main problem with wind energy in weak grids is the variation of steady-state voltage [65] and is the main design criterion for connection of wind turbines to the grid especially the medium voltage system. In a grid without wind energy, the normal voltage profile for a feeder is that the highest voltage is at the bus bar at the substation and it drops as the distance increases until the end where the highest drop is experienced as shown in Figure 2.14. The voltage profile when wind turbines are connected to the same feeder as consumers is much different from the no wind case and is illustrated in Figure 2.15 for different wind scenarios and loading [45].

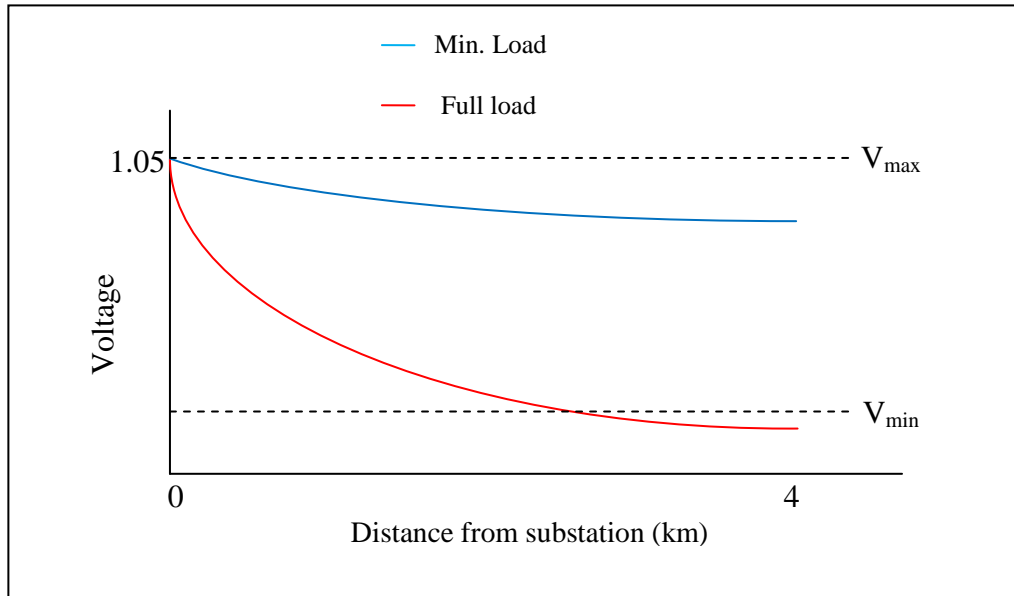


Figure 2.14 Voltage Profile of a feeder without wind

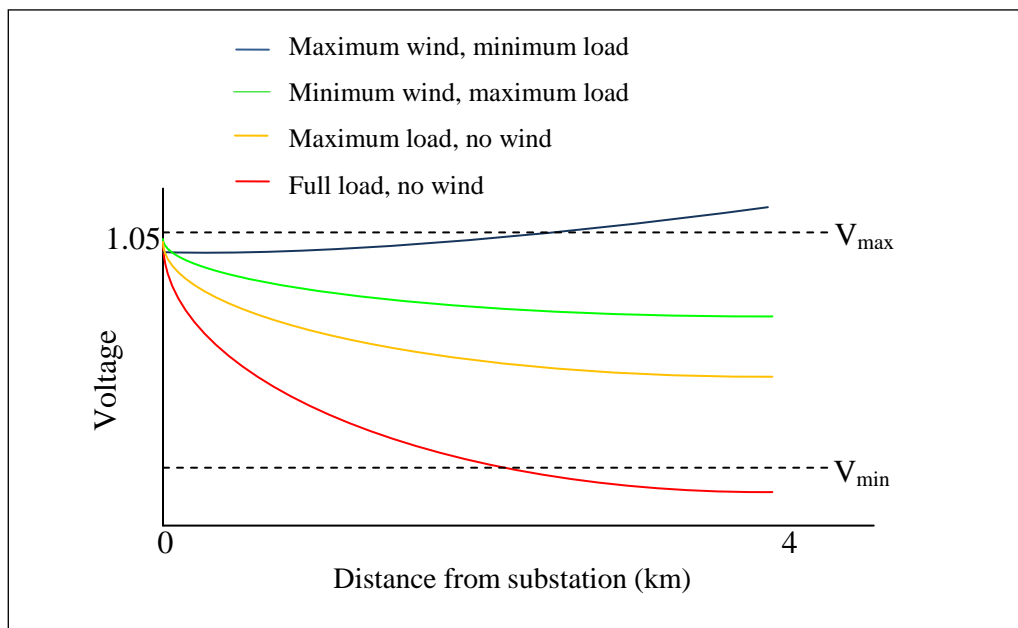


Figure 2.15 Voltage profile of a feeder with wind energy

Due to the power production at the wind turbine the voltage level in most cases will be higher than in the no wind case and can exceed the maximum allowed when the consumer load is low and the power output from the wind turbines is high. This is what limits the capacity of the feeder or grid [44, 45, 66, 67]. The voltage profile depends on the line or grid impedance, the point of common coupling or connection

(PCC), the wind power production and the consumer load. The impact of wind turbines on an existing grid is mainly local, that is, the effect is felt in the areas close to the PCC [68].

If the load demand in the no wind case is low, the voltage level usually exceeds the maximum limit.

2.6.2 *Change in voltage Level*

Most of the grids where wind energy has enjoyed some level of success involve strong or “stiff” grids, but weak grids have peculiar challenges. In many practical situations, the expected steady-state voltage change due to the operation of the wind turbines (WTs) are the most important criterion in determining the required grid reinforcements. It depends on the impedance at the PCC.

The best solution for the determination of the steady-state voltage change caused by WT's would be a load flow calculation and the general method is an extreme values deterministic approach where only the maximum voltage change at the PCC is computed [69, 70]. The following formula can be applied:

$$\Delta V = \frac{S_w}{S_k} \cos(\psi - \phi) \quad (2.76)$$

where ΔV is voltage change at the PCC, S_k is the network short circuit capacity at the PCC, ψ is the angle of the network impedance at the PCC. S_w is the WT rated capacity and ϕ is the respective power factor angle at rated power. If the wind generator operated at unity power factor (i.e. $Q = 0$), then the voltage rise in a lightly loaded radial circuit is given approximately by:

$$\Delta V = V - V_0 = \frac{PR}{V_0} \quad (2.77)$$

When the generator is operated at a leading power factor when reactive power is absorbed it reduces the voltage rise. The voltage rise in pu is given by [2]:

$$\Delta V = V - V_0 = \frac{(PR - QX)}{V_0} \quad (2.78)$$

The impedance of 33kV and 11kV distribution circuit may, typically, have a ratio of inductive reactance to resistance (X/R) ratio of 2. An uncompensated induction generator at rated output, typically, has a power factor of 0.89 leading, that is, $P = -2Q$ [71]. Thus, under these conditions, there is no apparent voltage rise in the circuit at full power. However the real power loss (w) in the circuit is given approximately by:

$$w = \frac{(P^2 + Q^2)R}{V_o^2} \quad (2.79)$$

The reactive power drawn by the generator acts to limit the voltage rise but higher real power losses are incurred in the connecting circuit. Equations (2.76) - (2.79) are approximations only and do not apply to heavily loaded circuits. A simple but precise calculation for voltage rise in any radial network may be carried out by conducting a load flow.

2.6.3 *Reactive power effects*

All wind farms consume reactive power in one form or the other (even wind turbines that produce at unity power consume reactive power in other areas) and at the same time feed reactive power to the grid. These two factors reduce the power factor at the conventional power stations. At the primary side of wind farm substations, the wind farms affect the reactive power of:

- wind turbine themselves, especially wind turbines with directly grid connected induction generators;
- step-up transformers between wind turbines and wind farms feeders;
- wind farm feeders;
- substation transformers.

2.7 **Per Unit System**

The per unit system used mostly in this thesis is a means of carrying out network calculations in power system analysis without expressing the quantities in their actual

volts, amperes, or ohms by using the per unit (p.u.) system. The method is well known and widely documented; some can be found in references [72-76] on which the following analysis is based.

In the per unit system, quantities are expressed as a fraction of a reference value commonly known as the base. There are four base quantities - base volts, base amperes, base voltamperes, and base ohms. They are closely related so choosing base values for any two of them determines the base values of the remaining two. The basic relationship of the per unit system is given in (2.80) and if the value is required in percent, (2.92) is used.

$$\text{per unit quantity} = \frac{\text{actual quantity}}{\text{base quantity}} \quad (2.80)$$

$$\text{percent quantity} = \frac{\text{actual quantity}}{\text{base quantity}} \times 100 \quad (2.81)$$

where “actual quantity” refers to the given values in ohms (Ω), amperes (A), volts (V) and voltamperes (VA), etc. In the following discussion, the subscript “pu” will indicate a per unit value, the subscript “base” will indicate a base value and quantities without subscripts represent the actual values and I, Z, V and S have their usual meanings, where $S = P + jQ$.

If the four base quantities are known, the per unit quantities are defined in equations (2.82a).

$$I_{\text{pu}} = \frac{I}{I_{\text{base}}} \quad (2.82a)$$

$$V_{\text{pu}} = \frac{V}{V_{\text{base}}} \quad (2.82b)$$

$$S_{\text{pu}} = \frac{S}{S_{\text{base}}} \quad (2.82c)$$

$$Z_{\text{pu}} = \frac{Z}{Z_{\text{base}}} \quad (2.82d)$$

2.7.1 *Basic Procedure in Per Unit System*

Analysis in per unit is generally achieved by following some basic steps:

- Selection of a base value.
- Conversion of actual quantities to their per unit values by dividing by the base value.
- Performing calculations using the per unit values.
- There may be a need to change a per unit value on one base to a per unit value on another base; this will be done during the calculations.
- The results in per unit would be converted to actual values if required.

2.7.2 *Selecting Base Values*

The most important requirement of the per unit system is that correct answers should be obtained as it would be if actual values were used in the calculations. The common practice is to assign base values to kVA and voltage and they should satisfy the fundamental laws of electricity and the foundational equation is the ohms law represented in (2.83).

$$I_{\text{base}} = \frac{V_{\text{base}}}{Z_{\text{base}}} \quad (2.83)$$

Generally in power system analysis, the preferred base voltage is the nominal system voltage at one point in the system and MVA can be the MVA rating of one of the predominant pieces of system equipment, such as a generator or a transformer; but usual practice is to choose a convenient round number such as 10 for the base MVA. The advantage of this round number is that there is a sharing of common characteristics especially when several studies are made. On the other hand, choosing the MVA of one the equipment means that conversion to new base is not required for at least one piece of equipment [72]. Base amperes and base ohms are then determined for each voltage level in the system.

Where two or more systems with different voltage levels are interconnected through transformers, the MVA base is common for all systems; but the base voltage of each system is determined by the primary and secondary voltages of the transformer

connecting the systems. Base ohms and base amperes will thus be correspondingly different for systems of different voltage levels. Once the system quantities are converted to per unit values the various systems with different voltage levels can be treated as a single system. It is only when reconverting the per unit values to actual voltage and current values that the different base voltages exist throughout the system.

It is important to note that all base values are only magnitudes and not associated with any angle but per unit values are phasors. The phase angles of the current and voltages and the power factor of the circuit are not affected by conversion to per unit values.

2.7.3 *Three-Phase System*

For a three-phase system, the impedance is in ohms per phase and the base MVA is the three-phase value. The base impedance and base current are related by (2.84) and (2.85a). The nominal line-to-line system voltages are the usual base values. The derived values of the remaining two quantities are:

$$I_{\text{base}} = \frac{S_{\text{base}}}{\sqrt{3} V_{\text{base}}} \quad (2.84)$$

$$Z_{\text{base}} = \frac{V_{\text{base}}^2}{S_{\text{base}}} \quad (2.85a)$$

$$Z_{\text{base}} = \frac{V_{\text{base}}^2}{VA_{\text{base}}} \quad (2.85b)$$

or

$$Z_{\text{base}} = \frac{kV_{\text{base}}^2}{MVA_{\text{base}}} \quad (2.86)$$

2.7.4 *Single Phase System*

For single phase systems (2.87) and (2.88a) are used:

$$I_{\text{base}} = \frac{S_{\text{base}}}{V_{\text{base}}} \quad (2.87)$$

$$Z_{\text{base}} = \frac{V_{\text{base}}^2}{S_{\text{base}}} \quad (2.88a)$$

$$Z_{\text{base}} = \frac{V_{\text{base}}^2}{\text{VA}_{\text{base}}} \quad (2.88b)$$

$$Z_{\text{base}} = \frac{\text{kV}_{\text{base}}^2}{\text{kVA}_{\text{base}}} \times 10^3 \quad (2.88c)$$

$$Z_{\text{base}} = \frac{\text{kV}_{\text{base}}^2}{\text{MVA}_{\text{base}}} \quad (2.88d)$$

On a single phase basis:

$$I_{\text{base}} Z_{\text{base}} = \frac{V_{\text{LL}}}{\sqrt{3}} \quad (2.89)$$

where the subscript “LL” indicates line value and

S_{base} = apparent power base in voltamperes (VA)

I_{base} = current base in amperes (A)

V_{base} = voltage base in volts (V)

2.7.5 *Change of Base*

Occasionally, the need arises to convert a per unit value on a different base to another base. For example, on a transformer nameplate, per cent impedance is normally given using the transformer full load VA as the base. Thus the transformer Z must be converted to the VA_B being used in the study. Equation (2.90) is the requirement for the conversion.

$$Z_{\text{pu}(1)} Z_{\text{base}(1)} = Z_{\text{pu}(2)} Z_{\text{base}(2)} \quad (2.90)$$

$$Z_{pu(2)} = Z_{pu(1)} \frac{Z_{base(1)}}{Z_{base(2)}} \quad (2.91)$$

where Z_{1pu} is the per unit value to be changed and Z_{2pu} is the new per unit value after changing the base. Using (2.88a), equation (2.91) becomes:

$$Z_{pu(2)} = Z_{pu(1)} \frac{\left(\frac{(V_{base(1)})^2}{S_{base(1)}} \right)}{\left(\frac{(V_{base(2)})^2}{S_{base(2)}} \right)} \quad (2.92)$$

Equation (2.92), can be rewritten as:

$$Z_{pu(2)} = Z_{pu(1)} \left(\frac{V_{base(1)}}{V_{base(2)}} \right)^2 \left(\frac{S_{base(2)}}{S_{base(1)}} \right) \quad (2.93)$$

2.7.6 Advantages of the per unit system

The basic advantages of the per unit system are:

- The values of various components lie within a narrow range regardless of equipment rating.
- The need for $\sqrt{3}$ in calculations is removed which is particularly use star and delta quantities in balanced three-phase systems.
- Impedances of a network can simply be added together irrespective of different voltage levels in the system
- It simplifies computer simulations

2.8 Important Considerations for Wind Integration

2.8.1 Strength of Grid

Electrical grid is an interconnected complex structure consisting of power sources, transmission and subtransmission networks, distribution networks and a variety of

energy consumers. It can be categorized as weak or strong based on the short-circuit level, and it can be inductive or resistive based on the network impedance phase angle (ψ).

The grid impedance as seen by the wind turbine induction generator, among other factors, is an indication of the ‘strength’ of a network. If the network is strong the impedance will be small, leading to a large short-circuit level. On the other hand, a weak system will have large impedance and low short-circuit level. The grid impedance is therefore very important and has to be taken into account in order to draw valid conclusions. A strong network would likely resist voltage changes when wind power is integrated to it.

For distribution networks, resistance effects are more apparent than at the transmission or subtransmission level with the X/R ratio ranging from typically 10 for transmission networks to 2 for distribution networks [71].

2.8.2 *Point of Common Coupling or Connection*

A very important factor for adding new generation to an existing grid is the point of common coupling or connection (PCC). Grid Codes demand requirements are at the PCC and not at the individual wind turbine generator terminals. The definition of PCC in IEEE 519 arose out of the need to reduce distortions caused by power electronic equipment on the power system so as to increase the quality of power delivered to consumers. The PCC is defined as “*a point of metering, or any point as long as both the utility and the consumer can either access that point for direct measurement of the harmonic indices meaningful to both or can estimate the harmonic indices at point of interference (POI) thorough mutually agreeable methods. Within an industrial plant, the PCC is the point between the nonlinear load and other loads.*” [77]. The definition has been interpreted in many ways and in some cases misapplied [78].

The PCC could be between an existing network and a generator, another network or a wind farm, and therefore determines the effect of the incoming component on the existing network. In relation to wind power, the PCC is the point in the network most affected by the connection of a wind farm to the network and reflects the condition of

that network. Impedance which is a major determinant of the state of a grid is usually determined at the PCC.

2.8.3 *Short-Circuit level*

The short-circuit level at the PCC is a measure of the strength of a network and particularly aids the prediction of voltage change in the network. The lower the short circuit level the higher the voltage change ΔV at the PCC when a new source is connected to the grid [44, 79].

In a balanced three-phase system, the short-circuit level is defined as $S_k = \sqrt{3}V_0 I_{sc}$, where V_0 is the line voltage and I_{sc} is the short-circuit current, but is often calculated as $S_k = V_0^2 / Z^*$. A low short-circuit level therefore implies a high network source impedance, Z , and an indication of a grid whose voltage would easily vary with the level of power injected at the PCC. A network is said to be weak if the short-circuit ratio, S_k/S_w , is less than 25 and strong if it is greater than 25 [80].

2.8.4 *Impedance angle (ψ)*

Transmission grids are mostly inductive with a network impedance of angle typically between 55° and 85° . Large wind farms are usually connected to such networks. Smaller wind farms are generally connected to distribution grids that are more resistive with ψ ranging from 25° to 55° [80].

2.9 **Weak Grid**

Weak grids are often found in remote places where feeders are long and operated at medium voltage. Such grids are designed for relatively small loads [45]. The definition of an electrically weak grid can be applied to a grid integrated with wind power or a grid without wind energy. The behaviour of or expectations from a grid under these two conditions are slightly different [45]. A weak grid can therefore be defined under the following headings:

a) Generally

A weak grid is one in which the power flows (P and Q) in the network are likely to cause significant voltage fluctuations and change in voltage levels at that point

considering the load and production cases. That is, the grid impedance is an important determining factor in drawing valid conclusions.

b) Without wind energy

A weak is such that when the rated load is exceeded, there is a drop in voltage and/or the thermal limits may be exceeded.

c) With wind energy

In wind integrated network, it can be defined as one where the amount of wind energy that can be integrated at the PCC is limited by the grid capacity (or impedance) and not necessarily by the operating limits of the conventional generation or the thermal limits of the grid.

2.10 Voltage Variation Due to Wind Integration

A number of factors determine the level of wind energy that can be integrated into a grid but the key design factor is the steady-state voltage variation of the grid [81, 71, 70]. The permitted voltage change, ΔV , at the PCC is usually required to be less than 2% of nominal voltage [69]. Variations in the steady-state voltage at the PCC influence the performance of a wind farm and losses in the induction generators. A wind farm can operate from no load to full load and may be located at any point in the network. For low voltages, the no-load losses decrease slightly due to reduced iron losses, whereas the full-load losses increase due to increased currents in the generator windings [67].

If the output from a distributed wind turbine generator is absorbed locally by an adjacent load the effect on the distribution network voltage and losses is likely to be beneficial. However, if it is necessary to transport the power through the distribution network, increased losses may occur and slow voltage variations (ΔV) may become excessive. The PCC is the meeting point between the wind farm and the electrical grid. The grid, seen from the PCC, can be modelled as a stiff voltage source in series with an impedance Z . The major network components in the impedance path between the wind farm and grid are transformers, underground cables and overhead lines.

Consider Figure 2.14 which represents the grid connection of a wind farm. The impedance Z represents loads, all transmission lines, cables and transformers feeding the grid and V is the voltage at the PCC while V_0 is the nominal voltage of the grid. S_k is the short circuit capacity at the PCC. The higher the voltage deviation (ΔV) at the PCC, the lower the short circuit capacity (S_k) and therefore the lower the ability of a grid to absorb wind energy.

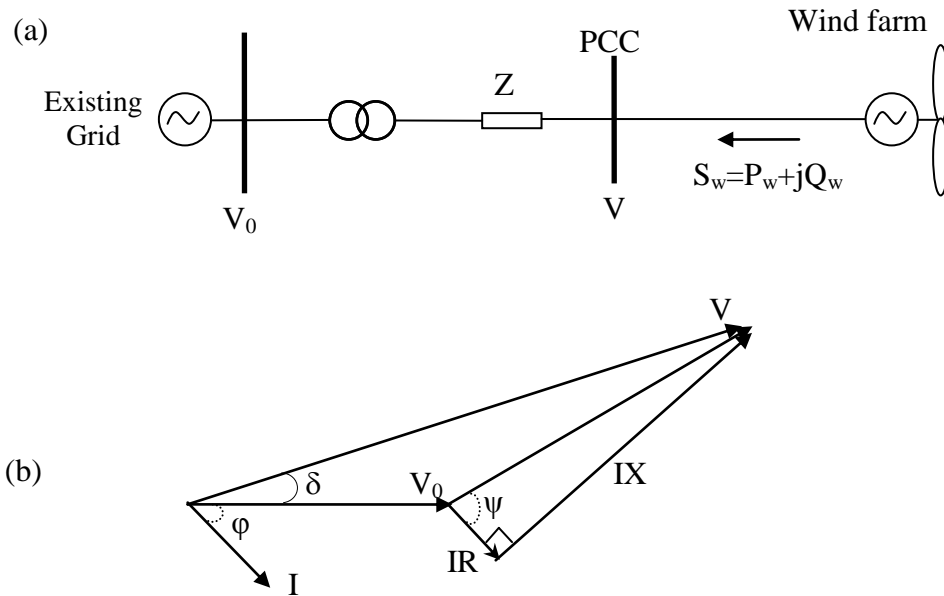


Figure 2.16. Grid connection of a wind farm

2.10.1 Determination of Voltage Variation and Short-circuit ratio in a Weak Grid

In a weak grid the short circuit ratio and voltage change of the grid can be derived from

Figure 2.17 and basic power analysis equations derived from [80]. Assuming the production P , Q and the network parameters are known, where V is the voltage at the supply point and V_0 is the voltage at any point under consideration, then

$$V = V_0 + (R + jX)I \tag{2.94}$$

Recall: $S = VI^*$

$$I = \frac{S^*}{V^*} = \frac{P - jQ}{V^*} \quad (2.95)$$

Combining (2.94) and (2.95) yields:

$$VV^* = V_o V_o^* + (R + jX)(P - jQ) \quad (2.96)$$

Also,

$$V = |V|e^{j\delta} = |V|(\cos \delta + j \sin \delta) \quad (2.97)$$

Substituting for V in (2.97) yields:

$$|V|^2 = V_o |V| = |V| \cos \delta + PR + QX + j(PX - QR - V_o V \sin \delta) \quad (2.98)$$

If V_o is assumed to be real, then $PX - QR - V_o V \sin \delta = 0$. Therefore,

$$\cos \delta = \frac{\sqrt{(V_o |V|)^2 - (PX - QR)^2}}{V_o |V|} \quad (2.99)$$

From (2.98) and (2.99):

$$|V|^2 = \left[(V_o |V|)^2 - (PX - QR)^2 \right]^{\frac{1}{2}} + (PR + QX) \quad (2.100)$$

Solving for $|V|$ in (2.100):

$$|V|^2 - (PR + QX) = \left[(V_o |V|)^2 - (PX - QR)^2 \right]^{\frac{1}{2}} \quad (2.101)$$

$$|V|^4 - 2|V|^2(PR + QX) + (PR + QX)^2 - (V_o |V|)^2 + (PX - QR)^2 = 0 \quad (2.102)$$

$$(|V|^2)^2 - [2(PR + QX) + (V_o)^2]|V|^2 - [(PR + QX)^2 + (PX - QR)^2] = 0 \quad (2.103)$$

$$|V|^2 = \frac{[V_o^2 + 2(PR - QX)] \pm \sqrt{[(PR + QX) - V_o]^2 - 4[(PR + QX)^2 + (PX - QR)^2]}}{2} \quad (2.104)$$

$$\therefore |V| = \left\{ \frac{V_o^2 + 2(RP + QX) + [V_o^4 + 4(RP + QX)V_o^2 - 4(XP - RQ)^2]^{\frac{1}{2}}}{2} \right\}^{\frac{1}{2}} \quad (2.105)$$

The voltage change at the PCC is obtained as:

$$\Delta V = |V| - |V_0| \quad (2.106)$$

Voltage change as a function of the network impedance is

$$\tan \psi = \frac{X}{R} \quad (2.107)$$

The short-circuit ratio is

$$S_r = \frac{S_k}{S_w} = \frac{V_0^2}{\sqrt{R^2 + X^2}} \bigg/ \frac{1}{\sqrt{P^2 + Q^2}} = \frac{V_0^2}{\sqrt{R^2 + X^2}} \cdot \frac{1}{\sqrt{P^2 + Q^2}} \quad (2.108)$$

2.10.2 *Reactive power control*

Whether motoring or generating, the induction machine consumes reactive power because of the magnetizing reactance, and the system must supply this. There is therefore a need for reactive power compensation at the terminal of the induction generator. The level of compensation depends on the loading condition, being a maximum at no load and reducing at full load.

The steady-state voltage deviations may be kept within acceptable limits by controlling the reactive power flow and its effectiveness depends on the network short circuit ratio, S_r , and the impedance angle, ψ . To maintain zero voltage deviation in network with ψ up to 55° , relatively high reactive power compensation is required. Hence, in resistive grids (i.e. distribution grids), reactive power compensation is a less effective measure to control the voltage. Networks with larger impedance angles ($70 - 85^\circ$) require smaller amounts of reactive power to maintain zero voltage deviation. An exception is the extreme case of $S_k/S_w=1$ and $\psi=85^\circ$, where a power factor of 0.87 (capacitive) is required. Otherwise the power factor required is between unity and 0.95.

The reactive power required to maintain a specific voltage is

$$Q = \frac{1}{R^2 + X^2} \left\{ |V|^2 X - \left[|V|^2 (2RP + V_0^2)(R^2 + X^2) - |V|^4 R^2 - P^2 (R^2 + X^2) \right]^{1/2} \right\} \quad (2.109)$$

2.11 Voltage Variation in a Strong Grid

At high S_k/S_w , (above 25) that is for a strong grid, the voltage deviation can be reasonably approximated by:

$$\Delta V \approx \frac{PR + QX}{V_0} \quad (2.110)$$

If $X \gg R$ as is often the case, $Q \propto \Delta V$, which means voltage change is directly connected to reactive power flow [82]. The reactive power requirement for maintaining zero voltage deviation for $S_k/S_w > 25$ is thus approximately independent of the network strength and is simply given by the X/R of the network:

$$\frac{S_w}{Q} \approx \frac{X}{R} = -\tan \psi \quad (2.111)$$

The short circuit power, S_k , the PCC can be calculated generally as

$$S_k = \frac{V_0^2}{Z^*} \quad (2.112)$$

2.12 Load Flow Analysis

The best method for determining the steady-state voltage change ΔV caused by the WT is the load flow analysis [45, 64]. Equations for calculating voltage change, ΔV , in a radial network can be used but load flow solution is proposed for this work because it gives a picture of all the situations of the network including the loads and the WT's [47].

Load-flow analysis is at the heart of power systems analysis and forms the basis of other types of analyses. It plays an important role in power system planning during which additions or extensions are decided. It also helps to determine voltages levels during contingency conditions and to identify weak points. In load flow, voltages at all the buses in the system are calculated to get a grip on the state of the system because, once the bus voltages are known, bus powers, bus currents, line flows and line currents can be directly calculated.

2.12.1 Power System Basics

All electric power systems consist of three main stages: generation, transmission, and utilization stages.

- The main component at the generation state is a generator which produces electrical power.
- At the utilization stage are loads that consume the electrical power
- Transmission stage comprises, transmission, lines, transformers, etc that transport electrical power to the loads.

A simple power system is illustrated in Figure 2.17, where G_1 and G_2 are generators, T_1 and T_2 are transformers. The lines connecting the components are the transmission lines. In power system analysis, transmission lines, transformers, shunt capacitors and reactors are considered as static components and are represented by their equivalent circuits consisting of resistance, inductance, and capacitance, that is, the R, L, C elements. The network formed by these elements is viewed as a linear network represented by their impedance matrix or admittance matrix. In load flow calculation, generators and loads are treated as nonlinear components. The categorization is shown in the block diagram of Figure 2.18 adapted from [83].

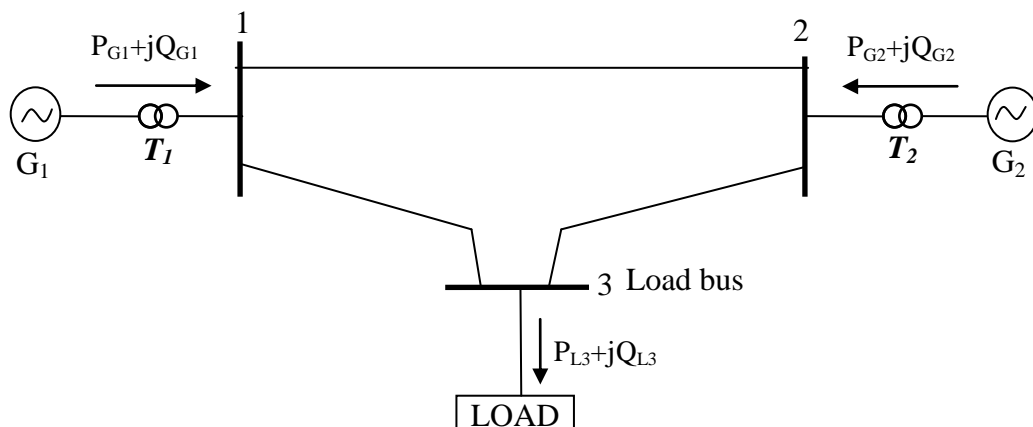


Figure 2.17 Typical power system

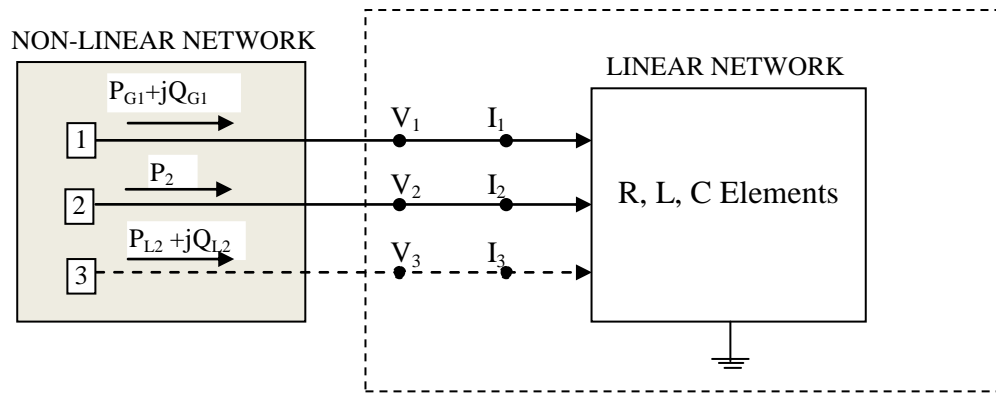


Figure 2.18 Block diagram of the simple power system

2.12.2 Types of Buses

Four possible variables characterize the electrical condition of buses and they are real power P , reactive power Q , voltage magnitude V and voltage angle δ . In load flow analysis, classification of buses is based on the two specified quantities at each bus. Three distinct types of buses are identified as shown in Table 2.2.

Table 2.3 Types of buses and the quantities

Type of Bus	Known Quantities	Unknown quantities
Slack bus ($V\delta$)	V, δ	P, Q
Generator Bus (PV)	P, V	Q, δ
Load Bus (PQ)	P, Q	V, δ

1. Slack bus

A generator bus is chosen to be the slack bus where the nodal voltage magnitude, V and angle δ are specified. It sets the angular reference for all other buses and the angle is usually chosen as 0° . It is expected to compensate for real power and losses that are not known in advance.

2. Generator Bus

This is a bus in which a generating source is connected and the node voltage is controlled by injecting or absorbing reactive energy through the generator excitation.

The generated power P_G and bus voltage V are kept constant; therefore P and V can be specified for this bus which is why the bus is also called P-V bus. Constant voltage operation is only possible when the generator is within its reactive power generation limits.

3. Load bus

In this bus only a load is connected, there is no generator. Any generator connected to a load bus is outside its reactive power limits. The load at this bus is defined by real power P and reactive power Q and so the bus is also referred to as P-Q bus.

2.12.3 Power Flow Equations

The power flow equation can be stated concisely as

$$S_i = V_i I_i^* \quad (i=1, 2, \dots, N) \quad (2.113)$$

For a network with a total of N buses, (2.1) is obtained as:

$$\begin{bmatrix} I_1 \\ I_2 \\ \cdot \\ I_i \\ \cdot \\ I_N \end{bmatrix} = \begin{bmatrix} y_{11} & y_{12} & \cdot & \cdot & \cdot & y_{1N} \\ y_{21} & y_{22} & \cdot & \cdot & \cdot & y_{2N} \\ \cdot & \cdot & \cdot & \cdot & \cdot & \cdot \\ y_{i1} & \cdot & \cdot & \cdot & \cdot & y_{iN} \\ \cdot & \cdot & \cdot & \cdot & \cdot & \cdot \\ y_{N1} & y_{N2} & \cdot & \cdot & \cdot & y_{NN} \end{bmatrix} \begin{bmatrix} V_1 \\ V_2 \\ \cdot \\ V_i \\ \cdot \\ V_N \end{bmatrix} \quad (2.114)$$

Let $Y = G + jB$ denote the admittance matrix of the power system and I_i be the total current injection into any node. I_i is actually the sum of all other nodes that physically connect to i . For any node i , the current is $I_{in} = V_n Y_{in}$. In view of equation (2.114) all nodes that could possibly be connected to i yield the equation,

$$I_i = \sum_{n=1}^N Y_{in} V_n \quad (i=1, 2, \dots, N) \quad (2.115)$$

Therefore,

$$S_i = V_i I_i^* = V_i \sum_{n=1}^N Y_{in} V_n \quad (2.116)$$

$$S_i = \sum_{n=0}^N V_i V_n e^{j(\delta_i - \delta_n)} (G_{ik} - jB_{ik}) \quad (2.117)$$

$$S_i = \sum_{n=1}^N V_i V_n [\cos((\delta_i - \delta_n) + j\sin(\delta_i - \delta_n))] (G_{ik} - jB_{ik}) \quad (2.118)$$

Separating the real and imaginary parts gives

$$\left. \begin{aligned} P_i - \sum_{n \in i}^N V_i V_n (G_{in} \cos \delta_{in} + B_{in} \sin \delta_{in}) \\ Q_i - \sum_{n \in i}^N V_i V_n (G_{in} \sin \delta_{in} - B_{in} \cos \delta_{in}) \end{aligned} \right\} (i = 1, 2, \dots, N) \quad (2.119)$$

$$F(x) = 0 \quad (2.120)$$

$$F(x) = \begin{cases} P_i - \sum_{n \in i}^N V_i V_n (G_{in} \cos \delta_{in} + B_{in} \sin \delta_{in}) \\ Q_i - \sum_{n \in i}^N V_i V_n (G_{in} \sin \delta_{in} - B_{in} \cos \delta_{in}) \end{cases} (i = 1, 2, \dots, N) \quad (2.121)$$

where P_i and Q_i are the active and reactive powers injected at node i respectively, G_{in} is the real part of the element in row i and column n of the admittance matrix while B_{in} is the imaginary part. δ_{in} is the difference in voltage angle between bus i and bus n , that is, ($\delta_{in} = \delta_i - \delta_n$). N is the total number of buses in the system. The power mismatch function can be defined by (2.120), where x is the vector of nonlinear functions consisting of voltage magnitudes and angles.

Equation (2.121) is the system of nonlinear equations usually solved to find the solution of the power/load flow problem. A nonlinear system may have more than one equilibrium point because nonlinear equations generally have more than one solution unlike linear systems. Iterative procedures are commonly used to solve the load flow equations, but like any iterative solution pose some challenges as pointed

out in [84]. There is therefore a strong proposition for direct methods which has led to the development of the *Holomorphic Embedding load flow* method [51]. The classical iterative procedures include Gauss-Seidel, Newton-Raphson, and the Fast Decoupled load flow methods. Other Methods are Fuzzy Logic, Genetic Algorithm application, Particle swarm method and recently the direct load flow method - Holomorphic Load flow analysis.

2.12.4 *Direct methods and Iterative methods in Load Flow solutions*

Problems have been identified with iterative load flow solutions which include the existence of both “*physical and virtual solutions* [85] to the nonlinear equation and subject to ill-conditioning and convergence problems especially in large scale power systems [84, 86]. In view of the above, direct methods are proposed in [51, 85] The holomorphic embedding load flow (HELM) is a direct method reputed to provide an accurate physical solution to the load-flow and advise when one does not exist [85].

Direct methods necessarily require factorization of matrices which is not always necessary in iterative methods. This means that iterative operations can be executed at very high efficiency on most current computer architectures which are designed for iterative rather than for direct methods. Also, iterative methods are usually simpler to implement than direct methods, and since no full factorization has to be stored, they can handle much larger systems than direct methods mainly because of memory constraints. High level parallelism is easier to achieve with iterative solvers than with direct solvers [42, 60].

2.12.5 *Diakoptics in Load Flow Analysis*

The ever increasing size and complexity of power systems imposes great burdens on the usual centralized analyses resulting in large quantities of core storage and high computation times. Tearing the system before the load flow analyses will reduce the core storage and in most cases the computation times. However, a literature survey on load flow analysis of power systems with or without wind integration has shown that the advantages of using the concept of diakoptics in load flow analysis have not been extensively explored.

Diakoptic load flow solutions involve the solution of the load flow equations in (2.119) but instead of solving the whole system as a piece the system, it is torn into subsystems before combining and modifying the solutions to obtain the solution of the original system. The electrical network can be divided into segments, or areas, where an area is defined as a group of buses which may or may not correspond to geographical boundaries or ownership restrictions. When some transmission lines which connect buses are cut so that subnetworks are obtained, this is branch tearing because cutting is done on the lines rather than the buses. Once the network has been divided, the solution process is independent of network size. Various methods have been proposed and some are summarized below.

2.12.6 *Diakoptics in Impedance Matrix Load Flow*

In general, load flow programmes are based on the node impedance matrix or admittance matrix. The diakoptic formulation of the load flow problem had been presented by Andretich et al and extended by others [38, 39, 43]. Their work was based mainly on impedance, Z matrix load flow; the major differences in their works are in the methods of decomposing the system and ordering the system buses after tearing. The impedance matrix load flow method based on diakoptics has been reviewed in section 2.3 and applied mathematically in the linear analysis of the network of Figure 2.5. The currents are updated at each iteration using:

$$I_{n(\text{new})} = I_{n(\text{old})} + \Delta I_n \quad (2.122)$$

where $I_{n(\text{new})}$ is the new value of the current iteration while $I_{n(\text{old})}$ is the previous iteration value and ΔI_n is the change in injected current. The other variables are computed as shown in section 2.3. The node voltage of the original network at bus n is computed using

$$E_n^{k+1} = E_n^k + \Delta E_n \quad (2.123)$$

The change in voltage ΔE_n is computed using

$$\Delta E_n = Z_{nc} \Delta I_c + Z_n \Delta I_n \quad (2.124)$$

where Z_{nc} is the impedance matrix of the subnetworks without considering effect of cut lines ΔI_c is the change in injected currents entering each subnetwork through cut lines. ΔI_n is the change in system current and Z_n is the impedance of the network.

The load flow method is based on injected currents which require the computation of injected currents from injected powers first. Also, though one slack bus is used, the subnetworks without the original slack are computed with a different set of equations and the program is such as require the identification of subnetworks without slack buses.

2.12.7 *Piecewise Load Flow by Admittance Matrix Method*

In reference paper [40], the impedance matrix and admittance matrix models for load flow are discussed. There is a departure from Andretich et al's methods [38, 39, 43] in three areas - the diakoptic formulation of the load-flow problem is based on graph theory. Another difference is that the load-flow formulation is not based on the usual assumption of a fixed slack bus. The total transmission losses form an important part of the load-flow scheme. Admittance matrix is used in the formulation, which is an advantage because network admittance matrices are easier to build.

Another admittance method is by treating the power system analysis as a circuit analysis problem as presented in [14]. All generators and loads are converted into equivalent current sources except the slack bus which is eliminated. For a 5-bus network with the system of equation in (2.125), effect of bus 5 is eliminated. This is added to the solution as given by equation (2.126).

$$\begin{bmatrix} I_1 \\ I_2 \\ I_3 \\ I_4 \\ I_5 \end{bmatrix} = \begin{bmatrix} y_{11} & y_{12} & y_{13} & y_{14} & y_{15} \\ y_{21} & y_{22} & y_{23} & y_{24} & y_{25} \\ y_{31} & y_{32} & y_{33} & y_{34} & y_{35} \\ y_{41} & y_{42} & y_{43} & y_{44} & y_{45} \\ y_{51} & y_{52} & y_{53} & y_{54} & y_{55} \end{bmatrix} \begin{bmatrix} V_1 \\ V_2 \\ V_3 \\ V_4 \\ V_5 \end{bmatrix} \quad (2.125)$$

$$\begin{bmatrix} I_1 \\ I_2 \\ I_3 \\ I_4 \end{bmatrix} = \begin{bmatrix} y_{11} & y_{12} & y_{13} & y_{14} \\ y_{21} & y_{22} & y_{23} & y_{24} \\ y_{31} & y_{32} & y_{33} & y_{34} \\ y_{41} & y_{42} & y_{43} & y_{44} \end{bmatrix} \begin{bmatrix} V_1 \\ V_2 \\ V_3 \\ V_4 \end{bmatrix} + \begin{bmatrix} y_{15} \\ y_{25} \\ y_{35} \\ y_{45} \end{bmatrix} [V_5] \quad (2.126)$$

This representation is very convenient for diakoptic analysis with added advantage of being able to analyse a large system on small commodity computers. The convergence of the network solution was also found to be good. Again, the load flow is by current injection which is not commonly used in the load flow packages available. And because bus quantities are usually not specified as currents, conversion of a large system's generators and loads to currents is likely to increase the computation burden.

2.12.8 Diakoptics and Large Change Sensitivity Method

A brief analysis of large change sensitivity (LCS) is given in section 2.3 and engaged in the solution of the sample network in Figure 2.5. For iterative solution of nonlinear systems, equations (2.47), (2.48a) and (2.62) translate to (2.127), (2.128) and (2.129) respectively.

$$\frac{\partial \mathbf{g}(\mathbf{y}^k)}{\partial \mathbf{y}} = \left[\begin{array}{cccc|c} \frac{\partial g_1}{\partial y_1} & & & & \lambda_1 \\ & \frac{\partial g_2}{\partial y_2} & & & \lambda_2 \\ & & \ddots & & \vdots \\ & & & \frac{\partial g_s}{\partial y_s} & \lambda_s \\ \hline F_1 & F_2 & \dots & F_s & (F-1)\tau \end{array} \right] \quad (2.127)$$

$$\mathbf{y}^k = \begin{bmatrix} y_1^k \\ y_2^k \\ \vdots \\ y_s^k \\ i_f^k \end{bmatrix}, \quad \mathbf{i}_f^k = \begin{bmatrix} i_1 \\ i_2 \\ \vdots \\ i_t \end{bmatrix}, \quad \mathbf{g}(\mathbf{y}^k) = \begin{bmatrix} g_1(y_1^k) + \lambda_1 i_f^k \\ g_2(y_2^k) + \lambda_2 i_f^k \\ \vdots \\ g_s(y_s^k) + \lambda_s i_f^k \\ \sum_{i=1}^s F \lambda_i^t y_i^k + (F-1)\tau i_f^k \end{bmatrix} \quad (2.128)$$

$$\begin{bmatrix} \mathbf{V}_A^k \\ \mathbf{V}_B^k \\ \mathbf{i}_f^k \end{bmatrix} = \begin{bmatrix} \mathbf{V}_{A0}^k \\ \mathbf{V}_{B0}^k \\ \mathbf{0} \end{bmatrix} = \begin{bmatrix} \mathbf{Y}_A^{-1} & \mathbf{0} & \mathbf{Y}_A^{-1}\mathbf{L}_A \\ \mathbf{0} & \mathbf{Y}_B^{-1} & \mathbf{Y}_B^{-1}\mathbf{L}_B \\ \mathbf{L}_A^t & \mathbf{L}_B^t & -\boldsymbol{\tau} \end{bmatrix} \times \begin{bmatrix} \mathbf{0} \\ \mathbf{0} \\ \boldsymbol{\tau} \end{bmatrix} \mathbf{i}_f^k \quad (2.129)$$

The LCS and diakoptics have been applied in [9] for transient analysis using load flow analysis, and in [42] for Fast decoupled load flow (FDLF) analysis where the ideal switches in Figure 2.11b are replaced by ideal circuit breakers, but the concept is the same. In the FDLF analysis, for the original equations:

$$\mathbf{B}' \Delta \boldsymbol{\delta} = \frac{\Delta \mathbf{P}}{|\mathbf{V}|} \quad (2.130a)$$

$$\mathbf{B}'' |\mathbf{V}| = \frac{\Delta \mathbf{Q}}{|\mathbf{V}|} \quad (2.130b)$$

where \mathbf{B}' is the imaginary part of the admittance matrix; other variables have the usual meanings in power systems. Applying LCS in (2.130a) yields (2.131). A corresponding equation has been written for (2.130b).

$$\begin{bmatrix} \mathbf{B}_A' & \mathbf{0} & \mathbf{L}_A \\ \mathbf{0} & \mathbf{B}_B' & \mathbf{L}_B \\ \mathbf{F}_A & \mathbf{F}_B & (\mathbf{F}-1)\boldsymbol{\tau} \end{bmatrix} \begin{bmatrix} \Delta \boldsymbol{\delta}_A^{k+1} \\ \Delta \boldsymbol{\delta}_B^{k+1} \\ \Delta \mathbf{P}_f^{k+1} \end{bmatrix} = \begin{bmatrix} \frac{\mathbf{P}_{1sp} - (\mathbf{P}_{1cal}^k + \mathbf{L}_1 \mathbf{P}_f^k)}{|\mathbf{V}_1^k|} \\ \frac{\mathbf{P}_{2sp} - (\mathbf{P}_{2cal}^k + \mathbf{L}_2 \mathbf{P}_f^k)}{|\mathbf{V}_2^k|} \\ \mathbf{F}_A \Delta \boldsymbol{\delta}_A^{k+1} + \mathbf{F}_B \Delta \boldsymbol{\delta}_B^{k+1} + (\mathbf{F}-1)\boldsymbol{\tau} \Delta \mathbf{P}_f^{k+1} \end{bmatrix} \quad (2.131)$$

where $\mathbf{F}_A = \mathbf{F} \mathbf{L}_A^t$ and $\mathbf{F}_B = \mathbf{F} \mathbf{L}_B^t$

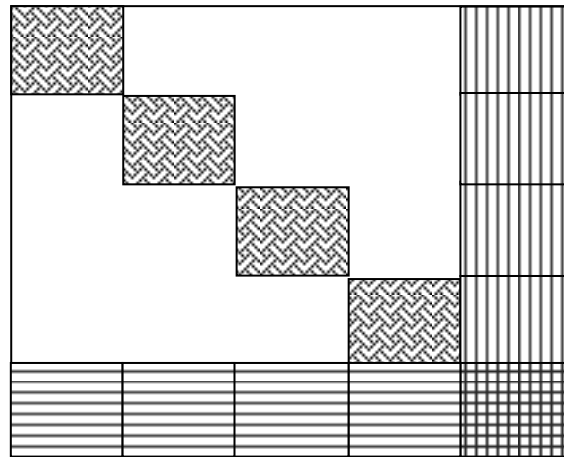
The results for the first iteration are shown to be the same as in one-piece solution but the same number of iterations is obtained as in the one piece solution using the original FDLF. Apart from tearing the network, the advantage of this method over the one-piece solution is not clear.

2.13 Proposed Method

Immittance matrices are important elements in the analysis of electrical power networks. The admittance matrix (Y_{bus}) is preferred in load flow analysis while impedance matrix (Z_{bus}) commonly uses in fault analysis [75]. In diakoptic analysis, the BBD matrices include constants that reflect the connection pattern of the tearing branches or nodes between subnetworks. Forming the Z_{bus} of a network is more laborious than forming the Y_{bus} which can be done by inspection. This is reflected in the codes for forming Y_{bus} and Z_{bus} directly in appendices A4 and A5 respectively. The Y_{bus} of a typical power system is sparse because many nodes are not usually connected together; Z_{bus} on the other hand is a full matrix and therefore require more computer space. Furthermore, the sparseness of the Y_{bus} can be manipulated faster than the Z_{bus} is power system analysis where every element of the Z_{bus} must be operated with during iteration [87, 83]. The Y_{bus} load flow presents a better choice than Z_{bus} in computer aided load flow analysis because the advantage of requiring less memory space [88]. The advantages due to the sparseness of the Y_{bus} makes it the chosen matrix in the proposed method.

Early load flow methods were compared in [89, 90]. Comparison of number of iterations between nodal ZBUS and nodal Y_{bus} load flow methods by Freris et al [89] did not follow any specific pattern in that some systems had higher iteration with Y_{bus} load flow and less in the ZBUS load flow and vice versa. The conclusion in [90] is that there was still no method that is much better than the existing ones. This assertion does not seem to have changed even after several years but the direct method developed in [85] promises a much better performance and as it unfolds for wider use this will be clearer.

The general form of the diakoptic matrix is shown Figure 2.19. In impedance matrix analysis, the formation of the elements M_2 , M_2^t and M_4 is more difficult than in admittance matrix method which can be done by inspection. In addition, Z_{bus} are full matrices while Y_{bus} for electrical power systems are sparse. In Y_{bus} method, M_2 and M_2^t contain only +, -1 and 0; M_4 contains only diagonal elements when branch cutting is employed. This is illustrated with the matrices of (2.34) and (2.37) for the same network of Figure 2.5.



LEGEND

-  M_1 = Impedance or admittance matrices of subnetworks
 M_2 = Impedance, admittance or connection matrix of the network
 M_3 = Transpose of M_2
 M_4 = Intersubdivision impedance or admittance matrix

Figure 2.19. Typical BBD matrix typical for diakoptic analysis

In the diakoptic impedance load flow presented in [43], the process of computing the removed branch currents and modifying the subnetworks solutions is long and difficult for every power system analyst to understand and apply. Also with this method, the swing bus and generator axis in the BBDF matrix have to be removed and incorporated later in another complicated process. There is also the process of re-ordering the line data to fit into the solution process. All these technicalities make the method unattractive.

The admittance method proposed in [40] is different from the conventional procedure in that the total transmission line losses are determined at each iteration and the slack bus is treated like a load bus. This method applied G-S load flow and convergence was said to be faster in one-piece solution, but this assertion was not conclusive. Also, when the method was incorporated into diakoptics convergence was slower. This method is a departure from the present load flow methods which require a slack

bus and therefore will not fit into the existing softwares that have already been developed.

The method proposed in this work seeks to remove the difficulties and complications of the methods discussed while making use of their merits in developing a new algorithm. Two new algorithms have been developed for linear and nonlinear analysis and because they are based on diakoptics, are suitable for sequential and parallel computing.

An improved method of forming the diakoptic matrix is produced and branch modifier techniques that can easily be applied to linear systems to obtain results that are exactly the same as one-piece solutions. The new algorithm, the Slack Voltage Updating Diakoptics, which is an extension of the Branch Voltage Modifier Technique, makes use of admittance matrices in the general form currently used in centralized load flow analyses. This is combined with the qualities of diakoptics to produce a hybrid algorithm for load flow analysis. The resulting algorithm would fit into existing load flow analysis packages without complications.

2.14 Summary

In chapter one, a review of literature on the various applications of diakoptics as a tool that has transcended electrical power system analysis and is now viewed as a general mathematical tool applicable to mathematics, computer science and other fields of engineering was presented. In this chapter, the emphasis of the review has been on application of diakoptics in electrical engineering where the concept of diakoptics was explained. Different methods particularly relevant to this work were reviewed analytically by applying the principles in the literatures on a sample network and drawing conclusions.

A brief technical review of the effects of wind power electricity on a weak grid is also presented where the effect on steady-state voltage level of the receiving grid was underlined as the major cause for concern. This forms a basis for analyzing the response of the Nigeria grid to wind power integration. Since load flow is recommended as the best method for assessing the effect of wind power electricity on the grid, a brief review of load flow is presented.

3 NOVEL ANALYSIS METHODS: THE BVMT AND THE SVUD METHOD OF LOAD FLOW

3.1 Introduction

This chapter describes the process of developing novel methods proposed for the solution of power systems problems – the branch voltage multiplier technique (BVMT) and the slack voltage updating diakoptics (SVUD) load flow methods. The BVMT and the SVUD have their root from diakoptics and as explained in chapter one, diakoptics is a means of solving a problem in parts and obtaining the same results as would be obtained when solved as a whole piece. It was noted from extant literature that diakoptics is generally presented in a complicated form which has limited its acceptability and use in power system analysis. The methodology therefore focuses on producing ‘user friendly’ diakoptics such that it can be appreciated and easily adopted by practicing power systems engineers, especially in their final forms. Another advantage of the proposed load flow method is that the main algorithm can easily be incorporated into existing softwares for power system analyses.

3.2 The Foundational Principle of BVMT and SVUD Methods

Diakoptics requires that a network be torn into parts or subnetworks before solving each subnetwork independently. Effects between subnetworks are communicated via connection matrices and removed branch voltages. The crux of diakoptics is combining and modifying the separate solutions of subnetworks to yield the solution of the original untorn network as if it was solved as whole piece.

Usually, in separate subnetworks solutions, computation of branch or link currents is required before the subnetwork solutions can be modified to get the complete solution [43, 38, 61]. In the branch voltage modifier technique, the need for calculating branch

currents has been removed thereby simplifying the solution. The assumptions in the analyses are balanced, three-phase, steady-state conditions and the topology of the network consists of buses and lines each of which connect at least two buses.

When a line or branch is removed to tear a network, the important element for reconciling the separate solutions to obtain the final solution of the original network is the removed branch voltage or voltage vector, if two or more lines are removed. Usually, this is obtained by first calculating the removed line current in a complicated manner. The BVMT simplifies the process and eliminates the need to compute a removed branch current first. The algorithm is a new diakoptic algorithm which is easy to understand and utilize in the analysis of linear networks and in networks where injected currents are known.

The most common load flow packages offer iterative solutions of nonlinear power system equations. The second algorithm, the SVUD is a method of load flow analysis which can easily be incorporated into the existing softwares thereby saving time and cost of producing completely new and likely expensive software. Updating the slack bus voltage of temporary slack bus is the novel way of varying their voltages as if they were in one-piece load flow analysis. In reference [9], ill-condition due to tearing is solved by adding a pair of symmetrical shunt elements to torn buses. The SVUD solves the ill-conditioning problem without adding extra elements to the network.

3.2.1 *Basic Solution Steps of the BVMT and the SVUD*

As schematically presented in Figure 3.1, the BVMT and SVUD methods consist of four basic stages: tearing, solution of torn parts, modelling solutions of torn parts and obtaining results of original network. These stages are typical of the diakoptic concept on which the new algorithms are built. Results of BVMT and SVUD are compared with results from calculations based on formal methods of solving the system as a whole piece.

When an electrical network is to be analysed, for example in load flow analysis, the impedance or admittance matrix would be formed which, for large systems, takes a great part of computer time. But if torn into smaller networks, the matrices to be formed are greatly reduced in size.

Step 1

In Figure 3.1, the network (a) to be analysed is first torn into M parts by removing the required branches or lines: lines (3 - 4), (5 - 6), (9 - 11) and (4 - 12). The tearing is usually theoretical when dealing with real systems.

Step 2

The M parts are solved separately and the results obtained at this stage are not yet the required solutions of the original network. For example, computed voltages at nodes 1, 2, 3 and 5 in subnet A in

Figure 3.1c will not be the same as computed voltages at the same nodes in the full network of Figure 3.1a. Complete solution of the whole network is obtained in each subnet after modification of the separate solutions of the subnetworks.

Step 3

Apart from the subnetworks, A, B, C... M, an extra network, the $(m+1)^{\text{th}}$ network, is constructed from the removed branches. This network plays a very important role in the solution process to obtain the correct solution of the full network; it has to be utilised in updating the subnetworks' solutions. It is a miniature form of the original network and in view of its important role, has been called the *intersection network*, *managerial system* and *central brain* [4].

Step 4

The m solutions of the subnetworks obtained separately are not the required solution of the original network. To obtain the required results, the m solutions are combined and modified using $(m+1)^{\text{th}}$ network and the complete network solution is obtained. The modified subnetworks node voltages at this stage are the same as node voltages in Figure 3.1a, that is, as if it was not torn but solved as a piece.

There many different approaches to the diakoptic solution of power systems but the fundamental equations are the same. Derivation of the fundamental equations of diakoptics is summarised in sections and 2.1 and 2.3.

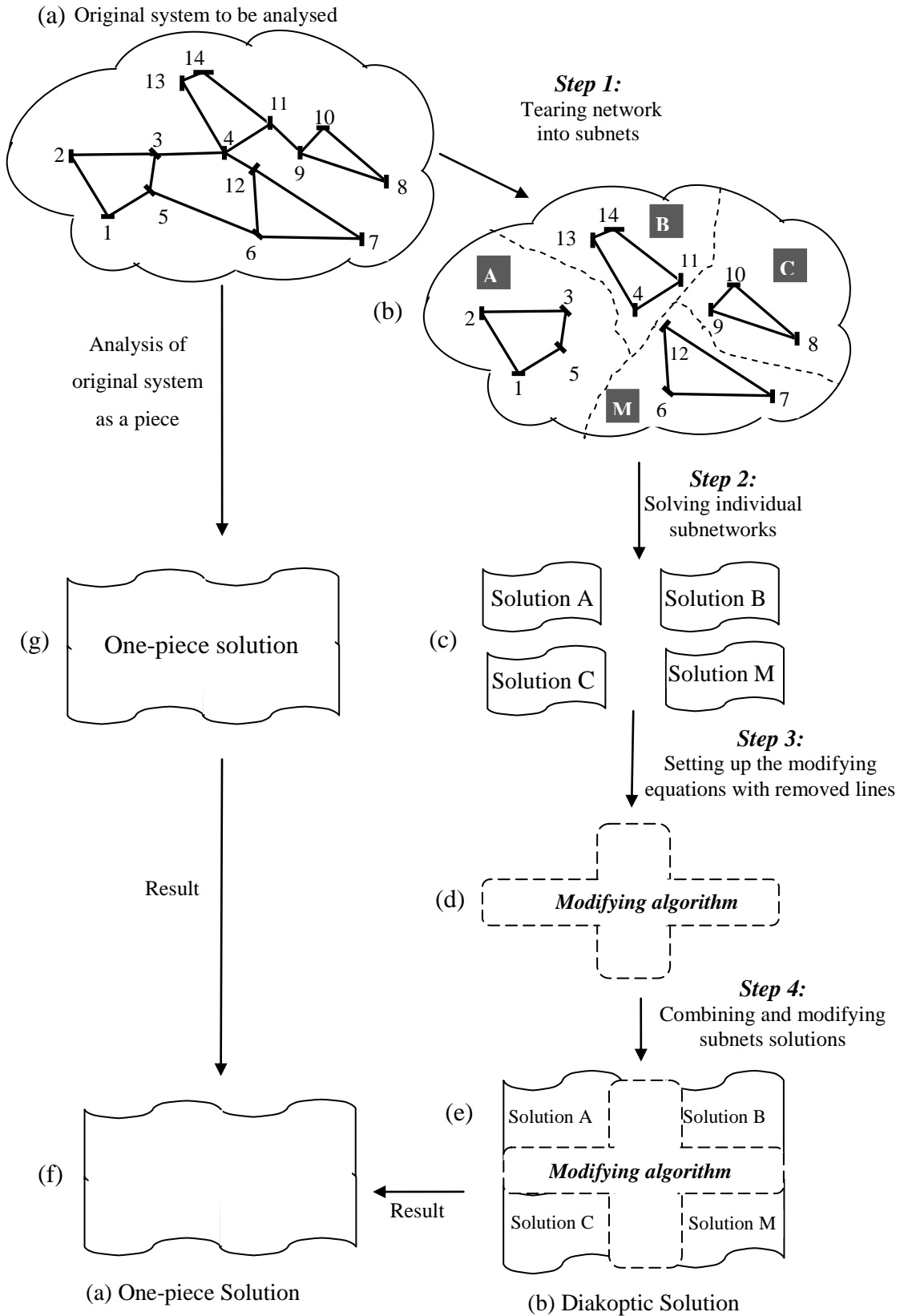


Figure 3.1. Schematic diagram of basic diakoptic steps and one-piece solution

3.3 Choosing Method of Tearing for BVMT and SVUD

3.3.1 Methods of Tearing

Diakoptic approach is also known as “method of tearing” [91, 92]. The most common methods of tearing an electrical network are branch tearing and node tearing but there are other variations that combine the qualities of both methods. Points of tear are also of importance in relation to speed of convergence where the requirement is to cut branches that are loosely coupled that is, branches with highest reactance or smaller susceptances [93, 94]. Tearing methods are demonstrated using Figure 3.2.

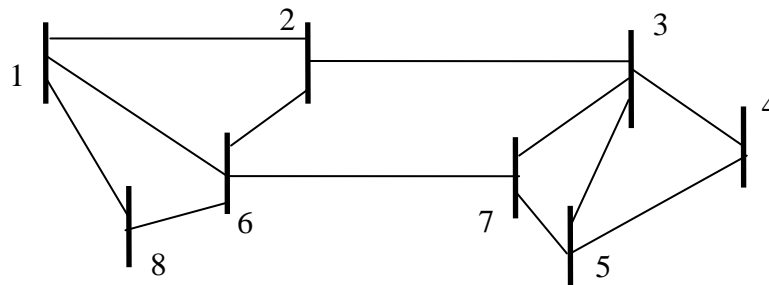


Figure 3.2. An 8-bus system

3.3.1.1 Branch Tearing

Let the network of Figure 3.2 be torn into two parts. The point of tear is such that there is no mutual coupling between the subnetworks. In Figure 3.3, lines between buses 2-3 and 6-7 are completely removed, yielding two separate networks. The removed branches then form a third network which will serve as the managerial system when the separate solutions of the two networks are being reconciled.

A clear advantage of branch tearing is seen in Figure 3.3b where the unknown currents flowing in the removed branches are not part of the currents in the subnetworks. This reduces the number of unknowns in the subnet by a great percentage [7]. Another very important advantage is that since the solutions of the subnetworks are completely separate, each subnet can be connected with other subnetworks (Figure 3.3c) or other networks (Figure 3.3) in any desired manner

without re-solving the subnetworks again, for each type of connection [4, 5, 7, 61, 92].

Breakers can be used to tear the network as demonstrated in [95] where a system was simulated with the aid of PSCAD (Power System Computer Aided Design) [96]. Circuit breakers were inserted on the branches to be torn. The breakers were opened to split the network into two. The subnetworks were then analysed in parallel. The nodal voltages compared to when the subnetworks were solved separately were the same. This method had been applied [9] in for node tearing.

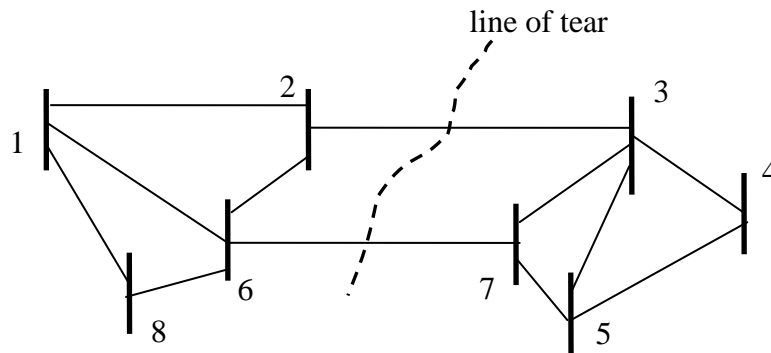


Figure 3.3(a) Branch tearing –original network with proposed line of tear

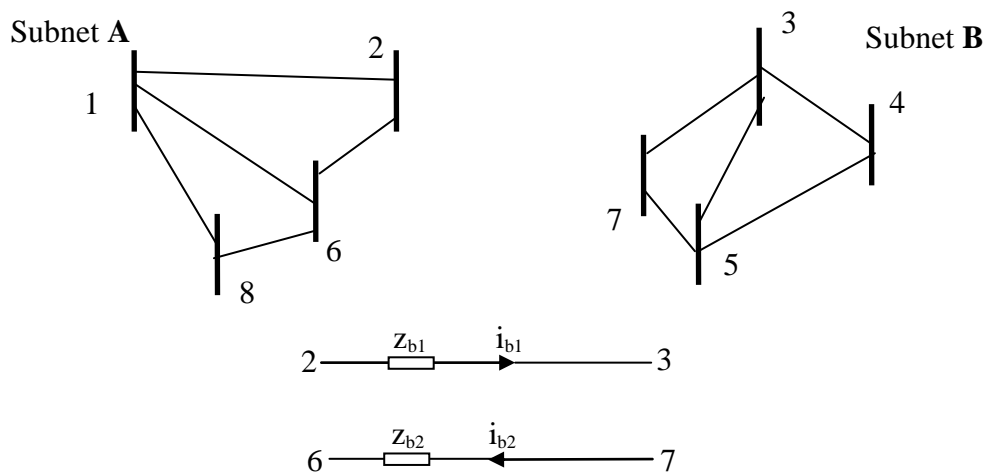


Figure 3.3(b) Branch tearing – branches removed to obtain two subnetworks

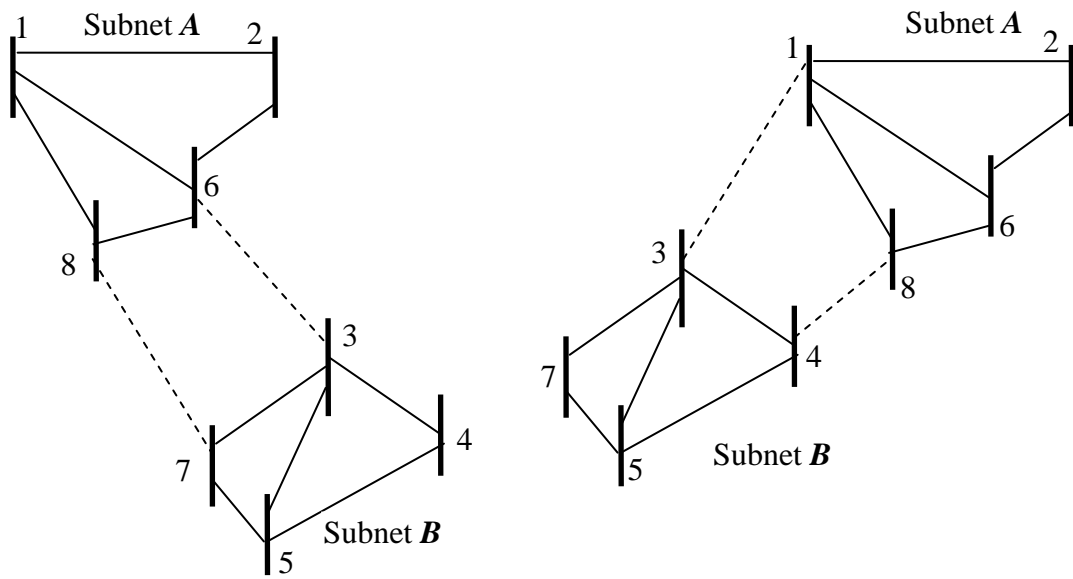


Figure 3.3(c) Branch tearing with connections to different set of buses

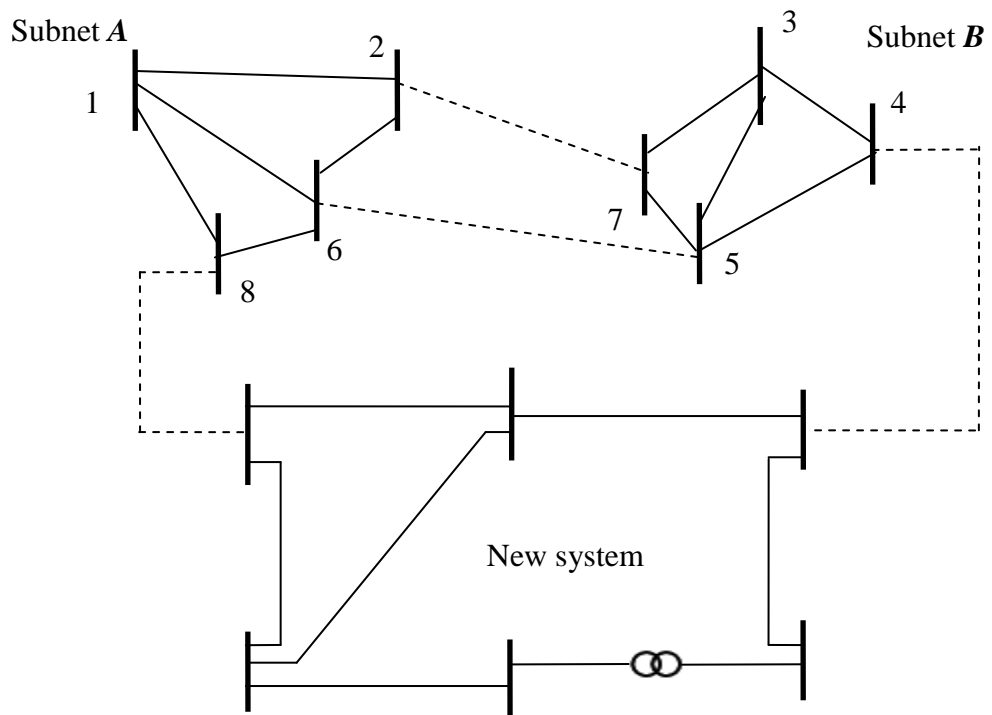


Figure 3.3(d) Branch tearing with subnetworks connected to another network not part of original network

3.3.1.2 Node Tearing

Two variations of the node tearing method are illustrated in Figure 3.4. In Figure 3.4(a) and (b); designated buses are removed thereby separating the subnetworks completely from each other. This method is presented in [4]. In the second approach, the lines of tear pass through buses or nodes [4, 9, 15] and so the cut buses are part of each subsystem (Figure 3.4 (c) and (d)). The cut buses are then connected via ideal switches or circuit breakers shown in Figure 3.4(d). Opening the switches tears the network and closing yields the original network. In the various forms of tearing, the characteristic matrix for diakoptic analysis is a BBD matrix shown in Figure 2.19.

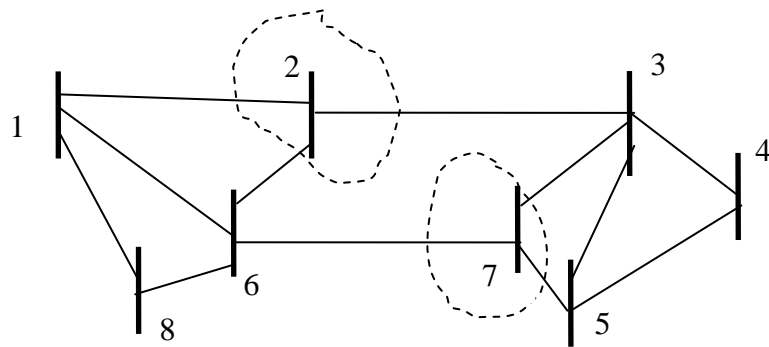


Figure 3.4 (a) Nodes to be removed or cut

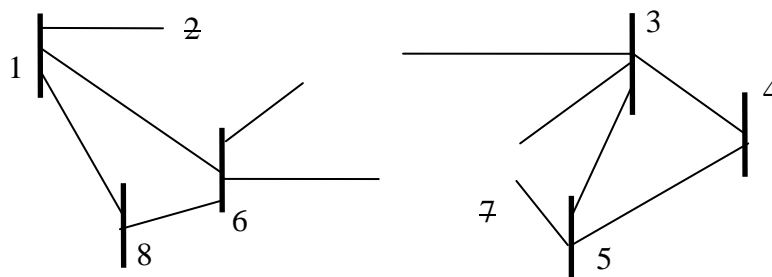


Figure 3.4 (b) Subnetworks completely

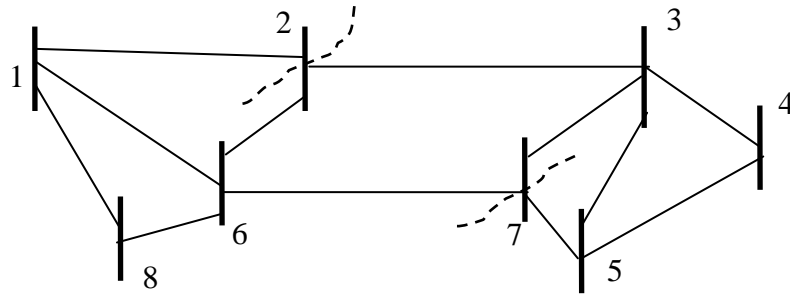


Figure 3.4 (c) Nodes cut into two

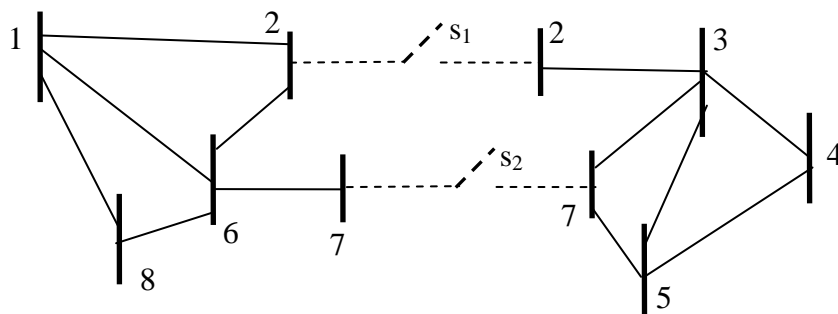


Figure 3.4 (d) Cut nodes separated by ideal switches

3.3.1.3 Overlapping Decomposition Method

In the methods considered so far, a network is torn either by cutting branches or cutting nodes, but a third possibility, proposed by Sasson [94], where the disconnecting branches are cut twice. This applied in [97] for piecewise Newton-Raphson load flow.

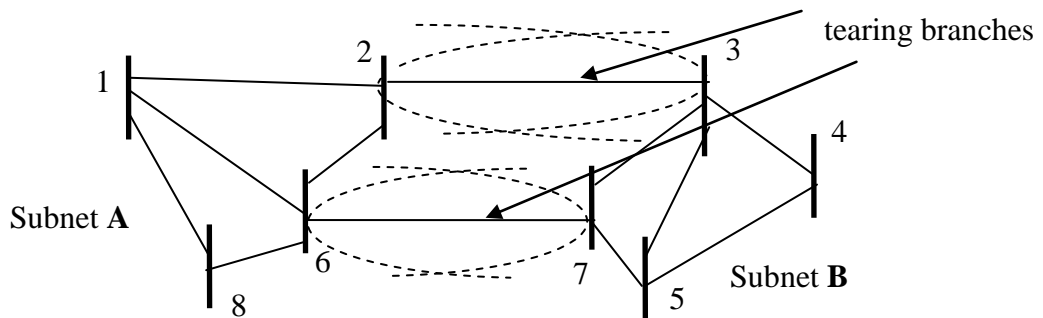


Figure 3.5a. Chosen branches showing overlap of the nodes

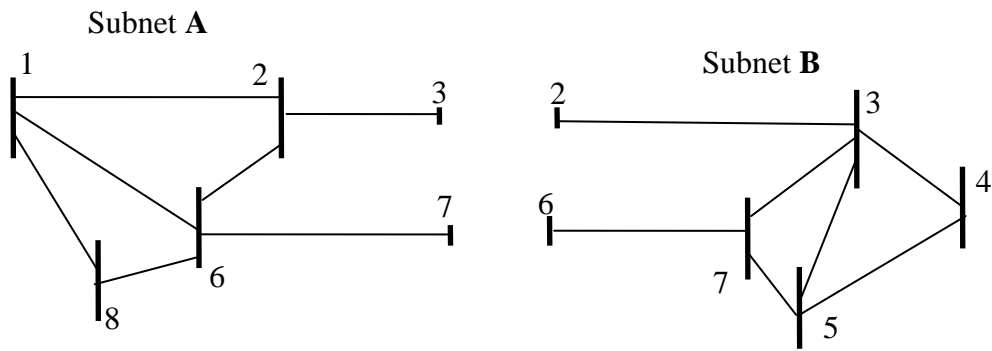


Figure 3.5b. Cut branches form part of each subnet

The method is demonstrated with the sample network in Figure 3.5, where bus 1 is the slack bus. In this method, the cut branch is not removed, but is present as part of both subnetworks. This results in overlapping subsystems. When subnet A is being solved, nodes 3 and 7 remain part of the solution. When subnet B is being solved buses 2 and 6 remain part of the solution.

Chosen method

Branch tearing was chosen for the BVMT and SVUD because of the advantages explained in this section. The first step is to identify branches which, when removed, will effectively decouple the subnetworks. Current directions on the chosen branches serve as a guide when forming the connection matrices. If directions of currents, i_b , are not indicated in the original network, they are chosen arbitrarily as a guide. It is important that once the current directions are chosen, the sign conventions are strictly followed in forming the connection matrices denoted as K or L in this work.

3.4 Formulation of the BVMT Equations for Solution

In extant literatures on diakoptics, two sets of equations are generally derived called the *fundamental equations of diakoptics* [13] and determination of the equations is summarized in section 2.3.2 and the equations are (2.29) and (2.30).

Evidence from literature shows that every diakoptic analysis is based on these equations; the major difference is usually in the method of realizing and solving the

two equations to obtain *the equation of solution* and required results. In this section, a new method of solving the equations is devised which deviates from the general method. The final equations of solution devised here have been broken down into functions that are easier to understand and apply to network solutions.

Consider the network of Figure 3.3; removing branches 2-3 and 6-7 effectively separates the network into two subnetworks shown in Figure 3.3b. If impedances of the removed branches are z_{b1} and z_{b2} , then the fundamental equations stated by (2.29) and (2.30) can be rewritten as in (3.1) and (3.2).

$$\mathbf{Y}_d \mathbf{V} - \mathbf{L} \mathbf{i}_b = \mathbf{I} \quad (3.1)$$

$$\mathbf{L}^t \mathbf{V} + \mathbf{Z}_b \mathbf{i}_b = \mathbf{0} \quad (3.2)$$

Where:

\mathbf{V} = vector of node voltages

\mathbf{Y} = block diagonal matrix with each block consisting of admittance matrix of a subnet

\mathbf{L} = Connection matrices of the subnetworks

\mathbf{L}^t = transpose of \mathbf{L}

\mathbf{I} = vector of injected currents

\mathbf{i}_b = vector of removed branch currents

\mathbf{Z}_b = is the diagonal impedance matrix of the removed branches.

Equations (3.1) and (3.2) are combined in matrix form in (3.3). For the network shown in Figure 3.12, equation (3.3) is expanded to give (3.5), and for any number of subnetworks equation (3.5) is obtained. The unknown values in (3.5) are the node voltages \mathbf{V} , and branch currents \mathbf{i}_b . \mathbf{V}_A and \mathbf{V}_B are vectors of node voltages and \mathbf{I}_A and \mathbf{I}_B are the vectors of injected currents in the subnetworks \mathbf{A} and \mathbf{B} . The voltages are determined using (3.6). Connection matrices of the subnetworks are \mathbf{L}_A and \mathbf{L}_B . \mathbf{Y}_A and \mathbf{Y}_B represent the admittance matrices of the subnetworks, vector of removed branch currents is \mathbf{i}_b and \mathbf{Z}_b is the diagonal matrix of the removed branches impedances. The matrices \mathbf{L}_A^t and \mathbf{L}_B^t are the transposed forms of \mathbf{L}_A and \mathbf{L}_B .

$$\begin{bmatrix} \mathbf{Y} & -\mathbf{L} \\ \mathbf{L}^t & \mathbf{Z}_b \end{bmatrix} \begin{bmatrix} \mathbf{V} \\ \mathbf{i}_b \end{bmatrix} = \begin{bmatrix} \mathbf{I} \\ \mathbf{0} \end{bmatrix} \quad (3.3)$$

$$\begin{bmatrix} \mathbf{Y}_A & & -\mathbf{L}_B \\ & \mathbf{Y}_B & -\mathbf{L}_B \\ \mathbf{L}_A^t & \mathbf{L}_B^t & \mathbf{Z}_b \end{bmatrix} \begin{bmatrix} \mathbf{V}_A \\ \mathbf{V}_B \\ \mathbf{i}_b \end{bmatrix} = \begin{bmatrix} \mathbf{I}_A \\ \mathbf{I}_B \\ \mathbf{0} \end{bmatrix} \quad (3.4)$$

$$\begin{bmatrix} \mathbf{Y}_A & & & & -\mathbf{L}_A \\ & \mathbf{Y}_B & & & -\mathbf{L}_B \\ & & \ddots & & \vdots \\ & & & \mathbf{Y}_M & -\mathbf{L}_M \\ \mathbf{L}_A^t & \mathbf{L}_B^t & \cdots & \mathbf{L}_M^t & \mathbf{Z}_b \end{bmatrix} \begin{bmatrix} \mathbf{V}_A \\ \mathbf{V}_B \\ \vdots \\ \mathbf{V}_M \\ \mathbf{i}_b \end{bmatrix} = \begin{bmatrix} \mathbf{I}_A \\ \mathbf{I}_B \\ \vdots \\ \mathbf{I}_M \\ \mathbf{0} \end{bmatrix} \quad (3.5)$$

$$\begin{bmatrix} \mathbf{V}_A \\ \mathbf{V}_B \\ \vdots \\ \mathbf{V}_M \\ \mathbf{i}_b \end{bmatrix} = \begin{bmatrix} \mathbf{Y}_A & & & & -\mathbf{L}_A \\ & \mathbf{Y}_B & & & -\mathbf{L}_B \\ & & \ddots & & \vdots \\ & & & \mathbf{Y}_M & -\mathbf{L}_M \\ \mathbf{L}_A^t & \mathbf{L}_B^t & \cdots & \mathbf{L}_M^t & \mathbf{Z}_b \end{bmatrix}^{-1} \begin{bmatrix} \mathbf{I}_A \\ \mathbf{I}_B \\ \vdots \\ \mathbf{I}_M \\ \mathbf{0} \end{bmatrix} \quad (3.6)$$

Let:

$$\mathbf{F} = \begin{bmatrix} \mathbf{Y}_A & & & & -\mathbf{L}_A \\ & \mathbf{Y}_B & & & -\mathbf{L}_B \\ & & \ddots & & \vdots \\ & & & \mathbf{Y}_M & -\mathbf{L}_M \\ \mathbf{L}_A^t & \mathbf{L}_B^t & \cdots & \mathbf{L}_M^t & \mathbf{Z}_b \end{bmatrix} = \begin{bmatrix} \mathbf{Y} & -\mathbf{L} \\ \mathbf{L}^t & \mathbf{Z}_b \end{bmatrix} \quad (3.7)$$

By applying the formula in [98] for inverse of partitioned matrices to (3.7), equation (3.8) is obtained, where

$$\mathbf{Y}_i \in \mathbb{C}^{n_i \times n_i}, \mathbf{L}_i = \mathbb{C}^{n_i \times n_{z_b}}, \mathbf{Z}_b \in \mathbb{C}^{n_{z_b} \times n_{z_b}}, n_{z_b} + n_Y = n \text{ with } n_Y := \sum_{i=1}^M n_i.$$

$$\mathbf{F}^{-1} = \begin{bmatrix} \mathbf{Y}_d^{-1} - \mathbf{Y}_d^{-1} \mathbf{L} \mathbf{D}'^{-1} \mathbf{L}' \mathbf{Y}_d^{-1} & \mathbf{Y}_d^{-1} \mathbf{L} \mathbf{D}'^{-1} \\ -\mathbf{D}'^{-1} \mathbf{L}' \mathbf{Y}_d^{-1} & \mathbf{D}'^{-1} \end{bmatrix} \quad (3.8)$$

where $\mathbf{D}' = \mathbf{Z}_b + \mathbf{L}' \mathbf{Y}_d^{-1} \mathbf{L}$.

$$\mathbf{Z}_b = \begin{bmatrix} z_{b1} & \cdot \\ \cdot & z_{b2} \end{bmatrix} \quad (3.9)$$

$$\mathbf{L}' \mathbf{Y}_d^{-1} \mathbf{L} = \begin{bmatrix} \mathbf{L}'_A & \mathbf{L}'_B \end{bmatrix} \begin{bmatrix} \mathbf{Y}_A^{-1} & \cdot \\ \cdot & \mathbf{Y}_B^{-1} \end{bmatrix} \begin{bmatrix} \mathbf{L}_A \\ \mathbf{L}_B \end{bmatrix} \quad (3.10)$$

Since \mathbf{D}' is a multiplier with \mathbf{L} in (3.8), let $\mathbf{D} = -\mathbf{D}'$, then

$$\mathbf{D} = -(\mathbf{Z}_b + \mathbf{L}' \mathbf{Y}_d^{-1} \mathbf{L}) \quad (3.11)$$

Equations (3.5) and (3.6) and are now as shown in (3.9) and (3.10).

$$\begin{bmatrix} \mathbf{V}_A \\ \mathbf{V}_B \\ \vdots \\ \mathbf{V}_M \\ \mathbf{i}_b \end{bmatrix} = \begin{bmatrix} \mathbf{Y}_A & & & & \mathbf{L}_A \\ & \mathbf{Y}_B & & & \mathbf{L}_B \\ & & \ddots & & \vdots \\ & & & \mathbf{Y}_M & \mathbf{L}_M \\ \mathbf{L}'_A & \mathbf{L}'_B & \cdots & \mathbf{L}'_M & -\mathbf{Z}_b \end{bmatrix}^{-1} \begin{bmatrix} \mathbf{I}_A \\ \mathbf{I}_B \\ \vdots \\ \mathbf{I}_M \\ \mathbf{0} \end{bmatrix} \quad (3.12)$$

$$\begin{bmatrix} \mathbf{V} \\ \mathbf{i}_b \end{bmatrix} = \begin{bmatrix} \mathbf{Y}_d^{-1} + \mathbf{Y}_d^{-1} \mathbf{L} \mathbf{D}^{-1} \mathbf{L}' \mathbf{Y}_d^{-1} & -\mathbf{Y}_d^{-1} \mathbf{L} \mathbf{D}^{-1} \\ \mathbf{D}^{-1} \mathbf{L}' \mathbf{Y}_d^{-1} & -\mathbf{D}^{-1} \end{bmatrix} \begin{bmatrix} \mathbf{I} \\ \mathbf{0} \end{bmatrix} \quad (3.13)$$

The branch current \mathbf{i}_b in (3.10) does not contribute to the complete solution of the network and is therefore neglected. The node voltages are then computed using

(3.11). This is the final equation for calculating the nodal voltages and corresponds to the so called equation of solution found in [13] where \mathbf{Y} is the block diagonal matrix of the torn network. In reference [13] the inversion of the whole diagonal matrix is required during the computation.

$$\mathbf{V} = (\mathbf{Y}_d^{-1} + \mathbf{Y}_d^{-1} \mathbf{L} \mathbf{D}^{-1} \mathbf{L}^t \mathbf{Y}_d^{-1}) \mathbf{I} \quad (3.14)$$

Equation (3.11) is the new equation of solution for a whole network and is extended in the following sections to enable the inversion of matrices of subnetworks individually. Individual handling of subnetworks has been done in [10, 60, 61]; the main difference is in the method of communicating with other subnetworks for complete solution.

3.4.1 *Obtaining Complete Solution of the Subnetworks Separately*

In the following analysis, the devised algorithm is such that a complete network solution can be obtained by solving each subnet separately, which is a deviation from the method in [23]. This is important especially when subnetworks represent networks in different parts of a country managed by separate operators.

3.4.1.1 Expansion of the Equation of Solution

If a network is torn into two subnetworks, each of the matrices in (3.14) is defined by the following submatrices.

$$\mathbf{V} = \begin{bmatrix} \mathbf{V}_A \\ \mathbf{V}_B \end{bmatrix} \quad (3.15)$$

$$\mathbf{I} = \begin{bmatrix} \mathbf{I}_A \\ \mathbf{I}_B \end{bmatrix} \quad (3.16)$$

$$\mathbf{Y}_d = \begin{bmatrix} \mathbf{Y}_A & \\ & \mathbf{Y}_B \end{bmatrix} \quad (3.17)$$

$$\mathbf{Y}_d^{-1} = \begin{bmatrix} \mathbf{Y}_A^{-1} & \\ & \mathbf{Y}_B^{-1} \end{bmatrix} \quad (3.18)$$

$$\mathbf{L} = \begin{bmatrix} \mathbf{L}_A \\ \mathbf{L}_B \end{bmatrix} \quad (3.19)$$

$$\mathbf{L}^t = [\mathbf{L}_A \quad \mathbf{L}_B] \quad (3.20)$$

Equations (3.15) - (3.20) are substituted in (3.14) in stages from (3.21) - (3.24) to obtain (3.24).

$$\mathbf{Y}_d^{-1} \mathbf{L} \mathbf{D}^{-1} = \begin{bmatrix} \mathbf{Y}_A^{-1} & \\ & \mathbf{Y}_B^{-1} \end{bmatrix} \begin{bmatrix} \mathbf{L}_A \\ \mathbf{L}_B \end{bmatrix} \mathbf{D}^{-1} = \begin{bmatrix} \mathbf{Y}_A^{-1} \mathbf{L}_A \mathbf{D}^{-1} \\ \mathbf{Y}_B^{-1} \mathbf{L}_B \mathbf{D}^{-1} \end{bmatrix} \quad (3.21)$$

$$\mathbf{L}^t \mathbf{Y}_d^{-1} = [\mathbf{L}_A^t \quad \mathbf{L}_B^t] \begin{bmatrix} \mathbf{Y}_A^{-1} & \\ & \mathbf{Y}_B^{-1} \end{bmatrix} = [\mathbf{L}_A^t \mathbf{Y}_A^{-1} \quad \mathbf{L}_B^t \mathbf{Y}_B^{-1}] \quad (3.22)$$

$$\mathbf{Y}_d^{-1} \mathbf{L} \mathbf{D}^{-1} \mathbf{L}^t \mathbf{Y}_d^{-1} = \begin{bmatrix} \mathbf{Y}_A^{-1} \mathbf{L}_A \mathbf{D}^{-1} \\ \mathbf{Y}_B^{-1} \mathbf{L}_B \mathbf{D}^{-1} \end{bmatrix} [\mathbf{L}_A^t \mathbf{Y}_A^{-1} \quad \mathbf{L}_B^t \mathbf{Y}_B^{-1}] \quad (3.23)$$

$$= \begin{bmatrix} \mathbf{Y}_A^{-1} \mathbf{L}_A \mathbf{D}^{-1} \mathbf{L}_A^t \mathbf{Y}_A^{-1} & \mathbf{Y}_A^{-1} \mathbf{L}_A \mathbf{D}^{-1} \mathbf{L}_B^t \mathbf{Y}_B^{-1} \\ \mathbf{Y}_B^{-1} \mathbf{L}_B \mathbf{D}^{-1} \mathbf{L}_A^t \mathbf{Y}_A^{-1} & \mathbf{Y}_B^{-1} \mathbf{L}_B \mathbf{D}^{-1} \mathbf{L}_B^t \mathbf{Y}_B^{-1} \end{bmatrix}$$

$$\begin{bmatrix} \mathbf{V}_A \\ \mathbf{V}_B \end{bmatrix} = \begin{bmatrix} \mathbf{Y}_A^{-1} & \\ & \mathbf{Y}_B^{-1} \end{bmatrix} \begin{bmatrix} \mathbf{I}_A \\ \mathbf{I}_B \end{bmatrix} + \begin{bmatrix} \mathbf{Y}_A^{-1} \mathbf{L}_A \mathbf{D}^{-1} \mathbf{L}_A^t \mathbf{Y}_A^{-1} & \mathbf{Y}_A^{-1} \mathbf{L}_A \mathbf{D}^{-1} \mathbf{L}_B^t \mathbf{Y}_B^{-1} \\ \mathbf{Y}_B^{-1} \mathbf{L}_B \mathbf{D}^{-1} \mathbf{L}_A^t \mathbf{Y}_A^{-1} & \mathbf{Y}_B^{-1} \mathbf{L}_B \mathbf{D}^{-1} \mathbf{L}_B^t \mathbf{Y}_B^{-1} \end{bmatrix} \begin{bmatrix} \mathbf{I}_A \\ \mathbf{I}_B \end{bmatrix} \quad (3.24)$$

Combining the right hand side of (3.24) gives

$$\begin{bmatrix} \mathbf{V}_A \\ \mathbf{V}_B \end{bmatrix} = \begin{bmatrix} \mathbf{Y}_A^{-1} + \mathbf{Y}_A^{-1} \mathbf{L}_A \mathbf{D}^{-1} \mathbf{L}_A^t \mathbf{Y}_A^{-1} & \mathbf{Y}_A^{-1} \mathbf{L}_A \mathbf{D}^{-1} \mathbf{L}_B^t \mathbf{Y}_B^{-1} \\ \mathbf{Y}_B^{-1} \mathbf{L}_B \mathbf{D}^{-1} \mathbf{L}_A^t \mathbf{Y}_A^{-1} & \mathbf{Y}_B^{-1} + \mathbf{Y}_B^{-1} \mathbf{L}_B \mathbf{D}^{-1} \mathbf{L}_B^t \mathbf{Y}_B^{-1} \end{bmatrix} \begin{bmatrix} \mathbf{I}_A \\ \mathbf{I}_B \end{bmatrix} \quad (3.25)$$

If a network is torn into three subnetworks, equation (3.25) becomes

$$\begin{bmatrix} \mathbf{V}_A \\ \mathbf{V}_B \\ \mathbf{V}_C \end{bmatrix} = \begin{bmatrix} \mathbf{Y}_A^{-1} + \mathbf{Y}_A^{-1} \mathbf{L}_A \mathbf{D}^{-1} \mathbf{L}_A^t \mathbf{Y}_A^{-1} & \mathbf{Y}_A^{-1} \mathbf{L}_A \mathbf{D}^{-1} \mathbf{L}_B^t \mathbf{Y}_B^{-1} & \mathbf{Y}_A^{-1} \mathbf{L}_A \mathbf{D}^{-1} \mathbf{L}_C^t \mathbf{Y}_C^{-1} \\ -\mathbf{Y}_B^{-1} \mathbf{L}_B \mathbf{D}^{-1} \mathbf{L}_A^t \mathbf{Y}_A^{-1} & \mathbf{Y}_B^{-1} + \mathbf{Y}_B^{-1} \mathbf{L}_B \mathbf{D}^{-1} \mathbf{L}_B^t \mathbf{Y}_B^{-1} & \mathbf{Y}_B^{-1} \mathbf{L}_B \mathbf{D}^{-1} \mathbf{L}_C^t \mathbf{Y}_C^{-1} \\ \mathbf{Y}_C^{-1} \mathbf{L}_C \mathbf{D}^{-1} \mathbf{L}_A^t \mathbf{Y}_A^{-1} & \mathbf{Y}_C^{-1} \mathbf{L}_C \mathbf{D}^{-1} \mathbf{L}_B^t \mathbf{Y}_B^{-1} & \mathbf{Y}_C^{-1} + \mathbf{Y}_C^{-1} \mathbf{L}_C \mathbf{D}^{-1} \mathbf{L}_C^t \mathbf{Y}_C^{-1} \end{bmatrix} \begin{bmatrix} \mathbf{I}_A \\ \mathbf{I}_B \\ \mathbf{I}_C \end{bmatrix} \quad (3.26)$$

Separating (3.12) into two parts yields:

$$\begin{bmatrix} \mathbf{V}_A \\ \mathbf{V}_B \\ \mathbf{V}_C \end{bmatrix} = \begin{bmatrix} \mathbf{Y}_A^{-1} & & \\ & \mathbf{Y}_B^{-1} & \\ & & \mathbf{Y}_C^{-1} \end{bmatrix} \begin{bmatrix} \mathbf{I}_A \\ \mathbf{I}_B \\ \mathbf{I}_C \end{bmatrix} + \begin{bmatrix} \mathbf{Y}_A^{-1} \mathbf{L}_A \mathbf{D}^{-1} \mathbf{L}_A^t \mathbf{Y}_A^{-1} & \mathbf{Y}_A^{-1} \mathbf{L}_A \mathbf{D}^{-1} \mathbf{L}_B^t \mathbf{Y}_B^{-1} & \mathbf{Y}_A^{-1} \mathbf{L}_A \mathbf{D}^{-1} \mathbf{L}_C^t \mathbf{Y}_C^{-1} \\ \mathbf{Y}_B^{-1} \mathbf{L}_B \mathbf{D}^{-1} \mathbf{L}_A^t \mathbf{Y}_A^{-1} & \mathbf{Y}_B^{-1} \mathbf{L}_B \mathbf{D}^{-1} \mathbf{L}_B^t \mathbf{Y}_B^{-1} & \mathbf{Y}_B^{-1} \mathbf{L}_B \mathbf{D}^{-1} \mathbf{L}_C^t \mathbf{Y}_C^{-1} \\ \mathbf{Y}_C^{-1} \mathbf{L}_C \mathbf{D}^{-1} \mathbf{L}_A^t \mathbf{Y}_A^{-1} & \mathbf{Y}_C^{-1} \mathbf{L}_C \mathbf{D}^{-1} \mathbf{L}_B^t \mathbf{Y}_B^{-1} & \mathbf{Y}_C^{-1} \mathbf{L}_C \mathbf{D}^{-1} \mathbf{L}_C^t \mathbf{Y}_C^{-1} \end{bmatrix} \begin{bmatrix} \mathbf{I}_A \\ \mathbf{I}_B \\ \mathbf{I}_C \end{bmatrix} \quad (3.27)$$

Let $\mathbf{Y}_d^{-1} \mathbf{L} \mathbf{D}^{-1} = \boldsymbol{\gamma}$ and $\mathbf{Y}_d^{-1} \mathbf{L}^t = \boldsymbol{\gamma}^t$, then (3.31) reduces to:

$$\begin{bmatrix} \mathbf{V}_A \\ \mathbf{V}_B \\ \mathbf{V}_C \end{bmatrix} = \begin{bmatrix} \mathbf{Y}_A^{-1} & & \\ & \mathbf{Y}_B^{-1} & \\ & & \mathbf{Y}_C^{-1} \end{bmatrix} \begin{bmatrix} \mathbf{I}_A \\ \mathbf{I}_B \\ \mathbf{I}_C \end{bmatrix} + \begin{bmatrix} \boldsymbol{\gamma}_A \boldsymbol{\gamma}_A^t & \boldsymbol{\gamma}_A \boldsymbol{\gamma}_B^t & \boldsymbol{\gamma}_A \boldsymbol{\gamma}_C^t \\ \boldsymbol{\gamma}_B \boldsymbol{\gamma}_A^t & \boldsymbol{\gamma}_B \boldsymbol{\gamma}_B^t & \boldsymbol{\gamma}_B \boldsymbol{\gamma}_C^t \\ \boldsymbol{\gamma}_C \boldsymbol{\gamma}_A^t & \boldsymbol{\gamma}_C \boldsymbol{\gamma}_B^t & \boldsymbol{\gamma}_C \boldsymbol{\gamma}_C^t \end{bmatrix} \begin{bmatrix} \mathbf{I}_A \\ \mathbf{I}_B \\ \mathbf{I}_C \end{bmatrix} \quad (3.28)$$

3.4.1.2 Obtaining Branch Voltage Equation for BVMT

The branch voltage equation can be obtained by analysing (3.28) which can be re-written as:

$$\begin{bmatrix} \mathbf{V}_A \\ \mathbf{V}_B \\ \mathbf{V}_C \end{bmatrix} = \begin{bmatrix} \mathbf{Y}_A^{-1} & & \\ & \mathbf{Y}_B^{-1} & \\ & & \mathbf{Y}_C^{-1} \end{bmatrix} \begin{bmatrix} \mathbf{I}_A \\ \mathbf{I}_B \\ \mathbf{I}_C \end{bmatrix} + \begin{bmatrix} \gamma_A \\ \gamma_B \\ \gamma_C \end{bmatrix} \begin{bmatrix} \gamma_A^t & \gamma_B^t & \gamma_C^t \end{bmatrix} \begin{bmatrix} \mathbf{I}_A \\ \mathbf{I}_B \\ \mathbf{I}_C \end{bmatrix} \quad (3.29)$$

Isolating the subnetworks equations in (3.29) yields:

$$\mathbf{V}_A = \mathbf{Y}_A^{-1} \mathbf{I}_A + \gamma_A (\gamma_A^t \mathbf{I}_A + \gamma_B^t \mathbf{I}_B + \gamma_C^t \mathbf{I}_C) \quad (3.30)$$

$$\mathbf{V}_B = \mathbf{Y}_B^{-1} \mathbf{I}_B + \gamma_B (\gamma_A^t \mathbf{I}_A + \gamma_B^t \mathbf{I}_B + \gamma_C^t \mathbf{I}_C) \quad (3.31)$$

$$\mathbf{V}_C = \mathbf{Y}_C^{-1} \mathbf{I}_C + \gamma_C (\gamma_A^t \mathbf{I}_A + \gamma_B^t \mathbf{I}_B + \gamma_C^t \mathbf{I}_C) \quad (3.32)$$

If a network torn into \mathbf{m} number of subnetworks, for any subnet J, with admittance matrix \mathbf{Y}_J , the vector of nodal voltages is:

$$\mathbf{V}_J = \mathbf{Y}_J^{-1} \mathbf{I}_J + \gamma_J (\gamma_A^t \mathbf{I}_A + \gamma_B^t \mathbf{I}_B + \dots + \gamma_J^t \mathbf{I}_J + \dots + \gamma_M^t \mathbf{I}_M) \quad (3.33)$$

$$\mathbf{V}_J = \mathbf{Y}_J^{-1} \mathbf{I}_J + \gamma_J \sum_{m=A}^M \gamma_m^t \mathbf{I}_m \quad (m = A, B, \dots, J, \dots, M) \quad (3.34)$$

where $\gamma_J = \mathbf{Y}_J^{-1} \mathbf{L}_J \mathbf{D}^{-1}$ and $\gamma_J^t = \mathbf{L}_J^t \mathbf{Y}_J^{-1}$

Let:

$$\mathbf{e}_{b(\text{BVMT})} = \sum_{m=A}^M \gamma_m^t \mathbf{I}_m \quad (m = A, B, \dots, M) \quad (3.35)$$

Then, the complete solution for any subnet J is given in (3.36).

$$\mathbf{V}_J = \mathbf{Y}_J^{-1} \mathbf{I}_J + \gamma_J \mathbf{e}_{b(\text{BVMT})} \quad (3.36)$$

The branch voltage vector is common to all subnetworks, that is, $\mathbf{e}_{b(\text{BVMT})}$ need only be computed once for use in transforming the separate solutions of the subnetworks. This is similar to the equations obtained in [61] but it is easier understand how the subnetworks parameters fit into the solution of the original network in this analysis.

Let $\mathbf{V}_{0J} = \mathbf{Y}_J^{-1} \mathbf{I}_J$ and $\mathbf{v}_J = \gamma_J \mathbf{e}_b$, then (3.22) becomes:

$$\mathbf{V}_J = \mathbf{V}_{0J} + \mathbf{v}_J \quad (3.37)$$

\mathbf{V}_{0J} is voltage vector of subnet J when computed separately without the effect of interconnection to other subnetworks. The vector \mathbf{v}_J is the modifying voltage for subnet J . \mathbf{V}_J is voltage vector of subnet J that gives the complete solution of the original network for which subnet J is a part, as if it was solved as a piece. In view of (3.37) the voltage vector for the whole network can be written as:

$$\mathbf{V} = \mathbf{V}_0 + \mathbf{v} \quad (3.38)$$

Equation (3.38) is sufficient for load flow by current injection. The matrices γ and γ^t do not change during iteration and could be computed and stored permanently. This reduces the demand on the core storage on the computer [93]. The method of obtaining the equation of solution by direct inverse and the consequent branch voltage is in a novel idea that makes it easy to understand the tearing algorithm.

3.5 Slack Bus Voltage-Updating Diakoptic (SVUD) Load Flow

The integration of wind energy into an existing network poses challenges to the existing load flow techniques especially because their characteristics when working with conventional generation are still being investigated. In view of the advantages of iterative procedures outlined in section 1.4, especially in parallel computing, a most successful method will be that which combines the benefits of diakoptics with the advantages of iterative solutions for modern computing.

The slack bus voltage-updating diakoptics (SVUD) is a novel load flow method based on mixed methods. Although the idea of combining diakoptics with load flow is not new, the method of linking the subnetworks' solutions and updating the temporary slack bus voltage are new. Temporary slack buses are those in subnetworks that do not contain the slack bus of the original network. At the conception of diakoptics, linearity of a system was necessary for finding direct analytical solutions [3] but several attempts have been made to solve nonlinear systems using iterative procedures [42, 38, 43]. This is therefore another attempt to apply diakoptics to load flow analysis of power systems without linearizing. Therefore, detailed algorithms for embedding diakoptics into the Gauss-Seidel load flow are presented in this chapter in which the nonlinearity of the power system is retained. First, the algorithm for determining the branch voltage, $e_{b(SVUD)}$ is devised for application to the analysis of nonlinear systems. Secondly, the devised e_b is used in load flow analysis that involves updating e_b and slack bus voltage during the load flow process.

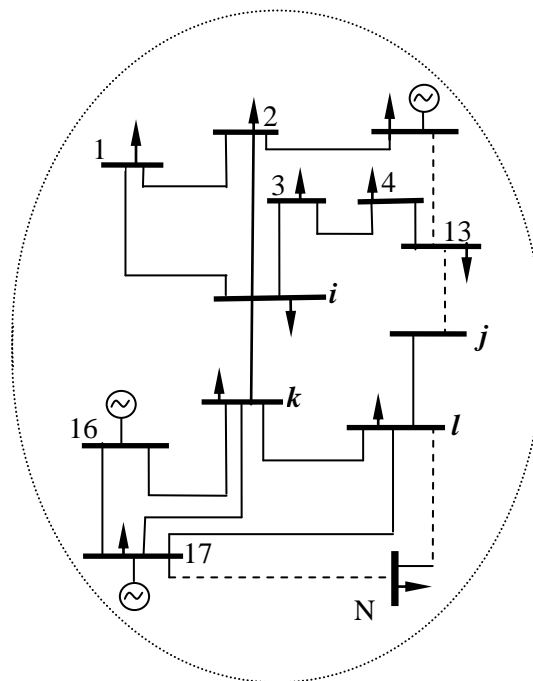


Figure 3.6. An N-bus network

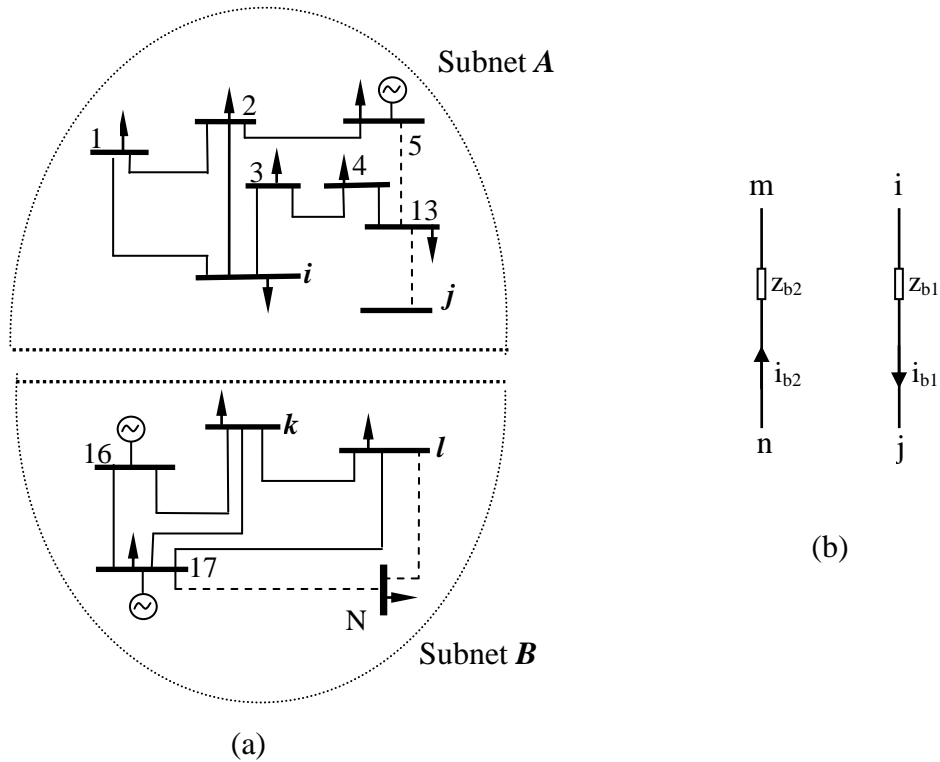


Figure 3.7. The n-bus network torn into two (a) Subnetworks (b) removed branches

3.5.1 Subnetworks

In large power systems, areas are interconnected by tie lines and contingency analysis of the tie line(s) is also an important feature in power system planning and operation studies. Figure 3.6 describes a large network with two areas interconnected by two lines $i-k$ and $j-l$ having series impedances z_{b1} and z_{b2} . If the interconnectors, $i-k$ and $j-l$ are removed, then, the admittance matrices \mathbf{Y}_A of subnet **A** and \mathbf{Y}_B of subnet **B** can be formed. Because there is no coupling between the subnetworks and between removed branches, the impedance matrix of the branch elements, \mathbf{Z}_b is a diagonal matrix.

3.5.2 Load Flow Studies

Load flow analysis has become an indispensable tool in the planning and operation of electrical power systems and forms the basis for solutions of other power system problems. The procedure is fundamentally a network analysis problem and involves

the solution of large sparse linear systems expressed in the general mathematical term as

$$\mathbf{Ax} = \mathbf{b} \quad (3.39)$$

In power systems analysis, \mathbf{x} represents the voltage vector of unknowns, \mathbf{b} is a known vector which represents the current, and the \mathbf{A} is usually a large sparse square matrix representing the admittance matrix. The load flow solution contains voltages and their angles at all the buses from which the real and reactive power generation, load levels at all buses, and the real and reactive flows across all circuits can be determined.

The load flow equation based on linear equation of (3.39) and expressed in terms of current (\mathbf{I}) and voltage (\mathbf{V}) is shown in (3.43) when the \mathbf{Y} matrix consists of only passive transmission elements and are therefore constant. When active elements like transformers, reactive power compensating devices are introduced into the matrix, the equation will no longer be linear.

$$\mathbf{YV} = \mathbf{I} \quad (3.40)$$

Equation (3.40) is the linear current-voltage (IV) flow equations. In an interconnected system, where the net current injected into the network at bus i is I_i , and V_i is voltage at bus i , the complex conjugate power at bus i is given by (3.41). This is the traditional power-voltage (SV) flow equations which is nonlinear quadratic type.

$$S_i^* = V_i^* I_i \quad (3.41)$$

In a network with N buses, the current I_i is the total current between bus i and all other nodes from 1 to N physically connected to i . If these nodes are indicated by n , Y_{in} is the admittances of all the links in the network, and V_n is the voltage difference between nodes i and n , the current at node i is given in (3.42).

$$I_i = \sum_{n=1}^N Y_{in} V_n \quad (3.42)$$

The complete set of power flow equations is expressed explicitly as

$$S_i^* = P + jQ = V_i^* I_i = V_i^* \sum_{n=1}^N Y_{in} V_n \quad (3.43)$$

$$S_i^* = (P_i - jQ_i) = V_i^* Y_{ii} V_i + V_i^* \sum_{\substack{n=1 \\ n \neq i}}^N Y_{in} V_n \quad (3.44)$$

$$V_i = \frac{1}{Y_{ii}} \left[\frac{P_i - jQ_i}{V_i^*} - \sum_{\substack{n=1 \\ n \neq i}}^N Y_{in} V_n \right] \quad (3.45)$$

3.5.2.1 Systems of Equations in Load flow analysis

In load flow analysis, two main constraints are normally applied; the linear equality constraints and the nonlinear equality constraints explained in [84]. The linear formulation, which is the **IV** formulation, involves the solution of the linear system of equations defined by (3.40) based on current injection. In this formulation, the constraints that apply to the general system are linear, while the nonlinear constraints are localized at the buses and transmission elements. Nonlinear formulation, on the other hand, is a PQV (or PV, QV) formulation represented by equations (3.56) which is a nonlinear system of equations. In this formulation, the constraints operating throughout the network is nonlinear while linear constraints are localized. Load flow analyses with linear solvers are therefore, generally faster than nonlinear solvers [84].

3.5.2.2 Classical Gauss-Seidel Load Flow Equation

Gauss-Seidel and Newton-Raphson are two of the earliest and presently the most commonly used iterative load flow methods for power systems analysis. The two methods are featured in this work but the emphasis here is on Gauss-Seidel method because of its simplicity and the need to develop an effective and ‘user friendly’ load flow method. Both methods were applied in the solution of the network in Figure 3.8 before tearing. After tearing the networks, only Gauss-Seidel was found to converge for the two subnetworks. Newton-Raphson failed to converge for subnet B because of the topology of the system.

The load flow equation given by (3.45) is a nonlinear equation which makes it difficult to solve exactly mathematically and is normally solved by iterative methods

to specified accuracy. In the G-S algorithm, the equation is utilized to find the final bus voltage at bus i in successive steps of iterations using (3.46).

$$V_i^{k+1} = \frac{1}{Y_{ii}} \left[\frac{P_i - jQ_i}{V_i^{*k}} - \sum_{\substack{n=1 \\ n \neq i}}^N Y_{in} V_n^k \right] \quad (3.46)$$

The error difference between successive iterations is given by $\Delta V_i^{k+1} = V_i^{k+1} - V_i^k$. To satisfy convergence the error difference should be within specified value. $\Delta V_i^{k+1} \approx \varepsilon$. This is usually dictated by the reason for the load flow, which is, planning, contingency analysis, etc.

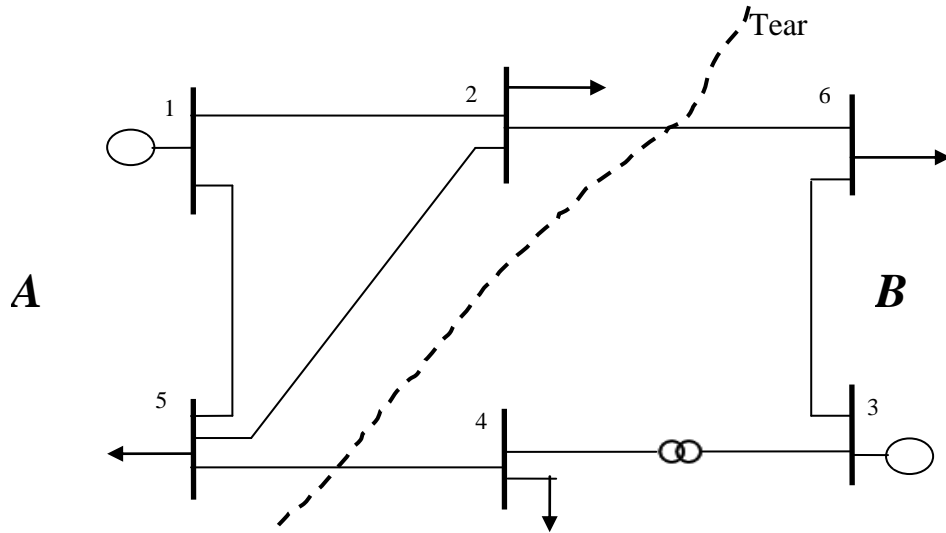


Figure 3.8. Six-bus network

3.5.2.3 Formulation of the SVUD Load Flow

The SVUD solves the nonlinear load flow equation iteratively in a new way which allows a temporary slack bus voltage to vary during the process like in a one piece solution.

Before this work, no slack bus voltage-updating load flow of torn networks has been found in literature although voltage correction is a general principle in load flow analysis as presented in [99].

3.5.2.4 Branch Voltage for SVUD Analysis

The branch voltage is a key factor for modifying solutions of subnetworks obtained separately. In power systems, the given data at the nodes are usually combinations of two of the following – voltages V , voltage angles δ , active powers P , and reactive powers Q . The derived branch voltage equation given in (3.35) for $e_{b(BVMT)}$ is not convenient for direct application to nonlinear systems which would entail conversion of given quantities to current injections as in [43, 61]. For direct and easier application, the algorithm is extended such that the nonlinearity of power flow equations is retained. Expansion (3.35) for two subnetworks yields:

$$\mathbf{e}_{b(SVUD)} = (\boldsymbol{\gamma}_A^t \mathbf{I}_A + \boldsymbol{\gamma}_B^t \mathbf{I}_B) \quad (3.47)$$

But $\boldsymbol{\gamma}^t = \mathbf{L}^t \mathbf{Y}_d^{-1}$

$$\therefore \mathbf{e}_{b(SVUD)} = (\mathbf{L}_A^t \mathbf{Y}_A^{-1} \mathbf{I}_A + \mathbf{L}_B^t \mathbf{Y}_B^{-1} \mathbf{I}_B) \quad (3.48)$$

Substituting $\mathbf{I} = \mathbf{Y}\mathbf{V}$ in equation (3.48) for all subnetworks yields

$$\mathbf{e}_{b(SVUD)} = (\mathbf{L}_A^t \mathbf{Y}_A^{-1} \mathbf{Y}_A \mathbf{V}_{0A} + \mathbf{L}_B^t \mathbf{Y}_B^{-1} \mathbf{Y}_B \mathbf{V}_{0B}) \quad (3.49)$$

$$\therefore \mathbf{e}_{b(SVUD)} = (\mathbf{L}_A^t \mathbf{V}_{0A} + \mathbf{L}_B^t \mathbf{V}_{0B}) \quad (3.50)$$

For any number of subnetworks M , $e_{b(SVUD)}$ can be obtained using (3.51)).

$$\mathbf{e}_{b(SVUD)} = \sum_{m=A}^M \mathbf{L}_m^t \mathbf{V}_{0m} \quad (m = A, B, \dots, M) \quad (3.51)$$

where \mathbf{V}_{0m} is the voltage vector of subnetworks computed when they are completely decoupled. Equation (3.51) is a much easier method of obtaining the branch voltage. This further simplifies the determination of branch voltage equation which is applicable in (3.45).

The connection matrices, \mathbf{L}_A and \mathbf{L}_B , for the network of Figure 3.7, are given in equations (3.29) and (3.30) and the voltage vectors are given in equations (3.31) and (3.32).

$$\mathbf{L}_A^t = \begin{bmatrix} 0 & 0 & \dots & 1 & 0 & \dots & 0 \\ 0 & 0 & \dots & 0 & 1 & \dots & 0 \end{bmatrix} \quad (3.52)$$

$$\mathbf{L}_B^t = \begin{bmatrix} 0 & 0 & \dots & -1 & 0 & \dots & 0 \\ 0 & 0 & \dots & 0 & -1 & \dots & 0 \end{bmatrix} \quad (3.53)$$

$$\mathbf{V}_{0A} = \begin{bmatrix} \mathbf{V}_{0A1} \\ \mathbf{V}_{0A2} \\ \vdots \\ \mathbf{V}_{0Ai} \\ \mathbf{V}_{0Aj} \\ \vdots \\ \mathbf{V}_{0A13} \end{bmatrix} \quad (3.54)$$

$$\mathbf{V}_{0B} = \begin{bmatrix} \mathbf{V}_{0B16} \\ \mathbf{V}_{0B17} \\ \vdots \\ \mathbf{V}_{0Bk} \\ \mathbf{V}_{0Bl} \\ \vdots \\ \mathbf{V}_{0BN} \end{bmatrix} \quad (3.55)$$

Substituting (3.52) - (3.55) in (3.51) yields:

$$\mathbf{e}_{b(SVUD)} = \begin{bmatrix} 0 & 0 & \dots & 1 & 0 & \dots & 0 \\ 0 & 0 & \dots & 0 & 1 & \dots & 0 \end{bmatrix} \begin{bmatrix} \mathbf{V}_{0A1} \\ \mathbf{V}_{0A2} \\ \vdots \\ \mathbf{V}_{0Ai} \\ \mathbf{V}_{0Aj} \\ \vdots \\ \mathbf{V}_{0A13} \end{bmatrix} + \begin{bmatrix} 0 & 0 & \dots & -1 & 0 & \dots & 0 \\ 0 & 0 & \dots & 0 & -1 & \dots & 0 \end{bmatrix} \begin{bmatrix} \mathbf{V}_{0B16} \\ \mathbf{V}_{0B17} \\ \vdots \\ \mathbf{V}_{0Bk} \\ \mathbf{V}_{0Bl} \\ \vdots \\ \mathbf{V}_{0BN} \end{bmatrix} \quad (3.56)$$

$$\therefore \mathbf{e}_{\mathbf{b(SVUD)}} = \begin{bmatrix} \mathbf{V}_{0Ai} \\ \mathbf{V}_{0Aj} \end{bmatrix} + \begin{bmatrix} -\mathbf{V}_{0Bk} \\ -\mathbf{V}_{0Bl} \end{bmatrix} \quad (3.57)$$

$$= \begin{bmatrix} \mathbf{V}_{0Ai} - \mathbf{V}_{0Bk} \\ \mathbf{V}_{0Aj} - \mathbf{V}_{0Bl} \end{bmatrix} \quad (3.58)$$

Equations (3.51) and (3.58) are the new equations for computing the branch voltage and are more appropriate in iterative load flow procedures and for load flow using current injections. Evaluation of (3.58) shows that V_{0Ai} , V_{0Am} in subnet A and V_{0Bj} , V_{0Bn} in subnet B are the voltages of terminating buses computed when the subnetworks are uncoupled. Equations (3.51) and (3.58) show that the branch voltage, e_b , can be computed directly from the initial bus voltages. It should be noted that (3.51) and (3.58) can also be applied directly for linear analysis. This method of obtaining branch voltage is different from the methods surveyed in literature especially in the original formulations of diakoptics in that the whole voltage vector can be used directly in the determination without selecting the boundary bus voltages. Although this method of obtaining the branch voltage was discovered experimentally and mathematically proved independently in this research, the idea is somewhat related to the ideas presented in [43] [100] [75]. The key difference is that in the references, the usual principle of voltage drop across lines is assumed while in this work it has been derived by the application of diakoptics and connection matrices to basic power system equations. Also, applications in the references are based on impedance methods for load flow and contingency analysis. The major advance of the method of analysis in this work is that each stage of the derivation can easily be identified with and applied in diakoptic analysis.

3.5.3 *Modelling Voltages of Subnetworks*

As already explained in section 3.2, the voltages of individual subnetworks obtained in their separate calculations need to be modelled using information from the removed branches to obtain the required node voltages for the original system. In view of (3.51), vector of voltages of the complete network is

$$\mathbf{V} = \mathbf{Y}_d^{-1}\mathbf{I} + \gamma\mathbf{e}_b(\text{SVUD}) \quad (3.59)$$

Let $\mathbf{V}_0 = \mathbf{Y}^{-1}\mathbf{I}$ and $\mathbf{v} = \gamma\mathbf{e}_b$, then (3.59) becomes,

$$\mathbf{V} = \mathbf{V}_0 + \mathbf{v} \quad (3.60)$$

Where \mathbf{V}_0 is vector of subnetworks voltages computed separately, \mathbf{v} is the modifying voltage vector and \mathbf{V} is the vector of updated subnetworks voltages that give the solution of the complete network. Again, equation (3.60) is also applicable to linear systems. \mathbf{V}_0 can be computed using any chosen method but Gauss-Seidel load flow method is applied in this analysis. For the network of Figure 3.8 when torn into two along the line of tear,

$$\mathbf{V}_0 = \begin{bmatrix} \mathbf{V}_{0A} \\ \mathbf{V}_{0B} \end{bmatrix} = \begin{bmatrix} \mathbf{Y}_A^{-1} & \\ & \mathbf{Y}_B^{-1} \end{bmatrix} \begin{bmatrix} \mathbf{I}_A \\ \mathbf{I}_B \end{bmatrix} \quad (3.61)$$

and

$$\mathbf{v} = \begin{bmatrix} \mathbf{v}_A \\ \mathbf{v}_B \end{bmatrix} = \begin{bmatrix} \gamma_A \\ \gamma_B \end{bmatrix} [\mathbf{e}_b(\text{SVUD})] \quad (3.62)$$

The complete solution of the network solved separately is given in (3.63) and (3.64).

$$\mathbf{V}_A = \mathbf{V}_{0A} + \mathbf{v}_A \quad (3.63)$$

$$\mathbf{V}_B = \mathbf{V}_{0B} + \mathbf{v}_B \quad (3.64)$$

The voltage vectors in view of equations (3.63) and (3.64) are

$$\mathbf{V}_A = \begin{bmatrix} \mathbf{V}_{A1} \\ \mathbf{V}_{A2} \\ \vdots \\ \mathbf{V}_{Ai} \\ \mathbf{V}_{Aj} \\ \vdots \\ \mathbf{V}_{A13} \end{bmatrix} \quad (3.65)$$

$$\mathbf{V}_B = \begin{bmatrix} \mathbf{V}_{B16} \\ \mathbf{V}_{B17} \\ \vdots \\ \mathbf{V}_{Bk} \\ \mathbf{V}_{Bl} \\ \vdots \\ \mathbf{V}_{BN} \end{bmatrix} \quad (3.66)$$

3.5.3.1 SVUD Equations for Solution

The admittance matrix \mathbf{Y} represents the topology and parameters of the network to be analysed and comprises all the admittances in the network. The diagonal admittance matrix composed of the subnetworks admittances \mathbf{Y}_A and \mathbf{Y}_B do not represent the whole network because some branches have been removed to tear the network. The SVUD algorithm is presented in this section where the G-S load flow equation is embedded in SVUD equation to obtain a new load flow method which takes advantage of network tearing. For subnet A, (3.40) – (3.45) are expressed in (3.67) – (3.74).

$$\mathbf{I}_A = \mathbf{Y}_A \mathbf{V}_{0A} \quad (3.67)$$

In view of equation (3.42) the current injection at node i of subnet A is

$$I_{Ai} = \sum_{n=1}^{N_A} Y_{Ain} V_{0An} \quad (3.68)$$

where N_A is the total number of buses in subnet A. The complex power at node i is

$$S_{0Ai}^* = V_{0Ai}^* I_{Ai} \quad (3.69)$$

Substituting (3.68) in (3.69) yields

$$S_{0Ai}^* = V_{0Ai}^* \sum_{n=1}^{N_A} Y_{Ain} V_{0An} \quad (3.70)$$

Analysis of equation (3.70) gives equations (3.71) – (3.74).

$$S_{0Ai}^* = V_{0Ai}^* Y_{Aii} V_{0Ai} + V_{0Ai}^* \sum_{\substack{n=1 \\ n \neq i}}^{N_A} Y_{Ain} V_{0An} \quad (3.71)$$

$$\frac{S_{0Ai}^*}{V_{0Ai}^*} = Y_{Aii} V_{0Ai} + \sum_{\substack{n=1 \\ n \neq i}}^{N_A} Y_{Ain} V_{0An} \quad (3.72)$$

$$V_{0Ai} = \frac{1}{Y_{Aii}} \left[\frac{S_{0Ai}^*}{V_{0Ai}^*} - \sum_{\substack{n=1 \\ n \neq i}}^{N_A} Y_{Ain} V_{0An} \right] \quad (3.73)$$

$$V_{0Ai} = \frac{1}{Y_{Aii}} \left[\frac{P_{0Ai} - jQ_{0Ai}}{V_{0Ai}^*} - \sum_{\substack{n=1 \\ n \neq i}}^{N_A} Y_{Ain} V_{0An} \right] \quad (3.74)$$

V_{0Ai} in (3.74) is the voltage at node i of subnet A ; applying iteration steps yields equation (3.75). Equation (3.76) is similarly written for subnet B .

$$V_{0Ai}^{k+1} = \frac{1}{Y_{Aii}} \left[\frac{P_{0Ai} - jQ_{0Ai}}{V_{0Ai}^{*k}} - \sum_{\substack{n=1 \\ n \neq i}}^{N_A} Y_{Ain} V_{0An}^k \right] \quad (3.75)$$

$$V_{0Bi}^{k+1} = \frac{1}{Y_{Bii}} \left[\frac{P_{0Bi} - jQ_{0Bi}}{V_{0Bi}^{*k}} - \sum_{\substack{n=1 \\ n \neq i}}^{N_B} Y_{Bin} V_{0Bn}^k \right] \quad (3.76)$$

The voltage vectors, V_{0Ai} and V_{0Bi} obtained in load flow analysis of the subnetworks separately are not the values that would be obtained in one-piece solution. To obtain the required node voltages, some changes must be made to the G-S load flow equations of each subnet in (3.75) and (3.76) to take care of the effect of connection to other subnetworks. The voltages v_A and v_B in equations (3.77) and (3.78) represent the voltage values which when added to the subnetworks results would modify the

individual subnet solutions to give the desired node voltages as in the original system before tearing; the voltages v_A and v_B are as defined in (3.62).

$$V_{0Ai}^{k+1} = \frac{1}{Y_{Aii}} \left[\frac{P_{0Ai} - jQ_{0Ai}}{V_{0Ai}^{*k}} - \sum_{\substack{n=1 \\ n \neq i}}^N Y_{Ain} V_{0An}^k \right] + v_A \quad (3.77)$$

$$V_{0Bi}^{k+1} = \frac{1}{Y_{Bii}} \left[\frac{P_{0Bi} - jQ_{0Bi}}{V_{0Bi}^{*k}} - \sum_{\substack{n=1 \\ n \neq i}}^N Y_{Bin} V_{0Bn}^k \right] + v_B \quad (3.78)$$

3.5.4 Updating Algorithm for Temporary Slack Bus Voltage

Iterative load flow analysis is based on the principle of voltage updating which is explained in [99] for normal one-piece network analysis where the slack bus voltage is kept constant throughout the iterative process. A special feature of the SVUD is the slack bus voltage updating algorithm which causes the temporary slack bus voltage to vary like other buses during the iterative process.

Diakoptics involves at least two networks (subnetworks) derived from a whole network. When the analyses of these subnetworks are computed with normal load flow algorithm, there is a need for extra or temporary slack buses. Buses in the subnetworks that do not contain the original slack bus would either be a load or generator buses; in the one-piece load flow solution, the complex voltages of these temporary buses are not constant. However, if any of the load or generator buses is chosen as a slack bus, its voltage will remain constant as the original slack bus voltage and this affects the results. Updating the temporary slack bus voltage after each iteration makes it behave as if it was in a one-piece load flow iterative process. The updating algorithms for the temporary buses are laid out in this section.

3.5.4.1 Load Bus Updating Algorithm

Consider bus i where the scheduled or specified real and reactive power inputs are P_{is} and Q_{is} . Let the computed current injection at bus i be $I_i = (a_i + jb_i)$ and computed

voltage be $V_i = (e_i + jf_i)$. The calculated power corresponding to this voltage and current is

$$P_{ic} + jQ_{ic} = V_i I_i = (e_i + jf_i)(a_i + jb_i) \quad (3.79)$$

$$= (a_i e_i + b_i f_i) + j(a_i f_i - b_i e_i) \quad (3.80)$$

Separating real and imaginary parts:

$$P_{ic} = (a_i e_i + b_i f_i) \quad (3.81)$$

$$Q_{ic} = j(a_i f_i - b_i e_i) \quad (3.82)$$

The computed power is different from the scheduled power. Let ΔP_i and ΔQ_i be the deviations from the scheduled values and the corrective voltage be $\Delta V_i = \mu_i + j\lambda_i$. The corrective current due to this voltage is $\Delta I_i = Y_{ii} \Delta V_i$, where $Y_{ii} = G_{ii} + jB_{ii}$ is the diagonal element of the bus admittance matrix. The corrected currents and voltages are $(I_i + \Delta I_i)$ and $(V_i + \Delta V_i)$. The corrected current with the corrected voltage produce the scheduled power in (3.89).

$$P_{is} + jQ_{is} = (V_i + \Delta V_i)(I_i + \Delta I_i)^* \quad (3.83)$$

Substituting the expressions for V_i , I_i , ΔV_i and ΔI_i , in (3.89) gives:

$$\begin{aligned} P_{is} + jQ_{is} &= [(e_i + jf_i) + (\mu_i + j\lambda_i)][(a_i + jb_i) + (G_{ii} + jB_{ii})(\mu_i + j\lambda_i)]^* \\ &= [(e_i + jf_i) + (\mu_i + j\lambda_i)][(a_i + jb_i) + (G_{ii}\mu_i + jG_{ii}\lambda_i) + jB_{ii}\mu_i - B_{ii}\lambda_i]^* \\ &= [(e_i + jf_i) + (\mu_i + j\lambda_i)][(a_i + G_{ii}\mu_i - B_{ii}\lambda_i) - j(b_i + G_{ii}\lambda_i + B_{ii}\mu_i)]^* \\ &= e_i a_i + e_i G_{ii} \mu_i - e_i \lambda_i B_{ii} - j(e_i b_i + e_i G_{ii} \lambda_i + e_i B_{ii} \mu_i) \\ &\quad + jf_i a_i + jf_i G_{ii} \mu_i - jf_i \lambda_i B_{ii} + f_i b_i + f_i G_{ii} \lambda_i + f_i B_{ii} \mu_i \\ &\quad - \mu_i a_i + \mu_i^2 G_{ii} - \mu_i B_{ii} \lambda_i - j(\mu_i b_i + \mu_i G_{ii} \lambda_i + \mu_i^2 B_{ii}) \\ &\quad + j\lambda_i a_i + j\lambda_i G_{ii} \mu_i - j\lambda_i^2 B_{ii} + \lambda_i b_i + \lambda_i^2 G_{ii} + \lambda_i B_{ii} \mu_i \end{aligned} \quad (3.84)$$

$$\begin{aligned}
 P_{is} + jQ_{is} = & e_i a_i + e_i G_{ii} \mu_i - e_i \lambda_i B_{ii} + f_i b_i + f_i G_{ii} \lambda_i + f_i B_{ii} \mu_i + \lambda_i b_i + \lambda_i^2 G_{ii} \lambda_i B_{ii} \mu_i \\
 & - \mu_i a_i + \mu_i^2 G_{ii} - \mu_i B_{ii} \lambda_i - j(e_i b_i + e_i G_{ii} \lambda_i + e_i B_{ii} \mu_i) + j f_i a_i + j f_i G_{ii} \mu_i \\
 & - j f_i \lambda_i B_{ii} - j(\mu_i b_i + \mu_i G_{ii} \lambda_i + \mu_i^2 B_{ii}) + j \lambda_i a_i + j \lambda_i G_{ii} \mu_i - j \lambda_i^2 B_{ii}
 \end{aligned} \quad (3.85)$$

Analysis of (3.85) produces the scheduled real and reactive power in equations (3.86) and (3.87).

$$\begin{aligned}
 P_{is} = & \mu_i (e_i G_{ii} + f_i B_{ii} + a_i) + \lambda_i (-e_i B_{ii} + f_i G_{ii} + b_i) + e_i a_i + f_i b_i \\
 & + G_{ii} (\mu_i^2 G_{ii} + \lambda_i^2)
 \end{aligned} \quad (3.86)$$

$$\begin{aligned}
 Q_{is} = & \mu_i (e_i B_{ii} + f_i G_{ii} + b_i) + \lambda_i (-e_i G_{ii} + f_i B_{ii} + a_i) + e_i b_i + f_i a_i \\
 & + B_{ii} (\mu_i^2 + \lambda_i^2)
 \end{aligned} \quad (3.87)$$

The voltages, μ_i and λ_i are usually small, so the higher order terms are neglected. The resulting equations are therefore

$$P_{is} = \mu_i (e_i G_{ii} + f_i B_{ii} + a_i) + \lambda_i (-e_i B_{ii} + f_i G_{ii} + b_i) + e_i a_i + f_i b_i \quad (3.88)$$

$$Q_{is} = \mu_i (e_i B_{ii} + f_i G_{ii} + b_i) + \lambda_i (-e_i G_{ii} + f_i B_{ii} + a_i) + e_i b_i + f_i a_i \quad (3.89)$$

Equations (3.96) and (3.97) are the real and reactive power deviations from the scheduled values.

$$\Delta P_i = P_{is} - P_{ic} \quad (3.90)$$

$$\Delta Q_i = Q_{is} - Q_{ic} \quad (3.91)$$

Substituting for P_{is} , P_{ic} , in (3.96) from (3.81) and (3.85) yields (3.92). Similarly, substitution for Q_{is} , Q_{ic} from (3.82) and (3.86) in (3.91) yields (3.93).

$$\Delta P_i = \mu_i (e_i G_{ii} + f_i B_{ii} + a_i) + \lambda_i (-e_i B_{ii} + f_i G_{ii} + b_i) \quad (3.92)$$

$$\Delta Q_i = \mu_i (-e_i B_{ii} + f_i G_{ii} - b_i) + \lambda_i (-e_i G_{ii} + f_i B_{ii} + a_i) \quad (3.93)$$

Equations (3.92) and (3.93) are solved simultaneously to obtain the voltage deviation, $\Delta V_i = (\mu_i + j\lambda_i)$. At any iteration, the terms in brackets are considered constants for node i , therefore let:

$$c_1 = (e_i G_{ii} + f_i B_{ii} + a_i) \quad (3.94)$$

$$c_2 = (-e_i B_{ii} + f_i G_{ii} + b_i) \quad (3.95)$$

$$m_1 = (-e_i B_{ii} + f_i G_{ii} - b_i) \quad (3.96)$$

$$m_2 = (-e_i G_{ii} + f_i B_{ii} + a_i) \quad (3.97)$$

Substituting equations (3.94) - (3.97) in (3.92) and (3.93), they become:

$$\Delta P_i = c_1 \mu_i + c_2 \lambda_i \quad (3.98)$$

$$\Delta Q_i = m_1 \mu_i + m_2 \lambda_i \quad (3.99)$$

The corrective voltages μ_i and λ_i are the unknown quantities required for updating the voltage, therefore the equations are solved for the two unknowns as follows.

From (3.99),

$$\mu_i = \left(\frac{\Delta Q_i - m_2 \lambda_i}{m_1} \right) \quad (3.100)$$

Substituting for μ_i in (3.98) and solving yields,

$$\begin{aligned} \Delta P_i &= \frac{c_1 \Delta Q_i - m_2 \lambda_i}{m_1} + c_2 \lambda_i \\ &= \frac{c_1 \Delta Q_i}{m_1} - \left(\frac{c_1 m_2}{m_1} - c_2 \right) \lambda_i \end{aligned} \quad (3.101)$$

From which:

$$\left(\frac{c_1 m_2}{m_1} - \frac{m_1 c_2}{m_1} \right) \lambda_i = \frac{c_1 \Delta Q_i}{m_1} - \frac{m_1 \Delta P_i}{m_1}$$

$$\lambda_i = \frac{c_1 \Delta Q_i - m_1 \Delta P_i}{c_1 m_2 - m_1 c_2} \quad (3.102)$$

Substituting for λ_i in (3.100) yields:

$$\Delta P_i = c_1 \mu_i + c_2 \left(\frac{c_1 \Delta Q_i - m_1 \Delta P_i}{c_1 m_2 - m_1 c_2} \right) \quad (3.103)$$

$$\mu_i = \frac{\Delta P_i}{c_1} - \frac{c_2}{c_1} \left(\frac{c_1 \Delta Q_i - m_1 \Delta P_i}{c_1 m_2 - m_1 c_2} \right)$$

$$= \frac{\Delta P_i c_1 m_2 - \Delta P_i c_2 m_1 - c_1 c_2 \Delta Q_i - c_2 m_1 \Delta P_i}{c_1 (c_1 m_2 - m_1 c_2)} \quad (3.104)$$

$$= \frac{\Delta P_i c_1 m_2 - c_1 c_2 \Delta Q_i}{c_1 (c_1 m_2 - m_1 c_2)}$$

$$\therefore \mu_i = \frac{m_2 \Delta P_i - c_2 \Delta Q_i}{(c_1 m_2 - m_1 c_2)} \quad (3.105)$$

Let $(k_1 m_2 - m_1 k_2) = C_1$, then equations (3.104) and (3.102) become:

$$\mu_i = C_1^{-1} (m_2 \Delta P_i - c_2 \Delta Q_i) \quad (3.106)$$

$$\lambda_i = C_1^{-1} (c_1 \Delta Q_i - m_1 \Delta P_i) \quad (3.107)$$

Equations (3.106) and (3.107) are the corrective equations for the temporary slack bus if it was originally a load bus.

3.5.4.2 Generator Bus Updating Algorithm

If the temporary slack bus was originally a generator bus, the voltage correction principle is slightly different. In a generator bus the active power and voltage

magnitude are specified but the load flow process is started with a complete set of estimated voltage $V_n = (e_n + jf_n)$. Consider bus n , where power P_{ns} and the voltage V_{ns} are specified. The current $I_n = (a_n + jb_n)^*$ can be computed from (3.108). The power P_{nc} is obtained by multiplying this current with the voltage V_n and taking the real part of the product.

$$P_{nc} = (a_n e_n + b_n f_n) \quad (3.108)$$

$$|V_n|^2 = (e_n^2 + f_n^2) \quad (3.109)$$

Let the active power and voltage deviations be ΔP_n and $\Delta |V_n|$, then

$$\Delta P_n = P_{ns} - P_{nc} \quad (3.110)$$

$$\Delta |V_n|^2 = (|V_{ns}|^2 - |V_{nc}|^2) \quad (3.111)$$

Let the voltage that will be added to the calculated voltage to produce the scheduled power be

$$\Delta V_n = \mu_n + j\lambda_n \quad (3.112)$$

The scheduled power is therefore given as

$$P_{ns} + jQ_{ns} = (V_n + \Delta V_n)(I_n + \Delta I_n)^* \quad (3.113)$$

Expanding (3.113) and separating real and imaginary parts yields the active power in (3.114).

$$P_{ns} = \mu_n (e_n G_{nn} + f_n B_{nn} + a_n) + \lambda_n (-e_n B_{nn} + f_n G_{nn} + b_n) + e_n a_n + f_n b_n + G_{nn} (\mu_n^2 G_{nn} + \lambda_n^2) \quad (3.114)$$

In view of equations (3.108), (3.111) and (3.114), the power deviation is obtained as

$$\therefore \Delta P_n = \mu_n (e_n G_{nn} + f_n B_{nn} + a_n) + \lambda_n (-e_n B_{nn} + f_n G_{nn} + b_n) \quad (3.115)$$

$$\begin{aligned} V_n + \Delta V_n &= (e_n + jf_n) + (\lambda_n + j\lambda_n) \\ &= (e_n + \mu_n) + j(f_n + \lambda_n) \end{aligned} \quad (3.116)$$

$$\begin{aligned} |\mathbf{V}_n + \Delta\mathbf{V}_n|^2 &= (\mathbf{e}_n + \boldsymbol{\mu}_n)^2 + (\mathbf{f}_n + \boldsymbol{\lambda}_n)^2 \\ &= 2\mathbf{e}_n\boldsymbol{\mu}_n + 2\mathbf{f}_n\boldsymbol{\lambda}_n + \mathbf{e}_n^2 + \mathbf{f}_n^2 + (\boldsymbol{\mu}_n^2 + \mathbf{j}\boldsymbol{\lambda}_n^2) \end{aligned} \quad (3.117)$$

The voltage magnitude deviation is given as

$$\Delta|\mathbf{V}_n|^2 = |\mathbf{V}_n + \Delta\mathbf{V}_n|^2 - |\mathbf{V}_n|^2 \quad (3.118)$$

Neglecting the higher-degree terms

$$\Delta|\mathbf{V}_n|^2 = 2\mathbf{e}_n\boldsymbol{\mu}_n + 2\mathbf{f}_n\boldsymbol{\lambda}_n \quad (3.119)$$

Let:

$$\mathbf{c}_3 = (\mathbf{e}_n \mathbf{G}_{nn} + \mathbf{f}_n \mathbf{B}_{nn} + \mathbf{a}_n) \quad (3.120)$$

$$\mathbf{c}_4 = (-\mathbf{e}_n \mathbf{B}_{nn} + \mathbf{f}_n \mathbf{G}_{nn} + \mathbf{b}_n)$$

Equation (3.114) becomes

$$\therefore \Delta\mathbf{P}_n = \boldsymbol{\mu}_n \mathbf{c}_3 + \boldsymbol{\lambda}_n \mathbf{c}_4 \quad (3.121)$$

Equations (3.119) and (3.121) are solved simultaneously. From (3.121),

$$\boldsymbol{\mu}_n = \frac{\Delta\mathbf{P}_n - \boldsymbol{\lambda}_n \mathbf{c}_4}{\mathbf{c}_3} \quad (3.122)$$

$$\Delta|\mathbf{V}_n|^2 = 2\mathbf{e}_n \left(\frac{\Delta\mathbf{P}_n - \boldsymbol{\lambda}_n \mathbf{c}_4}{\mathbf{c}_3} \right) + 2\mathbf{f}_n \boldsymbol{\lambda}_n \quad (3.123)$$

$$\Delta|\mathbf{V}_n|^2 = \frac{2\mathbf{e}_n \Delta\mathbf{P}_n - \boldsymbol{\lambda}_n \mathbf{c}_4 + 2\mathbf{f}_n \boldsymbol{\lambda}_n \mathbf{c}_3}{\mathbf{c}_3} \quad (3.124)$$

$$\Delta|\mathbf{V}_n|^2 \mathbf{c}_3 = 2\mathbf{e}_n \Delta\mathbf{P}_n - \boldsymbol{\lambda}_n (\mathbf{c}_4 + 2\mathbf{f}_n \mathbf{c}_3) \quad (3.125)$$

$$\boldsymbol{\lambda}_n (\mathbf{c}_4 + 2\mathbf{f}_n \mathbf{c}_3) = 2\mathbf{e}_n \Delta\mathbf{P}_n - \Delta|\mathbf{V}_n|^2 \mathbf{c}_3 \quad (3.126)$$

$$\boldsymbol{\lambda}_n = \frac{2\mathbf{e}_n \Delta\mathbf{P}_n - \Delta|\mathbf{V}_n|^2 \mathbf{c}_3}{(\mathbf{c}_4 + 2\mathbf{f}_n \mathbf{c}_3)} \quad (3.127)$$

Let:

$$C_2 = (c_4 + 2f_n c_3) \quad (3.128)$$

$$\lambda_n = \frac{2e_n \Delta P_n - \Delta |V_n|^2 c_3}{C_2} = C_2^{-1} (2e_n \Delta P_n - \Delta |V_n|^2 c_3) \quad (3.129)$$

Substituting for λ_n in equation (3.119) and solving:

$$\mu_n c_3 = \Delta P_n - \frac{c_4 (2e_n \Delta P_n - \Delta |V_n|^2 c_3)}{C_2} \quad (3.130)$$

$$\mu_n = \frac{\Delta P_n}{c_3} - \frac{c_4 (2e_n \Delta P_n - \Delta |V_n|^2 c_3)}{c_3 C_2} \quad (3.131)$$

$$= \frac{\Delta P_n}{c_3} - \frac{c_4 2e_n \Delta P_n}{c_3 C_2} - \frac{\Delta |V_n|^2 c_3 c_4}{c_3 C_2} \quad (3.132)$$

$$= \Delta P_n c_3^{-1} - c_3^{-1} c_4 2e_n \Delta P_n C_2^{-1} - \Delta |V_n|^2 c_4 C_2^{-1} \quad (3.133)$$

$$\therefore \mu_n = \Delta P_n c_3^{-1} (1 - c_4 2e_n C_2^{-1}) - \Delta |V_n|^2 c_4 C_2^{-1} \quad (3.134)$$

The real and imaginary parts of the corrective voltage are μ_n and λ_n in (3.134) and (3.129).

3.6 Flow Charts for Slack Bus Voltage-Updating Diakoptics (SVUD) Load Flow

The flow charts of the proposed algorithm are shown in Figure 3.10 for sequential computing and Figure 3.11 for parallel computing. For very large systems, parallel computation will reduce the computation burden [101] and therefore lower memory computers can be used in parallel to perform the task of supercomputers with large memories. Two subnetworks A and B are presented in the flow charts for clarity but can be applied to any number of subnetworks.

In both methods the process starts by choosing the appropriate branches that will tear the network into the desired number of subnetworks. Data of subnetworks and removed branches are then loaded into the system. Alternatively, the whole system data can be loaded into the computer before choosing the branches to remove but this will negate one of the advantages of tearing which is reduced data handling.

3.6.1 *Flow Chart for Sequential Computing*

In sequential analysis, the admittance matrices \mathbf{Y}_A , \mathbf{Y}_B , connection matrices \mathbf{L}_A , \mathbf{L}_B of the subnetworks and impedance diagonal matrix, \mathbf{Z}_b of the removed branch impedances are formed. Gauss-Seidel load flow for the subnetworks is performed using (3.75) and (3.76). After $(k+1)^{\text{th}}$ iteration the voltage values are used to compute e_b^{k+1} from equation (3.58). The voltages of the subnetworks are then modified using (3.44) and (3.45). The chosen slack bus in subnet B is a load bus therefore, the next step is to update the slack bus voltage V_{B1} by applying (3.77) and (3.78) for load bus. If the convergence criterion is not met, the updated voltages including the slack bus in B would be used in the next iteration, $(k+2)$. This procedure is repeated until the convergence is achieved.

3.6.2 *Flow Chart for Parallel Computing*

In parallel computing for the two subnetworks A and B, three computers or a computer with duo core may be involved in the process (Figure 3.11). The computers A and B run the load flow of the individual networks separately the third computer which acts as the master or coordinator. The subnetworks computers send node voltages and connection matrices to the master computer which computes e_b at that iteration. The original data at subnet B slack bus is also loaded into the master. It uses this data to modify all subnetworks voltages and update the slack bus voltage and sends the results back to subnetworks computers. If there is no convergence, this new data is used by the subnetworks computers for the next iteration.

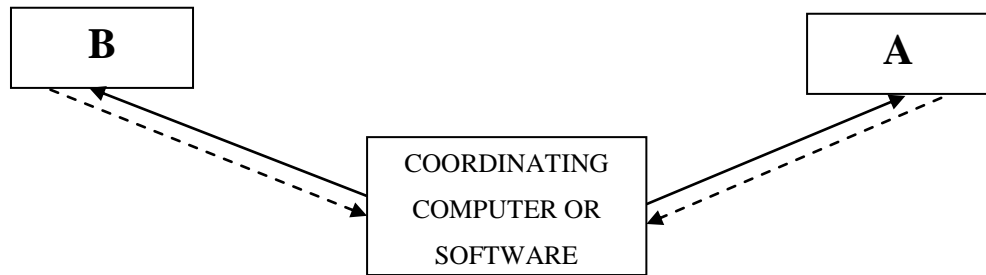


Figure 3.9. Parallel computing arrangement for two subnetworks

3.6.2.1 Forming Admittance Matrices

The available line data are $(R+jX)$, $B/2$, and transformer tap position if specified. Admittance matrices of subnetworks Y_A and Y_B are formed using the line data of the system.

3.6.2.2 Load Flow and Computation of $e_{b(SVUD)}$

The branch voltage, $e_{b(SVUD)}$, is a very important as it ensures that the solution of the subnetworks voltages are the same as if the network was solved as a piece. Load flows of the subnetworks are performed to obtain the node voltages. After $(k+1)^{th}$ iteration, voltages of the two subnetworks V_{0A}^{k+1} and V_{0B}^{k+1} are substituted in equation (3.58) to compute $e_{b(SVUD)}^{k+1}$ where k is the starting iteration.

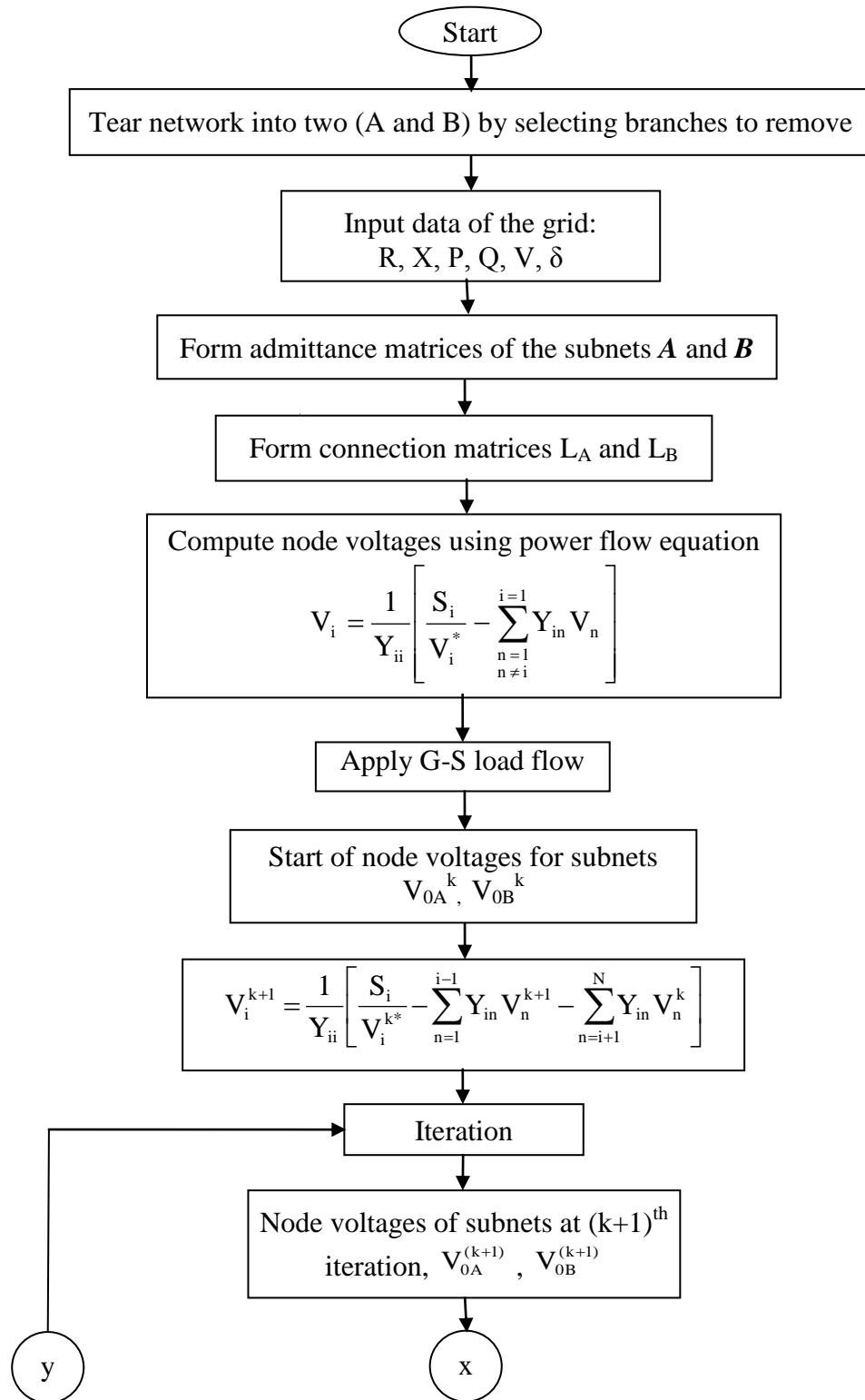


Figure 3.10a. Part 1 of flow chart for sequential implementation of SVUD load flow

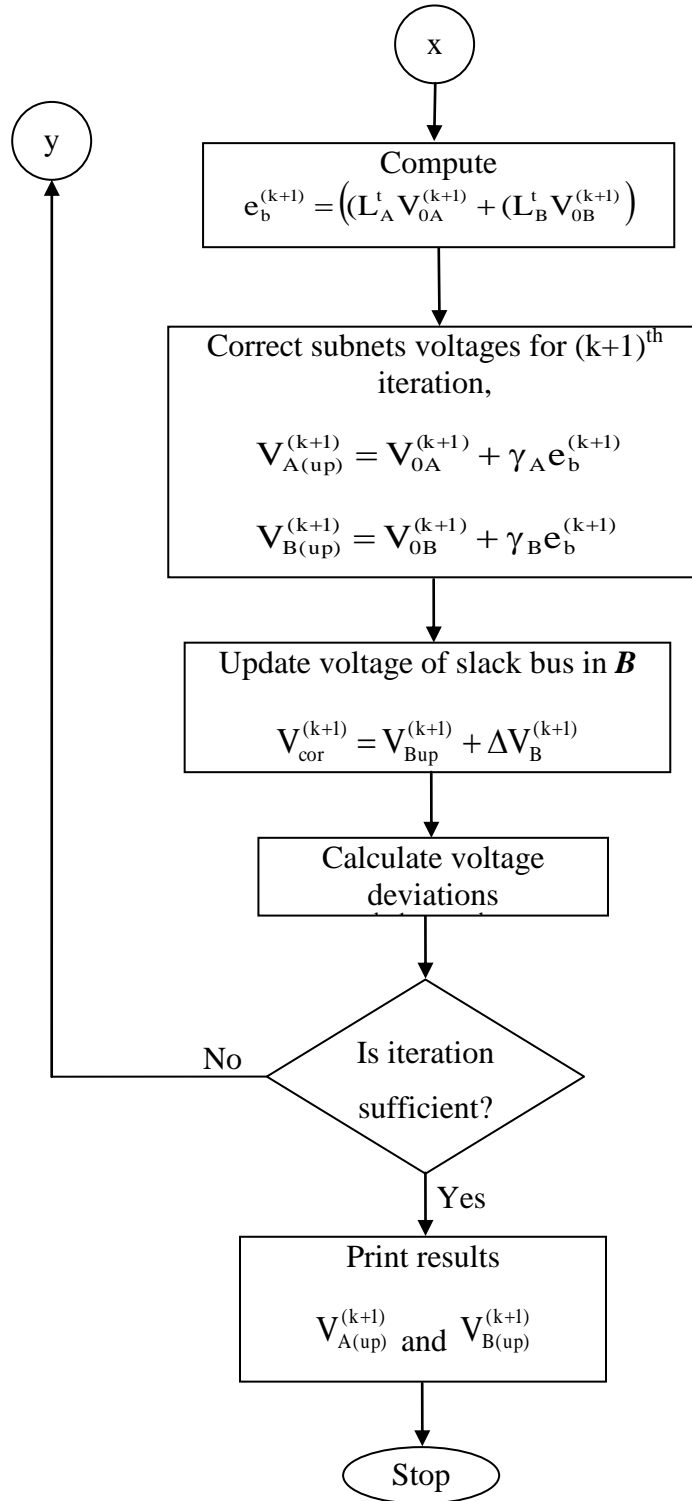


Figure 3.10b. Part 2 of flow chart for sequential implementation of SVUD load flow

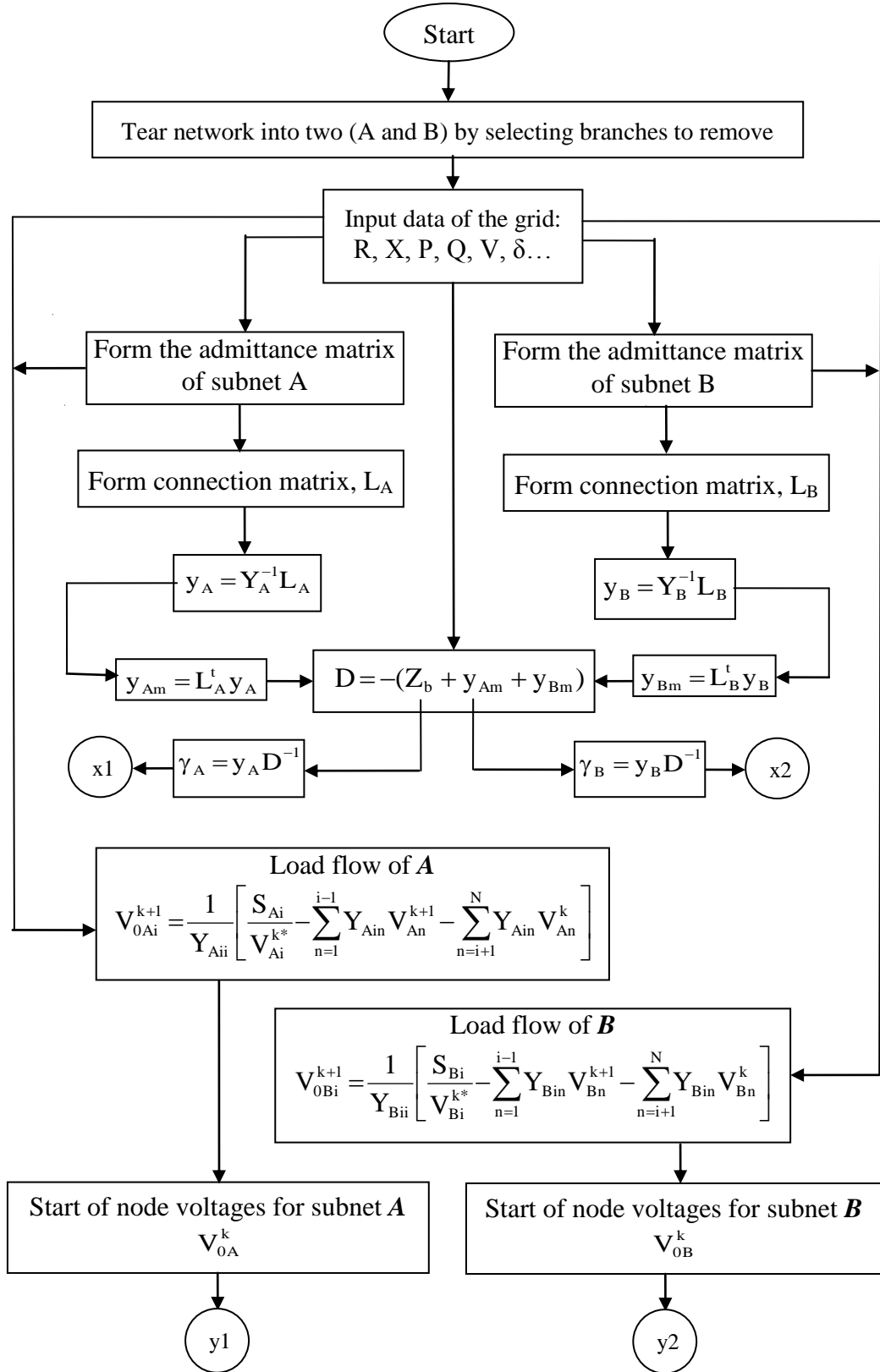


Figure 3.11a. Part 1 of flow chart for parallel implementation of SVUD load flow

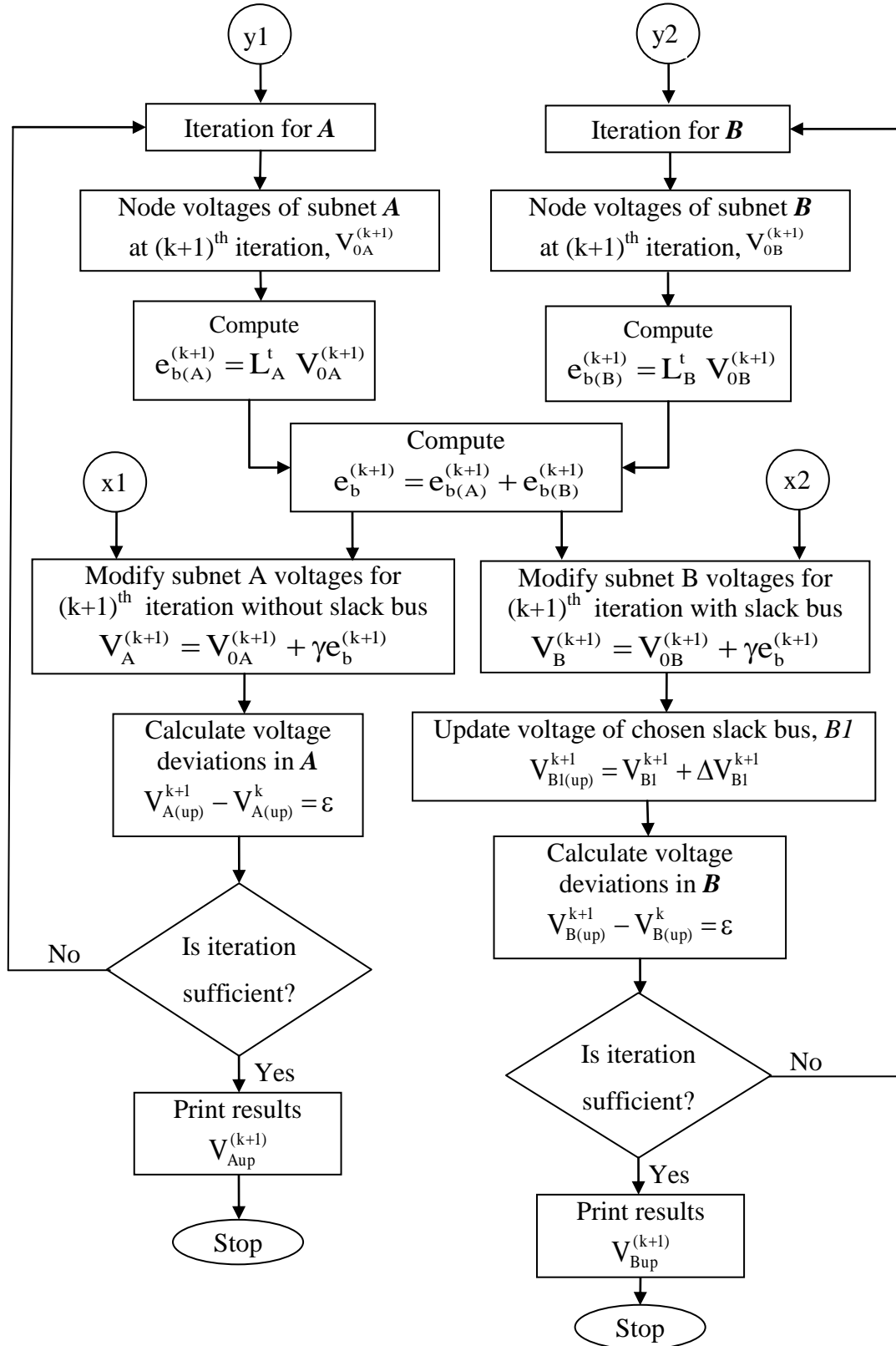


Figure 3.11b. Part 2 of flow chart for parallel implementation of SVUD load flow

3.7 Process of Modifying Node Voltages and Updating Slack Bus Voltage

Consider the network shown in Figure 3.12 torn into two subnetworks that were originally interconnected by two lines b_1 and b_2 . The numbers in the subnetworks represent the bus numbers in the original network. The bus numbers in brackets are the original numbers while the numbers next to them are new numbers using the subnetworks symbols.

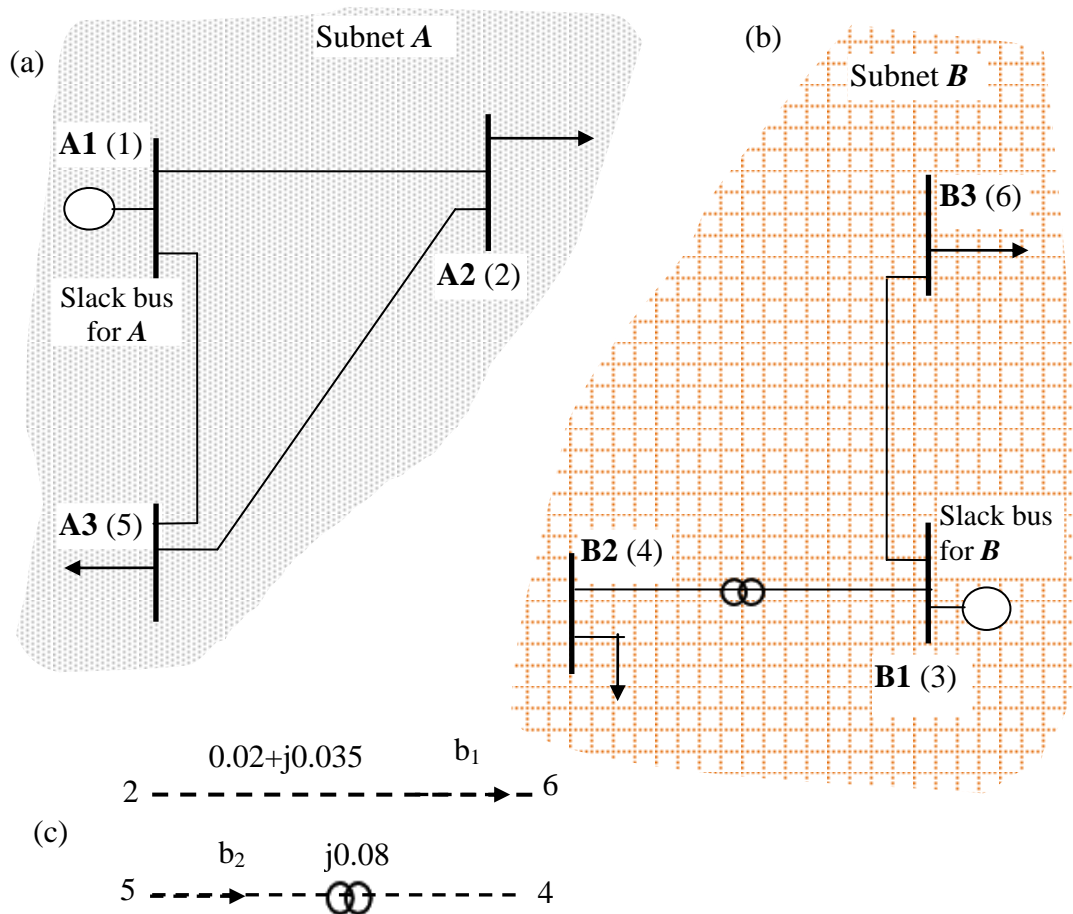


Figure 3.12 Network of Figure.3.8 torn into two
(a)Subnet A (b) Subnet B (c) Removed branches

The method of forming the connection matrices of a network is described in section 2.7. The first column in each matrix represents branch b_1 and the second column represents branch b_2 . The dimensions of the connection matrices are always such that

the number nodes in a subsystem is equal to the number of rows and the number of cut branches is equal to the number of columns. The connection matrices for the network of Figure 3.12 are L_A and L_B in **Error! Reference source not found.** and (3.136).

$$L_A = \begin{bmatrix} 0 & 0 \\ 1 & 0 \\ 0 & 1 \end{bmatrix} \quad (3.135)$$

$$L_B = \begin{bmatrix} 0 & 0 \\ 0 & -1 \\ -1 & 0 \end{bmatrix} \quad (3.136)$$

3.7.1 *Modifying Node Voltages at iteration k*

Let the voltages for subnetworks **A** and **B** at iteration (k+1) from their separate load flow analyses be V_{0A}^{k+1} and V_{0B}^{k+1} as given in (3.77) and (3.78). For the given network, the equations are given in (3.137) and (3.138). The voltages of the terminating buses are V_{02} , V_{06} and V_{05} , V_{04} . The branch voltages vector is computed as given in (3.139) and the corrective voltages given in (3.140) and (3.141).

$$V_{0A}^{k+1} = \begin{bmatrix} V_{01}^{k+1} \\ V_{02}^{k+1} \\ V_{05}^{k+1} \end{bmatrix} \quad (3.137)$$

$$V_{0B}^{k+1} = \begin{bmatrix} V_{03}^{k+1} \\ V_{04}^{k+1} \\ V_{06}^{k+1} \end{bmatrix} \quad (3.138)$$

$$\mathbf{e}_{b(SVUD)}^{k+1} = \mathbf{L}_A^t \begin{bmatrix} \mathbf{V}_{01}^{k+1} \\ \mathbf{V}_{02}^{k+1} \\ \mathbf{V}_{05}^{k+1} \end{bmatrix} - \mathbf{L}_B^t \begin{bmatrix} \mathbf{V}_{03}^{k+1} \\ \mathbf{V}_{04}^{k+1} \\ \mathbf{V}_{06}^{k+1} \end{bmatrix} \quad (3.139)$$

$$\mathbf{v}_A^{k+1} = \gamma_A \mathbf{e}_{b(SVUD)}^{k+1} \quad (3.140)$$

$$\mathbf{v}_B^{k+1} = \gamma_B \mathbf{e}_{b(SVUD)}^{k+1} \quad (3.141)$$

The values γ_A and γ_B do not change during the iteration process and can be considered constant.

$$\mathbf{V}_A^{k+1} = \mathbf{V}_{0A}^{k+1} + \mathbf{v}_A^{k+1} = \begin{bmatrix} \mathbf{V}_1^{k+1} \\ \mathbf{V}_2^{k+1} \\ \mathbf{V}_5^{k+1} \end{bmatrix} \quad (3.142)$$

$$\mathbf{V}_B^{k+1} = \mathbf{V}_{0B}^{k+1} + \mathbf{v}_B^{k+1} = \begin{bmatrix} \mathbf{V}_3^{k+1} \\ \mathbf{V}_4^{k+1} \\ \mathbf{V}_6^{k+1} \end{bmatrix} \quad (3.143)$$

Note that V_{01} is the original slack bus voltage of the untorn network and is therefore not evaluated; it is also the slack bus voltage of subnet A. \mathbf{V}_A^{k+1} and \mathbf{V}_B^{k+1} are the required voltages at (k+1) iteration. If there is no convergence, these values would be used in the next iteration (k+2), except the slack bus of subnet B, V_{03} , which has to be updated first.

3.7.2 Updating Temporary Slack Bus Voltage

Bus numbers in subnetworks are renumbered using the subnetworks' labels A and B as shown in Table 3.1 with the corresponding original numbers. Subnet B new bus numbers, B1, B2 and B3 are used in the updating algorithm. Subnet B does not incorporate the original slack bus and the temporary slack bus chosen is bus 3 or bus B1 which is a load bus, so P and Q are given. The corrected voltages of subnet B are given in (3.43) using the procedure in section 3.5.3.

Table 3.1 Bus numbers in original network and subnetworks

Bus numbers in original network	Bus numbers in subnetworks A and B
1	A1
2	A2
3	B1
4	B2
5	A3
6	B3

$$\mathbf{V}_B^{k+1} = \begin{bmatrix} \mathbf{V}_{B1}^{k+1} \\ \mathbf{V}_{B2}^{k+1} \\ \mathbf{V}_{B3}^{k+1} \end{bmatrix} = \begin{bmatrix} \mathbf{V}_3^{k+1} \\ \mathbf{V}_4^{k+1} \\ \mathbf{V}_6^{k+1} \end{bmatrix} \quad (3.144)$$

The complex power at bus 3 or bus B1, $S_{B1(cal)}$ is calculated in (3.145).

$$S_{B1(cal)}^{k+1} = \mathbf{V}_{03}^k \left(\mathbf{Y}_{B11} \mathbf{V}_{B1}^{*k+1} + \mathbf{Y}_{B12}^* \mathbf{V}_{B2}^{*k+1} + \mathbf{Y}_{B13}^* \mathbf{V}_{B3}^{*k+1} \right) \quad (3.145)$$

Let the scheduled power at bus B1 be $S_{B1(sch)} = P_{B1(sch)} + jQ_{B1(sch)}$, then the power difference is

$$\Delta S_{B1} = S_{B1(sch)} - S_{B1(cal)} \quad (3.146)$$

$$\Delta P_{B1} = \text{real } \Delta S_{B1}$$

$$\Delta Q_{B1} = \text{imaginary } \Delta S_{B1}$$

The currents due to the voltages \mathbf{V}_B^{k+1} is

$$\mathbf{I}_B^{k+1} = \mathbf{Y}_B \mathbf{V}_B^{k+1} \quad (3.147)$$

For bus 3 which is also bus B1 in subnet B:

$$a_{B1} = \text{real } \mathbf{I}_3^{k+1}$$

$$b_{B1} = \text{imaginary } I_3^{k+1}$$

$$e_{B1} = \text{real } V_3^{k+1}$$

$$f_{B1} = \text{imaginary } V_3^{k+1}$$

$$G_{B11} = \text{real } Y_{B11}$$

$$B_{B11} = \text{imaginary } Y_{B11}$$

Equations (3.94)– (3.95) for bus 3 or bus B1 are given in (3.148) - (3.151):

$$c_1 = (e_{B1}G_{B11} + f_{B1}B_{B11} + a_{B1}) \quad (3.148)$$

$$c_2 = (-e_{B1}B_{B11} + f_{B1}G_{B11} + b_{B1}) \quad (3.149)$$

$$m_1 = (-e_{B1}B_{B11} + f_{B1}G_{B11} - b_{B1}) \quad (3.150)$$

$$m_2 = (-e_{B1}G_{B11} + f_{B1}B_{B11} + a_{B1}) \quad (3.151)$$

The updating voltage for the slack bus, B1, of subnet B is calculated to give:

$$\mu_{B1} = C_1^{-1} (m_2 \Delta P_{B1} - c_2 \Delta Q_{B1}) \quad (3.152)$$

$$\lambda_{B1} = C_1^{-1} (c_1 \Delta Q_{B1} - m_1 \Delta P_{B1}) \quad (3.153)$$

The updating voltage for slack bus of subnet B is therefore given as

$$\Delta V_{B1}^{k+1} = \mu_{B1}^{k+1} + j \lambda_{B1}^{k+1} \quad (3.154)$$

The updated slack bus voltage at (k+1)th iteration is therefore given in (3.155) where bus B1 is the same as bus 3 in the original network.

$$V_{B1(\text{up})}^{k+1} = V_{B1}^{k+1} + \Delta V_{B1}^{k+1} \quad (3.155)$$

The voltage, $V_{B1(\text{up})}^{k+1}$, is used with other node voltages of B2 and B3 for the next iteration if the convergence criterion is not met. The complete solution of voltage of subnet B at iteration (k+1) is given in (3.156). If there is no convergence at this voltage, it will be used for the next iteration (k+2) and so on until convergence is achieved.

$$\mathbf{V}_B^{k+1} = \begin{bmatrix} \mathbf{V}_{B1(\text{up})}^{k+1} \\ \mathbf{V}_{B2}^{k+1} \\ \mathbf{V}_{B3}^{k+1} \end{bmatrix} \quad (3.156)$$

3.8 Summary

The methodologically rigorous derivations of two novel algorithms have been presented in this chapter. The step by step derivation of the algorithm with well-founded mathematical procedures makes it easy to understand and utilize. As already mentioned, an important finding, based on the extensive literature review, is that the fundamental equations of diakoptics are basically the same in all the methods studied. The main difference is the method of derivation and utilization of the equations which is generally cumbersome. In the BVMT the process of deriving the fundamental equations of diakoptics has been simplified and a reader can easily reconcile this with normal network analysis. One of the high points is the removal of the need for separate computation of link currents.

A detailed formulation of another novel method, the slack voltage update diakoptics (SVUD) has also been presented for torn networks equations embedded in Gauss-Seidel load flow. The branch voltage equation derived in section 3.4 is not convenient for iterative solutions. For the SVUD solution, the method of deriving the branch voltage equation is different and very simple and the derived equation is convenient for nonlinear analysis. It is worth noting that the branch voltage equation derived for nonlinear solution can also be applied to linear solutions.

In the SVUD, voltage correction of the temporary slack bus of subnetworks that do not contain the original slack bus of the whole system is a novel idea which is particularly significant. It is a new discovery and a contribution to knowledge in the field of electrical engineering and power systems analysis in particular. In the course of this research, a large volume of literature was studied in various forms but there is none where the SVUD method was been attempted. The accuracy and effectiveness of the developed algorithms were tested by applying to a number of sample networks which include IEEE benchmark systems. Some of the networks solutions are described in the next chapter.

4 IMPLEMENTATION OF THE BVMT AND THE SVUD LOAD FLOW METHOD

4.1 Introduction

Two diakoptic methods of solution developed in the course of this research work are described in chapter three. The contents of this chapter are basically how the developed methods are implemented in network calculations. The first algorithm, the BVMT, a new formulation and extension of the original diakoptic concept is applicable to linear network, and nonlinear network with current injections instead of power injection equations as explained in section 3.5.2.1. The second algorithm, the SVUD load flow applies to power systems in iterative solutions. And because tearing is synonymous with diakoptics, the computer tearing process is explained. The general structure of implementing the algorithms is laid out in the next section.

4.2 Layout of Implementation of Algorithms

The three main parts which highlight the general structure of implementation of the algorithms are described in Figure 4.1 are summarized:

1. The foundational method in this work is diakoptics and the first part of implementation is network tearing described in section 4.3. It describes the process of choosing line combinations that will successfully tear a network into the desired subnetworks automatically and “manually” using a computer programme. The computer programme developed for the SVUD solution incorporates this tearing algorithm in a modified form.
2. In the second part shown in section 4.4, the BVMT is implemented on a linear network and a nonlinear network with given current injections for the non-iterative solution of the power flow equations $[I]=[Y][V]$ and $S_r = V_r I_r^*$. Analysis and results are compared with one-piece solutions of the same

network to show its accuracy. The largeness of the full matrix of the whole network when compared with subnetworks matrices is exposed.

3. The SVUD load flow algorithm is implemented in sections 4.5 – 4.8 using sample networks which include IEEE benchmark networks. Each network is also analyzed without tearing using conventional Gauss-Seidel load flow method and in some cases Newton-Raphson is also applied. Unlike BVMT, the SVUD is an iterative method.

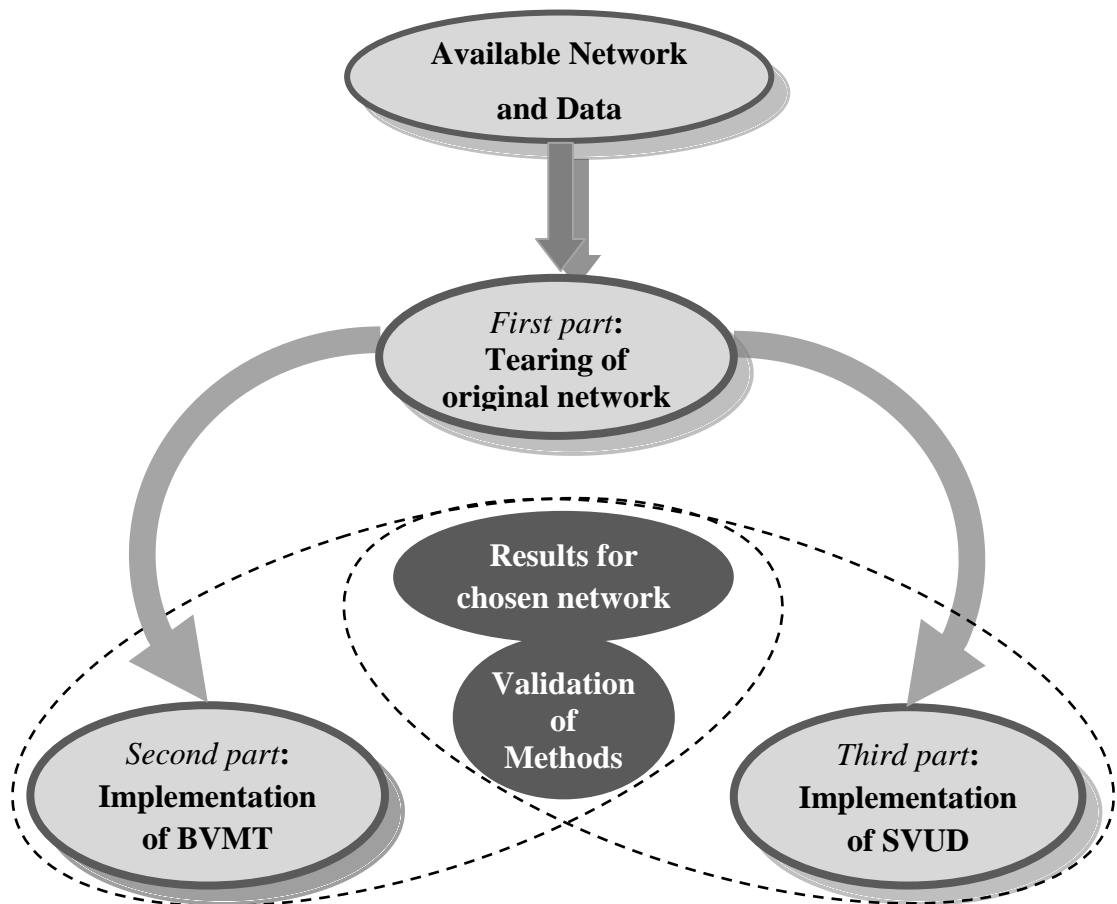


Figure 4.1. Implementation structure of devised methods

The overlapping procedure in the two methods is the validation of results obtained by comparing with results using one-piece methods that have been tested over time.

4.3 Network Tearing Algorithm

Network tearing is the basis of diakoptic analysis and is therefore applicable to the BVMT and the SVUD. To ensure automation of the SVUD load flow analysis method for large systems, a MATLAB programme was developed using some codes from MATLAB Central site, example of which can be found in [102]. MATLAB codes for G-S and N-R load flow methods are shown in Appendix A.1 and A.2. The code for splitting the network has two parts – first, the automatic tearing of the network where the code selects the links to remove to get the most appropriate size of subnetworks, and second is the “manual” tearing where the engineer inputs the chosen line numbers when prompted by the computer programme based on network topology. Each method has its merits as explained below.

4.3.1 Automatic Network Splitting

The global network to be torn is shown in Figure 4.2 which is adapted from Figure 3.8. From the array, “linedata” which is the input of network line parameters representing the arrangement of lines and buses, the computer first identifies the pairs of buses in the network that are joined by individual links using the code in Figure 4.3 and outputs the result shown in

Table 4.1. The code also outputs the network map of Figure 4.2 as Figure 4.4.

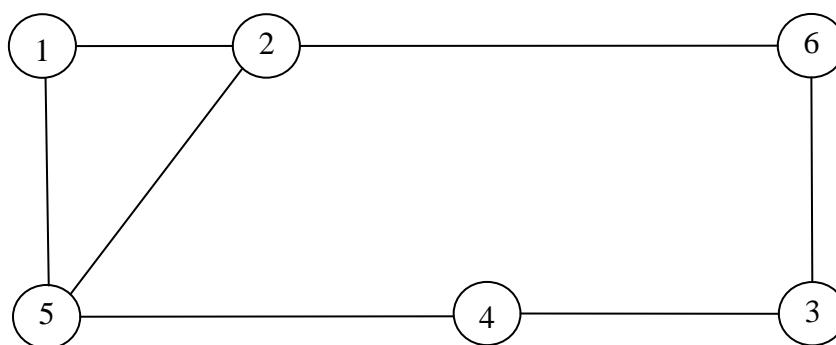


Figure 4.2. Network architecture of Figure 3.8

The first column is the lines identification numbers. The last two columns of the output identify the pairs of bus nodes in the network that are joined by individual links.

```

disp('Line numbers and bus numbers for network: ')
disp(' ')

disp('Line      From bus      To bus')

for nn=1:size(linedata,1)
    disp([num2str(nn)      '      '      num2str(linedata(nn,1))      '      '
num2str(linedata(nn,2))]
end

```

Figure 4.3. Algorithm for identifying line numbers and connections

If there are n links in a network, all possible cuts that could divide the original network into subnetworks are found using the code in Figure 4.5 [103]. For the network of Figure 4.2 with 6 nodes and 7 lines, the code finds 120 individual combinations of links that may be cut as listed in Table 4.2. MATLAB programme for finding combinations is shown in Appendix A.3. Only nine of the combinations can successfully split the original network into two isolated subnetworks shown in Table 4.3 and Figure 4.6a(1-4), Figure 4.6b(5-8) and Figure 4.6c(9). Table 4.4 and Figure 4.6c(10-11) show combinations that will split the network into three subnetworks. Other combinations that would separate the network into isolated subsystems are marked with asterisks in Table 4.2 but involve the removal of extra lines that are not necessary as shown in Figure 4.6c(12) where line 1 is removed in addition to the lines that have successfully torn the network into two already. This increases the number of computations required when combining the separate solutions to form the required solution of the whole network. This should be avoided where necessary.

Table 4.1 Line numbers and bus numbers for network

Line	From bus	To bus
1	1	2
2	2	5
3	1	5
4	2	6
5	5	4
6	3	4
7	3	6

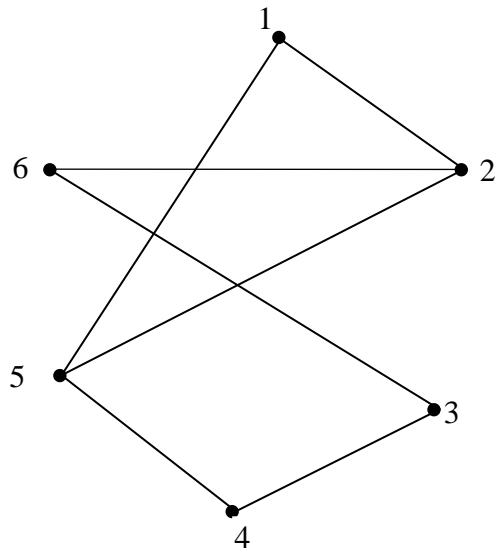


Figure 4.4. Graph of network of Figure 4.2

```
for n=1:size(linedata,1)
    cuts=combnans(1:size(linedata,1),n);
end
```

Figure 4.5. Code for finding possible combinations [103]

Table 4.2 Combinations of possible lines to cut in 6-node network

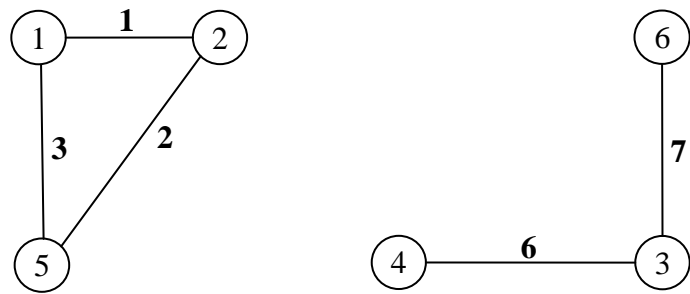
No of combinations	Combinations of links						
1	[1 2]	31	[1 4 5]*	61	[1 2 4 5]	91	[4 5 6 7]
2	[1 3]	32	[1 4 6]*	62	[1 2 4 6]	92	[1 2 3 4 5]
3	[1 4]	33	[1 4 7]	63	[1 2 4 7]	93	[1 2 3 4 6]
4	[1 5]	34	[1 5 6]	64	[1 2 5 6]	94	[1 2 3 4 7]
5	[1 6]	35	[1 5 7]*	65	[1 2 5 7]	95	[1 2 3 5 6]
6	[1 7]	36	[1 6 7]	66	[1 2 6 7]	96	[1 2 3 5 7]
7	[2	37	[2 3 4]	67	[1 3 4 5]	97	[1 2 3 6 7]
8	[2 4]	38	[2 3 5]*	68	[1 3 4 6]	98	[1 2 4 5 6]
9	[2 5]	39	[2 3 6]	69	[1 3 4 7]	99	[1 2 4 5 7]
10	[2 6]	40	[2 3 7]	70	[1 3 5 6]	100	[1 2 4 6 7]
11	[2 7]	41	[2 4 5]*	71	[1 3 5 7]	101	[1 2 5 6 7]
12	[3 4]	42	[2 4 6]*	72	[1 3 6 7]	102	[1 3 4 5 6]
13	[3 5]	43	[2 4 7]	73	[1 4 5 6]	103	[1 3 4 5 7]
14	[3 6]	44	[2 5 6]	74	[1 4 5 7]	104	[1 3 4 6 7]
15	[3 7]	45	[2 5 7]*	75	[1 4 6 7]	105	[1 3 5 6 7]
16	[4	46	[2 6 7]	76	[1 5 6 7]	106	[1 4 5 6 7]
17	[4 6]	47	[3 4 5]*	77	[2 3 4 5]	107	[2 3 4 5 6]
18	[4 7]	48	[3 4 6]*	78	[2 3 4 6]	108	[2 3 4 5 7]
19	[5 6]	49	[3 4 7]	79	[2 3 4 7]	109	[2 3 4 6 7]
20	[5 7]	50	[3 5 6]	80	[2 3 5 6]	110	[2 3 5 6 7]
21	[6 7]	51	[3 5 7]*	81	[2 3 5 7]	111	[2 4 5 6 7]
22	[1 2	52	[3 6 7]	82	[2 3 6 7]	112	[3 4 5 6 7]
23	[1 2	53	[4 5 6]	83	[2 4 5 6]	113	[1 2 3 4 5]
24	[1 2	54	[4 5 7]	84	[2 4 5 7]	114	[1 2 3 4 5]
25	[1 2	55	[4 6 7]	85	[2 4 6 7]	115	[1 2 3 4 6]
26	[1 2	56	[5 6 7]	86	[2 5 6 7]	116	[1 2 3 5 6]
27	[1 3	57	[1 2 3 4]	87	[3 4 5 6]	117	[1 2 4 5 6]
28	[1 3	58	[1 2 3 5]	88	[3 4 5 7]	118	[1 3 4 5 6]
29	[1 3	59	[1 2 3 6]	89	[3 4 6 7]	119	[2 3 4 5 6]
30	[1 3	60	[1 2 3 7]	90	[3 5 6 7]	120	[1 2 3 4 5 6]

Table 4.3 Configurations that can successfully split network into two subnetworks

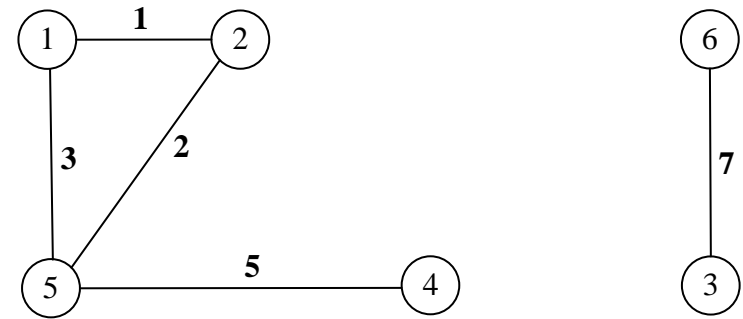
Number of configurations	Potential lines for tearing network	Number of subnetworks	Number of nodes in each subnet
1	[4 5]	2	[3 3]
2	[4 6]	2	[4 2]
3	[5 7]	2	[4 2]
4	[1 2 5]	2	[2 4]
5	[1 2 6]	2	[3 3]
6	[1 2 7]	2	[4 2]
7	[2 3 4]	2	[2 4]
8	[2 3 6]	2	[4 2]
9	[2 3 7]	2	[3 3]

Table 4.4 Configurations that can successfully split network into three subnetworks

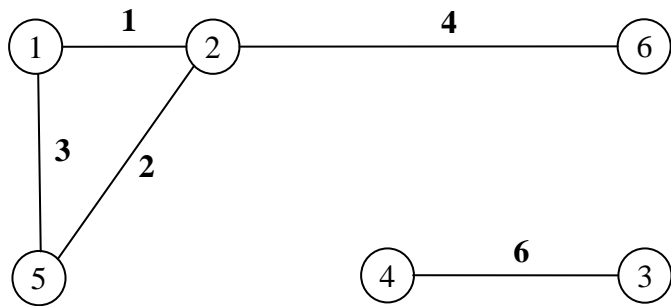
Number of configurations	Potential lines for tearing network	Number of subnets	Number of nodes in each subnet
1	[1 2 5 7]	3	[2 2 2]
2	[2 3 4 6]	3	[2 2 2]



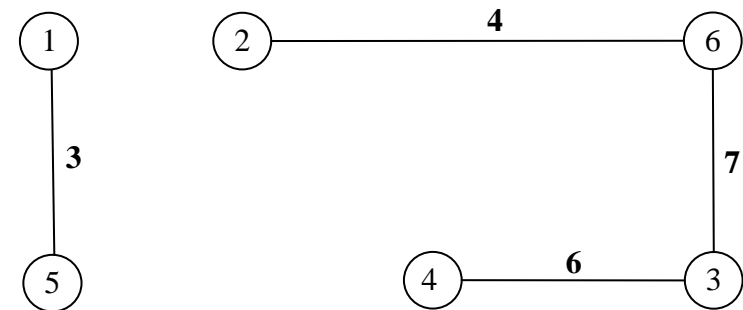
(1) Removed lines = 4, 5



(2) Removed lines = 4, 6

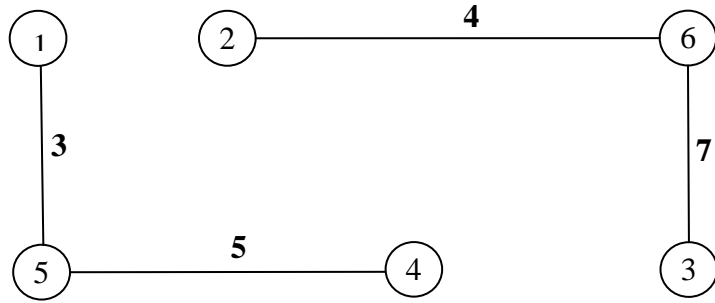


(3) Removed lines = 5, 7

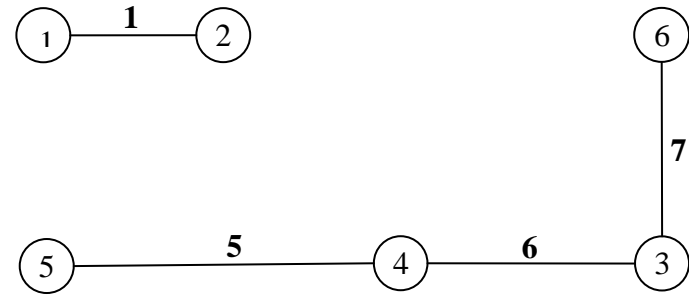


(4) Removed lines = 1, 2, 5

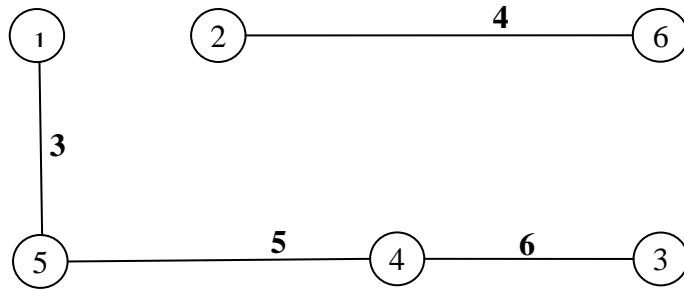
Figure 4.6a. Subnetworks formed by removing cut combinations (first set)



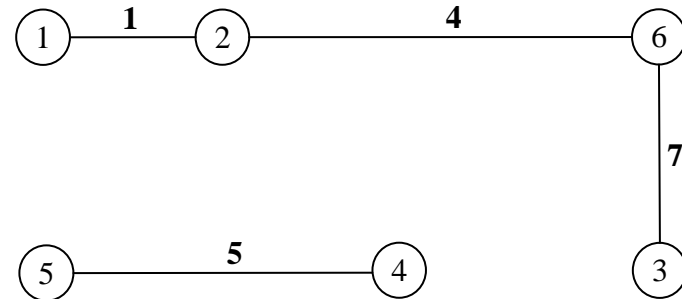
(5) Removed lines = 1, 2, 6



(6) Removed lines = 2, 3, 4

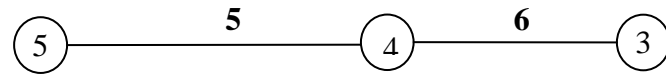
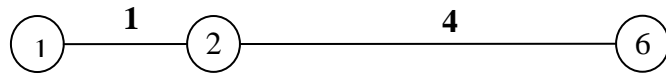


(7) Removed lines = 1, 2, 7

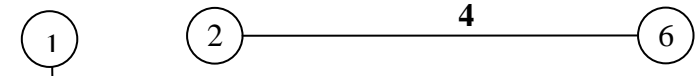


(8) Removed lines = 2, 3, 6

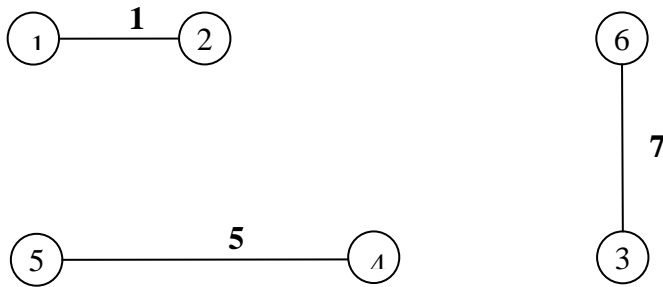
Figure 4.6b. Subnetworks formed by removing cut combinations (Second set)



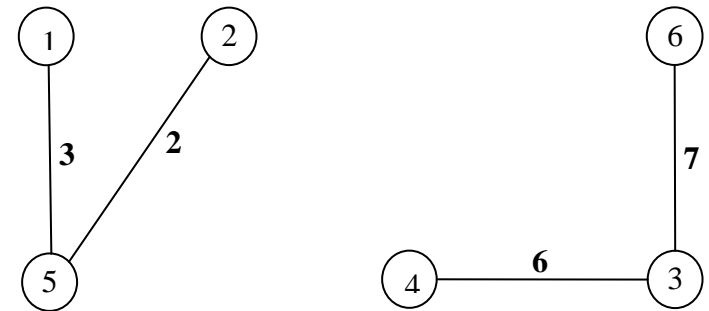
(9) Removed lines = 2, 3, 7



(10) Removed lines = 1, 2, 5, 7



(11) Removed lines = 2, 3, 4, 6



(12) Removed lines = 1, 4, 5 (Line 1 removed in addition)

Figure 4.6c. Subnetworks formed by removing cut combinations (third set)

4.3.2 *Forming Adjacency Matrix*

The adjacency matrix, also known as connection matrix, defines all links in a graph or network. It represents which node is adjacent or connected to which other node. It is worth noting that the formation of this connection matrix is slightly different from the connection matrix used in the actual diakoptic analysis explained in section 2.3.1.1, where the number of columns is equal to the number of removed branches and the total number of rows is equal to the total number of nodes in the network. Also, directions of currents in the removed branches determine the signs of the elements of the matrices. The connection matrix here will therefore henceforth be referred to as adjacency matrix to differentiate from connection matrix in the actual diakoptic analysis.

If there are N nodes in the network, the adjacency matrix is of size $N \times N$. The rows and columns represent the node numbers serially. Individual elements are set to 1 if the row and column index correspond to a link between related nodes in the network. If there is no link between any two nodes, the element is set to 0. An example is shown Table 4.5 for the graph of Figure 4.2 with six nodes which is how (4.1) was formed with the computer code.

Table 4.5 The adjacency matrix

Node numbers	1	2	3	4	5	6
1	0	1	0	0	1	0
2	1	0	0	0	1	1
3	0	0	0	1	0	1
4	0	0	1	0	1	0
5	1	1	0	1	0	0
6	0	1	1	0	0	0

4.3.3 *Algorithm for Automatic Assessment of Cut Configurations*

Sections of the algorithm to enable automatic assessment of the line combinations which when removed would successfully split the original network into a set of isolated subnetworks is explained below. This is adapted from [103] shown in appendix A.3.

Firstly, the adjacency matrix shown in (4.2) is formed for the network of Figure 4.2 using the code. Close inspection confirms that nonzero elements correspond to links between the nodes defined in the array “linedata”.

$$\mathbf{C} = \begin{vmatrix} 0 & 1 & 0 & 0 & 1 & 0 \\ 1 & 0 & 0 & 0 & 1 & 1 \\ 0 & 0 & 0 & 1 & 0 & 1 \\ 0 & 0 & 1 & 0 & 1 & 0 \\ 1 & 1 & 0 & 0 & 0 & 0 \\ 0 & 1 & 1 & 0 & 0 & 0 \end{vmatrix} \quad (4.1)$$

The adjacency matrix keeps changing during the analysis until the final one is obtained which gives the information of the cut subnetworks as follows. When a cut configuration is analysed, links that are cut have their corresponding elements set to zero in the adjacency matrix, as the cut links no longer connect the corresponding nodes. If links 4 and 5 are cut, the original links between node pairs (2, 6) and (4, 5) are no longer active, and so the adjacency matrix becomes (4.2). The “1’s” in row 2, column 6 and row 4 column 5 are replaced by “0”.

$$\mathbf{C} = \begin{vmatrix} 0 & 1 & 0 & 0 & 1 & 0 \\ 1 & 0 & 0 & 0 & 1 & 0 \\ 0 & 0 & 0 & 1 & 0 & 1 \\ 0 & 0 & 1 & 0 & 0 & 0 \\ 1 & 1 & 0 & 0 & 0 & 0 \\ 0 & 1 & 1 & 0 & 0 & 0 \end{vmatrix} \quad (4.2)$$

When a link has been cut, the nodes at either end should belong to two separate subnetworks. A two-step process follows - the algorithm then operates on a new matrix “D”, of equal size to C and initialised with zero elements.

STEP 1

Columns 2 and 6 in D, which should belong to subnetworks 1 and 2, are set to be equal to the corresponding columns in C, multiplied by the subnetwork number.

```

D=zeros(size(C))
D(:,2)=C(:,2)*1
D(:,6)=C(:,6)*2

```

Figure 4.7. Code for new adjacency matrix after a link is removed

$$\mathbf{D} = \begin{vmatrix} 0 & 1 & 0 & 0 & 0 & 0 \\ 0 & 0 & 0 & 0 & 0 & 0 \\ 0 & 0 & 0 & 0 & 0 & 2 \\ 0 & 0 & 0 & 0 & 0 & 0 \\ 0 & 1 & 0 & 0 & 0 & 0 \\ 0 & 1 & 0 & 0 & 0 & 0 \end{vmatrix} \quad (4.3)$$

STEP 2

The code in Figure 4.8 analyses the resulting adjacency matrix, checking each row of \mathbf{D} with at least one nonzero element. Every time there is a nonzero term in a row of \mathbf{D} , that row is updated to be equal to the corresponding row of \mathbf{C} multiplied by the subnetwork number. This effectively propagates the subnetwork number through to other connected nodes in the two subnetworks identified so far. If a row of \mathbf{D} already has two or more differently valued non-zero elements, this means the corresponding node is connected to more than one subnetwork, an indication that the cut configuration being tested is unsuitable for splitting network.

```

for i=1:nNodes
    A=unique(D(i,:));
    A=A(A~=0);
    if isempty(A)==0
        if numel(A)>1
            disp(['Node ' num2str(i) '
                Cut configuration unsuitable for
                splitting network.'])
            return
        else
            D(i,:)=C(i,:)*A;
        end
    end
end
end

```

Figure 4.8. Code for analysing the new matrix \mathbf{D}

Next, the two steps above are repeated but with columns then rows rather than rows then columns. New rows 2 & 6 of **D** are equal to the corresponding rows of **C** multiplied by subnetwork number using Figure 4.9 to obtain the output in (4.4).

$$\mathbf{D} = \begin{pmatrix} 0 & 1 & 0 & 0 & 1 & 0 \\ 0 & 0 & 0 & 0 & 0 & 0 \\ 0 & 0 & 0 & 2 & 0 & 2 \\ 0 & 0 & 0 & 0 & 0 & 0 \\ 1 & 1 & 0 & 0 & 0 & 0 \\ 0 & 1 & 0 & 0 & 0 & 0 \end{pmatrix} \quad (4.4)$$

D=zeros(size(C))

D(2,:)=C(2,)*1

D(6,:)=C(6,)*2

Figure 4.9 Reversed order of Figure 4.7

$$\mathbf{D} = \begin{pmatrix} 0 & 1 & 0 & 0 & 1 & 0 \\ 1 & 0 & 0 & 0 & 1 & 0 \\ 0 & 0 & 0 & 2 & 0 & 2 \\ 0 & 0 & 0 & 0 & 0 & 0 \\ 1 & 1 & 0 & 0 & 0 & 0 \\ 0 & 2 & 2 & 0 & 0 & 0 \end{pmatrix} \quad (4.5)$$

If more than one non-zero index, (node) is connected to more than one subnetwork, the cut configuration is not suitable for splitting network into subnetworks. The computer outputs the statement, “*Cut configuration is unsuitable*” otherwise (4.6) is output.

```

for i=1:nNodes
    A=unique(D(:,i));
    A=A(A~=0);
    if isempty(A) == 0
        if numel(A)>1
            return
        else
            D(:,i)=C(:,i)*A
        end
    end
end
end

```

Figure 4.10. Reversed row and column code of Figure 4.10

$$\mathbf{D} = \begin{vmatrix} 0 & 1 & 0 & 0 & 1 & 0 \\ 1 & 0 & 0 & 0 & 1 & 0 \\ 0 & 0 & 0 & 2 & 0 & 2 \\ 0 & 0 & 0 & 0 & 0 & 0 \\ 1 & 1 & 0 & 0 & 0 & 0 \\ 0 & 2 & 2 & 0 & 0 & 0 \end{vmatrix} \quad (4.6)$$

Now that links to the ends of the first cut have been identified, a second cut link in the list is considered. Cut 2 separates nodes 4 and 5. Repeating steps 1 and 2 until there is no change in \mathbf{D} in two consecutive applications of those steps, the final value of \mathbf{D} is obtained as (4.7).

$$\mathbf{D} = \begin{vmatrix} 0 & 1 & 0 & 0 & 1 & 0 \\ 1 & 0 & 0 & 0 & 1 & 0 \\ 0 & 0 & 0 & 2 & 0 & 2 \\ 0 & 0 & 2 & 0 & 0 & 0 \\ 1 & 1 & 0 & 0 & 0 & 0 \\ 0 & 0 & 0 & 0 & 0 & 0 \end{vmatrix} \quad (4.7)$$

Subnetwork numbers (SN) are assigned to a vector “SN” by scouring all elements of D, and reading the subnetwork number assigned to the node corresponding to a (row, column) position using Figure 4.11 and the output is (4.8). From the output, it can be seen that subnet A consists of nodes 1, 2, 5 and subnet 2 contains nodes 3, 4, 6. If a cut configuration does not separate individual subnetworks, the process is aborted and the cut configuration is removed from the list of potential configurations to be used in the network voltage analysis. In the case of this example, the cut configuration successfully splits the network into 2 exclusive subnetworks.

$$\mathbf{SN} = [1 \quad 1 \quad 2 \quad 2 \quad 1 \quad 2] \quad (4.8)$$

The split network is now as Figure 4.13 showing two distinct subnetworks. The code outputs Figure 4.14 with the dashed lines indicating the removed lines. Another cut configuration is shown in Figure 4.15 where lines 1, 2, 6 have been removed to also obtain two subnetworks. The SN of this new configuration would be as shown in equation (4.9). All cut configurations from successful tearing of the network are shown in Figure 4.6.

$$\mathbf{SN} = [1 \quad 2 \quad 2 \quad 1 \quad 1 \quad 2] \quad (4.9)$$

```

for i=1:nNodes
    for j=1:nNodes
        if D(i,j)~=0
            SN(i)=D(i,j);
            SN(j)=D(i,j);
        end
    end
end

```

Figure 4.11. Code that identifies the nodes in each subnetwork

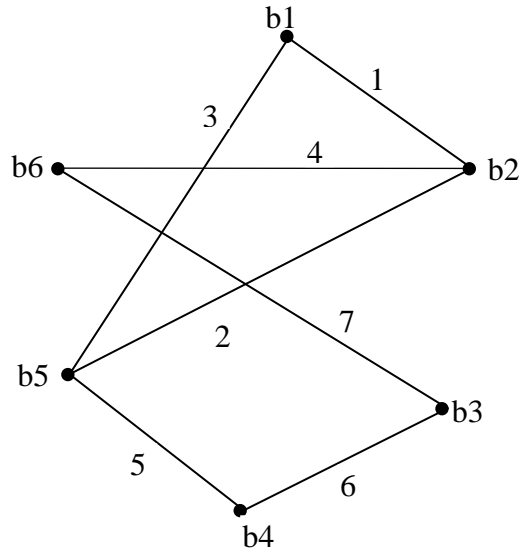


Figure 4.12. Computer representation of Figure 3.8 before cutting

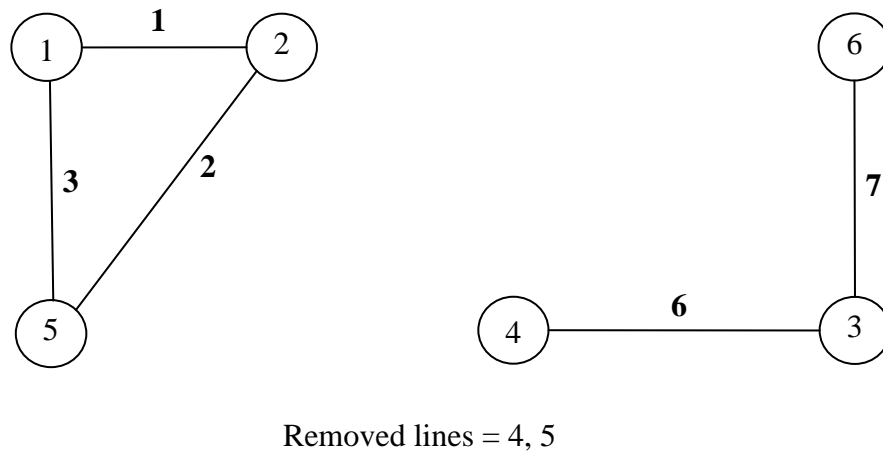


Figure 4.13. Network successfully split into two distinct subnetworks

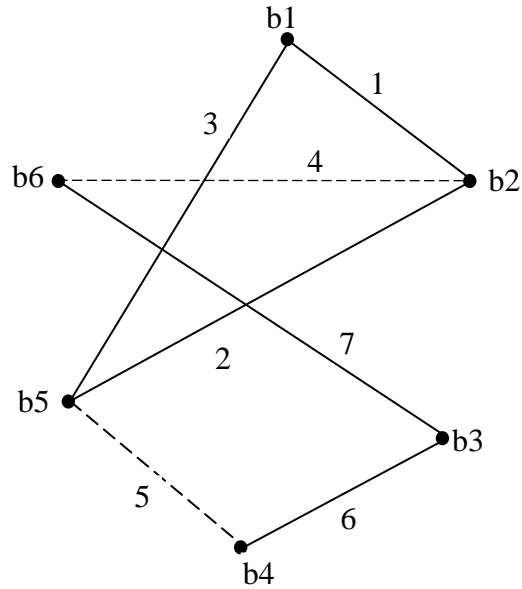


Figure 4.14. Cut network representation of Figure 4.5 (cut lines = 4, 5)

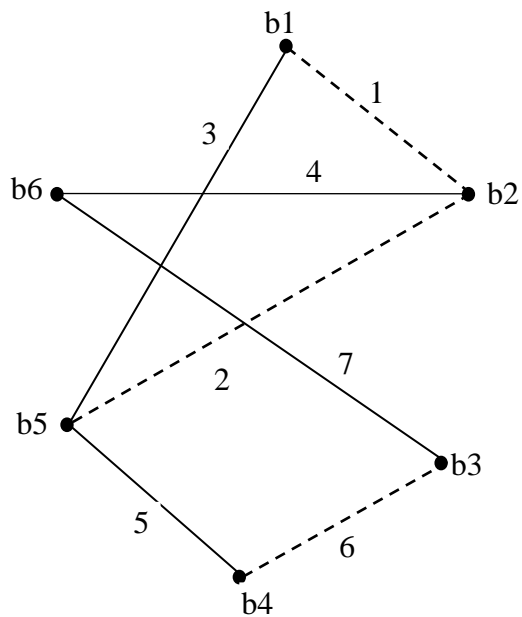


Figure 4.15. Another cut configuration for successful tearing into two distinct subnetworks (cut lines = 1, 2, 6)

4.3.4 Subnetwork Sizing

The most suitable cut configuration can be found by first finding the most uniform subnetwork sizing (i.e. the cut configuration which produces subnetworks of equal

size). This would ensure a similar timing for all threads when using parallel threaded code in solving for the voltages. Equal sizing is not practicable in real time electrical networks in most cases. Configurations with more subnetworks than cores available for parallel threading are filtered out in favour of configurations with fewer subnetworks. This prevents parallel threading having to run perhaps four parallel threads then a single one in the event of a five-subnetwork configuration on a 4-core machine, taking longer than four similarly balanced subnetworks in a single pass of the parallel thread.

A final filter is applied which analyses the number of nodes in the smallest subnetwork of each configuration, and chooses the configuration where this value is the largest. This filter would favour configurations where the smallest subnetwork has three nodes over one where the smallest subnetwork has just two nodes. This is based on the assumption that larger subnetworks produce more stable results and better convergence in iterations of the voltage solving algorithm. The computer used for this work has two cores and the largest number of subnetworks solved is three.

4.3.5 Automatic versus Manual Tearing of Network

In the automatic splitting of networks, the programme chooses the lines to cut and chooses the correct sizing of subnetwork as explained above. The MATLAB code is such that when run prompts for either automatic or manual cutting. The lines of cut were put in when prompted in the course of the computer analysis. If manual cutting is chosen, then there will be another prompt for the line numbers to be removed. Also, the slack buses for each subnetwork are selected. After all the slack buses are chosen, the power flow analysis is performed until convergence is reached. The process is long and increases processing time. But if the engineer chooses the lines to cut based on his knowledge of electrical network topology, the processing time reduces.

4.3.6 Tearing Times of Test Systems

Automatic tearing and “manual” tearing were applied to the network of Figure 3.8 and the IEEE 14-bus system and test systems in Figure 4.27 and Figure 4.28. Manual

selection times include the times for manually inputting chosen line numbers and running the programme for actual separation of networks into subnetworks. The duration of the tearing process was determined by using the MATLAB functions *tic* and *toc*. At $t=tic$ the internal stopwatch timer starts and ends at $t = toc$, giving the time elapsed since the start of the process.

For the 6-bus system, the lines chosen during the automatic process were (1, 2, and 6); these were then used in the manual tearing. The same results were obtained but Table 4.6 shows that automatic tearing took 5.367397s while manual tearing took 15.128001s. The manual solution time includes time to input the selected lines. The same network was torn based on engineering judgement of the topology of the network by removing manually, lines 4 and 5; the solution time was 13.652085s. The same procedure was followed for the 14-bus system and the times for the automatic and manual tearing were 21.623416s and 27.054145s respectively. However, as the number of buses increases, it becomes obvious that automatic tearing of networks has demerits especially in time.

Table 4.6 Computation times for tearing

Automatic tearing	First Manual selection of lines of tearing	Second Manual selection of lines of tearing
6-BUS TEARING		
cut lines = 1, 2, 6	cut lines = 1, 2, 6	cut lines = 4, 5
Elapsed time is 5.367397s	Elapsed time is 15.128001s	Elapsed time is 13.652085s
14-BUS TEARING		
Cut lines = 9, 10, 15	Cut lines = 9, 10, 15	Cut lines = 2, 5, 7, 16, 17
Elapsed time is 21.623416s	Elapsed time is 27.054145s	Elapsed time is 14.577079s
30-BUS NETWORK		
Network was not torn automatically even after the period below	Cut lines = 12, 14, 15, 36	
Elapsed time is 29,320.936s	Elapsed time is 24.166196s	

4.4 Implementation of the Branch Voltage Modifier Technique

The equations of solution for the Branch Voltage Modifier Technique (BVMT) have been developed in section 3.4 and computation in this section is based on equations (3.38) which is the new equation of solution and is suitable for solving linear system or system with injected currents.

4.4.1 Application of BVMT to Linear System

The algorithm is implemented on the 22-node network of Figure 4.16. For the purpose of comparison, the matrix of the full network for the nodal equation, $V=Y^{-1}I$ is shown in Table 4.8 to further explain the magnitude of data usually required for one-piece solution especially where thousands of nodes are involved. In the traditional diakoptics, the admittance matrices of subnetworks are used to form a diagonal matrix, Y_m of (2.31) presented in Figure 4.19 for the network and inverted as a whole. Inverting the whole block diagonal matrix is not required with this algorithm; each subnetwork admittance matrix is inverted separately and the link current is not computed.

The BVMT is also applied to the network of Figure 4.16 torn into six subnetworks by removing branches b1 - b8 to yield subnetworks A, B, C, D, E, and F of Figure 4.17, which is an expanded form of a figure from reference [13]. All the branch impedances are in ohms and all the injected currents are in amperes. The matrices as a result of decomposing the network are shown in Table 4.7.

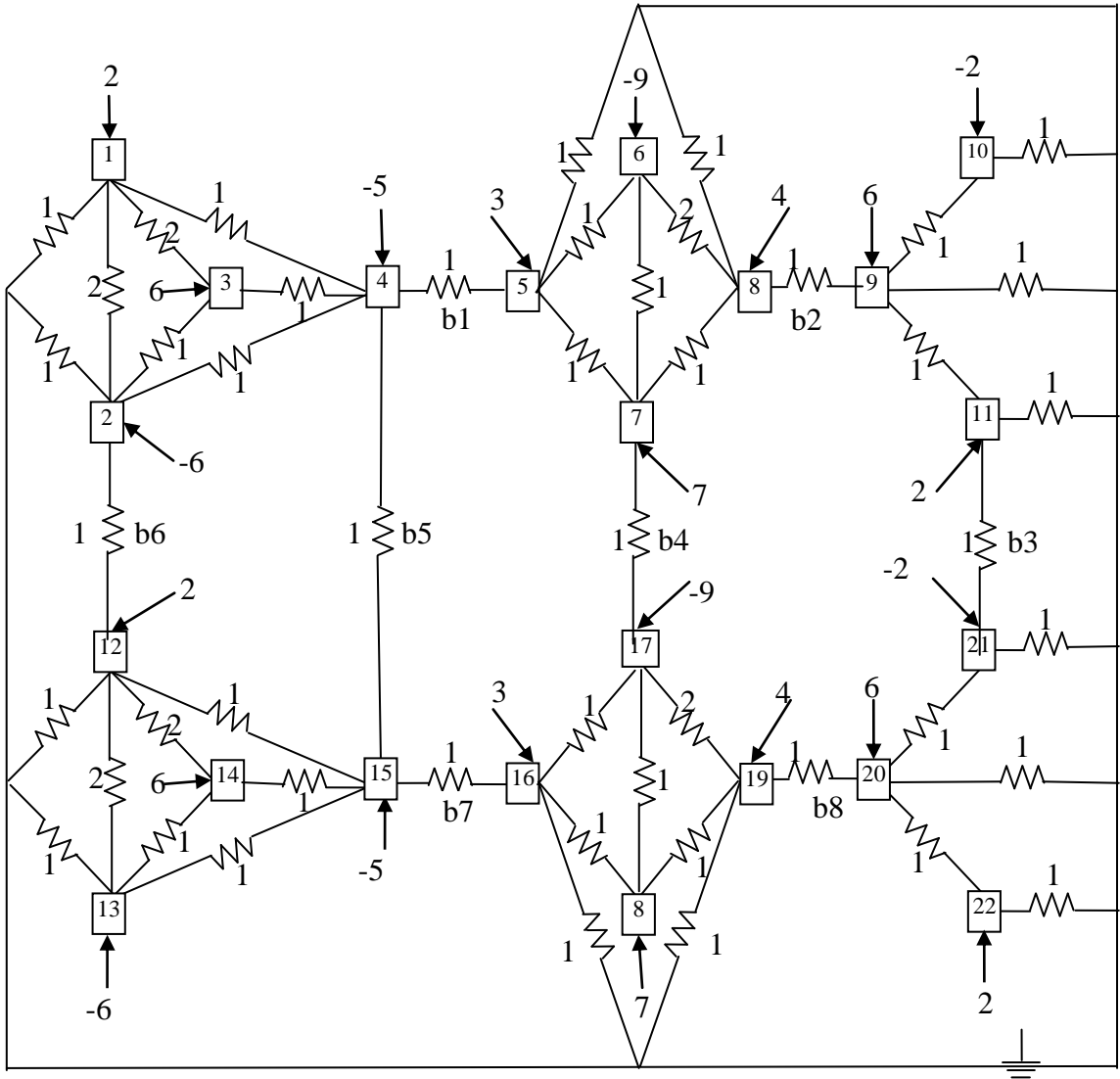


Figure 4.16. A 22-node network

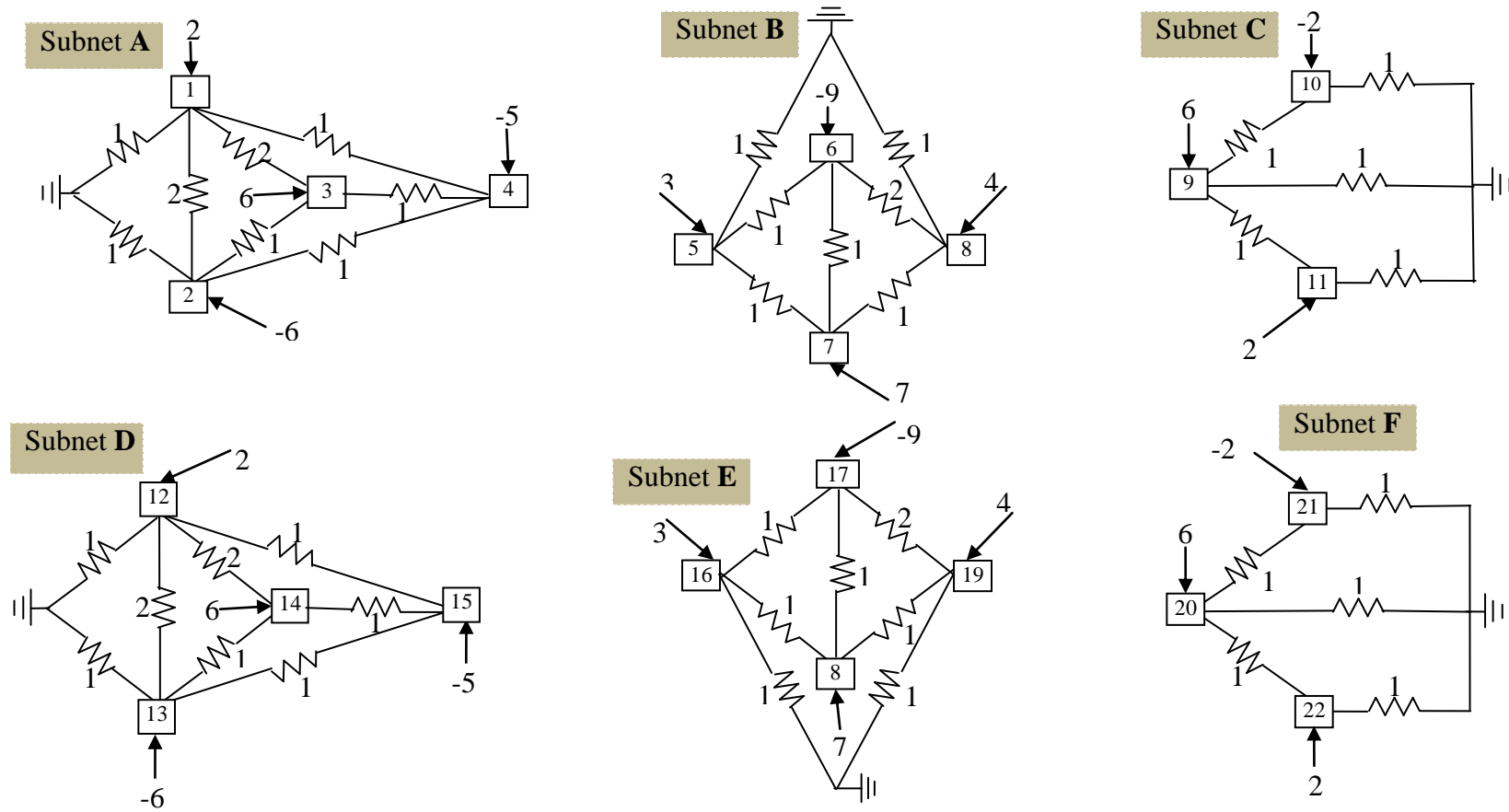


Figure 4.17. Network of Figure 4.1 decomposed into six subnetworks

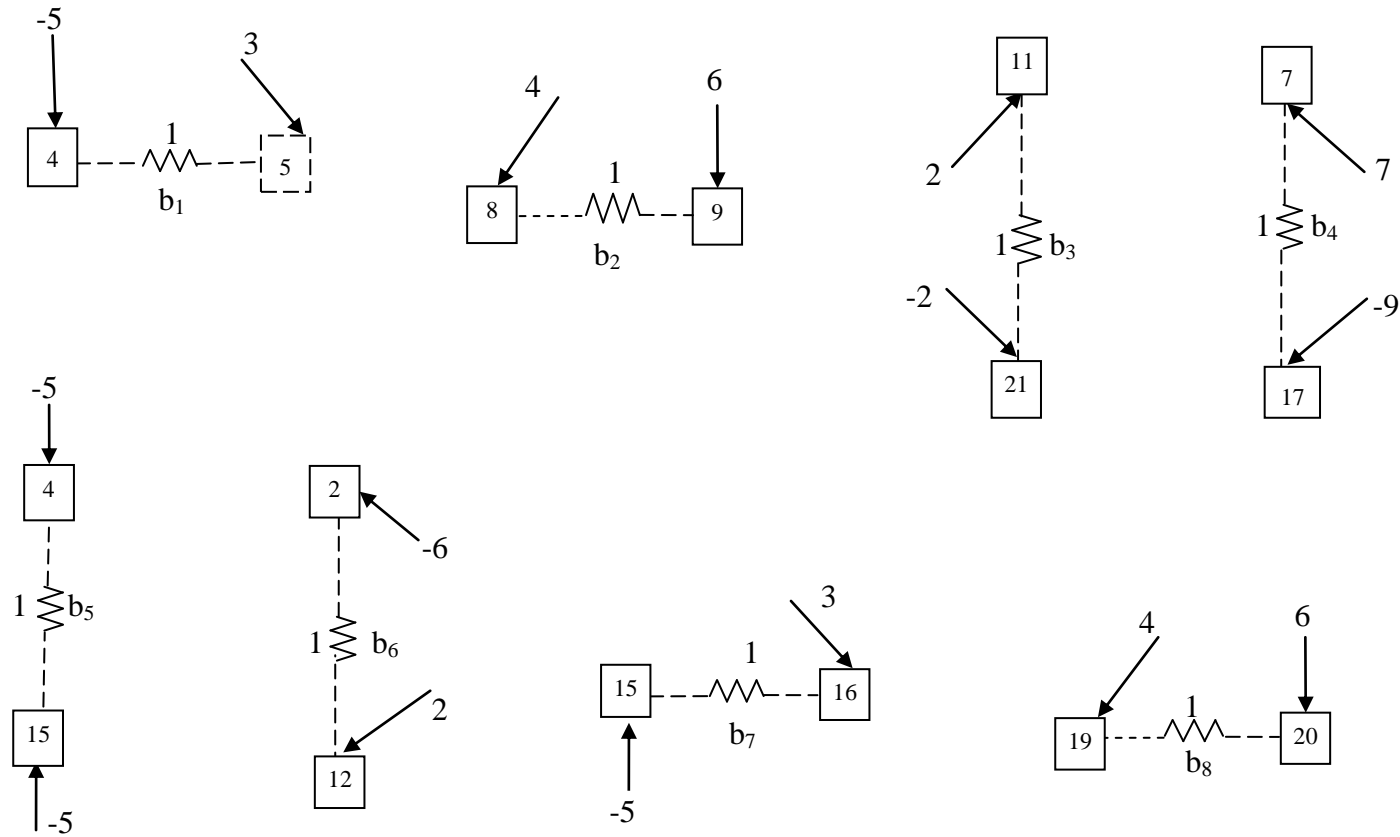


Figure 4.18. Removed branches of Figure 4.1

Table 4.7 Matrices of subnetworks from the torn network

Admittance matrices, \mathbf{Y}	Current vectors, \mathbf{I}	Connection matrices, \mathbf{L}																																																																	
<table border="1"> <thead> <tr> <th colspan="4">\mathbf{Y}_A</th> </tr> </thead> <tbody> <tr> <td>4</td> <td>-1</td> <td>-1</td> <td>-1</td> </tr> <tr> <td>-1</td> <td>4</td> <td>-1</td> <td>-1</td> </tr> <tr> <td>-1</td> <td>-1</td> <td>3</td> <td>-1</td> </tr> <tr> <td>-1</td> <td>-1</td> <td>-1</td> <td>3</td> </tr> </tbody> </table>	\mathbf{Y}_A				4	-1	-1	-1	-1	4	-1	-1	-1	-1	3	-1	-1	-1	-1	3	<table border="1"> <thead> <tr> <th>\mathbf{I}_A</th> </tr> </thead> <tbody> <tr> <td>2</td> </tr> <tr> <td>-6</td> </tr> <tr> <td>6</td> </tr> <tr> <td>-5</td> </tr> </tbody> </table>	\mathbf{I}_A	2	-6	6	-5	<table border="1"> <thead> <tr> <th colspan="8">\mathbf{L}_A</th> </tr> </thead> <tbody> <tr> <td>0</td> <td>0</td> <td>0</td> <td>0</td> <td>0</td> <td>0</td> <td>0</td> <td>0</td> </tr> <tr> <td>0</td> <td>0</td> <td>0</td> <td>0</td> <td>0</td> <td>1</td> <td>0</td> <td>0</td> </tr> <tr> <td>0</td> <td>0</td> <td>0</td> <td>0</td> <td>0</td> <td>0</td> <td>0</td> <td>0</td> </tr> <tr> <td>1</td> <td>0</td> <td>0</td> <td>0</td> <td>1</td> <td>0</td> <td>0</td> <td>0</td> </tr> </tbody> </table>	\mathbf{L}_A								0	0	0	0	0	0	0	0	0	0	0	0	0	1	0	0	0	0	0	0	0	0	0	0	1	0	0	0	1	0	0	0
\mathbf{Y}_A																																																																			
4	-1	-1	-1																																																																
-1	4	-1	-1																																																																
-1	-1	3	-1																																																																
-1	-1	-1	3																																																																
\mathbf{I}_A																																																																			
2																																																																			
-6																																																																			
6																																																																			
-5																																																																			
\mathbf{L}_A																																																																			
0	0	0	0	0	0	0	0																																																												
0	0	0	0	0	1	0	0																																																												
0	0	0	0	0	0	0	0																																																												
1	0	0	0	1	0	0	0																																																												
<table border="1"> <thead> <tr> <th colspan="4">\mathbf{Y}_B</th> </tr> </thead> <tbody> <tr> <td>3</td> <td>-1</td> <td>-1</td> <td>0</td> </tr> <tr> <td>-1</td> <td>3</td> <td>-1</td> <td>-1</td> </tr> <tr> <td>-1</td> <td>-1</td> <td>3</td> <td>-1</td> </tr> <tr> <td>0</td> <td>-1</td> <td>-1</td> <td>3</td> </tr> </tbody> </table>	\mathbf{Y}_B				3	-1	-1	0	-1	3	-1	-1	-1	-1	3	-1	0	-1	-1	3	<table border="1"> <thead> <tr> <th>\mathbf{I}_B</th> </tr> </thead> <tbody> <tr> <td>3</td> </tr> <tr> <td>-9</td> </tr> <tr> <td>7</td> </tr> <tr> <td>4</td> </tr> </tbody> </table>	\mathbf{I}_B	3	-9	7	4	<table border="1"> <thead> <tr> <th colspan="8">\mathbf{L}_B</th> </tr> </thead> <tbody> <tr> <td>-1</td> <td>0</td> <td>0</td> <td>0</td> <td>0</td> <td>0</td> <td>0</td> <td>0</td> </tr> <tr> <td>0</td> <td>0</td> <td>0</td> <td>0</td> <td>0</td> <td>0</td> <td>0</td> <td>0</td> </tr> <tr> <td>0</td> <td>0</td> <td>0</td> <td>1</td> <td>0</td> <td>0</td> <td>0</td> <td>0</td> </tr> <tr> <td>0</td> <td>1</td> <td>0</td> <td>0</td> <td>0</td> <td>0</td> <td>0</td> <td>0</td> </tr> </tbody> </table>	\mathbf{L}_B								-1	0	0	0	0	0	0	0	0	0	0	0	0	0	0	0	0	0	0	1	0	0	0	0	0	1	0	0	0	0	0	0
\mathbf{Y}_B																																																																			
3	-1	-1	0																																																																
-1	3	-1	-1																																																																
-1	-1	3	-1																																																																
0	-1	-1	3																																																																
\mathbf{I}_B																																																																			
3																																																																			
-9																																																																			
7																																																																			
4																																																																			
\mathbf{L}_B																																																																			
-1	0	0	0	0	0	0	0																																																												
0	0	0	0	0	0	0	0																																																												
0	0	0	1	0	0	0	0																																																												
0	1	0	0	0	0	0	0																																																												
<table border="1"> <thead> <tr> <th colspan="3">\mathbf{Y}_C</th> </tr> </thead> <tbody> <tr> <td>3</td> <td>-1</td> <td>-1</td> </tr> <tr> <td>-1</td> <td>2</td> <td>0</td> </tr> <tr> <td>-1</td> <td>0</td> <td>2</td> </tr> </tbody> </table>	\mathbf{Y}_C			3	-1	-1	-1	2	0	-1	0	2	<table border="1"> <thead> <tr> <th>\mathbf{I}_C</th> </tr> </thead> <tbody> <tr> <td>6</td> </tr> <tr> <td>-2</td> </tr> <tr> <td>2</td> </tr> </tbody> </table>	\mathbf{I}_C	6	-2	2	<table border="1"> <thead> <tr> <th colspan="8">\mathbf{L}_C</th> </tr> </thead> <tbody> <tr> <td>0</td> <td>-1</td> <td>0</td> <td>0</td> <td>0</td> <td>0</td> <td>0</td> <td>0</td> </tr> <tr> <td>0</td> <td>0</td> <td>0</td> <td>0</td> <td>0</td> <td>0</td> <td>0</td> <td>0</td> </tr> <tr> <td>0</td> <td>0</td> <td>1</td> <td>0</td> <td>0</td> <td>0</td> <td>0</td> <td>0</td> </tr> </tbody> </table>	\mathbf{L}_C								0	-1	0	0	0	0	0	0	0	0	0	0	0	0	0	0	0	0	1	0	0	0	0	0																	
\mathbf{Y}_C																																																																			
3	-1	-1																																																																	
-1	2	0																																																																	
-1	0	2																																																																	
\mathbf{I}_C																																																																			
6																																																																			
-2																																																																			
2																																																																			
\mathbf{L}_C																																																																			
0	-1	0	0	0	0	0	0																																																												
0	0	0	0	0	0	0	0																																																												
0	0	1	0	0	0	0	0																																																												
<table border="1"> <thead> <tr> <th colspan="4">\mathbf{Y}_D</th> </tr> </thead> <tbody> <tr> <td>4</td> <td>-1</td> <td>-1</td> <td>-1</td> </tr> <tr> <td>-1</td> <td>4</td> <td>-1</td> <td>-1</td> </tr> <tr> <td>-1</td> <td>-1</td> <td>3</td> <td>-1</td> </tr> <tr> <td>-1</td> <td>-1</td> <td>-1</td> <td>3</td> </tr> </tbody> </table>	\mathbf{Y}_D				4	-1	-1	-1	-1	4	-1	-1	-1	-1	3	-1	-1	-1	-1	3	<table border="1"> <thead> <tr> <th>\mathbf{I}_D</th> </tr> </thead> <tbody> <tr> <td>2</td> </tr> <tr> <td>-6</td> </tr> <tr> <td>6</td> </tr> <tr> <td>-5</td> </tr> </tbody> </table>	\mathbf{I}_D	2	-6	6	-5	<table border="1"> <thead> <tr> <th colspan="8">\mathbf{L}_D</th> </tr> </thead> <tbody> <tr> <td>0</td> <td>0</td> <td>0</td> <td>0</td> <td>0</td> <td>-1</td> <td>0</td> <td>0</td> </tr> <tr> <td>0</td> <td>0</td> <td>0</td> <td>0</td> <td>0</td> <td>0</td> <td>0</td> <td>0</td> </tr> <tr> <td>0</td> <td>0</td> <td>0</td> <td>0</td> <td>0</td> <td>0</td> <td>0</td> <td>0</td> </tr> <tr> <td>0</td> <td>0</td> <td>0</td> <td>0</td> <td>-1</td> <td>0</td> <td>1</td> <td>0</td> </tr> </tbody> </table>	\mathbf{L}_D								0	0	0	0	0	-1	0	0	0	0	0	0	0	0	0	0	0	0	0	0	0	0	0	0	0	0	0	0	-1	0	1	0
\mathbf{Y}_D																																																																			
4	-1	-1	-1																																																																
-1	4	-1	-1																																																																
-1	-1	3	-1																																																																
-1	-1	-1	3																																																																
\mathbf{I}_D																																																																			
2																																																																			
-6																																																																			
6																																																																			
-5																																																																			
\mathbf{L}_D																																																																			
0	0	0	0	0	-1	0	0																																																												
0	0	0	0	0	0	0	0																																																												
0	0	0	0	0	0	0	0																																																												
0	0	0	0	-1	0	1	0																																																												
<table border="1"> <thead> <tr> <th colspan="4">\mathbf{Y}_E</th> </tr> </thead> <tbody> <tr> <td>3</td> <td>-1</td> <td>-1</td> <td>0</td> </tr> <tr> <td>-1</td> <td>3</td> <td>-1</td> <td>-1</td> </tr> <tr> <td>-1</td> <td>-1</td> <td>3</td> <td>-1</td> </tr> <tr> <td>0</td> <td>-1</td> <td>-1</td> <td>3</td> </tr> </tbody> </table>	\mathbf{Y}_E				3	-1	-1	0	-1	3	-1	-1	-1	-1	3	-1	0	-1	-1	3	<table border="1"> <thead> <tr> <th>\mathbf{I}_E</th> </tr> </thead> <tbody> <tr> <td>3</td> </tr> <tr> <td>-9</td> </tr> <tr> <td>7</td> </tr> <tr> <td>4</td> </tr> </tbody> </table>	\mathbf{I}_E	3	-9	7	4	<table border="1"> <thead> <tr> <th colspan="8">\mathbf{L}_E</th> </tr> </thead> <tbody> <tr> <td>0</td> <td>0</td> <td>0</td> <td>0</td> <td>0</td> <td>0</td> <td>-1</td> <td>0</td> </tr> <tr> <td>0</td> <td>0</td> <td>0</td> <td>-1</td> <td>0</td> <td>0</td> <td>0</td> <td>0</td> </tr> <tr> <td>0</td> <td>0</td> <td>0</td> <td>0</td> <td>0</td> <td>0</td> <td>0</td> <td>0</td> </tr> <tr> <td>0</td> <td>0</td> <td>0</td> <td>0</td> <td>0</td> <td>0</td> <td>0</td> <td>1</td> </tr> </tbody> </table>	\mathbf{L}_E								0	0	0	0	0	0	-1	0	0	0	0	-1	0	0	0	0	0	0	0	0	0	0	0	0	0	0	0	0	0	0	0	1
\mathbf{Y}_E																																																																			
3	-1	-1	0																																																																
-1	3	-1	-1																																																																
-1	-1	3	-1																																																																
0	-1	-1	3																																																																
\mathbf{I}_E																																																																			
3																																																																			
-9																																																																			
7																																																																			
4																																																																			
\mathbf{L}_E																																																																			
0	0	0	0	0	0	-1	0																																																												
0	0	0	-1	0	0	0	0																																																												
0	0	0	0	0	0	0	0																																																												
0	0	0	0	0	0	0	1																																																												
<table border="1"> <thead> <tr> <th colspan="3">\mathbf{Y}_F</th> </tr> </thead> <tbody> <tr> <td>3</td> <td>-1</td> <td>-1</td> </tr> <tr> <td>-1</td> <td>2</td> <td>0</td> </tr> <tr> <td>-1</td> <td>0</td> <td>2</td> </tr> </tbody> </table>	\mathbf{Y}_F			3	-1	-1	-1	2	0	-1	0	2	<table border="1"> <thead> <tr> <th>\mathbf{I}_F</th> </tr> </thead> <tbody> <tr> <td>6</td> </tr> <tr> <td>-2</td> </tr> <tr> <td>2</td> </tr> </tbody> </table>	\mathbf{I}_F	6	-2	2	<table border="1"> <thead> <tr> <th colspan="8">\mathbf{L}_F</th> </tr> </thead> <tbody> <tr> <td>0</td> <td>0</td> <td>0</td> <td>0</td> <td>0</td> <td>0</td> <td>0</td> <td>-1</td> </tr> <tr> <td>0</td> <td>0</td> <td>-1</td> <td>0</td> <td>0</td> <td>0</td> <td>0</td> <td>0</td> </tr> <tr> <td>0</td> <td>0</td> <td>0</td> <td>0</td> <td>0</td> <td>0</td> <td>0</td> <td>0</td> </tr> </tbody> </table>	\mathbf{L}_F								0	0	0	0	0	0	0	-1	0	0	-1	0	0	0	0	0	0	0	0	0	0	0	0	0																	
\mathbf{Y}_F																																																																			
3	-1	-1																																																																	
-1	2	0																																																																	
-1	0	2																																																																	
\mathbf{I}_F																																																																			
6																																																																			
-2																																																																			
2																																																																			
\mathbf{L}_F																																																																			
0	0	0	0	0	0	0	-1																																																												
0	0	-1	0	0	0	0	0																																																												
0	0	0	0	0	0	0	0																																																												

Table 4.8 Matrix for one-piece solution

V	Y																				I		
V1	4	-1	-1	-1	0	0	0	0	0	0	0	0	0	0	0	0	0	0	0	0	0	-1	2
V2	-1	5	-1	-1	0	0	0	0	0	0	0	-1	0	0	0	0	0	0	0	0	0	0	-6
V3	-1	-1	3	-1	0	0	0	0	0	0	0	0	0	0	0	0	0	0	0	0	0	0	6
V4	-1	-1	-1	5	-1	0	0	0	0	0	0	0	0	0	-1	0	0	0	0	0	0	0	-5
V5	0	0	0	-1	4	-1	-1	0	0	0	0	0	0	0	0	0	0	0	0	0	0	0	3
V6	0	0	0	0	-1	3	-1	-1	0	0	0	0	0	0	0	0	0	0	0	0	0	0	-9
V7	0	0	0	0	-1	-1	4	-1	0	0	0	0	0	0	0	0	-1	0	0	0	0	0	7
V8	0	0	0	0	0	-1	-1	4	-1	0	0	0	0	0	0	0	0	0	0	0	0	0	4
V9	0	0	0	0	0	0	0	-1	4	-1	-1	0	0	0	0	0	0	0	0	0	0	0	6
V10	0	0	0	0	0	0	0	0	-1	2	0	0	0	0	0	0	0	0	0	0	0	0	-2
V11	0	0	0	0	0	0	0	0	-1	0	3	0	0	0	0	0	0	0	0	0	-1	0	2
V12	0	-1	0	0	0	0	0	0	0	0	0	5	-1	-1	-1	0	0	0	0	0	0	0	2
V13	0	0	0	0	0	0	0	0	0	0	0	-1	4	-1	-1	0	0	0	0	0	0	0	-6
V14	0	0	0	0	0	0	0	0	0	0	0	-1	-1	3	-1	0	0	0	0	0	0	0	6
V15	0	0	0	-1	0	0	0	0	0	0	0	-1	-1	-1	5	-1	0	0	0	0	0	0	-5
V16	0	0	0	0	0	0	0	0	0	0	0	0	0	0	-1	4	-1	-1	0	0	0	0	3
V17	0	0	0	0	0	0	-1	0	0	0	0	0	0	0	0	-1	4	-1	-1	0	0	0	-9
V18	0	0	0	0	0	0	0	0	0	0	0	0	0	0	0	-1	-1	3	-1	0	0	0	7
V19	0	0	0	0	0	0	0	0	0	0	0	0	0	0	0	0	-1	-1	4	-1	0	0	4
V20	0	0	0	0	0	0	0	0	0	0	0	0	0	0	0	0	0	0	-1	4	-1	-1	6
V21	0	0	0	0	0	0	0	0	0	0	-1	0	0	0	0	0	0	0	0	-1	3	0	-2
V22	0	0	0	0	0	0	0	0	0	0	0	0	0	0	0	0	0	0	0	0	-1	0	2

The current vectors, \mathbf{I} , in Table 4.7 are formed from the injected currents and the admittance matrices, \mathbf{Y} , of the subnetworks are formed by inspection using nodal analysis. It is assumed that all subnetworks are effectively decoupled from each other and therefore treated as separate entities. The branch impedance matrix, Z_b is the diagonal matrix of (4.10) arranged according to the branch numbers. Connections between the subnetworks are defined by the connection matrices, \mathbf{L} .

$$Z_b = \begin{bmatrix} 1 & . & . & . & . & . & . & . \\ . & 1 & . & . & . & . & . & . \\ . & . & 1 & . & . & . & . & . \\ . & . & . & 1 & . & . & . & . \\ . & . & . & . & 1 & . & . & . \\ . & . & . & . & . & 1 & . & . \\ . & . & . & . & . & . & 1 & . \\ . & . & . & . & . & . & . & 1 \end{bmatrix} \quad (4.10)$$

4.4.1.1 Results

The results in Table 4.9 show that the results for the one-piece solution and diakoptics using BVMT are exactly the same. Solutions of individual subnetworks before transformation shown in the third column are the partial solutions of the original network represented by V_0 in equation (3.23b). The vector \mathbf{v} is the modifying voltage for the subnetworks that takes care of effects of interconnection to other parts of the network to give the same results shown in the fourth column as if it was solved as a piece. For the network, the node voltages of separate subnetworks and modifying voltages are arranged:

$$V_0 = \begin{bmatrix} V_{0A} \\ V_{0B} \\ V_{0C} \\ V_{0D} \\ V_{0E} \\ V_{0F} \end{bmatrix} \quad \text{and} \quad \mathbf{v} = \begin{bmatrix} v_A \\ v_B \\ v_C \\ v_D \\ v_E \\ v_F \end{bmatrix}$$

Table 4.9 Node Voltages in pu for One-Piece Solution and BVMT

Nodes	One-piece nodal analysis of whole network	BVMD Results	
		Partial solution of network (V_0)	Complete solution of network using BVMD ($V=V_0+ v$)
		Volts	
	V_A	V_{0A}	V_A
1	0.4291	-0.7000	0.4291
2	-0.9776	-2.3000	-0.9776
3	1.5363	0.1250	1.5363
4	-0.8425	-2.6250	-0.8425
	V_B	V_{0B}	V_B
5	0.6871	2.3333	0.6871
6	-1.4907	0.0000	-1.4907
7	2.0815	4.0000	2.0815
8	1.7594	2.6667	1.7594
	V_C	V_{0C}	V_C
9	2.4466	3.0000	2.4466
10	0.2233	0.5000	0.2233
11	1.8037	2.5000	1.8037
	V_D	V_{0D}	V_D
12	-0.0108	-0.7000	-0.0108
13	-1.4175	-2.3000	-1.4175
14	1.2281	0.1250	1.2281
15	-0.8873	-2.6250	-0.8873
	V_E	V_{0E}	V_E
16	1.6064	2.3333	1.6064
17	0.3702	0.0000	0.3702
18	3.9424	4.0000	3.9424
19	2.8507	2.6667	2.8507
	V_F	V_{0F}	V_F
20	3.0901	3.0000	3.0901
21	0.9646	0.5000	0.9646
22	2.5450	2.5000	2.5450

4.4.2 Application of BVMT to Nonlinear system with Current Injections

The BVMT is utilized in the solution of a sample system with current injections to prove its effectiveness and validity. Figure 4.20 is a four-bus power system with two

generating stations G_1 and G_4 connected to bus 1 and bus 4, loads $L_1 - L_4$ and transformers $T_1 - T_4$, interconnected by transmission lines. The voltages at buses 1, 2, 3, and 4 are to be calculated.

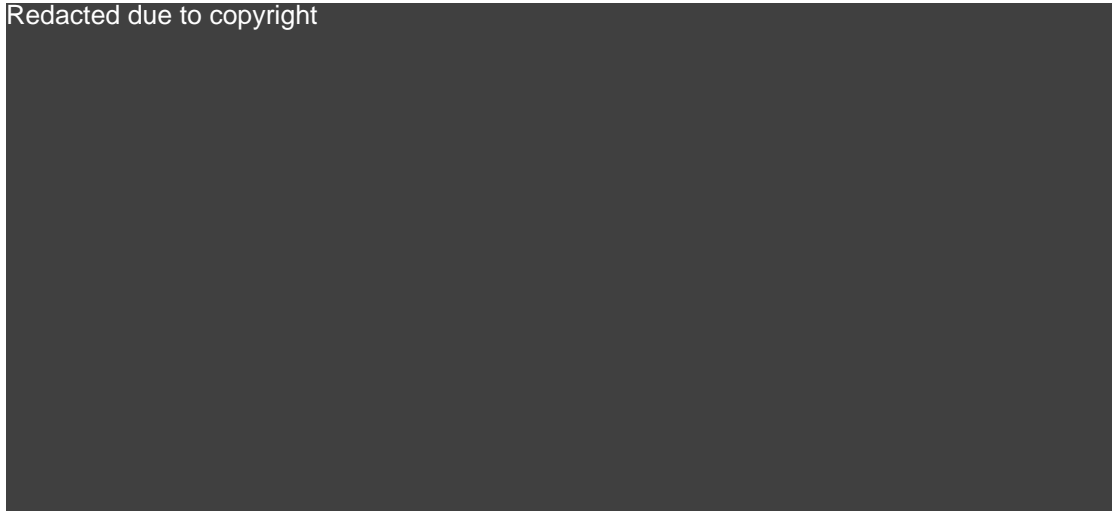


Figure 4.20. Power system with two generating stations [104]

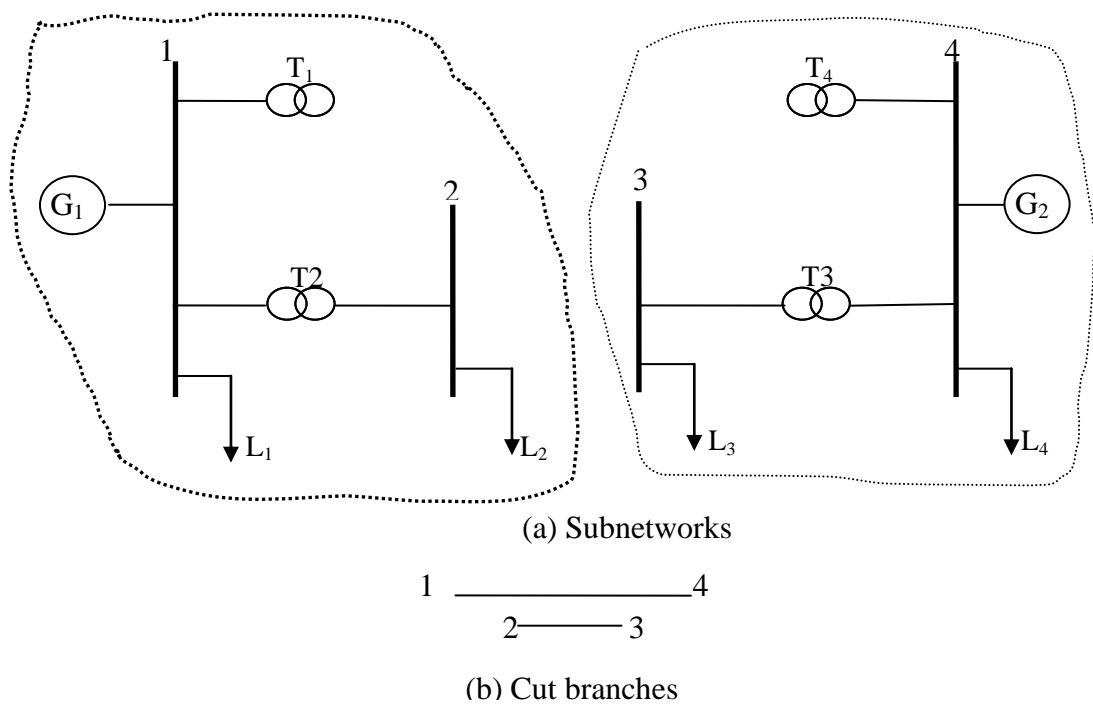


Figure 4.21. The system torn into two

Figure 4.22 is the admittance diagram of Figure 4.20 with power from generator converted to injected currents $I_1 = y_{G1}V_{G1}$ and $I_2 = y_{G2}V_{G2}$; the loads are represented by their admittances $y_{L1} - y_{L4}$ and the branch currents are i_{b1} and i_{b2} . The dashed line AB is the line of tear.

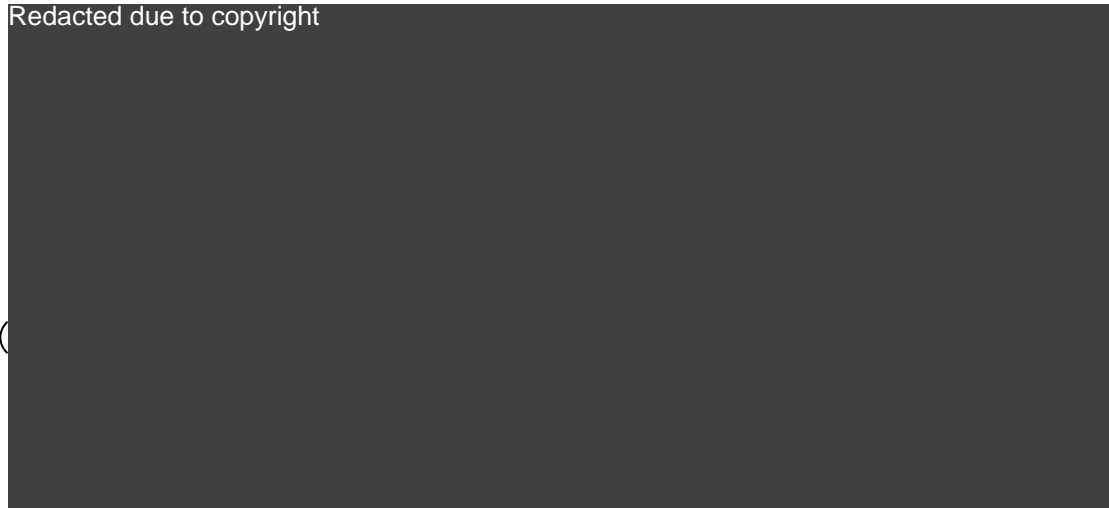


Figure 4.22. Network of current sources and per unit admittances [104] (AB = line of tear)



Figure 4.23. Network of current sources and per unit admittances [104] (AB = line of tear)

Table 4.10 Data for Figure 4.21

Line, load and generator tags	From bus	To bus	Admittances (pu)	Current injection (pu)
1	1	4	0.000 - 2.222i	I ₁ = 0.000-5.000i
2	1	2	0.000 - 6.250i	I ₂ =0
3	2	3	0.000 - 1.852i	I ₃ =0
4	3	4	0.000 - 5.000i	I ₄ =1.900-3.291i
L ₁	-	-	1.160 - 1.550i	-
L ₂	-	-	0.145 - 0.109i	-
L ₃	-	-	9.590 - 7.150i	-
L ₄	-	-	0.390 - 0.510i	-
G ₁	-	-	0.000 - 5.000i	-
G ₄	-	-	0.000 - 4.000i	-

The diagonal matrix for the network is (4.11), the current vector is (4.13), the removed line matrix is (4.14) and the connection matrices are in (4.16).

$$\mathbf{Y}_d = \begin{bmatrix} \mathbf{Y}_A & \cdot \\ \cdot & \mathbf{Y}_B \end{bmatrix}$$

$$= \begin{bmatrix} 0.1450 - j11.3590 & 0.0000 + j6.2500 & \cdot & \cdot \\ 0.0000 + j6.2500 & 9.5900 - j13.4000 & \cdot & \cdot \\ \cdot & \cdot & 1.1600 - j6.5500 & 0.0000 + j5.0000 \\ \cdot & \cdot & 0.0000 + j5.0000 & 0.3900 - j9.5100 \end{bmatrix}$$

(4.11)

where

$$\mathbf{Y}_d^{-1} = \begin{bmatrix} \mathbf{Y}_A^{-1} & \cdot \\ \cdot & \mathbf{Y}_B^{-1} \end{bmatrix}$$

$$= \begin{bmatrix} 0.0167 + 0.1033i & 0.0280 + 0.0282i & \cdot & \cdot \\ 0.0280 + 0.0282i & 0.0502 + 0.0519i & \cdot & \cdot \\ \cdot & \cdot & 0.0745 + 0.2307i & 0.0441 + 0.1195i \\ \cdot & \cdot & 0.0441 + 0.1195i & 0.0300 + 0.1667i \end{bmatrix}$$

(4.12)

$$\begin{bmatrix} \mathbf{I}_A \\ \mathbf{I}_B \end{bmatrix} = \begin{bmatrix} 0.0000 - 5.0000i \\ 0 \\ 0 \\ 1.9000 - 3.2910i \end{bmatrix} \quad (4.13)$$

$$\mathbf{L} = \begin{bmatrix} \mathbf{L}_A \\ \mathbf{L}_B \end{bmatrix} = \begin{bmatrix} 0 & 1 \\ 1 & 0 \\ -1 & 0 \\ 0 & -1 \end{bmatrix} \quad (4.14)$$

where

$$\mathbf{L}^t = [\mathbf{L}_A \quad \mathbf{L}_B] = \begin{bmatrix} 0 & 1 & -1 & 0 \\ 1 & 0 & 0 & -1 \end{bmatrix} \quad (4.15)$$

$$[\mathbf{Z}_b] = \begin{bmatrix} 0.5400i & . \\ . & j0.4500i \end{bmatrix} \quad (4.16)$$

The equations (4.11) – (4.16) are substituted in (3.36) to obtain the bus voltages in Table 4.11. Comparison with the one-piece solution shows they are exactly the same.

4.4.2.1 Results

The partial solutions of individual subnetworks before transformation are shown in the third column of Table 4.11 while the modifying voltages are shown in the fourth column. It can be seen that the results for the one-piece solution and BVMT are exactly the same.

Table 4.11 Results for for Figure 4.21

Buses	One-piece nodal solution of whole network	BVMT Results		
		Partial solution of network (V_0)	Modifying voltage for the partial solution (v)	Complete solution of network using BVMT ($V=V_0+ v$)
		pu		
	V_A	V_{0A}	v_A	V_A
1	0.5402 - 0.0445i	0.5167 - 0.0835i	0.0235 + 0.0391i	0.5402 - 0.0444i
2	0.1821 - 0.1325i	0.1409 - 0.1398i	0.0412 + 0.0073i	0.1821 - 0.1325i
	V_B	V_{0B}	v_B	V_B
3	0.3630 + 0.0018i	0.4769 + 0.0820i	-0.1140 - 0.0802i	0.3630 + 0.0018i
4	0.5420 + 0.1363i	0.6057 + 0.2181i	-0.0637 - 0.0818i	0.5420 + 0.1363i

4.5 Implementation of Slack Bus Voltage-updating Diakoptic (SVUD) Load Flow

Literature shows that load flow analysis and diakoptic analysis are well researched methods but little has been done in the area of applying diakoptics in load flow analysis of power systems. The reason is likely due to the success of sparsity techniques which were very successful in sequential computing [10]. The high speed of present computers which enables them to run load flows of large power systems could also account for the reduced interest in piecewise methods pioneered by Kron. But load flow analysis of power systems can be facilitated by the use of piecewise methods if properly utilised and would reduce computation burden which is a general concern in computer analyses. With the recent shift towards multiprocessors and the availability of cheap computers which can be run in parallel, there is renewed interest in diakoptic analysis of power systems but only a small proportion involves load flow.

Implementation of the SVUD load flow which is suitable for sequential and parallel computing is presented in this section. Because of the analysis of subnetworks separately, any system to be analysed would have more than one slack bus - one

original and chosen ones for the subnetworks that do not contain the main slack bus. The result is that during the iteration process, the voltages of these temporary slack buses remain constant instead of varying like they would in one-piece load flow analysis. To account for this, the given parameters (P, Q in the case of load buses and P, V in the case of generator buses) at the chosen buses are used to update the voltages during iteration.

4.5.1 *Summary of Application of SVUD to Test Systems*

The process of analysing the test networks using SVUD is summarized in Figure 4.24. Before a network is solved using the new load flow method, SVUD, it is first solved as a piece using the standard G-S method, and in some cases the N-R method. The results are then used as a benchmark for determining the accuracy of SVUD. Interface information is required in the process of solving subnetworks that were originally parts of a whole network.

The network in Figure 3.8 is used as the first case study for the new algorithm. The network data are shown in Table 4.12 and Table 4.13. In this analysis, all buses, except the slack bus, are assumed to be PQ buses. This assumption is close to reality because the number of PV buses in practical power networks is very small compared to PQ buses. In G-S load flow of the full network convergence was achieved after 27 iterations and the result is shown in Table 4.14; N-R load flow gave the same results but convergence was achieved after 6 iterations. This is typical because N-R has a faster convergence rate than G-S. But for this particular network, convergence could not be achieved for subnet **B** with N-R when the network was torn due to the topology of the network and the nature of the resultant Jacobian matrix.

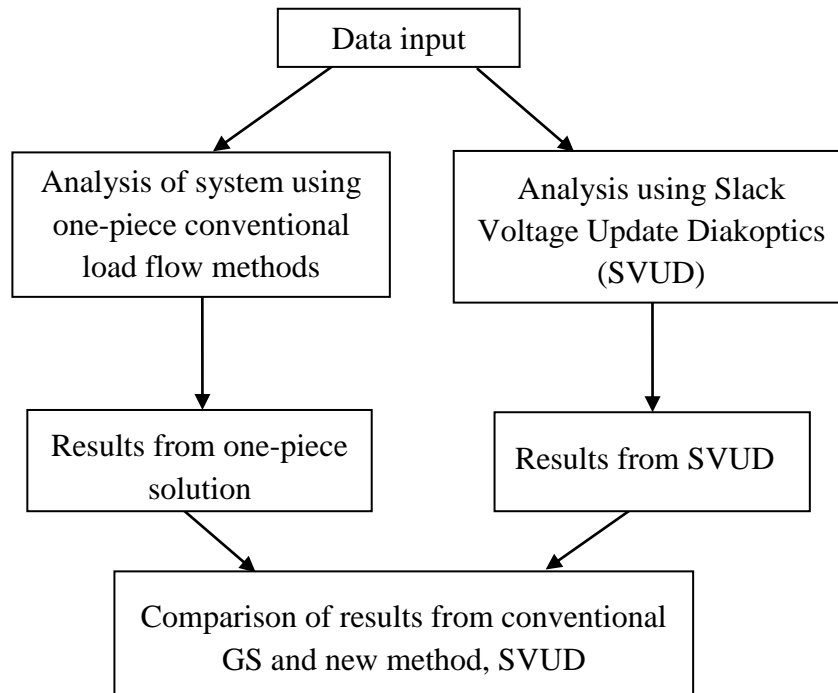


Figure 4.24 Procedure for analysis of test systems

4.5.2 Solution Procedure Slack Bus Voltage-Updating Load Flow

The network of Figure 3.8 was torn into two subnetworks, *A* and *B* shown in Figure 3.12 (a) and (b) by removing branches 2-6 and 4-5. In real systems the branches are not removed. The rearranged line data for the torn network is shown in Table 4.15.

Table 4.12 Bus data of the network of Figure 3.8

Bus	Voltage	Angle	Generation		Load	
			P_{Gi}	Q_{Gi}	P_{Li}	Q_{Li}
1	1.06	0	0.00	0.00	0.000	0.00
2	1.00	0	0.00	0.00	-0.100	-0.05
3	1.00	0	0.00	0.00	0.800	0.10
4	1.00	0	0.00	0.00	-0.250	-0.15
5	1.00	0	0.00	0.00	-0.200	-0.15
6	1.00	0	0.00	0.00	-0.577	-0.10

Table 4.13 Line data of the network

From bus	To bus	R	X	B/2	Transformer tap
1	2	0.01	0.030	0.030	-
2	5	0.04	0.150	0.035	-
1	5	0.05	0.180	0.010	-
2	6	0.02	0.035	0.000	-
5	4	0.00	0.080	0.000	-
3	4	0.00	0.060	0.000	1.02
3	6	0.03	0.080	0.030	-

Table 4.14 Result of load flow on full network

Bus	COMPLEX VOLTAGE (pu)	MAGNITUDE (pu)	ANGLE (degrees)	ITERATIONS
1	1.0600 - 0.0000i	1.0600	0.0000	27
2	1.0545 - 0.0066i	1.0545	-0.3568	
3	1.0644 + 0.0223i	1.0646	1.1994	
4	1.0381 + 0.0011i	1.0381	0.0617	
5	1.0425 - 0.0073i	1.0425	-0.3985	
6	1.0502 - 0.0103i	1.0502	-0.5615	

Table 4.15 Line data of torn network with buses reordered

Full network Numbering	Removed lines	From bus	To bus	R	X	B/2	Transformer tap
1- 2		A1	A2	0.01	0.030	0.030	
2-5		A2	A3	0.04	0.150	0.035	
1-5	line $z_{b1} =$	A1	A3	0.05	0.180	0.010	
2-6	line $z_{b2} =$	A2	B3	0.02	0.035	0.000	
4-5		A3	B2	0.00	0.080	0.000	
3-4		B1	B2	0.00	0.060	0.000	1.02
3-6		B1	B3	0.03	0.080	0.030	

4.5.2.1 Subnetwork Analysis

The slack bus voltage of subnet *A* is the slack bus of the untorn network which is $1.06\angle 0^\circ$; this value does not change during iteration and so does not need to be updated like the slack bus voltage of subnet *B*. Flat start of $1\angle 0^\circ$ pu is used for all other buses including the slack bus of subnet *B*.

Table 4.16 Results of each iteration and update

Nodes	Iteration 1	Iteration 2	Iteration 3	Iteration 4	Iteration 5
V_{Amod} (pu)					
VA2	1.0566 - 0.0048i	1.0573 - 0.0049i	1.0574 - 0.0049i	1.0574 - 0.0049i	1.0574 - 0.0049i
VA3	1.0473 - 0.0065i	1.0477 - 0.0065i	1.0478 - 0.0065i	1.0478 - 0.0065i	1.0478 - 0.0065i
V_{Bmod} (pu)					
VB1	1.0747 + 0.0242i	1.0749 + 0.0239i	1.0750 + 0.0239i	1.0750 + 0.0239i	1.0750 + 0.0239i
VB2	1.0463 + 0.0027i	1.0466 + 0.0025i	1.0467 + 0.0025i	1.0467 + 0.0025i	1.0467 + 0.0025i
VB3	1.0550 - 0.0090i	1.0556 - 0.0091i	1.0556 - 0.0091i	1.0557 - 0.0091i	1.0557 - 0.0091i
$VB1up$ (pu)					
Updated slack bus voltage	0.9969 + 0.0014i	1.0722 + 0.0241i	1.0719 + 0.0256i	1.0719 + 0.0255i	1.0719 + 0.0255i

4.5.2.2 Comparison of results with one-piece solution

Results from the SVUD and conventional G-S load flow of the whole network are compared in Table 4.18.

Figure 4.25 for voltage magnitudes and Figure 4.26 for the angles were generated using *Microsoft Excel* to compare results of the one-piece solution and the new method. The values prove the viability of the new algorithm. The likely reason for not obtaining exactly the same results as in linear analysis is explained in section 4.8.1 and this applies to all the iterative solutions employed. The bus voltages obtained by the one-piece load flow calculation are represented as $V(ONE)$ and the bus voltages obtained by using the SVUD method as $V(SVUD)$.

Table 4.17 Comparison of results

Original bus no.	Bus nos. in subnetworks	One-piece solution V(ONE)	SVUD solution V(SVUD)
Complex voltages (pu)			
1	A1	1.0600+0.0000i	1.0600 +0.0000i
2	A2	1.0545 - 0.0066i	1.0574 - 0.0049i
3	B1	1.0644 +0.0223i	1.0719+ 0.0255i
4	B2	1.0381 +0.0011i	1.0467+ 0.0025i
5	A3	1.0425 - 0.0073i	1.0478- 0.0065i
6	B3	1.0502 - 0.0103i	1.0557 - 0.0091i

Table 4.18 Comparison of results (magnitudes and angles)

Original bus no.	Bus no. in subnetworks	One-piece solution V(ONE)		SVUD solution V(SVUD)	
		Mag. (pu)	Ang.(deg)	Mag.(pu)	Ang.(deg)
1	A1	1.0600	0	1.0600	0
2	A2	1.0545	-0.36	1.0574	-0.27
3	B1	1.0646	1.20	1.0722	1.36
4	B2	1.0381	0.06	1.0467	0.14
5	A3	1.0425	-0.40	1.0478	-0.36
6	B3	1.0502	-0.56	1.0557	-0.49

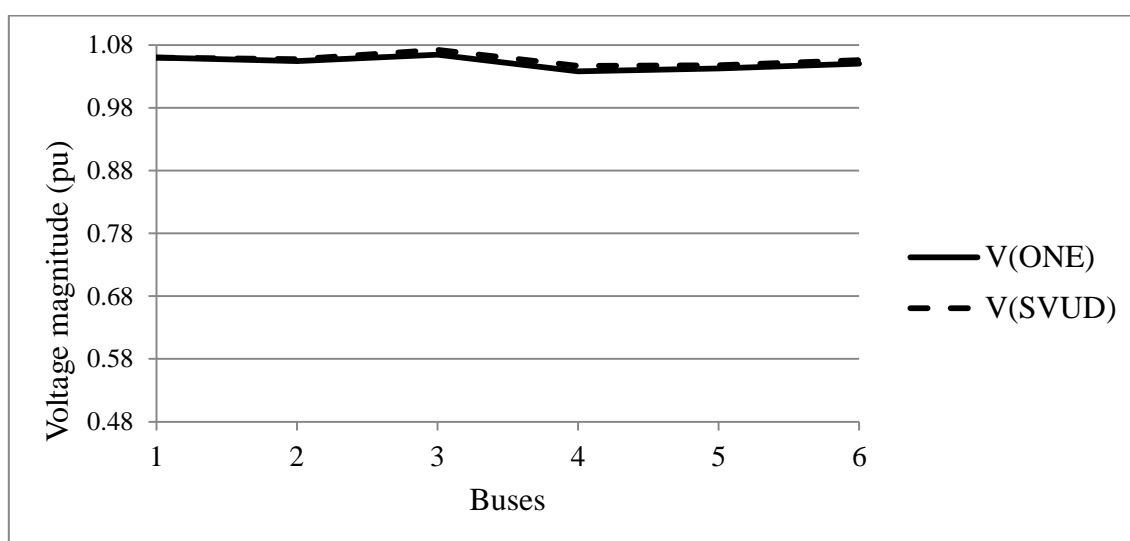


Figure 4.25 Plot of voltage magnitudes of one-piece load flow and SVUD method

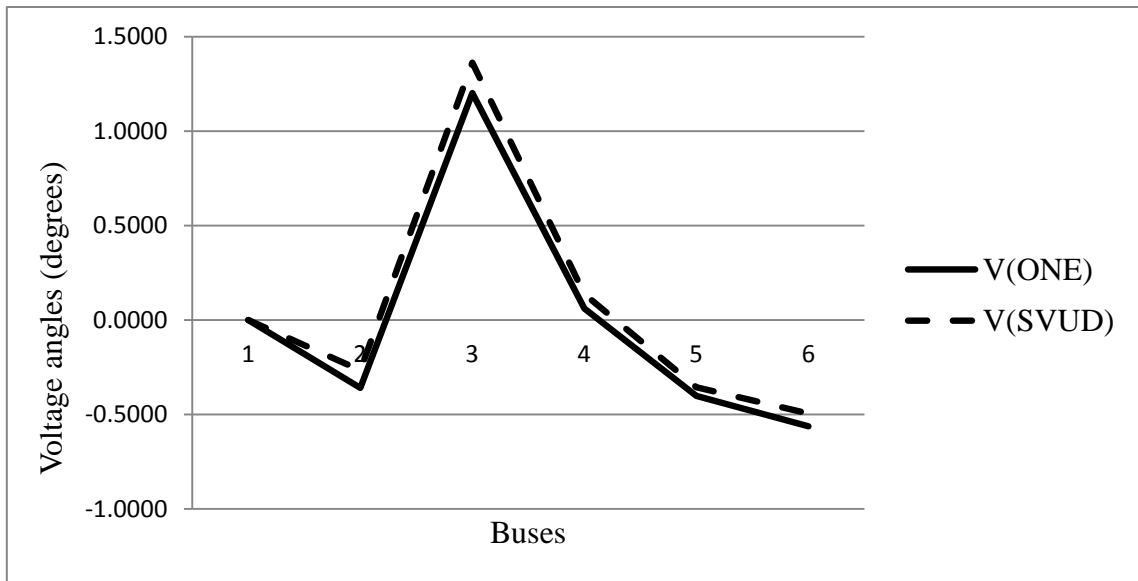


Figure 4.26. Plot of voltage angles of One-piece and SVUD solutions

4.5.2.3 Summary of Results

The dashed lines represent the one-piece results plot and full line the SVUD plots for voltage magnitudes and angles in degrees. The difference in the convergence rate between G-S of full network and the SVUD load flow is substantial. Even the sum of iterations in the two subnetworks is 10 with SVUD compared to 27 of the one-piece solution. Though some computing time is needed in the modifying and updating process, this is minimal. Another important aspect is the simplicity of the algorithm which, once written can be used for any network. It proves to be much easier than the piecewise load flow methods reviewed. Also the flow chart of Figure 3.11 indicates minimal communication between subnetworks and reduces the burden on the central computer thereby freeing some capacity to be utilized for other purposes like control.

4.6 Application of the SVUD Load Flow to IEEE Test Systems

In this section, the SVUD is applied to IEEE test systems to further ascertain the accuracy of the new method. The algorithm is also very useful in planning and contingency analysis where the accuracy desired is predictive.

The diakoptic load flow operates by updating information in each subnetwork with information from the other networks at each iteration. This method of updating is used in [42] but the method of analysis is quite different from the new algorithm in three major ways. In [42] bus tearing and fast decoupled load flow are employed and the analysis is based on large charge sensitivity derived basically from [15, 59]. In the SVUD, branch tearing is employed and G-S load flow method is used, partly as a way of improving its convergence characteristics. And then, there is the novel slack bus updating principle incorporated into the load flow iterative procedure.

4.6.1 *Application of SVUD to IEEE 14-Bus Test System*

The IEEE 14-bus system is shown in Figure 4.21 and the bus and line parameters are shown in Tables 4.14 and 4.15. The network is slightly modified in that the compensators in the original network are not used in this analysis. The line and bus data of the 14-bus system are shown in Table 4.19 and Table 4.20. The load flow was first performed using the standard G-S method in one-piece solution and results are shown in the second column of Table 4.22.

The MATLAB code developed for the SVUD load flow analysis is shown in appendix E. At the start of the SVUD solution procedure, there is a prompting to decide for automatic or manual tearing of the network where the message, *'would you like to manually cut network (1=yes, 0=no)'*: would be displayed. Equal sizes of subnetworks are not necessary; the best cuts can be determined by the engineer as explained in section 4.4. When the decision is for manual tearing, that is, *'yes'*, a *'1'* is input; the list of line numbers to choose for tearing would be displayed as in Table 4.21 in addition to the network map (Figure 4.28). The lines to remove for tearing the network can then be chosen. If lines 10, 18 and 20 are selected, the computer outputs Figure 4.30, where the dashed lines represent the cut lines.

The next decision is choosing the slack buses for the subnetworks. The message, *'Would you like to manually select slack buses for subnets? (1=yes, 0=no)'* would be displayed; if the answer is *'yes'*, the list of buses for each subnetwork is displaced. When the chosen buses are input, the computer

performs the load flow and outputs the bus voltages in the third column of Table 4.15. The voltage magnitudes of SVUD and one-piece results are shown in Table 4.23. Diakoptics was also employed in the same way as in SVUD but without updating the slack buses voltages. The load flow diverged in spite of the fact that the same lines of cut were selected. Since a divergent load flow cannot give reliable results, the most stable solution which was found at iteration 146 gave erroneous the results shown in Table 4.22.

Redacted due to copyright



Figure 4.27. IEEE 14-bus test system [105]

Table 4.19 Bus data of the IEEE 14-bus system [105]

Redacted due to copyright



Table 4.20 Line data of the IEEE 14-bus system [105]

Redacted due to copyright

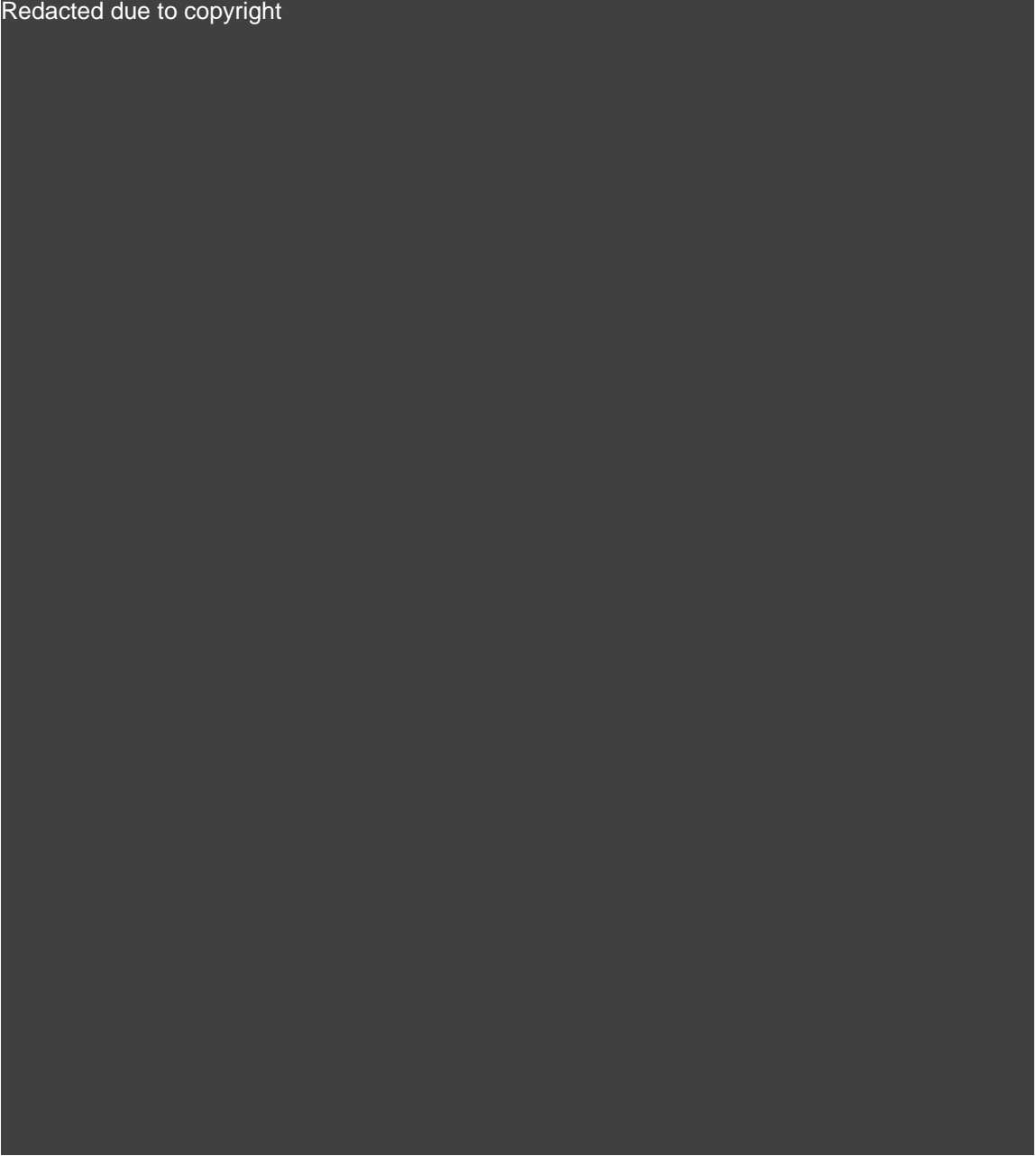


Table 4.21 Computer output of network line and bus numbers

Line no.	From bus	To bus
1	1	2
2	1	5
3	2	3
4	2	4
5	2	5
6	3	4
7	4	5
8	4	7
9	4	9
10	5	6
11	6	11
12	6	12
13	6	13
14	7	8
15	7	9
16	9	10
17	9	14
18	10	11
19	12	13
20	13	14

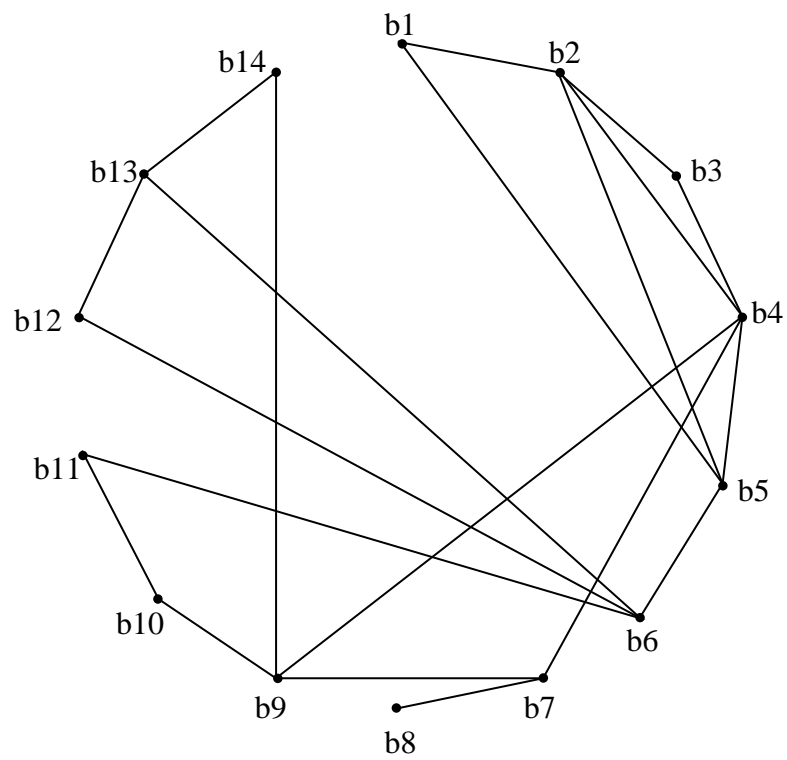


Figure 4.28 Network map 14-bus system showing bus numbers

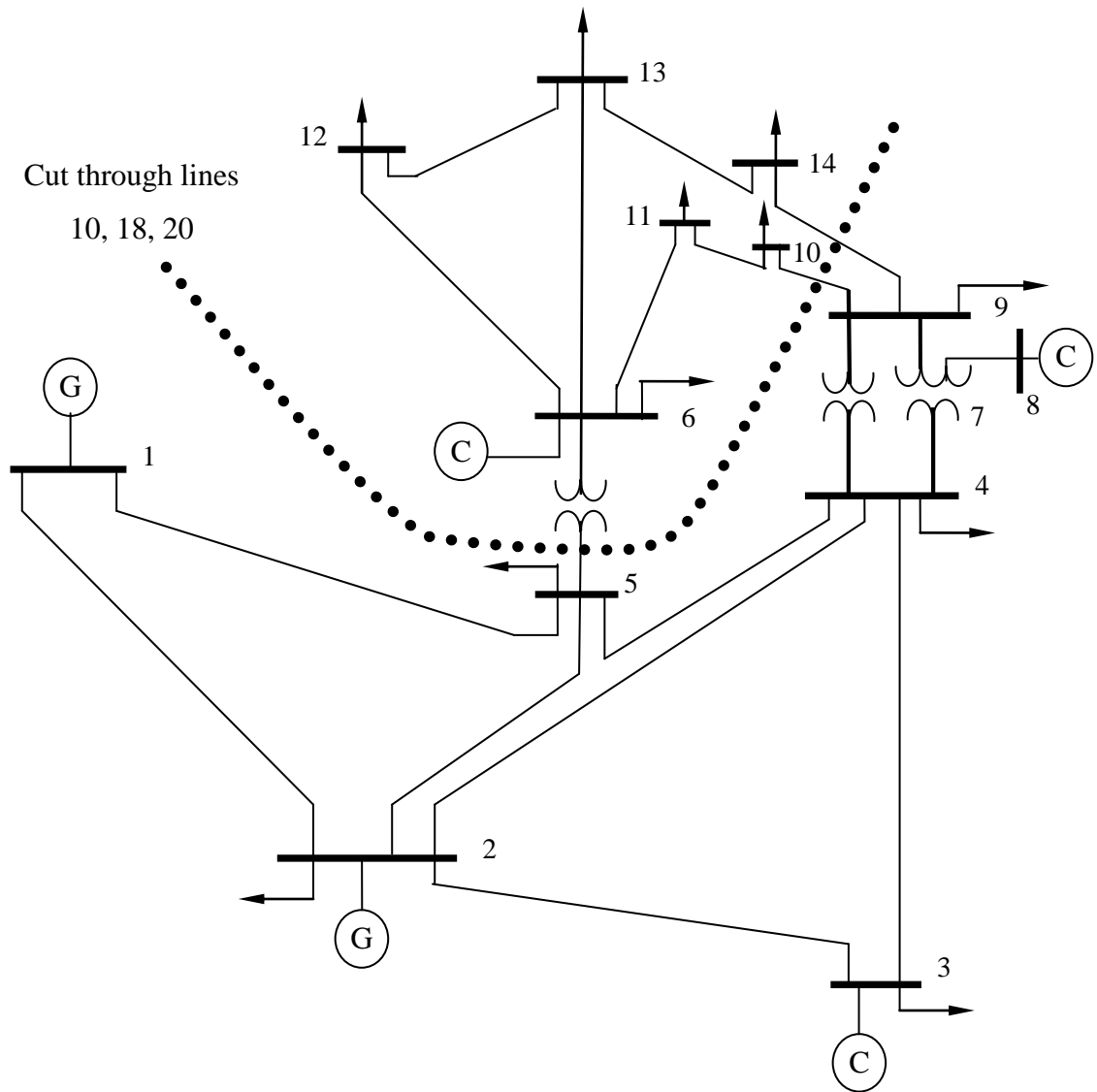


Figure 4.29. IEEE 14-bus test system showing cut= lines 10, 18, 20

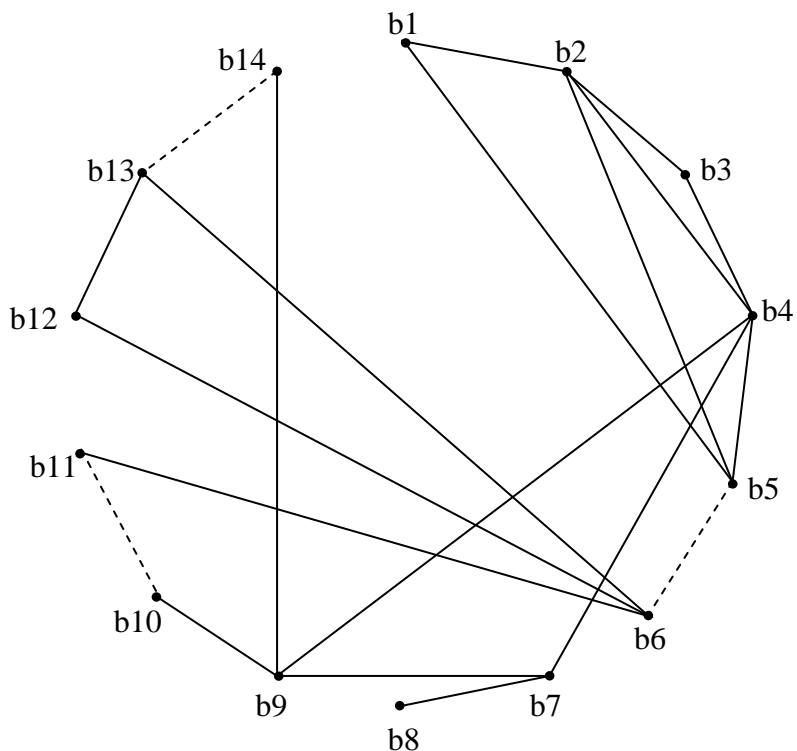


Figure 4.30 Computer output of the 14-bus network with cut =10, 18, 20

Table 4.22 Results of 14 bus network using different solution methods

Bus no.	One-Piece Gauss-Seidel	SVUD	Diakoptic Gauss-Seidel without slack bus update
	iterations = 106	Iterations = 5	Iterations = 146
	Voltages in pu		
1	1.0600 + 0.0000i	1.0600 + 0.0000i	1.0600 + 0.0000i
2	1.0304 - 0.1082i	1.0431 - 0.0970i	1.0667 + 0.0595i
3	0.9757 - 0.2423i	0.9969 - 0.2233i	1.0433 + 0.1734i
4	0.9702 - 0.1872i	0.9956 - 0.1633i	1.0514 + 0.1096i
5	0.9797 - 0.1609i	1.0089 - 0.1373i	1.0549 + 0.0906i
6	0.9719 - 0.2693i	0.9807 - 0.1626i	1.0529 + 0.1074i
7	0.9546 - 0.2415i	0.9754 - 0.2051i	1.0775 + 0.1051i
8	0.9546 - 0.2415i	0.9754 - 0.2051i	1.1150 + 0.1088i
9	0.9349 - 0.2679i	0.9529 - 0.2251i	1.0498 + 0.1194i
10	0.9322 - 0.2712i	0.9503 - 0.2233i	1.0427 + 0.1224i
11	0.9475 - 0.2715i	0.9594 - 0.1979i	1.0434 + 0.1175i
12	0.9505 - 0.2808i	0.9620 - 0.2099i	1.0368 + 0.1249i
13	0.9437 - 0.2798i	0.9561 - 0.2117i	1.0336 + 0.1257i
14	0.9145 - 0.2862i	0.9321 - 0.2305i	1.0227 + 0.1378i

Table 4.23 Voltage magnitudes of 14-bus solution in per unit

	SVUD Solution (pu)	One-Piece Solution (pu)
1	1.06	1.06
2	1.05	1.04
3	1.02	1.01
4	1.01	0.99
5	1.02	0.99
6	0.99	1.01
7	1.00	0.98
8	1.00	0.98
9	0.98	0.97
10	0.98	0.97
11	0.98	0.99
12	0.98	0.99
13	0.98	0.98
14	0.96	0.96

4.6.2 *SVUD Analysis of EEE 30-Bus Network*

A network can be cut into a number of subnetworks, as has been demonstrated already, as far as the number of removed branches is not too high as to compromise time [7, 17]. Analysis conducted in this work, shows that the lines of cut affect the results which corroborate Kron and Happ's statements [6, 7] that the chosen line of cut should be carefully chosen by the engineer. But as already stated, apart from a few tearing guidelines, the method of tearing remains heuristic. The same procedure as the 14-bus network is followed in analysis of the 30-bus network of Figure 4.27. The bus and line data are shown in Tables 4.17 and 4.18 respectively. Bus voltages obtained from load flow analysis are shown in Tables 4.19 and 4.20. The network maps before and after tearing are indicated by Figures 4.29, 4.30, 4.33 and 4.34 for different lines of tear.

Redacted due to copyright

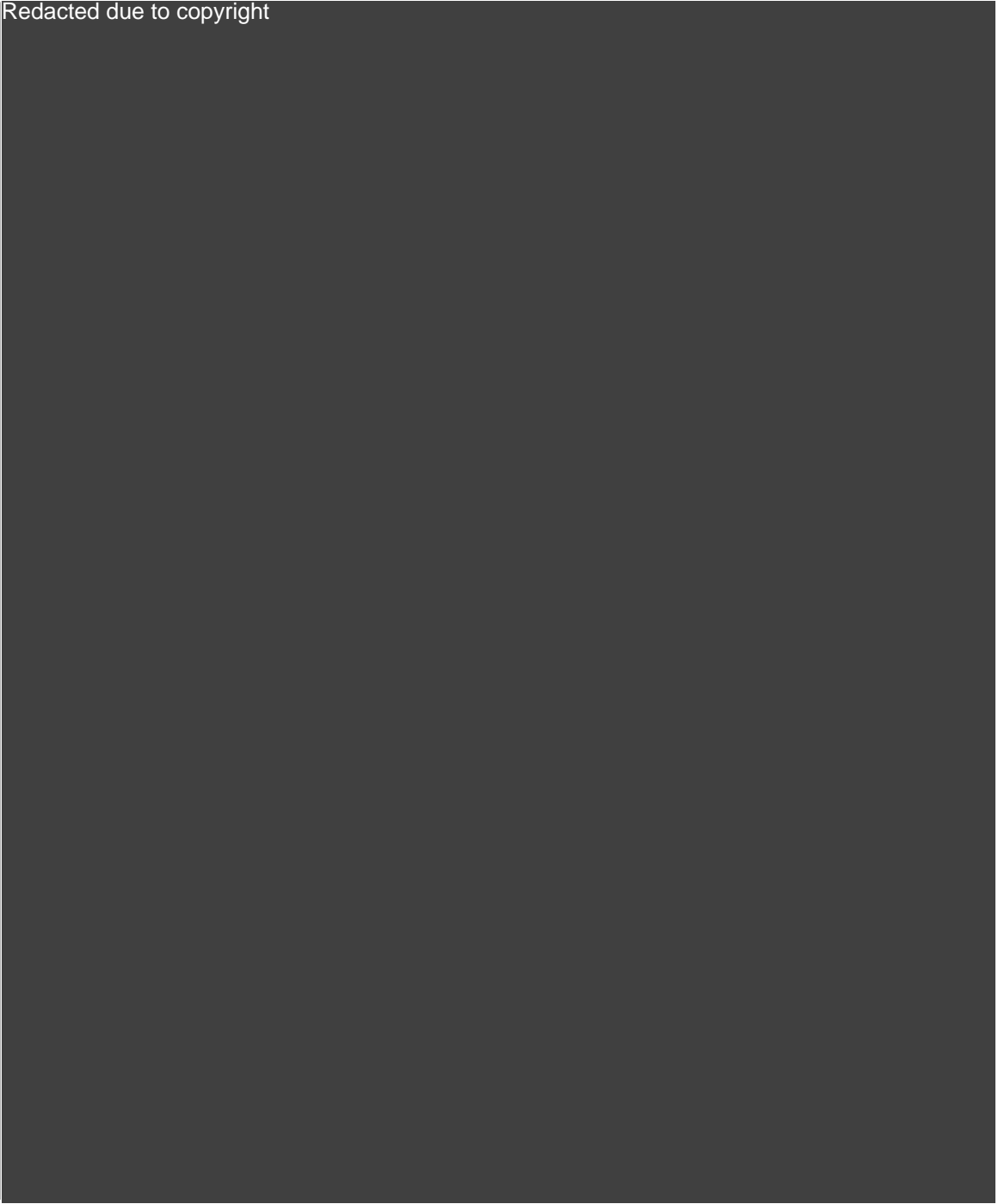


Figure 4.31. IEEE 30-bus test system [105]

Table 4.24 Bus data of the IEEE 30-bus system [106,107]

Redacted due to copyright

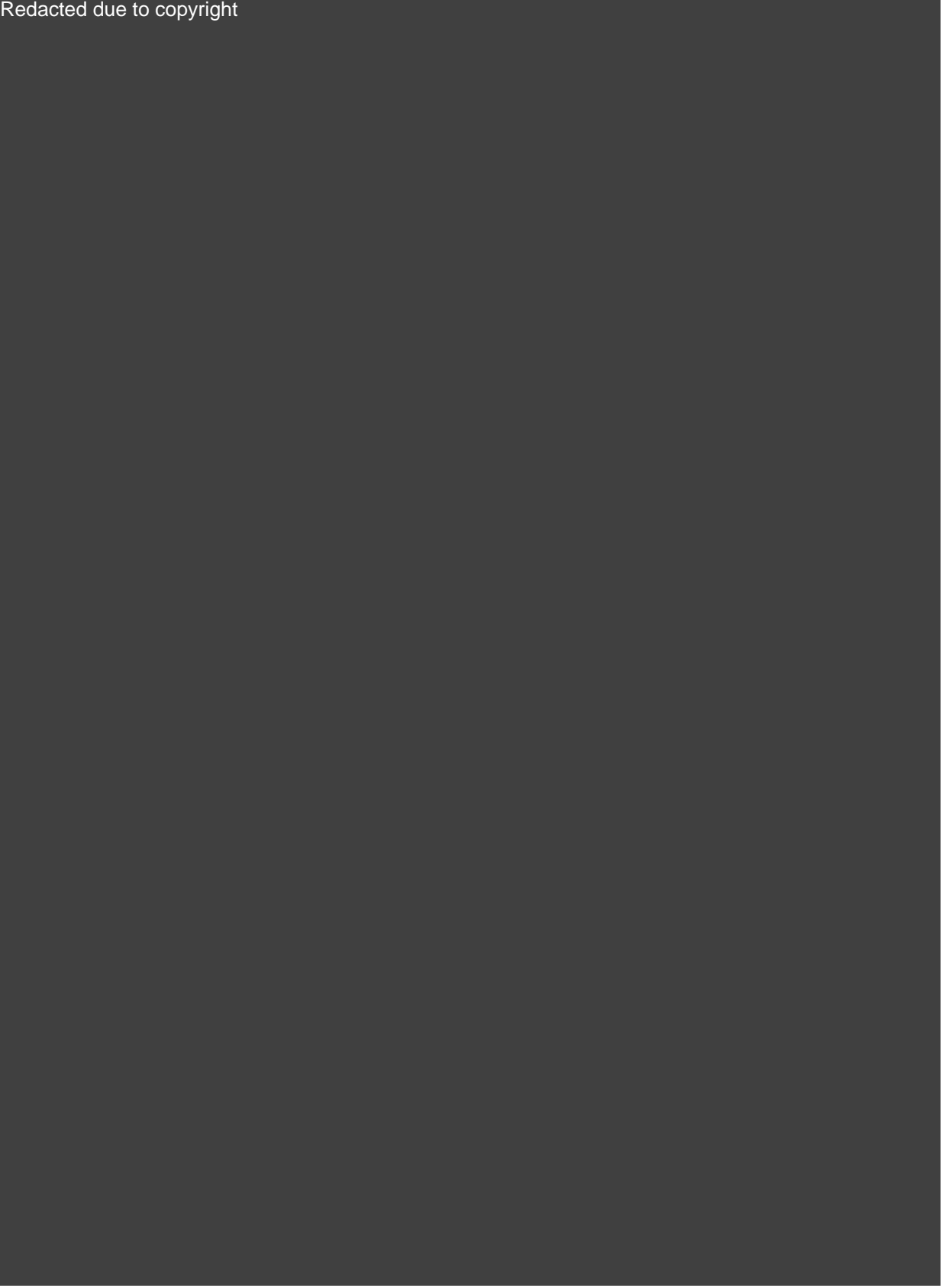


Table 4.25 Line data of the IEEE 30-bus system

Line no.	From bus	To bus	Line impedance (pu)		Charging (pu)	Tap Setting
			R	X	B/2	
1	1	2	0.0192	0.0575	0.0264	-
2	1	3	0.0452	0.1652	0.0204	-
3	2	4	0.0570	0.1737	0.0184	-
4	3	4	0.0132	0.0379	0.0042	-
5	2	5	0.0472	0.1983	0.0209	-
6	2	6	0.0581	0.1763	0.0187	-
7	4	6	0.0119	0.0414	0.0045	-
8	5	7	0.0460	0.1160	0.0102	-
9	6	7	0.0267	0.0820	0.0085	-
10	6	8	0.0120	0.0420	0.0045	-
11	6	9	0.0000	0.2080	0.0000	0.9780
12	6	10	0.0000	0.5560	0.0000	0.9690
13	9	11	0.0000	0.2080	0.0000	-
14	9	10	0.0000	0.1100	0.0000	-
15	4	12	0.0000	0.2560	0.0000	0.9320
16	12	13	0.0000	0.1400	0.0000	-
17	12	14	0.1231	0.2559	0.0000	-
18	12	15	0.0662	0.1304	0.0000	-
19	12	16	0.0945	0.1987	0.0000	-
20	14	15	0.2210	0.1997	0.0000	-
21	16	17	0.0824	0.1923	0.0000	-
22	15	18	0.1073	0.2185	0.0000	-
23	18	19	0.0639	0.1292	0.0000	-
24	19	20	0.0340	0.0680	0.0000	-
25	10	20	0.0936	0.2090	0.0000	-
26	10	17	0.0324	0.0845	0.0000	-
27	10	21	0.0348	0.0749	0.0000	-
28	10	22	0.0727	0.1499	0.0000	-
29	21	23	0.0116	0.0236	0.0000	-
30	15	23	0.1000	0.2020	0.0000	-
31	22	24	0.1150	0.1790	0.0000	-
32	23	24	0.1320	0.2700	0.0000	-
33	24	25	0.1885	0.3292	0.0000	-
34	25	26	0.2544	0.3800	0.0000	-
35	25	27	0.1093	0.2087	0.0000	-
36	28	27	0.0000	0.3960	0.0000	0.9680
37	27	29	0.2198	0.4153	0.0000	-
38	27	30	0.3202	0.6027	0.0000	-
39	29	30	0.2399	0.4533	0.0000	-
40	8	28	0.0636	0.2000	0.0214	-
41	6	28	0.0169	0.0599	0.0650	-

Table 4.26 Line and node numbers of the 30-bus

Line number	From bus	To bus
1	1	2
2	1	3
3	2	4
4	3	4
5	2	5
6	2	6
7	4	6
8	5	7
9	6	7
10	6	8
11	6	9
12	6	10
13	9	11
14	9	10
15	4	12
16	12	13
17	12	14
18	12	15
19	12	16
20	14	15
21	16	17
22	15	18
23	18	19
24	19	20
25	10	20
26	10	17
27	10	21
28	10	22
29	21	23
30	15	23
31	22	24
32	23	24
33	24	25
34	25	26
35	25	27
36	28	27
37	27	29
38	27	30
39	29	30
40	8	28
41	6	28

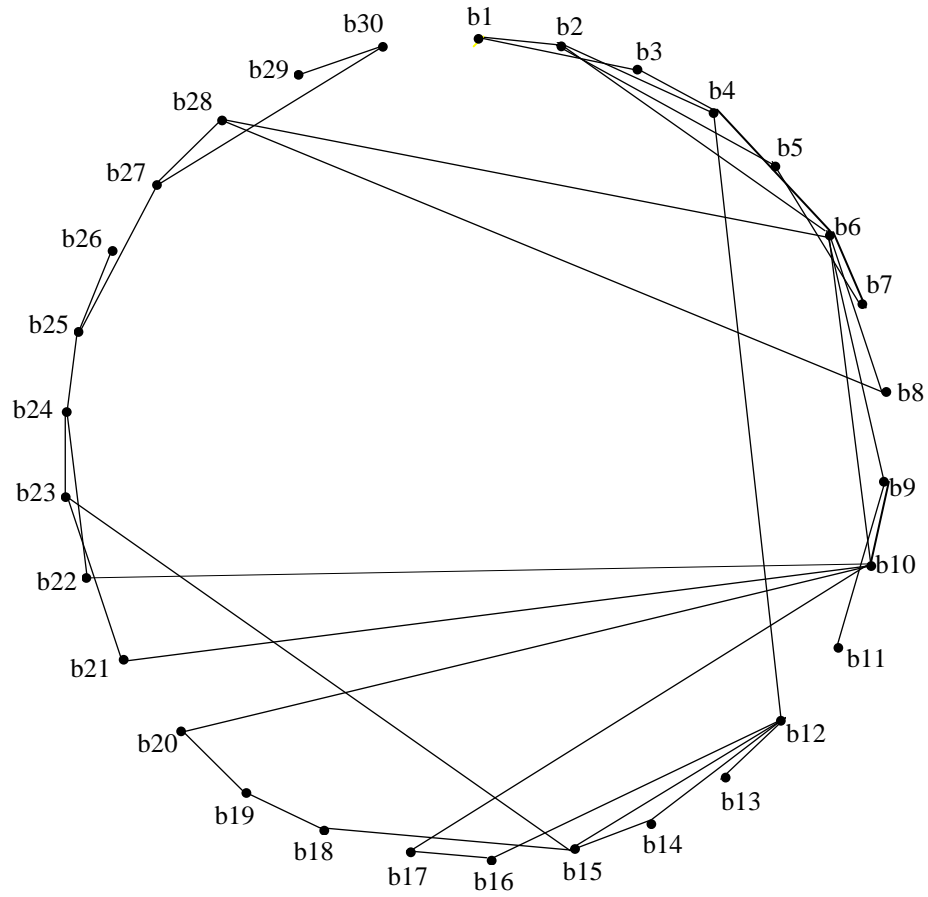


Figure 4.32. Network map of 30-bus test system before tearing

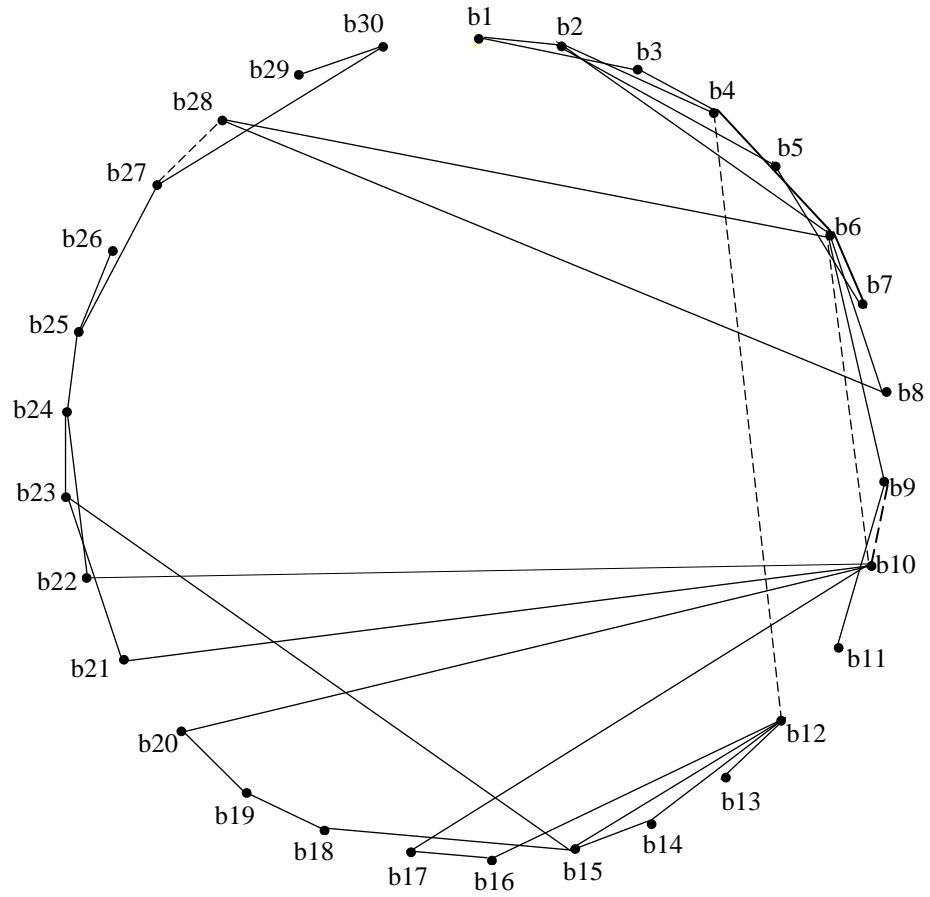


Figure 4.33. Network map of Figure 4.28 with cut lines = 12, 14, 15, 36

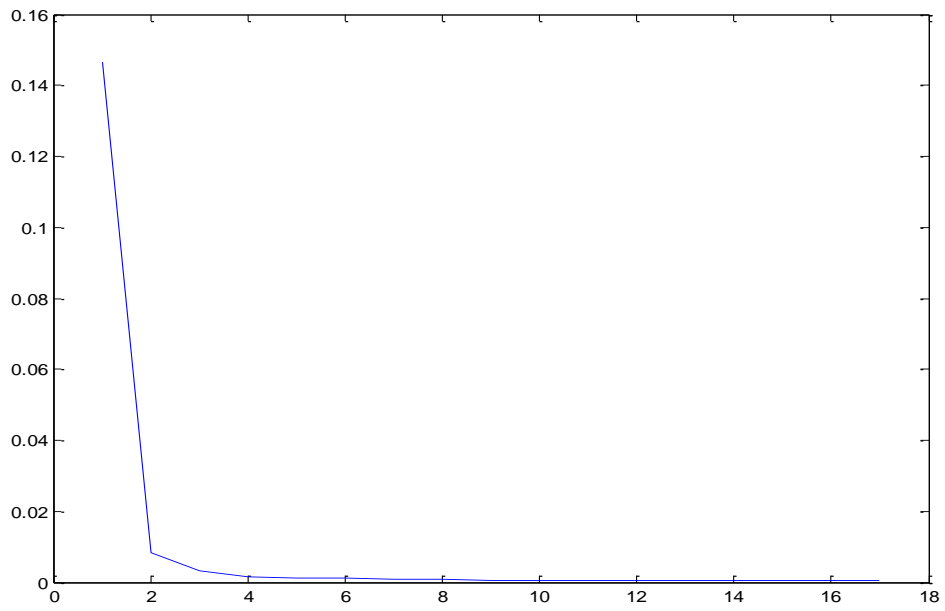


Figure 4.34. Convergence characteristics for cuts = 6,7,9,19,23,29,31,36

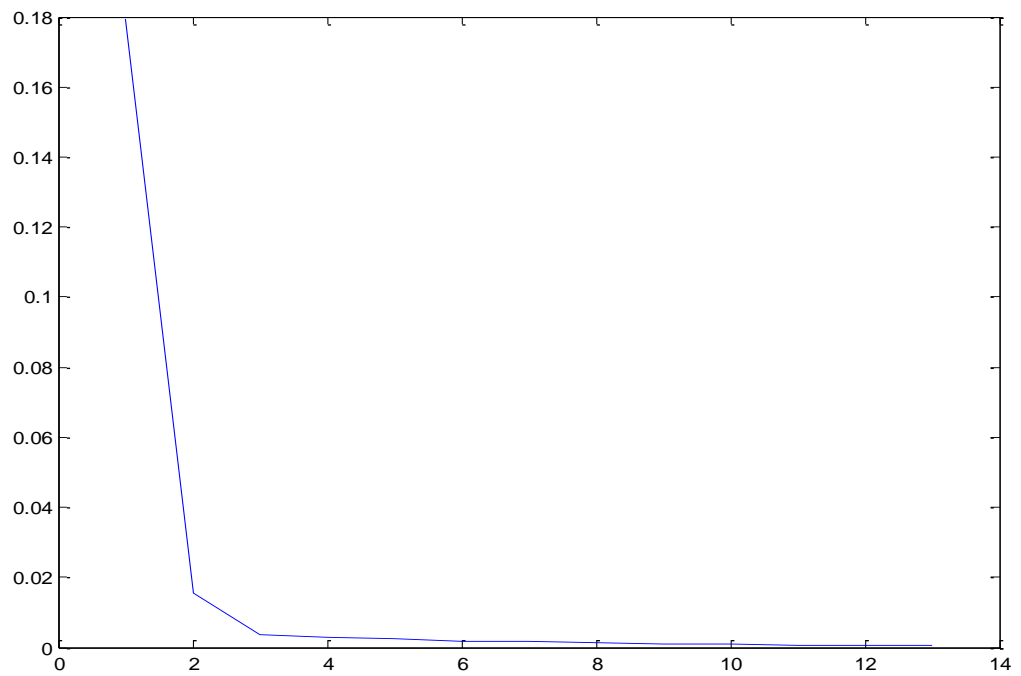


Figure 4.35. Convergence characteristics for cuts = 10,12,14,15,31,32,41

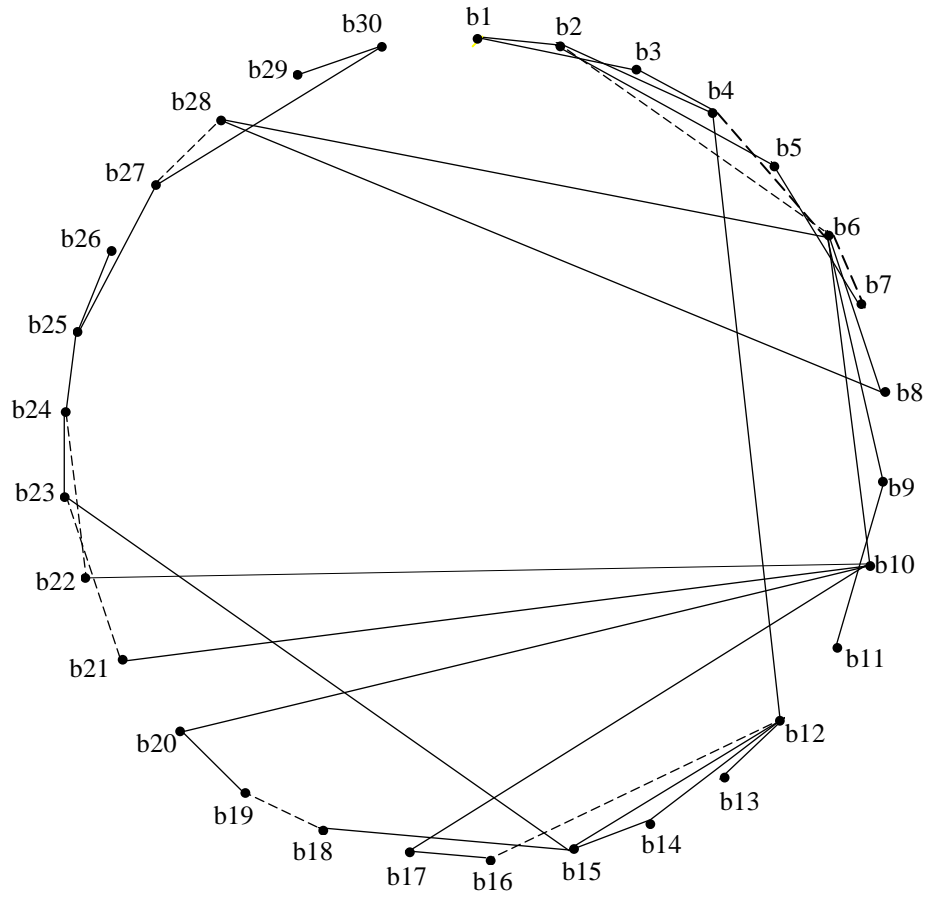


Figure 4.36. Network map for the 30-bus network for cuts = 6, 7, 9, 19, 23, 29, 31,

36.

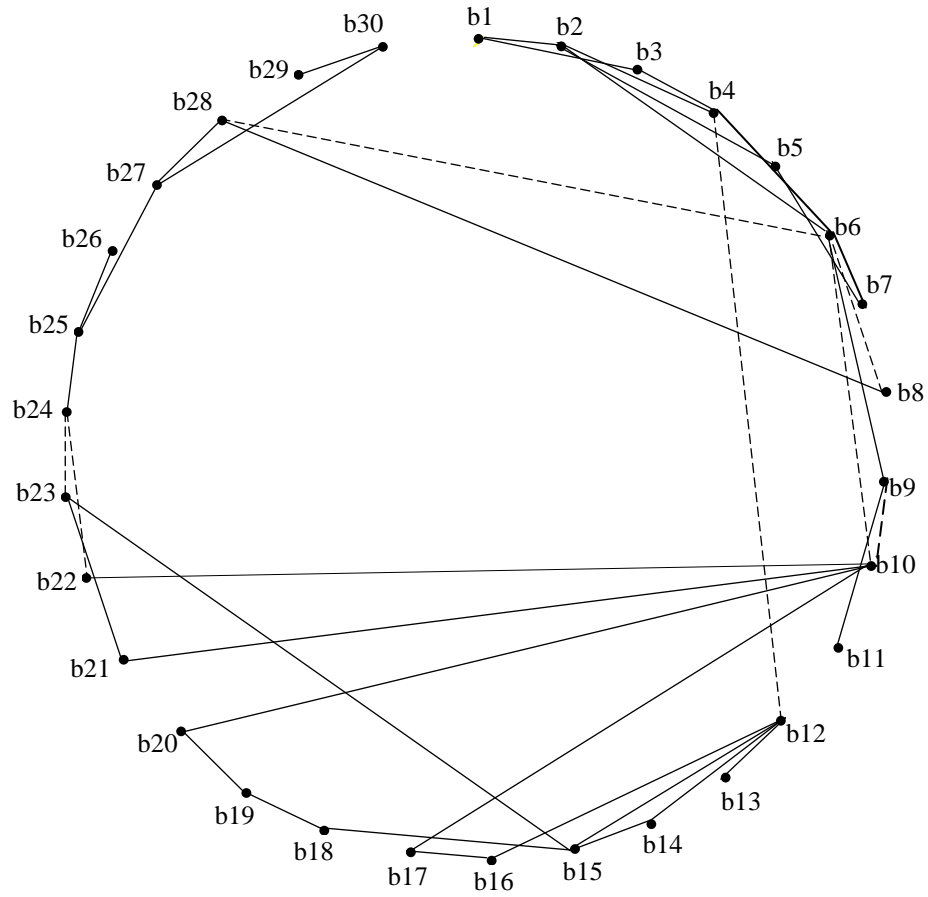


Figure 4.37. Network map for 30-bus cuts = 10,12,14,15,31,32,41

Table 4.27 Results for 30-bus system

Bus no.	G-S	SVUD	
	One-Piece	Two subnetworks Slack buses = 1, 6	Three subnetworks Slack buses = 1,8,12
	Iterations = 202	Iterations = 17	Iterations = 13
	No cut lines	Cuts lines = 6, 7, 9, 19, 23, 29, 31, 36	Cuts lines = 10, 12, 14, 15, 31, 32, 41
1	1.0600 + 0.0000i	1.0600 + 0.0000i	1.0600 + 0.0000i
2	1.0328 - 0.1182i	1.0322 - 0.0649i	1.0462 - 0.0426i
3	0.9962 - 0.1648i	1.0132 - 0.0911i	1.0419 - 0.0536i
4	0.9787 - 0.2013i	1.0007 - 0.1106i	1.0366 - 0.0649i
5	0.9694 - 0.2834i	0.9873 - 0.2013i	1.0048 - 0.1583i
6	0.9666 - 0.2367i	1.0030 - 0.0906i	1.0327 - 0.0729i
7	0.9580 - 0.2627i	0.9831 - 0.1587i	1.0135 - 0.1165i
8	0.9578 - 0.2469i	0.9896 - 0.1302i	0.9919 + 0.0787i
9	0.9812 - 0.3400i	1.0065 - 0.2258i	1.0438 - 0.0706i
10	0.9544 - 0.3839i	0.9823 - 0.2773i	1.0514 - 0.0356i
11	1.0247 - 0.3551i	1.0390 - 0.2328i	1.0335 - 0.0698i
12	1.0002 - 0.3549i	1.0268 - 0.2544i	1.0297 - 0.1044i
13	1.0292 - 0.3652i	1.0575 - 0.2622i	1.0611 - 0.1075i
14	0.9766 - 0.3688i	1.0028 - 0.2691i	1.0203 - 0.1209i
15	0.9663 - 0.3708i	0.9924 - 0.2698i	1.0174 - 0.1124i
16	0.9720 - 0.3690i	0.9992 - 0.2666i	1.0246 - 0.1027i
17	0.9532 - 0.3809i	0.9810 - 0.2761i	1.0255 - 0.0834i
18	0.9460 - 0.3824i	0.9731 - 0.2810i	1.0121 - 0.1122i
19	0.9382 - 0.3873i	0.9658 - 0.2851i	1.0062 - 0.1092i
20	0.9411 - 0.3871i	0.9688 - 0.2839i	1.0127 - 0.1023i
21	0.9418 - 0.3826i	0.9670 - 0.2783i	1.0186 - 0.0898i
22	0.9465 - 0.3817i	0.9678 - 0.2752i	1.0276 - 0.0883i
23	0.9431 - 0.3813i	0.9674 - 0.2772i	1.0159 - 0.0928i
24	0.9369 - 0.3778i	0.9498 - 0.2703i	1.0138 - 0.0996i
25	0.9433 - 0.3536i	0.9352 - 0.2383i	1.0138 - 0.1203i
26	0.9240 - 0.3542i	0.9081 - 0.2353i	0.9933 - 0.1264i
27	0.9565 - 0.3371i	0.9394 - 0.2187i	1.0245 - 0.1290i
28	0.9611 - 0.2494i	0.9905 - 0.1316i	1.0318 - 0.0763i
29	0.9302 - 0.3508i	0.8955 - 0.2293i	1.0006 - 0.1505i
30	0.9138 - 0.3611i	0.8673 - 0.2383i	0.9862 - 0.1658i

4.7 Comparison of SVUD with One-piece Gauss-Seidel Load Flow

The conventional GS load flow method and the SVUD approach results for different networks were compared in terms of the number of iteration and the accuracy of the results. An important quality of the SVUD method is its speed of convergence compared with the conventional Gauss-Seidel. The number of iterations using the SVUD is much lower where for example, instead of 202 iterations for the 30-bus network, 17 and 13 iterations were required as represented in Table 4.27. Results for 6-bus and 14-bus networks showed reduction in iteration from 27 to 5 and 106 to 5 respectively.

Table 4.28 Comparison of number of iterations for different networks

NETWORKS	One-Piece G-S	SVUD load flow
Sample 6-bus	27	5
IEEE 14-bus	106	5
IEEE 30-bus	202	17 (2 subnetworks) 13 (3 subnetworks)

The voltage mean square error, V_{MSE} is calculated [81] [108] for the results using the one-piece solution using G-S and the SVUD method by applying (4.17). The voltage magnitudes using G-S for one-piece solution is represented by $V_{i(ONE)}$ and the voltage magnitudes from SVUD method is represented by $V_{i(SVUD)}$. The total of number of buses in the network is N. The values in Table 4.22 indicate accuracy of the new algorithm.

$$V_{MSE} = \frac{1}{N} \sum_{i=1}^N (V_{i(ONE)} - V_{i(SVUD)})^2 \quad (4.17)$$

Table 4.29 Voltage mean Square errors (VMSE) between SVUD and one-piece G-S

NETWORKS	VMSE
6-bus with SVUD	0.0004
IEEE 14-bus with SVUD	0.0030
IEEE 30-bus with SVUD	0.0117

4.8 Convergence Characteristics of SVUD Load Flow

Load flow is generally an iterative solution of a set of equations representing Kirchhoff's current laws for electrical circuits. Convergence is said to be achieved in iterative solutions when the tolerance criterion is met by all nodes in a network. There are certain networks where convergence cannot be achieved and such networks may be ill-conditioned or initial conditions for the load flow are not properly chosen; in which case a few adjustments may ensure convergence. For example, the swing bus does not exist in physical power systems but is a basic requirement in power flow analysis. Since it is for computation convenience, choosing a different slack bus sometimes causes the load flow to converge. This has been proved in the analysis of some of the networks using SVUD. The plot in Figure 4.38 shows convergence when a right choice was made. The plots in Figure 4.39 and Figure 4.40 show oscillatory convergence and divergence of load flow analysis of the test systems when wrong choices were made for line cuts and temporary slack buses.

Convergence criteria in iterative solutions specify where the iterations should stop depending on the desired accuracy. The level of accuracy usually depends on the purpose of the load flow. The standard tolerance is 10^{-4} [100] but typical values are between 10^{-2} and 10^{-5} . For planning purposes a tolerance of 10^{-2} is sufficient. A load flow is said to converge if all the bus voltages meet the set tolerance.

As iteration goes on, the error difference should reduce until it is equal to or less than the desired tolerance. If a load flow diverges or the convergence is oscillatory, information obtained cannot be trusted to represent the physical power system so it is always good to ensure convergence. In contingency, such as a line outage, a previously converged power flow may diverge if a different slack bus is chosen. This also applies in diakoptic load flow analysis because it involves the disconnection of

some lines theoretically, to tear a network into subnetworks. Temporary slack buses for subnetworks that do not contain original slack bus were changed when there was no convergence.

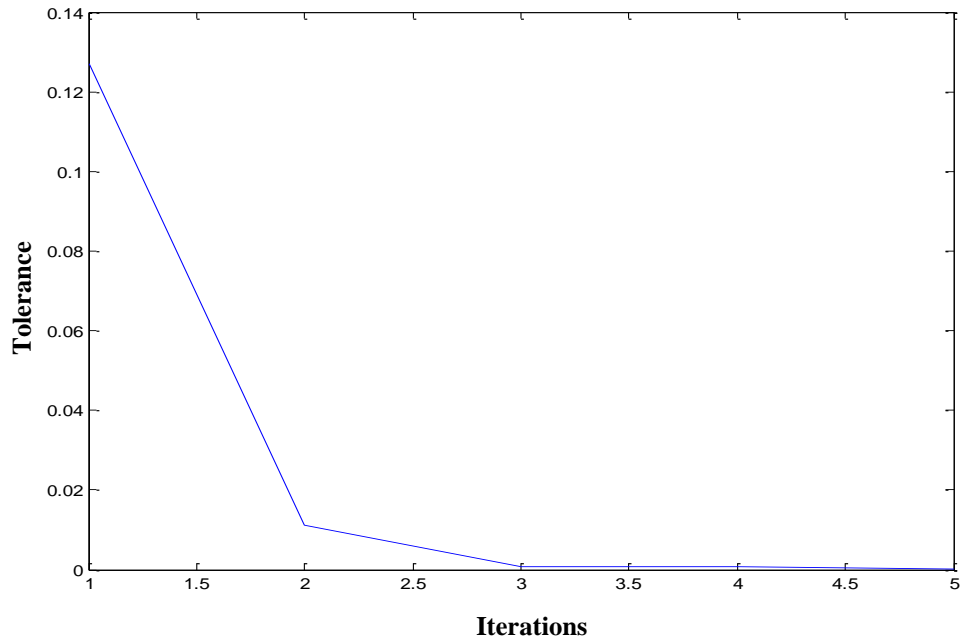


Figure 4.38. Convergence properties of 14-bus network for cut lines =10, 18, 20

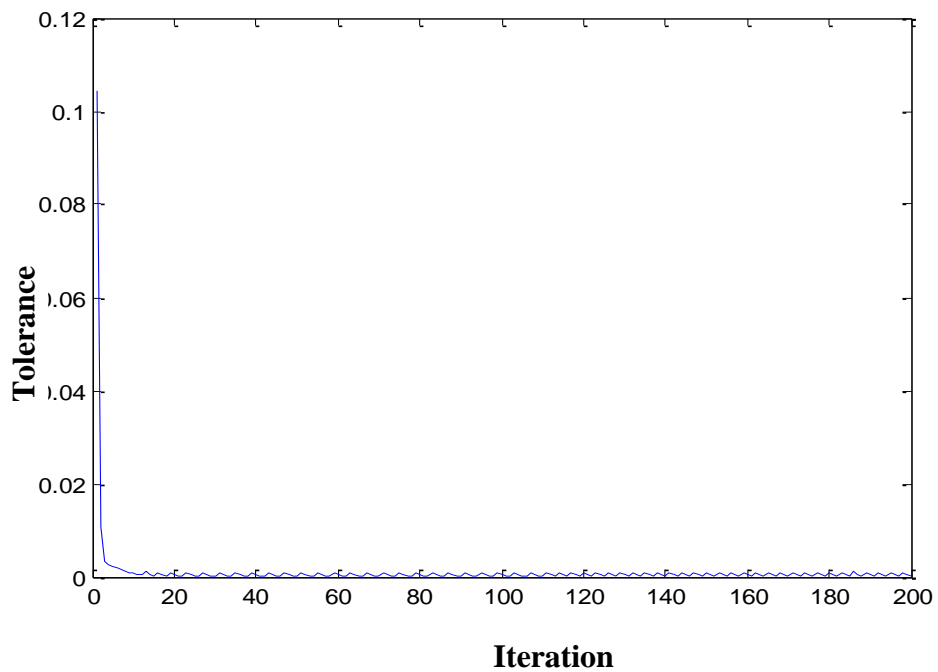


Figure 4.39. Oscillatory convergence of 30-bus for the cut lines 12,14,15,36

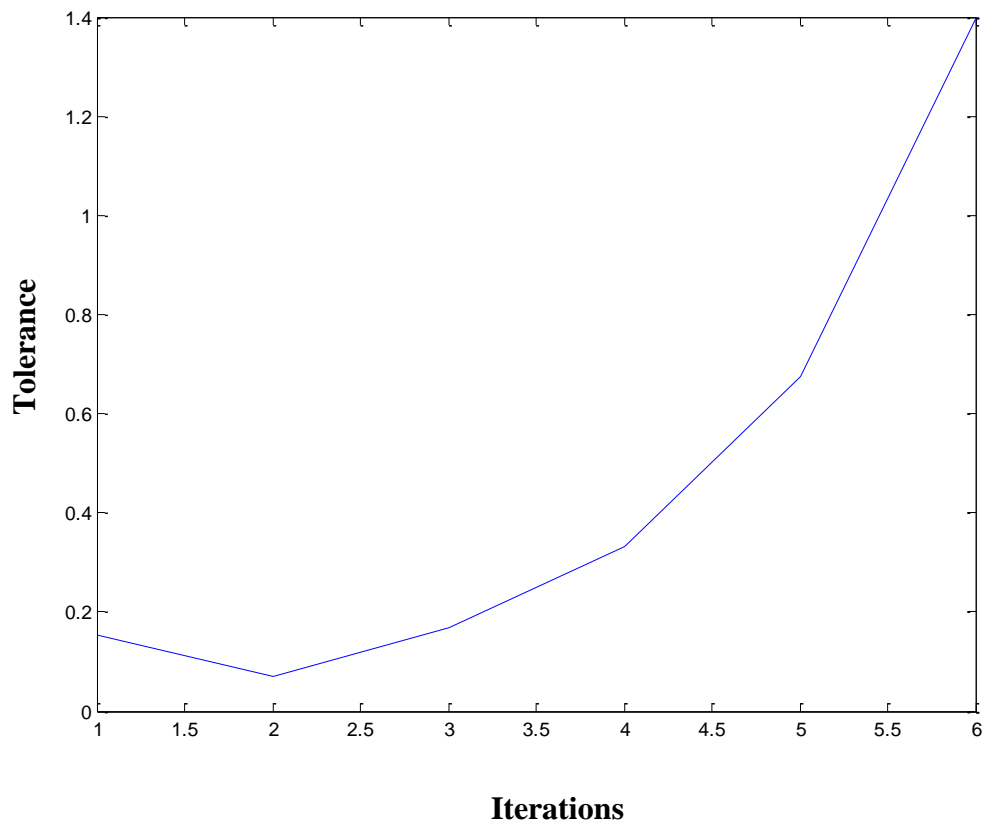


Figure 4.40. Divergence characteristic of Nigeria network with cut lines 13, 19

4.8.1 *SVUD and Effect of the Iterative Procedure*

In iterative solutions, results are often approximations because iteration itself involves successive approximations where the output of one iteration is used as input to the next. In load flow analysis, these approximations are pretty obvious as results for the same network obtained by different load flow analysis may be slightly different but accurate enough for the use to which they are to be put. Also, the iterative solution is a time dependent method of solution and the results may vary as shown in [109] where comparison of load flow methods involving standard Newton Raphson (SNR), Step Size Optimization (LFSSO) and Continuous Newton Power Flow (CNPf) converged at different rates for the same networks. In the solution of real systems or ill-conditioned systems, the NSR method diverged while others converged at 24 iterations or less. The same is true of SVUD when compared to the standard G-S.

Comparison of accuracy of load flow in [110] also shows differences because of the trade-off between accuracy and memory space.

The piecewise solutions are combined in different ways to obtain the result of the complete system. When dealing with linear systems, the same results are obtained as in one piece solution because in linear systems the output is a direct result of the combination of inputs and direct methods can easily be applied. But a nonlinear system is different and therefore there may be slight differences.

When a power system is torn, it is not only the boundary conditions that are affected; the whole system is affected especially, the parts close to the points of tear. The global effect on the network due to tearing, yields results that are slightly different because all the information required from subnetworks are not available to other subnetworks or are available in used forms. For example, voltage values communicated to other subnetworks are derived by using known powers at the nodes. This is particularly obvious in nonlinear systems where the output values do not have a constant difference like linear systems. Using the *fission elements* [7] to modify subnetworks solutions of a non-linear network therefore requires extra effort. In the SVUD load flow analysis, the subnetworks swap interface information at each iteration which is used with removed branches to update their results. The whole domain information is required, so the results may not be exactly equal to the one-piece results but are still accurate enough for taking action in system planning and operation.

4.9 Summary

A novel method for solving torn networks has been developed and validated by the results obtained when applied to credible benchmark systems. The low mean square errors of the SVUD load flow when compared to one-piece solutions prove that the algorithm is satisfactory. Also, in iterative load flow, convergence may be obtained without obtaining the desired results so results obtained may not be a true representation of the network [85]. This further shows that, SVUD is as good as other iterative procedures.

The SVUD method incorporates the conventional G-S load flow analysis and the result is a new G-S with a very fast rate of convergence compared to the classic one. Another merit of the new algorithm is that it can easily be implemented and incorporated into the existing conventional load flow methods. The G-S load flow method is known for its slow convergence but in this new algorithm its convergence properties were greatly improved. In all the analyses, no acceleration factor was applied to facilitate convergence of the iteration process.

5 THE NIGERIA ELECTRICAL POWER SYSTEM ANALYSIS

5.1 Introduction

Energy plays a most important role in the development and indeed the survival of any people. The quality of life of a people can be determined by the quality of available energy. Electrical energy is, undoubtedly, the cleanest energy to transport and utilize. Once the transport system (transmission and distribution lines) is in place, electrical energy drives itself to the points of utilization. It is also the easiest energy to produce in large quantities and is therefore the backbone of the economy of any nation or modern society. It also enhances general security as security equipment can operate uninterrupted. In spite of all the noise about information technology (IT), the main equipment still relies on electrical power. These and many more justify the enormous attention given to electrical energy all over the world.

In Nigeria, electrical energy was not given the required attention by several past governments which led to the near collapse of the electrical power system with the attendant adverse effects on the economy and the populace. Nigeria is a large country located in West Africa with abundant human and natural resources. Power generation started in Nigeria in 1896 but the growth of electricity was not commensurate with the population and industrial growth of the country. This led to a decline in industrial productivity as industries were forced to relocate or close down due to intermittent power supply and/or high cost of generating their own electricity. Individual productivity also declined as a result of electricity challenges experienced in offices and homes.

The electrical power system worldwide has experienced considerable changes due to the introduction of new types of power sources like wind and solar into the grid, giving rise to new challenges in the planning and operation of the grid. There is also the issue of new regulations and policies. The size and complexity of power systems make it imperative to produce improved analytical tools to reduce the burden of

computation. Analysing the system piecewise, while at the same getting the result of the system as if the whole system was analysed as a piece greatly improves the quality of information required for successful planning and operation of the system. Diakoptics lends itself here as a powerful concept and led to the development of the new tool, SVUD, in this research for load flow analysis of power systems. In diakoptics a system or network is torn into a suitable number of smaller systems, called subsystems or subnetworks in this work. In power systems points to tear often occur naturally and tearing the system at those points makes the solution easier. Such points could be the link between two nations' power systems collaborating in wind energy production and utilization or power networks in different parts of a country. When a system is torn for the purpose of analysis, hitherto hidden details or forces are exposed. This was shown in the analysis of the Nigerian power system where the state of the system was immediately exposed. Also, the part of the system which needs greater attention was spotted easily in the course of the solution. In this chapter, the Nigerian power system is analysed using the SVUD and the results are discussed.

5.2 Snapshot of the Nigeria Electrical Power System

A typical AC power system is a three-phase system consisting of three main stages - generation, transmission and distribution. Networks with voltage levels between transmission and distribution voltages are sometimes denoted as subtransmission network. In Nigeria, the transmission voltages are currently 330kV and 132kV while the distribution voltages are 33, 11 and 0.415kV; the generating voltage is between 10.5 and 16kV. The present installed capacity of the Nigerian power system is 7,876MW, made up of 76% thermal and 24% hydro generating systems. The transmission network consists of 4889.2km of 330kV lines, 6,319.33km of 132kV lines, 6,098MVA transformer capacity at 330/132kV and 8,090MVA transformer capacity at 132/33kV. Only a limited portion of the country is covered by the transmission system and the insufficient transmission capacity causes the network to be overloaded with a maximum electricity wheeling capacity of 4,000MW [111, 112, 113]. In addition, the network is radial and therefore the redundancies are inadequate.

The energy crisis is being addressed and substantial amount of money has been injected into the power sector in addition to the deregulation process. Before the

deregulation of the power sector, the operation has been a one-way flow of power as illustrated in Figure 5.1. All generation was into a pool from which it was transported to all parts of the country. The coordinating centre, known as the National Control Centre (NCC) located at Osogbo [114] in the western part of the country coordinates the activities of the power system and makes sure the grid code is followed. There are also supplementary and regional control centres in other parts of the country as depicted in Figure 5.2 [115].

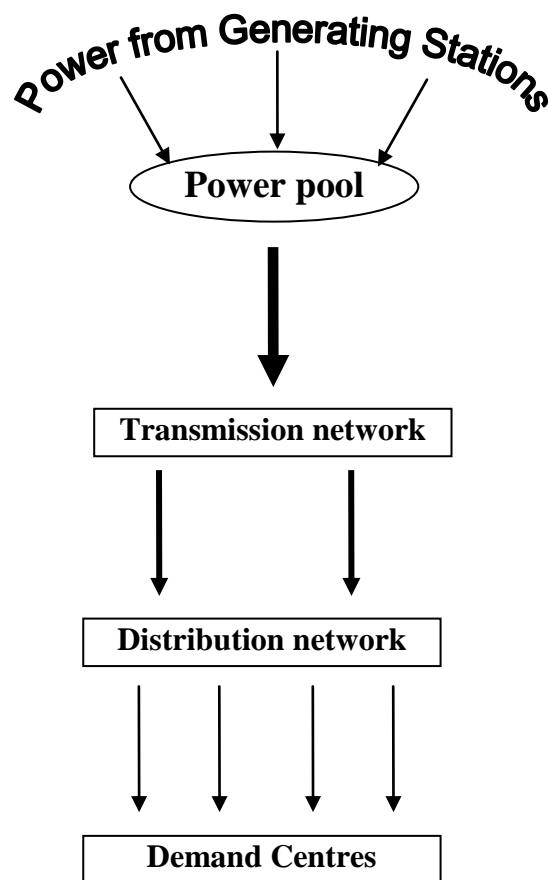


Figure 5.1. Schematic of Nigeria power System operation before deregulation

The map of Nigeria in Figure 5.3 adapted from [116] shows the arrangement of the 330kV transmission system with bus locations in the different states. Most of the lines are in the south west of the country and the longest lines are located in the north.

Redacted due to copyright



Figure 5.2. Structure of Nigeria Power System Control Centre [115].

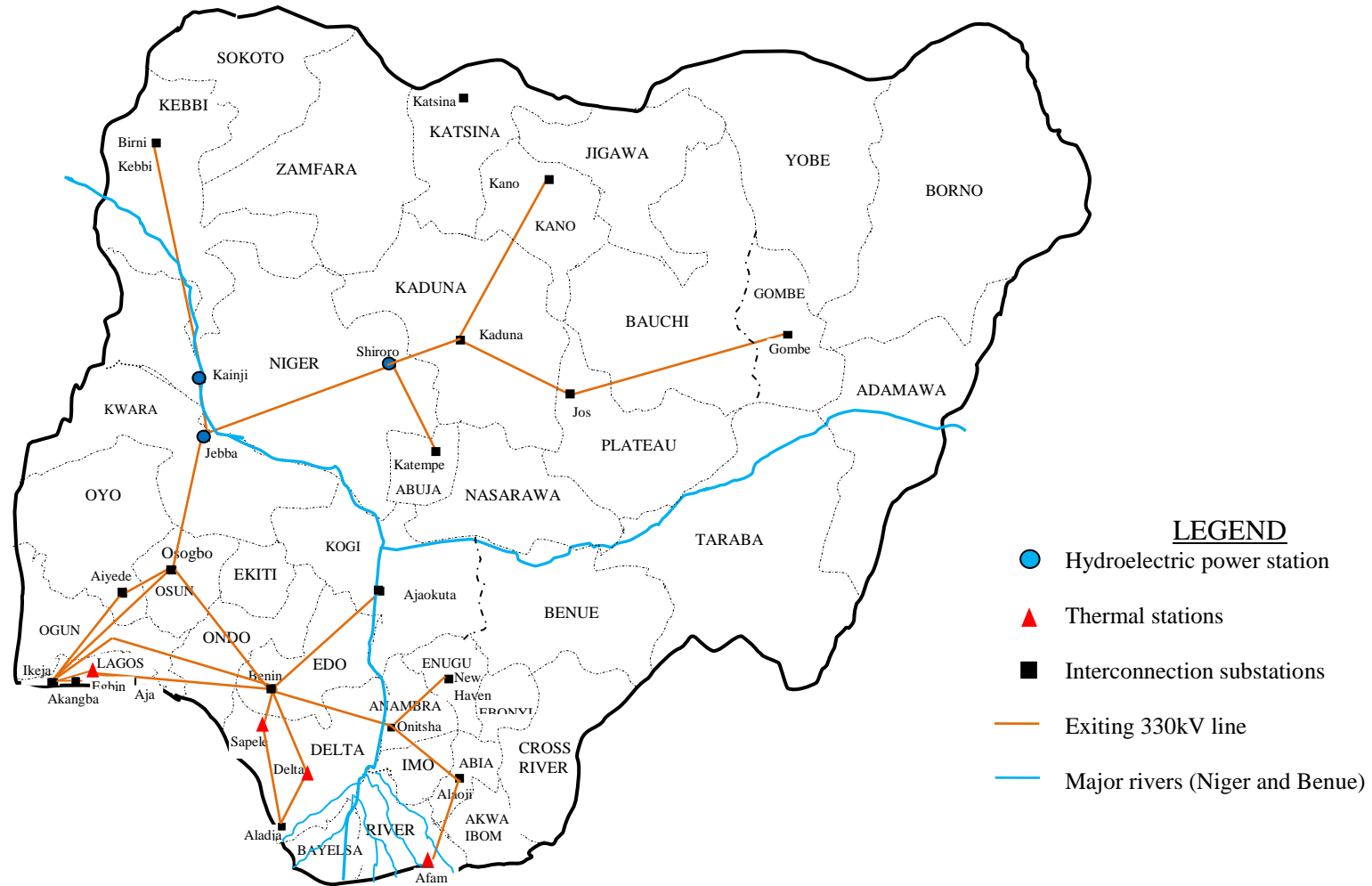


Figure 5.3. Map of Nigeria 330kV transmission network

5.2.1 *Nigeria Grid Codes for Transmission the System*

Grid codes generally define requirements for the successful operation of an electrical network. This ensures the efficient, safe and economic operation of the system and may be specified for generation, transmission and distribution systems as the case may be. Mandatory technical limits are specified including additional support that may be called on to maintain the quality and security of the system. There are also the issues of agreements between all operators of the system through market mechanisms [117].

The grid code for the Nigeria electricity transmission system is given in [118] and the area of interest here is Part 3, sections 2 and 3. The nominal frequency of the system is 50Hz and is to be maintained within $\pm 0.5\%$ by the Control Centre. This frequency can vary within $\pm 2.5\%$ when the system is under stress. At frequencies outside this range and in extreme fault conditions all generating units are to be disconnected unless there is a written agreement to the contrary. The busbar voltages are to be maintained within the ranges stated in Table 5.1. Under system stress or faults voltage deviation may go beyond these limits.

Table 5.1 Voltage Control Ranges of Nigeria Transmission system

Voltage level kV	Minimum voltage kV (pu)	Maximum voltage kV (pu)
330	313.5 (0.95)	346.5 (1.05)
132	118.8 (0.90)	145.0 (1.098)
33	31 (0.94)	34.98 (1.06)
16	15.2 (0.95)	16.8 (1.05)
11	10.45 (0.95)	11.55 (1.05)

5.2.2 *Overview of the SVUD Load Flow Method*

Load flow is the core of power systems analyses and a number of numerical methods for solving the power flow equations have been developed. The classical methods are Gauss-Seidel, Newton-Raphson and Fast Decoupled methods. Other methods are Fuzzy Logic, Genetic Algorithm and Particle swarm, but Gauss-Seidel and Newton-Raphson have remained on the forefront.

Load flow, computes the voltage at each bus, voltage drops on feeders and power flow in the lines in steady-state. Determination of bus voltages and their variation is the focus of this work. The solution requires the specification of two out of the four quantities voltage, voltage angle δ , active power P and reactive power Q at each bus. Generators regulate the voltage at their controlled buses as long as the generator's reactive power limits, Q_{\max} and Q_{\min} , have not been reached. If any generator reaches its maximum or minimum reactive power limit, the generator reactive power will be held at the respective limit, and the scheduled voltage becomes the unknown parameter for that bus.

The advantages of the classical G-S compared to N-R include simplicity less computer time per iteration, but the number of iterations increases with increase in the number of buses. It is therefore more suitable for the solution of small systems, however, small networks may require more iteration if the network is not well conditioned. G-S may be used on larger systems to obtain initial approximate solutions, for the N-R method [119].

This work set out to produce a simple diakoptic algorithm as a power analysis tool that reduces the volume of data handled per time, and at the same time to produce solutions as if the power network was solved as a piece. This led the development of the new method, the SVUD which, apart from reducing the volume of data handled, has improved the convergence characteristics of the traditional G-S method. The SVUD is a novel load flow algorithm based on diakoptics; SVUD load flow is explained in detail in chapter 3. The SVUD equations of solution are defined in (3.34) and (3.35). In the GS method, an accelerator is normally used to increase the rate of convergence but in the SVUD, it was not applied and yet the rate of convergence rate is much faster than the conventional G-S.

5.3 Analysis of the of the Nigeria 330kV transmission network

The Nigerian power system has been analysed by several researchers some of which can be found in [120-127] and the general verdict is that of a network with inadequate generating capacity, overloaded transmission lines, high losses and a generally weak

grid. This makes it prone to voltage instability and voltage collapse. The government is making efforts to improve the power system and simulation of the post reform network showed improvement in bus voltages, line loading and system stability [124].

A glance at the Nigeria transmission network arrangement in Figure 5.3 shows that the transmission capacity is grossly inadequate in view of the large land size of the country which is also accompanied by a large population. Individuals try to meet their energy needs with private generators in addition to uninterruptible power supplies (UPS's). This is financially very expensive, apart from air and noise pollution posed by the private generators. The short term plan of the government is to increase the generation capacity from the present installed capacity of 6000MW to 10,000MW and buses in the transmission network would be increased to forty nine [124].

5.3.1 *Application of SVUD the 330kV Transmission Network*

The major difference between different approaches hitherto taken in the analysis of the Nigerian 330kV network and the SVUD is that others are all one-piece approaches. By tearing a network, hidden characteristics are exposed; this was verified by applying one-piece G-S and N-R first to the subnet **A** and subnet **B** separately and both converged, but when SVUD was applied, only subnet **A** converged. Subnet **B** did not converge though all possible points of tear and different slack buses were exploited to ensure convergence. This part has been reported to be the weaker part of the network and this is a confirmation so SVUD immediately points to the part of a system that should be investigated further thereby saving time. This is akin to HELM mentioned in section 2.12.1 where a solution is either available or not available. This is an advantage of the SVUD over the methods adopted hitherto.

The SVUD is applied to Nigeria 330kV transmission network in Figure 5.5 which was chosen because it is a more general representation of the state of the power system. It forms the core of the system as it connects all the generating stations and distribution systems. Also, the size is sufficient to implement the main features of the algorithm. Tables 5.2 and 5.3 [121, 127] are the bus and line parameters of the network.

The process starts by inputting the bus and line data in the developed MATLAB programme and running. The first output is for the chance to choose between automatic or manual cutting of the network. If the decision is manual cutting, the computer outputs and the line numbers and the network map of Figure 5.4 showing the links between buses. The dots are buses denoted as b1 – b32 and the full lines represent the transmission lines. The line or lines which, if removed, would separate the network into individual subnetworks can easily be identified in the figure.

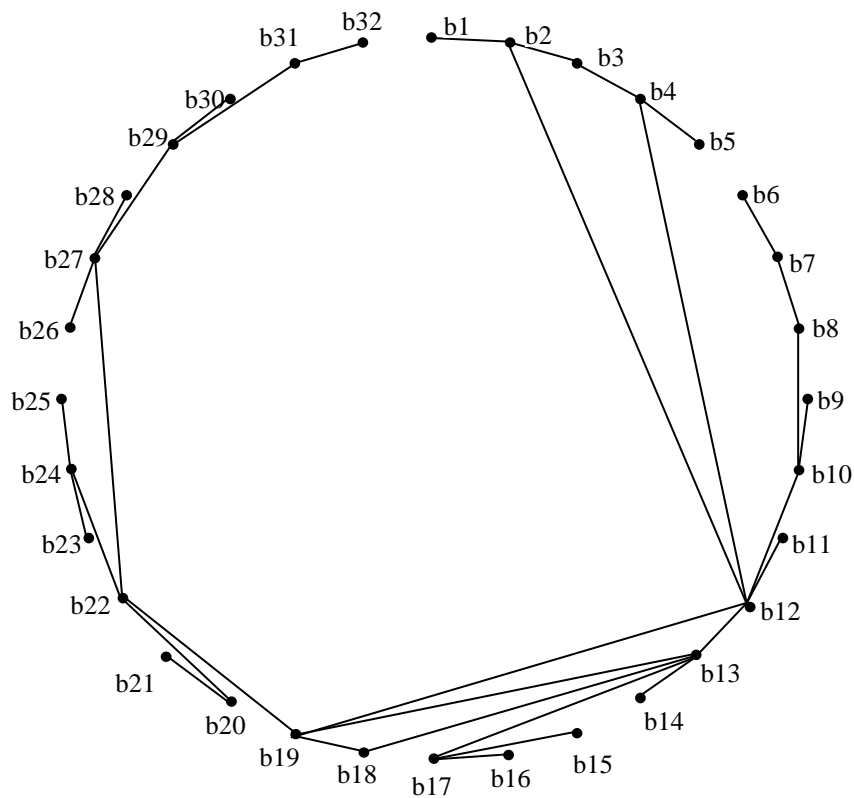


Figure 5.4. Computer arrangement of Nigeria 330kV system buses

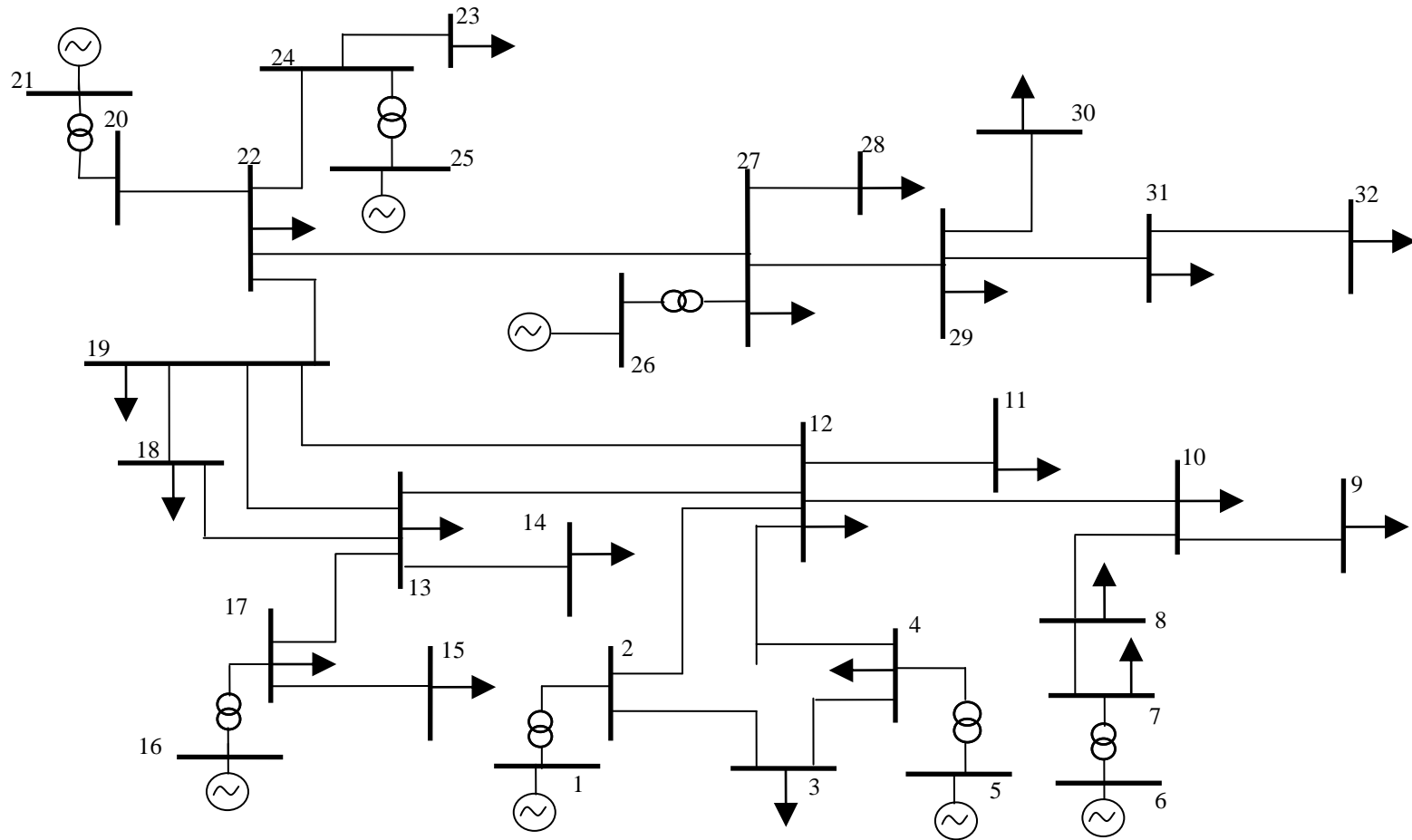


Figure 5.5. Nigeria 330kV transmission network

Table 5.2 Bus data of the Nigerian 330kV network

Bus no.	Voltage		Generation (pu)		Load (pu)		Reactive power limits (pu)		Bus names
	Magnitude (pu)	Angle (deg.)	P _G	Q _G	P _L	Q _L	Q _{min}	Q _{max}	
1	1.000	0	0.000	0	0.000	0.000	0.000	0.000	Sapele
2	1.000	0	0.000	0	0.000	0.000	0.000	0.000	SapeleHT
3	1.000	0	0.000	0	0.480	0.250	0.000	0.000	Aladja
4	1.000	0	0.000	0	0.000	0.000	0.000	0.000	DeltaHT
5	1.000	0	3.850	0	0.000	0.000	-2.000	5.000	DeltaGS
6	1.000	0	3.160	0	0.000	0.000	-2.000	5.000	Afam
7	1.000	0	0.544	0	0.000	0.000	0.000	0.000	AfamHT
8	1.000	0	0.000	0	2.480	0.530	0.000	0.000	Alaoji
9	1.000	0	0.000	0	1.820	1.120	0.000	0.000	New
10	1.000	0	0.000	0	1.460	0.770	0.000	0.000	Onitsha
11	1.000	0	0.000	0	0.720	0.450	0.000	0.000	Ajaokuta
12	1.000	0	0.000	0	1.360	0.840	0.000	0.000	Benin
13	1.000	0	0.000	0	4.840	3.000	0.000	0.000	Ikeja-
14	1.000	0	0.000	0	3.890	2.410	0.000	0.000	Akangba
15	1.000	0	0.000	0	2.000	1.240	0.000	0.000	Aja
16	1.000	0	6.670	0	0.000	0.000	-3.000	7.000	EgbinGS
17	1.000	0	0.000	0	0.800	0.600	0.000	0.000	EgbinTS
18	1.000	0	0.000	0	2.100	1.300	0.000	0.000	Aiyede
19	1.000	0	0.000	0	1.940	1.200	0.000	0.000	Oshogbo
20	1.000	0	0.000	0	0.000	0.000	0.000	0.000	JebbaHT
21	1.000	0	4.750	0	0.000	0.000	-2.000	5.000	Jebba GS
22	1.000	0	0.000	0	0.074	0.038	0.000	0.000	JebbaTS
23	1.000	0	0.000	0	0.890	0.550	0.000	0.000	Birni-
24	1.000	0	0.000	0	0.000	0.000	0.000	0.000	Kainji HT
25	1.000	0	3.200	0	0.000	0.000	-5.000	5.000	KainjiPS
26	1.000	0	3.200	0	0.000	0.000	-3.000	5.000	shiroroGS
27	1.000	0	0.000	0	0.000	0.000	0.000	0.000	shiroroTS
28	1.000	0	0.000	0	2.360	1.460	0.000	0.000	Katampe
29	1.000	0	0.000	0	2.600	1.610	0.000	0.000	Kaduna
30	1.000	0	2.102	0	0.000	1.400	0.000	0.000	Kano
31	1.000	0	0.000	0	1.140	0.900	0.000	0.000	Jos
32	1.000	0	0.000	0	1.300	0.800	0.000	0.000	Gombe

Table 5.3 Line data of the Nigerian 330kV network

Line no.	From bus	To bus	Line impedance (pu)		Half line charging (pu)	Tap setting (pu)
			R	X	B/2	
1	1	2	0.0000	0.0120	0.0000	-
2	2	12	0.0010	0.0074	0.3313	-
3	2	3	0.0025	0.0186	0.2087	-
4	4	12	0.0029	0.0216	0.2418	-
5	4	3	0.0010	0.0077	0.0861	-
6	5	4	0.0000	0.0133	0.0000	0.9
7	6	7	0.0000	0.0142	0.0000	-
8	7	8	0.0005	0.0037	0.1656	-
9	8	10	0.0060	0.0455	0.5101	-
10	10	9	0.0038	0.0284	0.3180	-
11	12	11	0.0077	0.0576	0.6460	-
12	12	10	0.0054	0.0405	0.4540	-
13	13	12	0.0005	0.0114	1.8850	-
14	13	14	0.0004	0.0027	0.1190	-
15	16	17	0.0000	0.0065	0.0000	-
16	17	13	0.0012	0.0092	0.4108	-
17	17	15	0.0003	0.0021	0.0928	-
18	18	13	0.0054	0.0405	0.4538	-
19	19	12	0.0029	0.0342	0.8315	-
20	19	18	0.0041	0.0041	0.3472	-
21	19	13	0.0016	0.0016	0.9805	-
22	22	19	0.0021	0.0155	0.0600	-
23	20	22	0.0002	0.0012	0.0530	-
24	21	20	0.0000	0.0193	0.0000	0.9
25	24	23	0.0122	0.0116	0.0269	-
26	24	22	0.0016	0.0120	0.0366	-
27	25	24	0.0000	0.0135	0.0000	0.9
28	26	27	0.0000	0.0164	0.0000	-
29	27	22	0.0001	0.0021	0.0165	-
30	27	29	0.0011	0.0142	0.6360	-
31	27	28	0.0025	0.0195	0.2130	-
32	29	30	0.0090	0.0280	0.0619	-
33	29	31	0.0077	0.0283	0.0526	-
34	31	32	0.0104	0.0283	0.0778	-

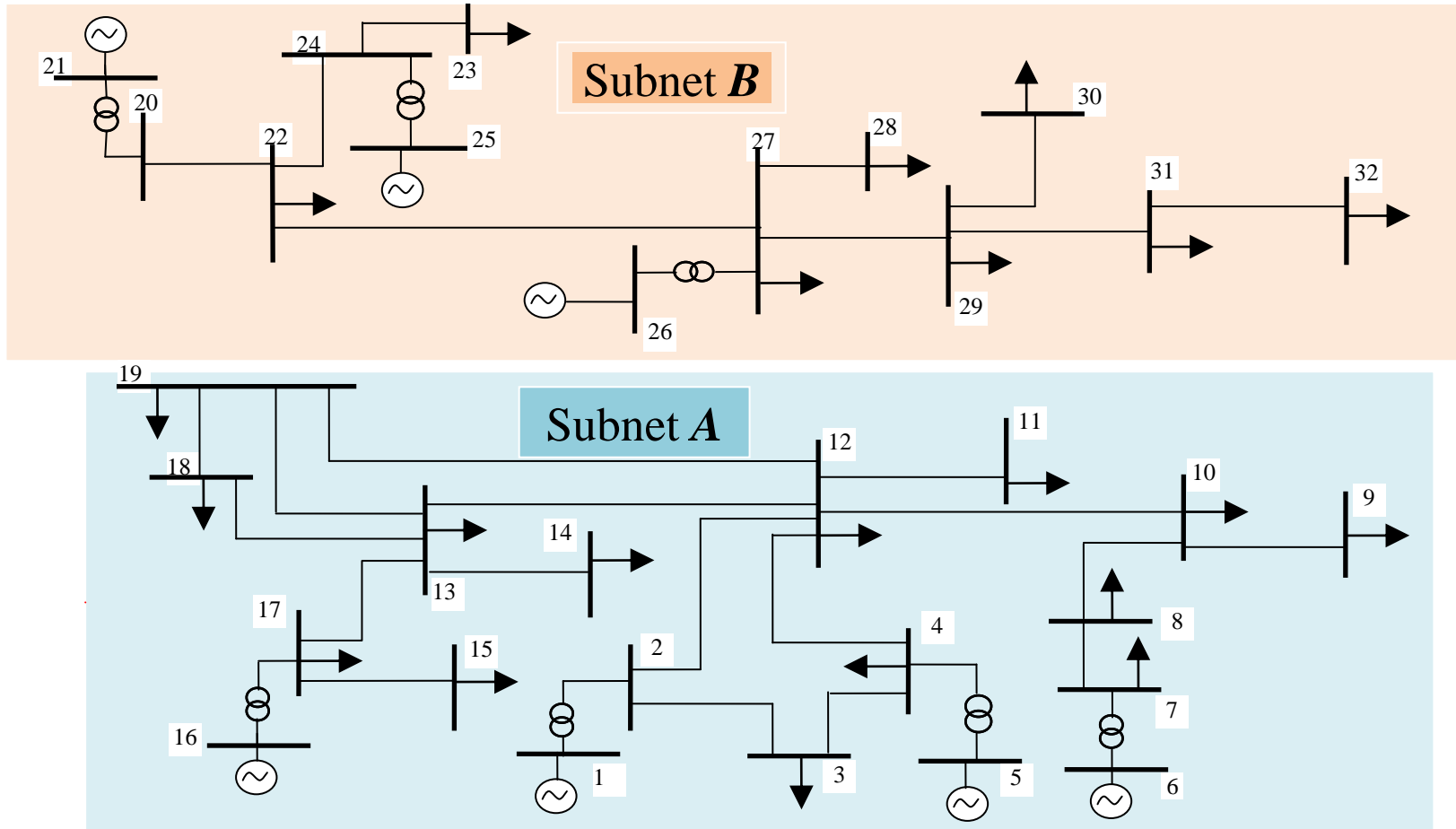


Figure 5.6. Subnetworks of Nigeria 330kV transmission network

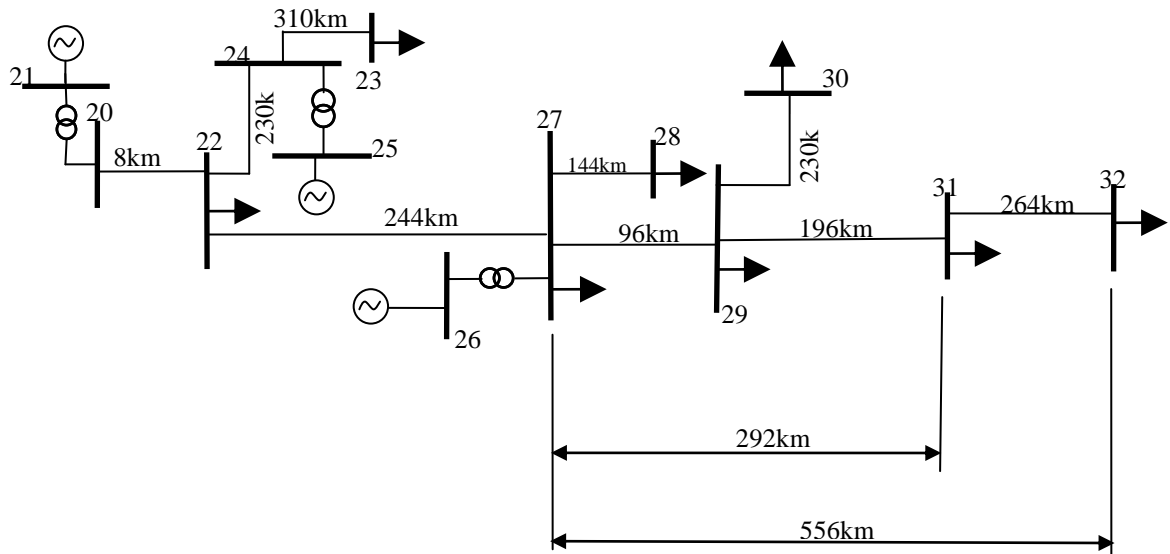


Figure 5.7. Subnet **B** of 330kV network showing long lines lengths.

5.3.2 Considerations for Choosing Lines of Cut

Apart from the few criteria for tearing a network given in [7, 3, 5, 13] it was discovered in the course of this research that in choosing lines to cut, each subnetwork should contain at least one generator bus. Secondly, the less the lines of cut, the closer the results are to the one-piece solution, this is also mentioned in view of time saving in [17]. Also, chosen lines of cut influence the convergence characteristics of the load flow analysis. It was also noticed that equal sizes of subnetworks do not always guarantee the best solution for nonlinear system analysis. Methods of determining the best lines of tear are somewhat heuristic.

It can be seen in Figure 5.4 that the least number of lines that would tear the network into separate subnetworks is the line between bus 19 and bus 22 which is line 22 as given in Table 5.3. The choice to remove line 22 was made for the programme after which Figure 5.8 was displayed showing the removed line as dashed. The resultant subnetworks are **A** and **B** in

Figure 5.6. When the choice for manual selection of slack buses is made, the bus parameters of subnet **A** in Table 5.4 are also output to enable the choice of slack bus for subnet **A**; when that is done, bus parameters for subnet **B** in Table 5.5 are output

and the slack bus for subnet B is chosen. This is the last decision, after which the load flow is performed to obtain the results shown in column 2 of Table 5.6.

Table 5.4 Bus data in subnet A of Nigeria network

Bus No.	Voltage (pu)	Angle (deg)	P_G (pu)	Q_G (pu)	P_L (pu)	Q_L (pu)	Q_{\min} (pu)	Q_{\max} (pu)
1	1.0000	0	0.0000	0.0000	0.0000	0.0000	0.0000	0.0000
2	1.0000	0	0.0000	0.0000	0.0000	0.0000	0.0000	0.0000
3	1.0000	0	0.0000	0.0000	0.4800	0.2500	0.0000	0.0000
4	1.0000	0	0.0000	0.0000	0.0000	0.0000	0.0000	0.0000
5	1.0000	0	3.8500	0.0000	0.0000	0.0000	-2.0000	5.0000
6	1.0000	0	3.1600	0.0000	0.0000	0.0000	-2.0000	5.0000
7	1.0000	0	0.5440	0.0000	0.0000	0.0000	0.0000	0.0000
8	1.0000	0	0.0000	0.0000	2.4800	0.5300	0.0000	0.0000
9	1.0000	0	0.0000	0.0000	1.8200	1.1200	0.0000	0.0000
10	1.0000	0	0.0000	0.0000	1.4600	0.7700	0.0000	0.0000
11	1.0000	0	0.0000	0.0000	0.7200	0.4500	0.0000	0.0000
12	1.0000	0	0.0000	0.0000	1.3600	0.8400	0.0000	0.0000
13	1.0000	0	0.0000	0.0000	4.8400	3.0000	0.0000	0.0000
14	1.0000	0	0.0000	0.0000	3.8900	2.4100	0.0000	0.0000
15	1.0000	0	0.0000	0.0000	2.0000	1.2400	0.0000	0.0000
16	1.0000	0	6.6700	0.0000	0.0000	0.0000	-3.0000	7.0000
17	1.0000	0	0.0000	0.0000	0.8000	0.6000	0.0000	0.0000
18	1.0000	0	0.0000	0.0000	2.1000	1.3000	0.0000	0.0000
19	1.0000	0	0.0000	0.0000	1.9400	1.2000	0.0000	0.0000

Table 5.5 Bus data in subnet B of Nigeria network

Bus No.	Voltage (pu)	Angle (deg)	P_G (pu)	Q_G (pu)	P_L (pu)	Q_L (pu)	Q_{\min} (pu)	Q_{\max} (pu)
20	1.0000	0	0.0000	0.0000	0.0000	0.0000	0.0000	0.0000
21	1.0000	0	4.7500	0.0000	0.0000	0.0000	-2.0000	5.0000
22	1.0000	0	0.0000	0.0000	0.0740	0.0380	0.0000	0.0000
23	1.0000	0	0.0000	0.0000	0.890	0.5500	0.0000	0.0000
24	1.0000	0	0.0000	0.0000	0.0000	0.0000	0.0000	0.0000
25	1.0000	0	3.2000	0.0000	0.0000	0.0000	-5.0000	5.0000
26	1.0000	0	3.2000	0.0000	0.0000	0.0000	-3.0000	5.0000
27	1.0000	0	0.0000	0.0000	0.0000	0.0000	0.0000	0.0000
28	1.0000	0	0.0000	0.0000	2.3600	1.4600	0.0000	0.0000
29	1.0000	0	0.0000	0.0000	2.6000	1.6100	0.0000	0.0000
30	1.0000	0	4.1018	3.9634	2.2600	1.4000	0.0000	0.0000
31	1.0000	0	0.0000	0.0000	1.1400	0.9000	0.0000	0.0000
32	1.0000	0	0.0000	0.0000	1.3000	0.8000	0.0000	0.0000

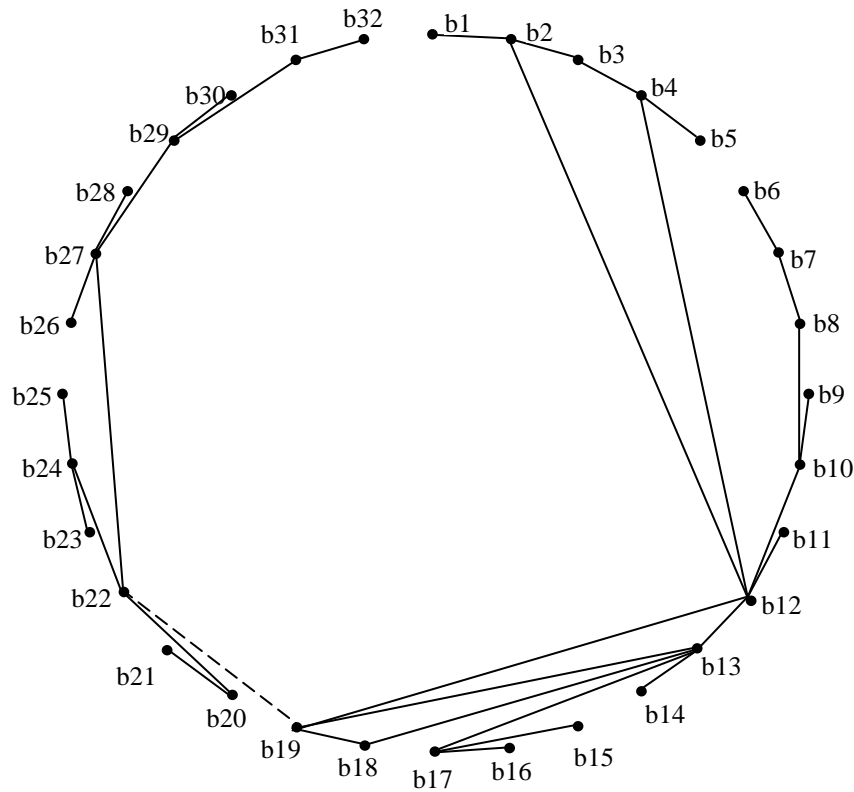


Figure 5.8. Nigeria 330-kV network map showing removed line

5.4 The Split Network Characteristics

Apart from line 22 which was removed to split the network into subnets *A* and *B*, other lines were also removed in an attempt to obtain desired subnetworks but there was no convergence so removing line 22 was the best option. In real systems, lines of cut often occur naturally like line 22 which effectively separates the network into north and south as it forms the major link between them. It is also the smallest number of lines that can tear the network when removed.

In the SVUD method the state of the network could be predicted by its convergence characteristics because ill-conditioned or weak network cannot stand alone when split as in the case of subnet *B* explained in section 5.3.1 when SVUD was applied. This part has very long transmission lines which are a condition that characterises weak networks [45].

Causes of load flow divergence could be physical or numerical. A physical condition is ill-conditioning or overloaded transmission system which would cause the system to operate very close to the critical loading condition leading to voltage collapse [45]. This is the Nigeria case where impedance of some of the lines had to be reduced slightly before convergence could be achieved. A numerical condition for load flow divergence could be due to choosing poor initial conditions [119] and can be corrected by choosing better initial conditions.

5.5 Comparison of Results of One-piece Solutions with SVUD Load Flow

The conventional G-S and N-R in one-piece solution, and SVUD approach were applied to the Nigerian 32-bus system in Figure 5.5. The major advantage of the SVUD method over the conventional G-S is the much lower number of iterations required to achieve convergence.

The SVUD results can be separated into subnetworks as shown in Table 5.7. This is particularly useful when information for a particular part of the system and how it relates with the other part of the system is required. Diakoptics is such that each subnetwork solution is as it would be if solved together with other parts as a piece, and as a result retains the relationship with other parts of the network.

Iterative solution is a special form of trial and error and so the results are not as conclusive as direct solutions. This is demonstrated by the one-piece solution using G-S and N-R methods for the same Nigeria network where the results are slightly different as shown in Table 5.6. The differences in results in iterative solutions have also been proved in [109] as explained in section 4.8.1.

Table 5.6 Results of different methods of analysis

Bus no.	SVUD	N-R One-piece	G-S One-piece
	Iterations = 6	Iterations = 6	Iterations = 330
Bus voltages in pu			
1	1.0000 + 0.0000i	1.0000 + 0.0000i	1.0000 + 0.0000i
2	1.0385 - 0.1212i	1.0262 - 0.1177i	1.0419 - 0.1110i
3	1.0800 - 0.1354i	1.0547 - 0.1272i	1.0843 - 0.1226i
4	1.0974 - 0.1377i	1.0668 - 0.1275i	1.1019 - 0.1239i
5	1.0423 - 0.0888i	0.9971 - 0.0760i	1.0458 - 0.0757i
6	0.9900 - 0.1495i	0.9891 - 0.1470i	0.9919 - 0.1272i
7	0.9877 - 0.1944i	0.9848 - 0.1917i	0.9912 - 0.1725i
8	0.9843 - 0.2076i	0.9808 - 0.2049i	0.9882 - 0.1861i
9	0.9296 - 0.2994i	0.9186 - 0.2963i	0.9369 - 0.2824i
10	0.9742 - 0.2615i	0.9639 - 0.2581i	0.9806 - 0.2438i
11	1.0317 - 0.2347i	1.0164 - 0.2302i	1.0386 - 0.2195i
12	1.0315 - 0.1924i	1.0172 - 0.1876i	1.0375 - 0.1774i
13	0.9831 - 0.2530i	0.9730 - 0.2489i	0.9901 - 0.2341i
14	0.9732 - 0.2602i	0.9630 - 0.2562i	0.9804 - 0.2414i
15	0.9771 - 0.2178i	0.9716 - 0.2147i	0.9809 - 0.1969i
16	0.9876 - 0.1719i	0.9856 - 0.1693i	0.9886 - 0.1505i
17	0.9809 - 0.2146i	0.9754 - 0.2116i	0.9846 - 0.1938i
18	0.9693 - 0.2939i	0.9583 - 0.2893i	0.9804 - 0.2731i
19	0.9989 - 0.2723i	0.9883 - 0.2669i	1.0116 - 0.2495i
20	1.0043 - 0.2690i	0.9965 - 0.2621i	1.0227 - 0.2403i
21	0.9706 - 0.1777i	0.9844 - 0.1761i	1.0073 - 0.1560i
22	0.9989 - 0.2723i	0.9897 - 0.2652i	1.0159 - 0.2436i
23	1.0280 - 0.2623i	1.0166 - 0.2539i	1.0521 - 0.2353i
24	1.0444 - 0.2626i	1.0331 - 0.2541i	1.0682 - 0.2353i
25	0.9914 - 0.2121i	0.9791 - 0.2032i	1.0193 - 0.1881i
26	1.0013 - 0.2335i	0.9753 - 0.2211i	0.9808 - 0.1953i
27	0.9828 - 0.2816i	0.9712 - 0.2740i	0.9962 - 0.2520i
28	0.9401 - 0.3130i	0.9279 - 0.3059i	0.9548 - 0.2846i
29	0.8703 - 0.3527i	0.8560 - 0.3462i	0.8872 - 0.3263i
30	0.7846 - 0.3767i	0.7684 - 0.3704i	0.8031 - 0.3529i
31	0.7725 - 0.3789i	0.7556 - 0.3726i	0.7913 - 0.3555i
32	0.7182 - 0.3899i	0.7000 - 0.3835i	0.7380 - 0.3683i

Table 5.7 SVUD Results separated into subnetworks

Subnet A		Subnet B	
Bus no.	Voltage in pu	Bus no.	Voltage in pu
1	1.0000 + 0.0000i	20	1.0043 - 0.2690i
2	1.0385 - 0.1212i	21	0.9706 - 0.1777i
3	1.0800 - 0.1354i	22	0.9989 - 0.2723i
4	1.0974 - 0.1377i	23	1.0280 - 0.2623i
5	1.0423 - 0.0888i	24	1.0444 - 0.2626i
6	0.9900 - 0.1495i	25	0.9914 - 0.2121i
7	0.9877 - 0.1944i	26	1.0013 - 0.2335i
8	0.9843 - 0.2076i	27	0.9828 - 0.2816i
9	0.9296 - 0.2994i	28	0.9401 - 0.3130i
10	0.9742 - 0.2615i	29	0.8703 - 0.3527i
11	1.0317 - 0.2347i	30	0.7846 - 0.3767i
12	1.0315 - 0.1924i	31	0.7725 - 0.3789i
13	0.9831 - 0.2530i	32	0.7182 - 0.3899i
14	0.9732 - 0.2602i		
15	0.9771 - 0.2178i		
16	0.9876 - 0.1719i		
17	0.9809 - 0.2146i		
18	0.9693 - 0.2939i		
19	0.9989 - 0.2723i		

Table 5.8 Voltage mean square error (VSME) in comparison with G-S one-piece

NETWORKS	VMSE
Nigeria 32-bus with SVUD	0.0007
Nigeria 32-bus with Newton Raphson	0.0003

The G-S one-piece solution of the Nigeria 330kv network converged after 330 iterations while the SVUD converged after 6 iterations for the particular point of cut. In Table 5.8, it can be seen that the voltage mean square error (VSME) of the SVUD compared with the one-piece G-S solution is 0.0007. The voltage mean square error of N-R one-piece solution compared with one-piece G-S is 0.0004; This is an indication of the accuracy of the SVUD load flow. It is worth noting that the number of iterations with SVUD depends on the line of cut, number of subnetworks and chosen slack bus but the number of iterations is still far below that of the one-piece

G-S solution. This is exemplified by the results of the IEEE 30-bus solution in Table 4.27 with two and three subnetworks.

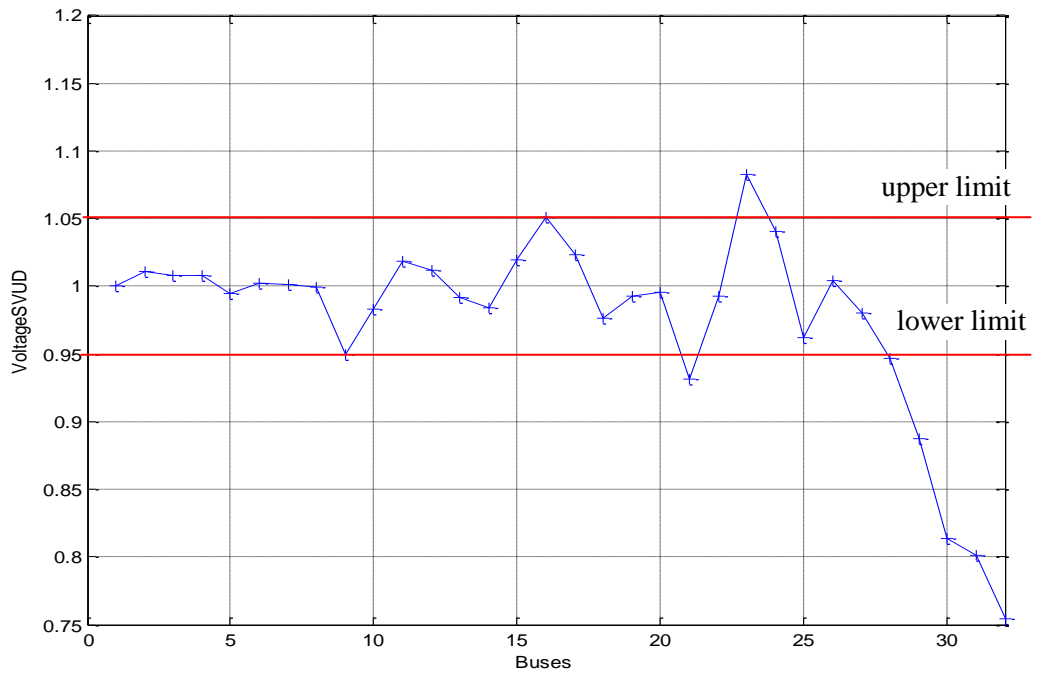


Figure 5.9. Voltage profile of 330kV network by SVUD

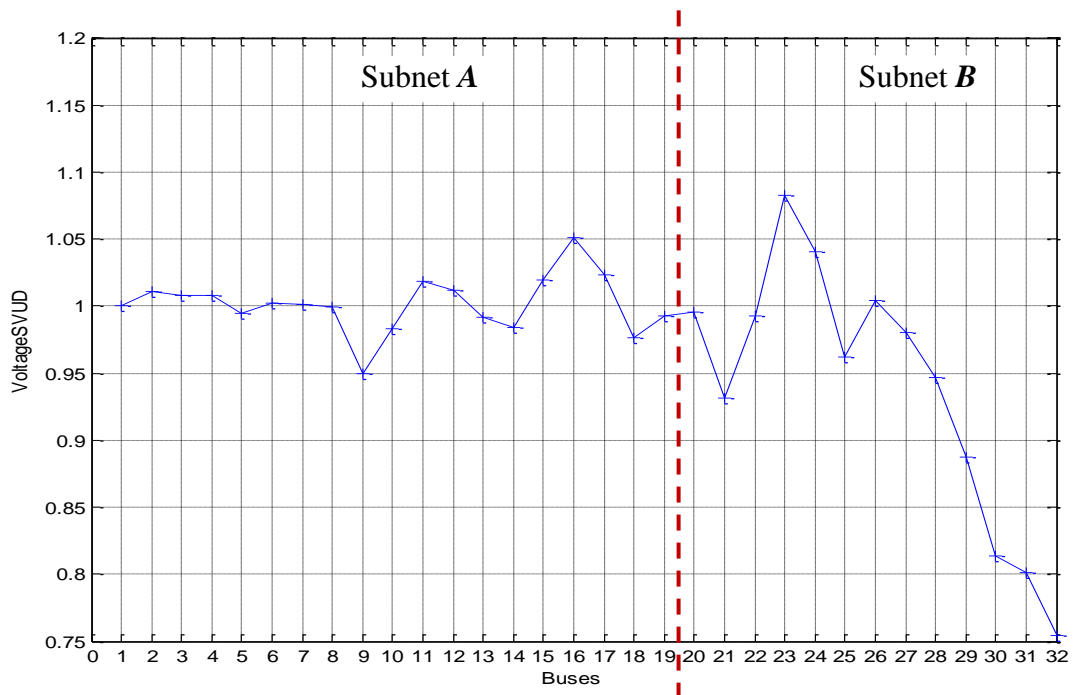


Figure 5.10. Voltage profile 330kV network showing subnetworks

5.6 Voltage profile of the system

One of the activities specified in the grid code [118] to be performed on the network by a System Operator is load flow studies with the intention of determining the level of power flowing in the system and the voltage profile for the existing network. The voltage profile of the 330kV network is shown in Figure 5.9 and Figure 5.10. Voltages of 7 buses are out of the accepted limits specified in Table 5.1. Out of thirteen buses in subnet **B**, buses 21, 23, 28, 29, 30, 31 and 32 voltages are out of limit which is 53.8%. In subnet **A**, voltages of two buses (9 and 16) are slightly out of limit but can be assumed to be on the limit. The large violations of voltage limits are an indication of a system that is weak, overloaded or ill-conditioned. In a weak grid, voltage limits are likely to be violated when demand and generation are considered [45]. Under-voltages have adverse effects on a system voltage stability margin and bulk power carrying capacity of transmission lines. If necessary measures are not put in place, this can lead to steady-state or dynamic voltage collapse [76]. Voltage collapse, though undesired, is a common phenomenon in the Nigerian power system and comes with blackouts for considerable lengths of time. Because energy is the 'live wire' of any nation's economy this has adversely impacted on the economy.

Voltages are unacceptably low in the northern part of the country represented by subnet **B**, especially buses 30, 31, and 32. Going by the definition in of voltage collapse in [76], the voltage at bus 32 could be termed a voltage collapse. Voltage instability usually precedes voltage collapse and is generally associated with weak grids, heavily loaded lines, long lines, radial networks, faults and/or reactive power shortages which can be identified with the Nigerian grid. A main cause of voltage collapse is the inadequate reactive power compensation [112]. Reactive power can be injected into the Nigerian grid system to improve the voltage profile but there is a limit this can be done to experience substantial improvement on the system voltage and general performance. Infrastructure reinforcement is a necessary requirement because the generating and transmission capacities are grossly inadequate.

5.7 Summary

The SVUD analysis of the Nigeria network agrees with the findings of other researchers on voltage profile and the fact that the system is weak. A lot needs to be

done in terms of providing more generating and transmission capacities in addition to reactive power compensation. Injection of reactive power would not cause any significant improvement in the grid.

The convergence characteristics of the 330kV network when using SVUD exposed its weakness, especially the part that is more challenged, that is, subnet **B**. This is an advantage of the SVUD over the one-piece methods used hitherto to analyse the network as explained in section 5.3.1. When a system is torn hidden nature of the system is revealed. A system that would converge when connected to other parts of the system may not converge when torn due to the nature of the resulting subnetworks. An electrical engineer can then work on the parts of the system represented by the subnetwork individually rather than search the whole network for the area of concern.

Another important advantage is that results of a certain part of the system can be obtained without analysing it in isolation as is done in [128]. In this reference, the basic N-R load flow was conducted on the part of the network represented as subnet **B** (Figure 5.6)). The results obtained do not take cognizance of the effect of other parts. SVUD on the other hand, gives results for subnet **B** separately (Table 5.7) and at the same time reflects the effect of subnet **A** on it. An alternative is to analyse the whole network as a piece and extract the required information for only subnet **B**, but this is extra work. This feature of the SVUD is particularly useful in interconnected systems between regions or countries where effects of interconnection can be determined during planning and operation.

6 ANALYSIS OF NIGERIA 330kV NETWORK INTEGRATED WITH WIND ENERGY

6.1 Introduction

The need to decarbonise electricity generation as a solution to climate change has led to increased integration of wind energy and other renewables into electrical power systems worldwide. Wind turbine technology has greatly advanced but integration issues have remained a challenge because ancillary services in the network such as, frequency and voltage control are provided by conventional generation. Some of these services can also be provided by separate systems such as capacitors or Static VAr Compensators but most of these are provided based on conventional generation. As already stated, the characteristics of wind energy generation are not as familiar as conventional generation, sizing and reorganising ancillary services to meet the requirements of a power system into which wind energy is integrated poses technical difficulties in planning and operation of system.

The Nigerian electrical power system was designed around conventional generation, mainly hydro and thermal stations but this is changing to include renewable energy as is currently the case in a number of countries which include Denmark, Germany, US and UK. But the system in its present state is not likely to derive much benefit from renewable energy. In weak transmission systems, integration of large wind energy presents such concerns as voltage regulation, system stability and post fault swings [71]. The Nigeria power system currently has limited grid transmission capacity coupled with the difficulties in matching electricity production with demand. It has been shown in the preceding chapter that the system is weak with many of the bus voltages much below acceptable limits. This could pose challenges when integrating electricity produced by wind energy into the present grid.

In this chapter, the effect of integrating the proposed wind farm to the Nigeria transmission network is assessed. And since more wind farms are proposed, the grid

is also simulated with increased wind power capacity. The 330kV network is the backbone of the grid as all the larger generating stations are connected to it from where the lower voltage network carry power to utilization points. A point on an electric grid may be characterised as being either weak or strong and may be with or without electrical power from wind integrated to it. The peculiar characteristic of a weak grid is that the voltage level is likely to fluctuate. Feeders in weak grids are usually long and are designed for relatively small loads. Long feeders in Nigeria grid have been identified in the preceding chapter.

The Nigeria grid was designed based on the load demand at the time it was established with some expansion thereafter which was sufficient. Subsequent increase in capacity that is supposed to follow increased demand was overlooked; the consequence is an overloaded and aged system with voltage levels generally below allowable minimum and thermal capacity of the grid often exceeded.

The feeder from Shiroro (bus 27) to Gombe (bus 32) is quite long, about 556km and is the furthest feeder from a generating station. This is evident in the voltage profile in Figure 5.9 and corroborates the fact that long feeders are likely to be weak points in the grid and therefore subject to voltages going beyond acceptable limits. In this case, load in excess of the design load is also a contributing factor. The effect of integrating wind energy to the grid in its present state can easily be predicted from various literatures on wind energy in weak grids like in [44, 45, 67, 69].

6.2 Choice of Wind Power for Electricity Generation

The large shortfall of electrical power in Nigeria has caused a very high percentage of individuals and organizations to generate their own electricity through the use of petrol and diesel generators. In an attempt to boost electricity produced by conventional generations, the abundant natural energy resources are now getting more attention. As a result, the National Energy Policy approved by the government of Nigeria seeks to exploit the renewable energy resources with substantial involvement of the private sector. This has led to the installation of a wind farm in Katsina State [130] and plans for more. This would improve the power system as a whole and reduce the emission of greenhouse gases.

Wind energy is considered the most cost-effective renewable source for electricity generation [129]. The cost comparison of renewable energy technologies in Table 6.1 shows that wind energy deserves the amount of attention currently given to it in the world. Investment and generation costs are lower compared to other new renewables. The efficiency ranges (Table 6.2) also make wind generation a good choice. Wind plants have much greater power capacity than photovoltaic (PV) plants [1].

Table 6.1 Cost Comparison of Renewable Electricity Technologies [130]

Redacted due to copyright



Table 6.2 Electrical efficiencies of electricity generation [131]

Redacted due to copyright



In the typical wind farm in Figure 6.1, the wind turbines are connected together by overhead lines or underground cables. Their collective output is connected through a low voltage line to a step-up transformer or transformers which raise the voltage to the existing grid voltage. The transformer output is connected to a high voltage bus.

This is the boundary bus between the wind farm and the existing grid and is commonly called, the point of common coupling or connection (PCC).

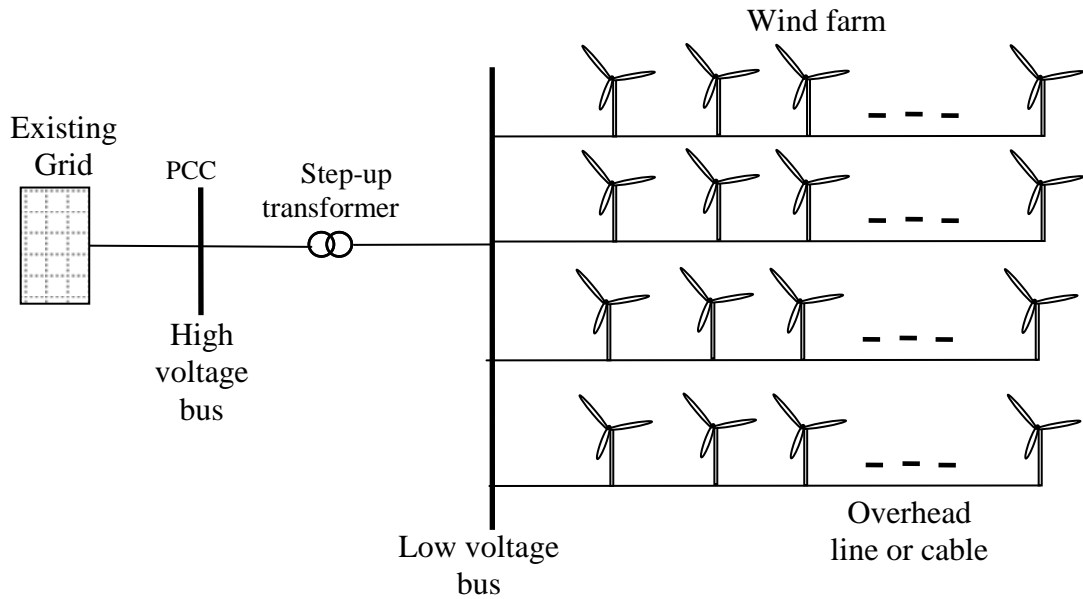


Figure 6.1. Wind farm layout

6.3 Wind Energy Prospects in Nigeria

Conventional generation development is financially and environmentally intensive; wind energy presents a good power supply to augment the existing conventional generation with reduced environmental impact.

Wind energy prospect in Nigeria is quite good especially in the north as shown in Figure 6.2 obtained from Nigeria Meteorological Agency (NIMET), Oshodi, Lagos State, Nigeria. The wind speed is in m/s. The data was arrived at from 40 years' measurements at 10 m height. For each location, the annual energy output and capacity factor are based on Weibull distribution [132]. In the economic analysis of wind energy in Algeria [133], it was shown that the cost per unit of electricity produced by wind depends on the type of turbines and the characteristics of the wind at the chosen site. This is common knowledge and partly informs the decision to locate the first main wind farm at Katsina where the wind speed is high, about 7m/s.

Redacted due to copyright



Figure 6.2. Nigeria with lines of equal wind speeds [132]

Wind energy is the dominant renewable energy for large scale electricity generation in the world today and several methods have been proposed and some are in place to ensure economic and quality supply when integrated into the existing grid.

6.4 The Nigeria Wind Farm Project

The capacity of a single wind turbine generator (WTG) is very small compared to conventional power generator. To obtain large amounts of electricity from wind turbines, several wind turbine generators are connected together by overhead lines or cables to form a wind farm or wind power generating station. The outputs of the generators are collected and transmitted to the grid through an AC or DC line after stepping up the voltage at the wind farm substation.

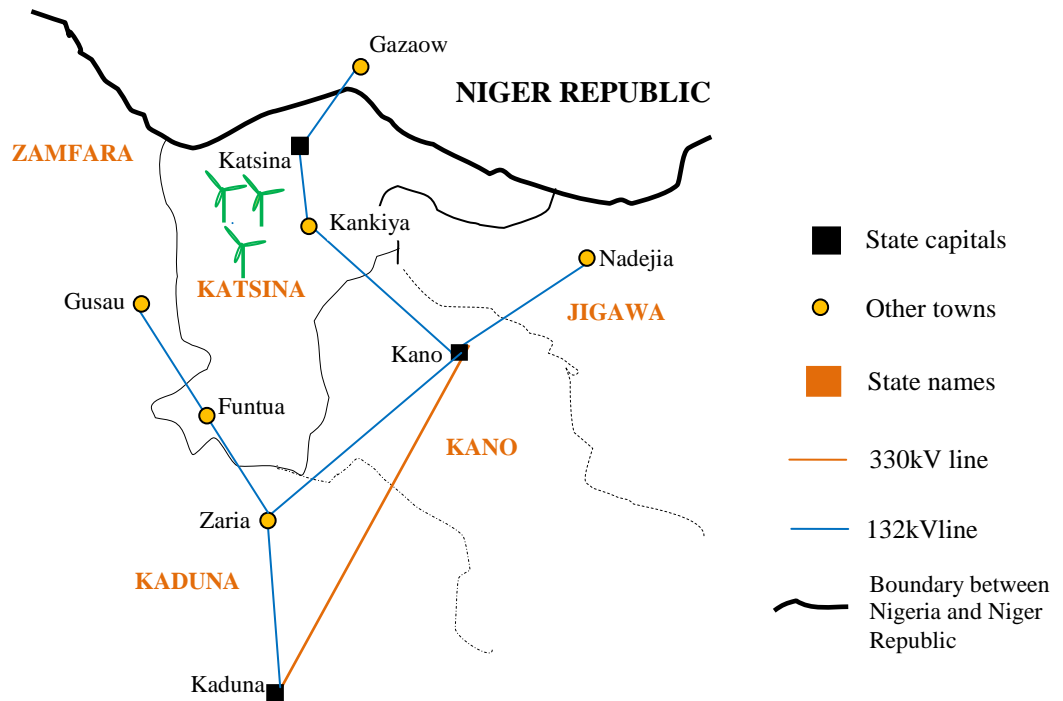


Figure 6.3. Section of map of Nigeria showing Katsina State - Location of the wind farm

Assessment of wind energy potential at six locations, (Katsina, Kaduna, Kano, Potiskum, Gusau, and Bauchi) in the northern part of Nigeria shows that all locations have a mean wind speed of 4.8m/s, but the speed could be as high as 9.839 m/s in Katsina and 7.767 m/s in Kano at certain times of the year. This was therefore concluded that Kano and Katsina are appropriate for wind farms and could produce wind power all the time. Gusau will be more productive if tall wind turbine towers are installed. Bauchi and Potiskum will yield wind energy electricity marginally [134]. The wind farm project is sited at Lamba Rimi in Katsina state [135]. Before the Katsina wind farm, the only wind electricity system is 5-kW system supplying Sayya Gidan Gada Village in Sokoto State [130].

Part of country showing the 330kV and 132kV transmission lines close to the wind farm is shown in Figure 6.3. The average annual mean monthly wind speed at 55m height for Katsina has been calculated as 6.044 m/s. The electrical layout of the wind farm in Figure 6.4 which consists of 37 GEV MP wind turbines each rated 275kW giving a total power of 10.175 MW. The generating voltage of the wind turbine is stepped up to 33kV by the transformers at the base of each turbine. The

substation is a 33/11kV substation with two 7.5MVA transformers connected through overhead lines to 11kV distribution network. Each turbine has two blades and the distance between two turbines in a wind farm is measured in rotor diameter, $d=32\text{m}$. The distance between turbines is $5d = 5 \times 32 = 160\text{m}$ and the distance between rows of turbines is $7d = 7 \times 32 = 224\text{m}$ [135].

Redacted due to copyright



Figure 6.4. Electrical layout of the Katsina wind farm [135]

6.5 Investigation of Effects Wind Energy Integration

Requirements for integrating wind energy electricity to a grid depend on the grid characteristics, the capacity of wind energy to be integrated and the variability of the wind source [136]. Wind farms are best situated at designated areas with good wind resources which are often in remote areas where the grid infrastructure is likely to be weak. Technical constraints related to weak grids limit the exploitation of wind energy for electricity production. These technical constraints are commonly associated with the effect that wind power has on voltage quality, and hardly the thermal capacity of the grid. The voltage-quality issues that may limit wind utilization in weak grids depend on the characteristics of both the wind turbine installation and the grid [80]. The focus of this work is on change in steady-state voltage level; other voltage quality constraints issues and thermal capacity are not investigated. The basic equations in the analysis of a wind integrated grid are given below. Analytical review of voltage variation due to wind integration is given in section 2.8 where the voltage

change at the PCC is given in (2.106) and voltage change as a function of the network impedance is given in (2.107). The short-circuit ratio is given in (2.108) and the short-circuit power is calculated using (2.112).

6.5.1 PSCAD Analysis of Integration of Wind Energy

The sample network [104] was analysed using the power system computer aided design (PSCAD) tool to review the effect of wind power on a grid. The investigation serves as guide in the analysis of the Nigeria system and conclusion on results.

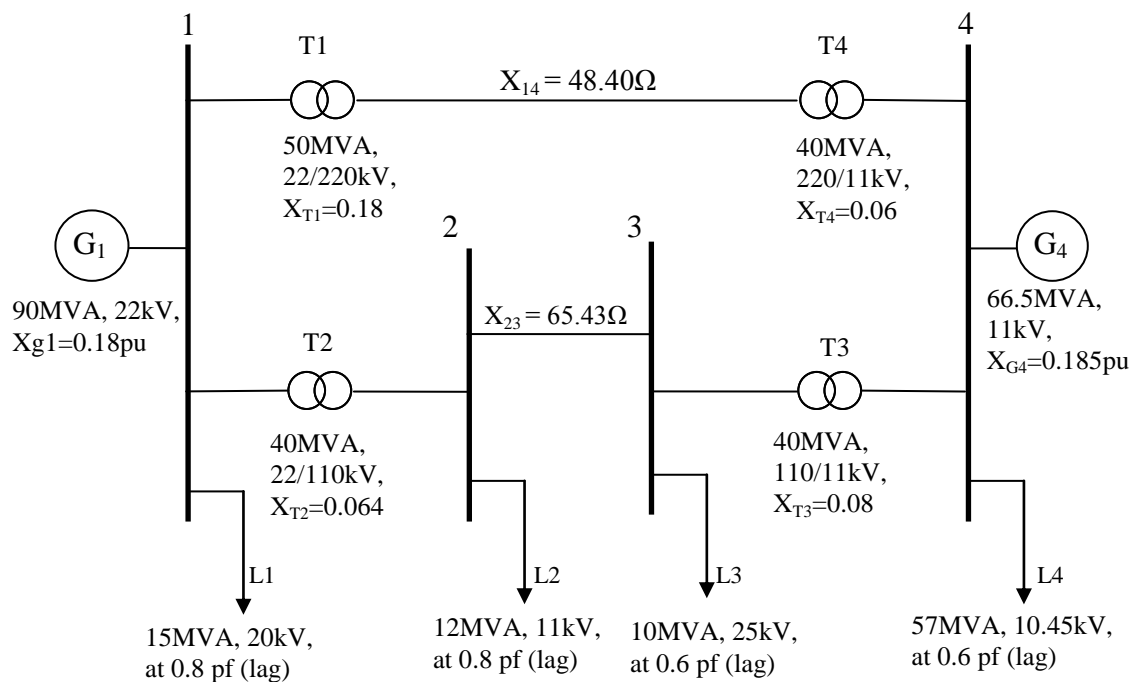


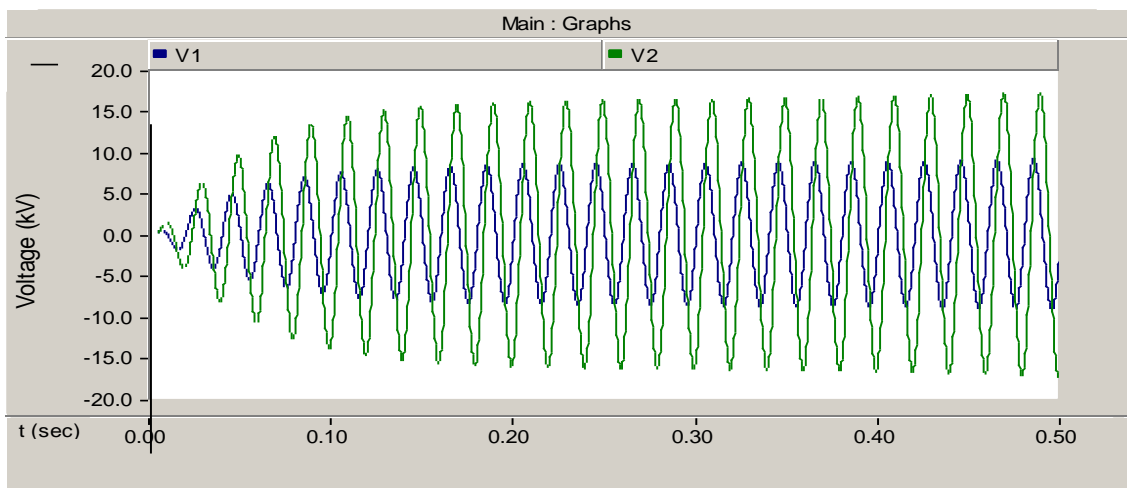
Figure 6.5 Four-bus test system for PSCAD simulation of wind integration

Effects of wind energy on the steady-state voltage of a grid have been reviewed in section 2.5. PSCAD is a very useful modelling and simulation tool for power system studies but it is “*exclusively an electromagnetic transients study environment*” [96]. It can though perform power flow for a system with few buses, such as the sample network used in the analysis below.

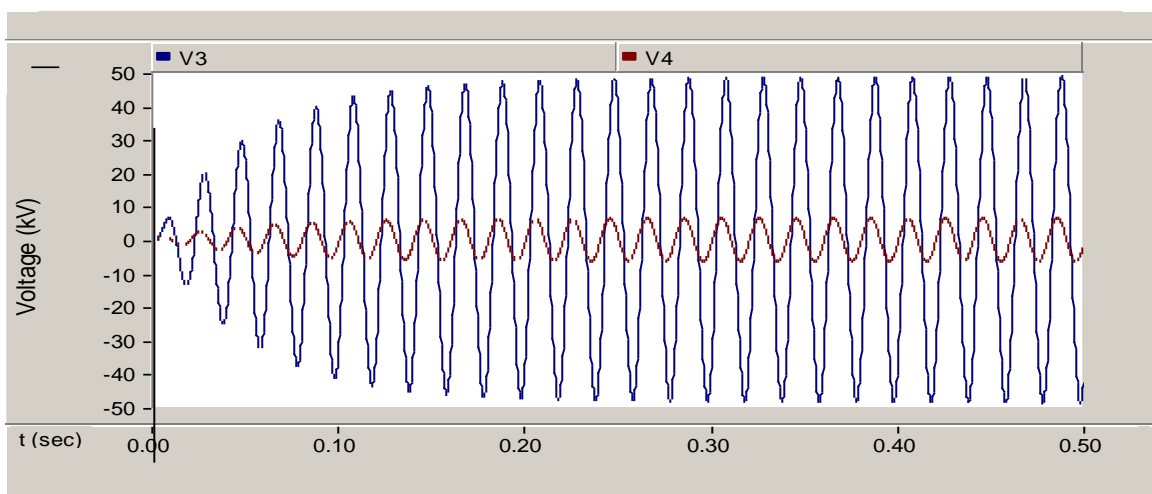
6.5.1.1 Simulation and Analysis

Investigation was carried out with PSCAD on the balanced three-phase, 4-bus, 2-machine system of Figure 6.5. Voltage levels were determined under the different scenarios:

- a) Original system with no wind
- b) Original system injected with wind power
- c) Original system weakened by increasing the grid impedance before injecting with wind energy.
- d) Reactive power injected into the weaker system with wind energy.



(a)



(b)

Figure 6.6. Voltages at the four buses (a) Voltages at buses 1 and 2 and (b) Voltages at buses 3 and 4

Results show the waveforms of voltages at the four buses (V_1 , V_2 , V_3 and V_4) in Figure 6.6. Only single phases are shown for clarity. There was no distortion in voltage waveforms under the different scenarios but the voltage levels were different. The values determined from the waveform are shown in Table 6.3.

Table 6.3 Steady-state voltage levels measured at the four buses

S/N	Node voltages Labels	Before Wind Integration	After Wind Integration		After Wind Integration + Reactive Power
		Original network (V_{or})	Original network (V_{or+w})	Weaker network ($V_{(k+w)}$)	Weaker network ($V_{(k+w+Q)}$)
		Voltage (kV)	Voltage (kV)		Voltage (kV)
1	V_1	10.41	9.58	9.37	9.50
2	V_2	22.01	20.53	18.49	18.72
3	V_3	39.70	38.74	45.18	45.25
4	V_4	6.05	5.96	6.27	6.28

Where

V_{or} is the voltage of the original network before wind integration

$V_{(or+w)}$ is the voltage of the original network after wind integration

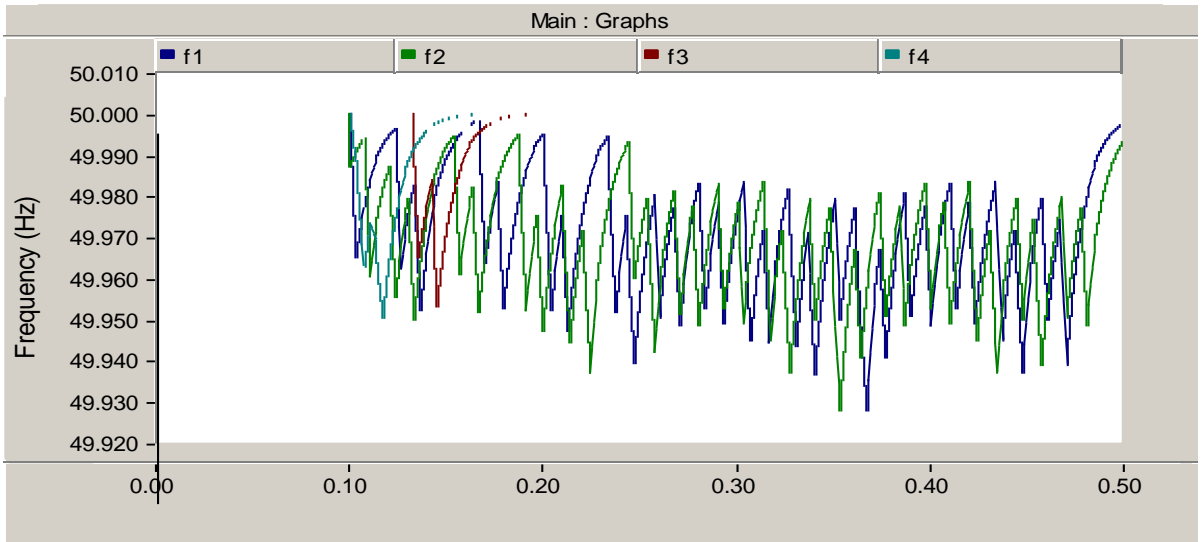
$V_{(k+w)}$ is the voltage of the weaker network after wind integration

$V_{(k+w+Q)}$ is the voltage of the weaker network after wind integration and reactive power compensation

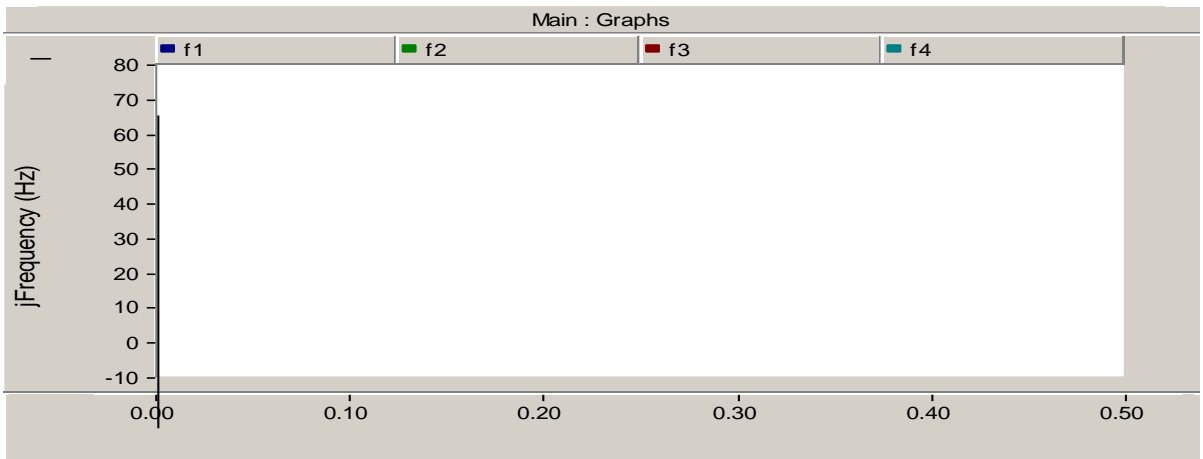
$\Delta V_{(or+w)}$ voltage change in original network after wind integration

$\Delta V_{(k+w)}$ voltage change in weaker network after wind integration

$\Delta V_{(k+w+Q)}$ voltage change in original network after wind integration and reactive power compensation.



(a)



(b)

Figure 6.7 Frequencies at the four buses during simulation (a) actual representation of system frequency (b) Average value

Table 6.4 Changes in voltage levels

S/N	Node voltages Labels	$V_{or} - V_{(or+w)}$	$V_{or} - V_{(k+w)}$	$V_{or} - V_{(k+w+Q)}$
		$\Delta V_{(or+w)}$ (kV)	$\Delta V_{(k+w)}$ (kV)	$\Delta V_{(k+w+Q)}$ (kV)
1	V_1	0.83	1.05	0.91
2	V_2	1.48	3.53	3.29
3	V_3	0.97	-5.47	-5.55
4	V_4	0.09	-0.22	-0.23

Table 6.5 Frequencies measured at the four buses

S/ N	Frequency (Hz)	Before Wind Integration		After Wind Integration				After Wind Integration + Reactive Power	
		Frequency (Hz)		Frequency (Hz)				Frequency (Hz)	
		Original network		Original network		Weaker network		Weaker network	
		Min	Max	Min	Max	Min	Max	Min	Max
1	f1	49.94	50.00	49.94	50.00	49.94	50.00	49.94	50.00
2	f2	49.94	50.00	49.94	50.00	49.94	50.00	49.94	50.00
3	f3	49.94	50.00	49.94	50.00	49.95	50.00	49.95	50.00
4	f4	49.94	50.00	49.95	50.00	49.95	50.00	49.95	50.00

6.5.1.2 Results and Discussion

All the buses experienced voltage changes, ΔV , because of wind integration; the weaker system experienced higher changes in voltage. The buses closest to the PCC experienced the highest change in voltage levels; the capacity of a grid to absorb wind power is usually determined at the PCC. When reactive power was introduced into the system there was a reduction in voltage change.

6.5.1.3 Determination of the Grid Type

The type of grid can be determined from the simulation results as follows. The equation, $\Delta V = S_w/S_k \cos(\psi - \phi)$ given in (2.76) shows that a higher the voltage deviation (ΔV) at the PCC indicates a lower short circuit capacity, S_k , and therefore the lower the ability of a grid to absorb wind energy. The grid, seen from the PCC, can be modelled as a stiff voltage source in series with an impedance Z .

a) Voltage Change before wind integration

Voltage difference based on equation (2.106) is obtained with PSCAD as

$$\Delta V_1 = \frac{\sqrt{3} \times 0.83}{\sqrt{2}} = 1.02 \text{ kV}$$

The nominal voltage of the system, $V_0 = 22\text{kV}$. The percentage change in voltage is therefore obtained as

$$\% \Delta V_1 = \frac{1.02}{22} \times 100 = 4.62\%$$

The permitted PCC voltage change, ΔV (%), is usually required to be less than 2% of nominal voltage. This is an indication that the system is a weak grid.

b) Voltage change after wind integration

Wind energy was integrated into the grid and the voltage change is computed below:

$$\Delta V_2 = \frac{\sqrt{3} \times 1.05}{\sqrt{2}} = 1.29\text{kV}$$

$$\% \Delta V_2 = \frac{1.29}{22} \times 100 = 5.85\%$$

The voltage change is higher which validates the research findings discussed in section 2.4.

c) Voltage change after wind integration and reactive power compensation

$$\Delta V_3 = \frac{\sqrt{3} \times 0.91}{\sqrt{2}} = 1.11\text{kV}$$

$$\% \Delta V_3 = \frac{1.11}{22} \times 100 = 5.07\%$$

One of the methods of reducing change in voltage in wind integrated grids is by reactive power compensation. In this case, the change in voltage at the PCC reduced from 5.85 to 5.07% after reactive power compensation.

Short Circuit Level

In the original network, the impedance measured at the PCC using PSCAD is $9.32/38.95^\circ\Omega$. The stiffness of the grid can also be determined by the short circuit level and is calculated using (2.112). Therefore, the short circuit level of the network is

$$S_{k1} = \frac{22^2}{9.32} = 51.93 \text{ MVA}$$

The short circuit level is quite low; another indication that the system is weak. The network was weakened further by increasing the impedance of some of the lines. The impedance of the weaker network measured at the PCC is $9.35/39.01^\circ \Omega$. The short circuit level is calculated as:

$$S_{k2} = \frac{22^2}{9.35} = 51.76 \text{ MVA}$$

This is lower than the level in the original network.

Short Circuit ratio

The short circuit ratio is calculated using (2.108) as

$$S_r = \frac{51.93}{23.45} = 2.21$$

For a weak grid, $S_k/S_w < 25$ and in extreme cases it is about 2.

Impedance angle

The impedance angle, ψ , at the PCC is 38.95° . This is a pointer that the network is resistive and therefore can be termed a distribution network. Relatively high power compensation is required to maintain zero voltage deviation in network. Reactive power compensation is a less effective measure to control the voltage in such networks.

6.5.1.4 Deductions from the Results

The PSCAD analysis has revealed that the weaker system experienced higher changes in voltage. Also the buses closest to the PCC experienced the highest change in voltage levels and the capacity of a grid to absorb wind power is usually determined at the PCC. The significant change in voltage level is related to the short circuit level being low ($S_k/S_w < 25$). Also, impedance phase angle shows that the network is resistive which suggests a distribution network. The findings are in line with the review in section 2.4.

6.6 SVUD Analysis of the Nigeria 330kV Network Integrated with wind Power

6.6.1 Grid Impedance and Short Circuit Ratio of the Network

The main factors influencing network voltage profile are the parameters of the distribution or transmission system overhead lines adjacent to the wind farm where grid impedance and short circuit ratio are the major determinants. Transmission lines are mainly inductive and so the X/R ratio is significantly greater than unity. Distribution lines are different in that X/R ratio may be close to unity.

When real power flows through a resistive element, the current is in phase with the voltage and therefore an in-phase voltage drop occurs across the network. There is no angular shift between the voltages at the sending-end and the receiving-end of the circuit. When real power flows through a purely reactive component, no in-phase voltage drop occurs but there is an angular shift between the voltages at the two nodes. So the transfer of active power has a major effect on the voltage profile on low-voltage systems, whereas reactive power transfer is the dominant factor on high-voltage systems. Apart from thermal loading considerations, this is one reason why it is important to connect large wind farms to higher voltage networks. In all cases reactive power transfer is the dominant factor in transformer voltage drop [81].

6.6.2 Determination of the grid impedance

The Katsina wind farm is connected to the 330kV network in this analysis as shown in Figure 6.8. The nearest 330kV bus is the Kano bus (bus 30) and is taken to be at the PCC.

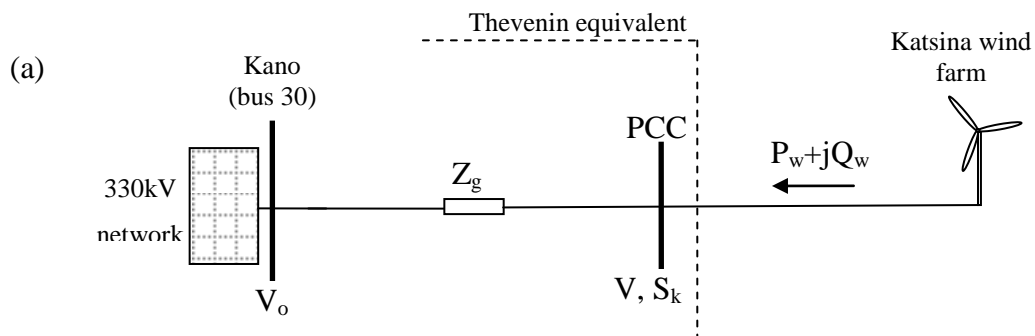


Figure 6.8. Thevenin equivalent at Kano

The estimated grid impedance looking at the 330kV network from the PCC is obtained using the method in [137, 138]. In the general method, two different load situations are obtained from which the voltages v_1 , v_2 and currents i_1 , i_2 are obtained. The impedance is computed using (6.1).

$$Z = \frac{v_1 - v_2}{i_1 - i_2} = \frac{\Delta v}{\Delta i} \quad (6.1)$$

The voltage v_{30a} and current i_{30a} at bus 30 which correspond to the Kano bus in Figure 6.8 is determined at rated load, S_{30a} . The load is varied to S_{30b} and the voltage and currents are determined as v_{30b} and i_{30b} . The grid impedance is estimated as

$$Z_{\text{grid}} = \frac{v_{30a} - v_{30b}}{i_{30a} - i_{30b}} = \frac{\Delta v}{\Delta i} \quad (6.2)$$

In the analysis of the system, balanced three-phase is assumed. The initial load at bus 30 is

$$S_{30a} = 2.260 + j1.400$$

The voltage v_{30a} and current i_{30a} at this load are obtained through load flow as:

$$v_{30a} = 0.74581 - 0.48397i$$

$$I_{30a} = 1.2756 - 2.7044i$$

The load at bus 30 is then increased to S_{30b} , and the voltage v_{30b} and current i_{30b} are determined at this new load:

$$S_{30b} = 3.260 + j2.400$$

$$v_{30b} = 0.54633 - 0.52175i$$

$$i_{30b} = 0.9273 - 5.2777i$$

The equivalent grid impedance is therefore obtained as:

$$Z_{\text{grid}} = \frac{(0.74581 - 0.48397i) - (0.54633 - 0.52175i)}{(1.2756 - 2.7044i) - (0.9273 - 5.2777i)}$$

$$= 0.0247 - 0.0742i \text{ pu}$$

The value in per unit is converted to real values as explained in section 2.7. The grid nominal voltage is 330kV and is taken as the base voltage, V_B , and the base MVA, S_B , is 100. The base impedance is obtained as:

$$Z_B = \frac{V_B^2}{S_B} = \frac{(330\text{kV})^2}{100\text{MVA}} \quad (6.3)$$

The impedance in ohms is computed using (6.4) derived from (2.82a)

$$Z_{\text{actual}} = Z_{\text{pu}} \cdot Z_B \text{ (}\Omega\text{)} \quad (6.4)$$

$$= Z_{\text{pu}} \cdot \frac{(\text{basekV})^2}{\text{baseMVA}}$$

$$= \frac{(0.0247 - 0.0742i)(330\text{kV})^2}{100}$$

$$= 26.9211 - 80.7745i$$

$$= 85.1427 \angle -71.5674^\circ \Omega$$

6.6.3 Short circuit ratio

The stiffness of the grid can be determined by the short circuit level. The magnitude of impedance at the PCC has been obtained as 85.1427 Ω . Therefore,

$$S_k = \frac{330^2}{85.1427}$$

$$= 38.7820\text{MVA}$$

The rated wind power output, S_w of the Katsina wind farm is 10.175 MW, therefore, the short circuit ratio is:

$$S_r = \frac{38.7820}{10.175}$$
$$= 3.8115.$$

A grid is considered weak for a short circuit ratio $S_r < 25$ and strong for $S_r > 25$. In extreme cases S_r can be close to 2. The computed short-circuit value with low wind power is 3.8115. This is very low, a clear indication that the network is weak and therefore integration of high wind power will likely compromise the reliability of the network. The system needs to be retrofitted and reinforcement is the only reasonable measure to enable the integration of large amount of wind power.

6.7 SVUD Assessment of Voltage Variation Introduced by Wind Energy in the 330kV Network

The power factor of wind turbines varies with the generated power [81] and consequently the reactive power consumption of wind turbines varies according to the output level of the generator. For the purpose of this work the power factor of the wind farm is assumed to be unity and so the rated wind power is 10.175MW. The analysis is carried out by integrating rated wind to the 330kV network at different buses and observing the voltage changes. Results are shown in Table 6.6. The voltage profile of the network when no wind is integrated and when rated wind is integrated shows almost no difference. This is reflected in Figure 6.9 where the blue and red lines overlap such that the blue line is not visible except at the PCC.

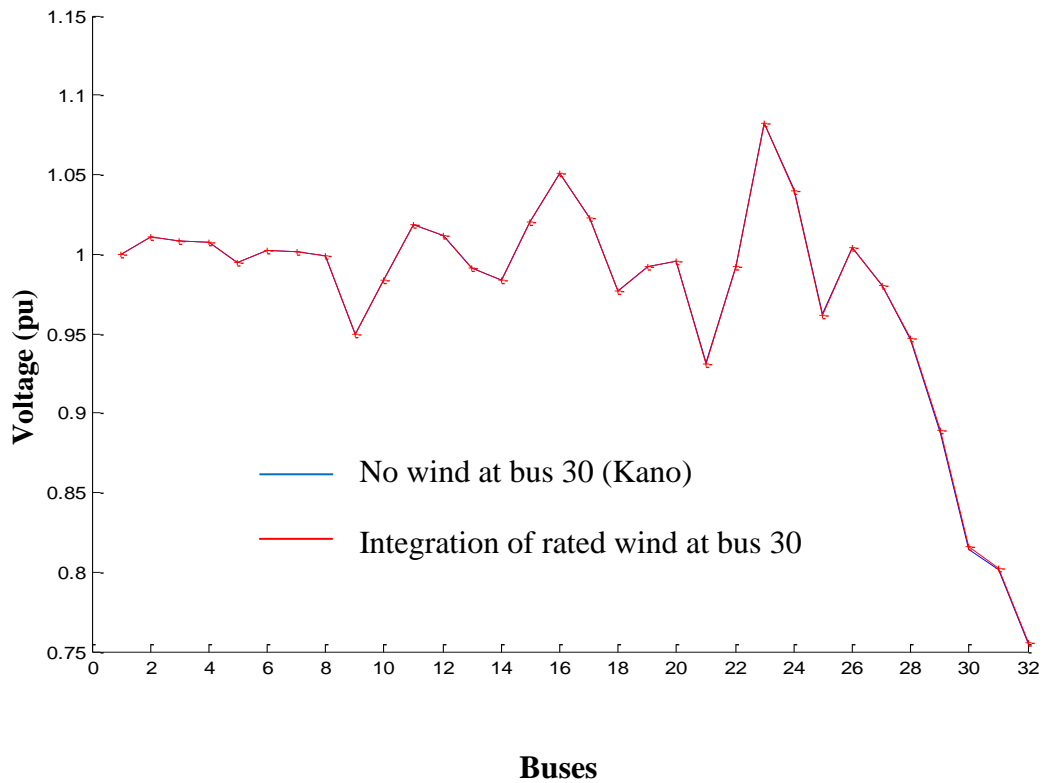


Figure 6.9. Voltage profiles without wind and with rated wind power

The rated wind power was then connected to different buses as a whole, then shared equally between two or three buses. There is no noticeable change in voltages because the wind power level is quite low, confirming the fact that only significant amount of wind causes appreciable effect on the power system. The profile when the wind farm is connected to buses close to conventional generating station like Shiroro showed almost no change in voltage. The slightly noticeable voltage change is seen at the PCC and buses close to the PCC (31 and 32) which connect the weakest part of the grid. The VMSE's for the different connections in Table 6.7 indicate the total voltage variation in each case when wind power is integrated.

Table 6.6a Effect of integrating rated wind power at different buses

Bus No	Voltages without wind	Voltages with rated wind at bus 30-Kano	Voltages with wind at bus Kano and Kaduna	Voltages with wind at bus Kano, Kaduna and Gombe	Voltages with wind at bus Birni-Kebbi	Whole wind at Kaduna	Whole wind at Shiroro
1	1.0000+0.0000i	1.0000+0.0000i	1.0000+0.0000i	1.0000 + 0.0000i	1.0000 + 0.0000i	1.0000 +0.0000i	1.0000+0.0000i
2	1.0037-0.1218i	1.0037-0.1217i	1.0049-0.1208i	1.0046 - 0.1210i	1.0037 - 0.1218i	1.0037 - 0.1218i	1.0037 - 0.1218i
3	1.0009-.1231i	1.001-0.12303i	1.0025-0.1220i	1.0021 - 0.1221i	1.0011 - 0.1231i	1.0010 - 0.1230i	1.0010 - 0.1231i
4	1.0004-0.1200i	1.0004-0.1199i	1.0021-0.1188i	1.0016 - 0.1189i	1.0005 - 0.1199i	1.0004 - 0.1199i	1.0005 - 0.1199i
5	0.9927-.0679i	0.9928-0.0678i	0.9945-0.06680i	0.9940 - 0.0669i	0.9928 - 0.0678i	0.9928 - 0.0678i	0.9928 - 0.0678i
6	0.9886-0.1635i	0.9887-0.1633i	0.9910-0.1615i	0.9903 - 0.1617i	0.9888 - 0.1633i	0.9887 - 0.1633i	0.9888 - 0.1633i
7	0.9798-0.2074i	0.9799-0.2072i	0.9823-0.2054i	0.9817 - 0.2056i	0.9800 - 0.2073i	0.9799 - 0.2073i	0.9800 - 0.2073i
8	0.9747-0.2203i	0.9748-0.2201i	0.9772-0.2183i	0.9766 - 0.2185i	0.9749 - 0.2202i	0.9748 - 0.2202i	0.9749 - 0.2202i
9	0.8986-0.3074i	0.8987-0.3073i	0.9014-0.3057i	0.9007 - 0.3059i	0.8988 - 0.3073i	0.8987 - 0.3073i	0.8988 - 0.3073i
10	0.9456-0.2695i	0.9457-0.2693i	0.9482-0.2678i	0.9475 - 0.2680i	0.9458 - 0.2694i	0.9457 - 0.2694i	0.9457 - 0.2694i
11	0.9897-0.2386i	0.9898-0.2385i	0.9919-0.2371i	0.9913 - 0.2373i	0.9899 - 0.2385i	0.9898 - 0.2385i	0.9899 - 0.2385i
12	0.9929-0.1958i	0.9930-0.1957i	0.9948-0.1943i	0.9943 - 0.1945i	0.9930 - 0.1957i	0.9930 - 0.1957i	0.9930 - 0.1957i
13	0.8975-0.4215i	0.8976-0.4213i	0.90136-0.4185i	0.9003 - 0.4188i	0.8978 - 0.4213i	0.8977 - 0.4213i	0.8978 - 0.4213i
14	0.8862-0.4269i	0.8863-0.4266i	0.8901-0.4239i	0.8890 - 0.4242i	0.8865 - 0.4267i	0.8864 - 0.4267i	0.8864 - 0.4267i
15	0.9350-0.4075i	0.9351-0.4073i	0.9387-0.40399i	0.9376 - 0.4043i	0.9353 - 0.4073i	0.9352 - 0.4073i	0.9352 - 0.4073i
16	0.9808-0.3770i	0.9809-0.3768i	0.9842-0.3733i	0.9832 - 0.3737i	0.9811 - 0.3768i	0.9810 - 0.3768i	0.9811 - 0.3768i

Table 6.6b Effect of integrating rated wind power at different buses

Bus No	Voltages without wind	Voltages with rated wind at bus 30 (Kano)	Voltages with wind at bus Kano and Kaduna	Voltages with wind at bus Kano, Kaduna and Gombe	Voltages with wind at bus Birni Kebbi	Whole wind at Kaduna	Whole wind at Shiroro
17	0.9392-0.4053i	0.9393-0.4053i	0.9428-0.4018i	0.9418 - 0.4021i	0.9395 - 0.4050i	0.9394 - 0.4050i	0.9394 - 0.4050i
18	0.8686-0.4466i	0.8688-0.4464i	0.8728-0.4439i	0.8717 - 0.4441i	0.8689 - 0.4464i	0.8688 - 0.4464i	0.8689 - 0.4464i
19	0.8989-0.4203i	0.8991-0.4201i	0.9029-0.4178i	0.9018 - 0.4180i	0.8992 - 0.4202i	0.8991 - 0.4202i	0.8992 - 0.4202i
20	0.9040-0.4171i	0.9040-0.4171i	0.9068-0.4169i	0.9056 - 0.4172i	0.9042 - 0.4172i	0.9041 - 0.4171i	0.9042 - 0.4171i
21	0.8771-0.3132i	0.8768-0.3130i	0.8773-0.3107i	0.8757 - 0.3106i	0.8772 - 0.3132i	0.8770 - 0.3131i	0.8772 - 0.3132i
22	0.8989-0.4203i	0.8991-0.4201i	0.9029-0.4177i	0.9019 - 0.4179i	0.8992 - 0.4202i	0.8991 - 0.4202i	0.8992 - 0.4202i
23	0.9517-0.5153i	0.9516-0.5149i	0.9543-0.5112i	0.9527 - 0.5111i	0.9589 - 0.5070i	0.9518 - 0.5150i	0.9520 - 0.5151i
24	0.9513-0.4211i	0.9512-0.4207i	0.9535-0.4171i	0.9522 - 0.4171i	0.9522 - 0.4198i	0.9514 - 0.4208i	0.9515 - 0.4208i
25	0.8944-0.355i	0.8941-0.3546i	0.8943-0.3505i	0.8928 - 0.3503i	0.8949 - 0.3537i	0.8943 - 0.3547i	0.8945 - 0.3548i
26	0.9256-0.3894i	0.9253-0.3887i	0.9257-0.3824i	0.9242 - 0.3823i	0.9257 - 0.3892i	0.9255 - 0.3888i	0.9257 - 0.3889i
27	0.8817-0.4276i	0.8820-0.4273i	0.8871-0.4231i	0.8862 - 0.4233i	0.8820 - 0.4275i	0.8820 - 0.4273i	0.8821 - 0.4273i
28	0.8316-0.4520i	0.8320-0.4516i	0.8374-0.4476i	0.8364 - 0.4478i	0.8319 - 0.4518i	0.8320 - 0.4516i	0.8320 - 0.4516i
29	0.7480-0.4783i	0.7499-0.4770i	0.7673-0.4639i	0.7681 - 0.4646i	0.7483 - 0.4782i	0.7495 - 0.4769i	0.7484 - 0.4780i
30	0.6530-0.4858i	0.6582-0.4830i	0.6889-0.4643i	0.6849 - 0.4682i	0.6533 - 0.4857i	0.6546 - 0.4846i	0.6534 - 0.4855i
31	0.6384-0.4848i	0.6405-0.4838i	0.6596-0.4732i	0.6722 - 0.4684i	0.6388 - 0.4847i	0.6401 - 0.4837i	0.6389 - 0.4845i
32	0.5784-0.4845i	0.5805-0.4836i	0.6004-0.4744i	0.6252 - 0.4643i	0.5788 - 0.4844i	0.5800 - 0.4835i	0.5789 - 0.4843i

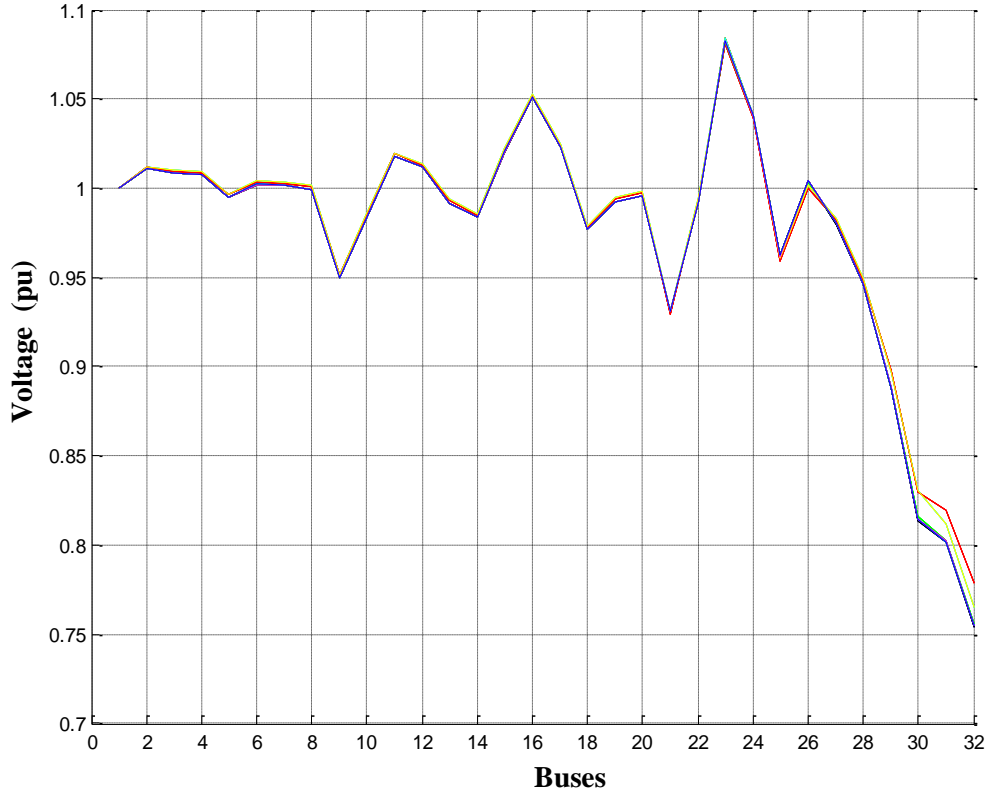
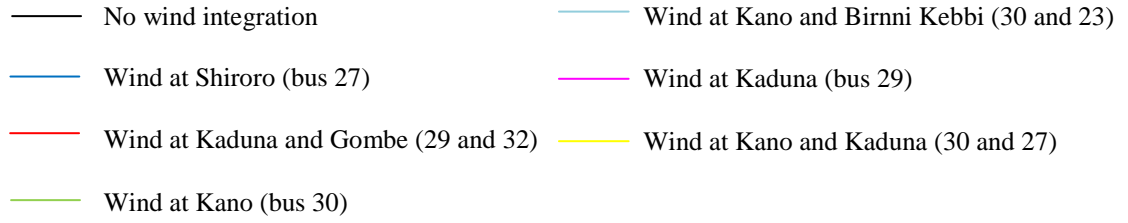


Figure 6.10. Voltage profiles for rated wind power at different buses

Table 6.7 VMSE for wind integration at different PCC's

Wind at Kano bus	Wind at Kano and Kaduna buses	Wind at Kano, Kaduna and Gombe buses	Wind at Birni Kebbi buses	Whole wind at Kaduna bus	Whole wind at Shiroro bus
8.4781e-07	6.2689e-05	9.8678e-05	2.0009e-06	2.8644e-07	5.5758e-08

6.8 Effect of Injecting Reactive Power on Voltage Change

The power produced by a wind turbine at any particular time depends on a number of parameters which include wind speed, location, local networks and the wind turbine generator manufacturer. The reactive power compensation system of a wind turbine plays a very important role in determining how much power it can deliver. Wind turbines are therefore fitted with basic reactive power compensation equipment that can deliver about 25% of start-up requirements [139]. The reactive power requirements of wind turbine generators affect both the generator and the grid to which it is integrated. The connection of reactive power equipment X_{PFC} is illustrated in Figure 6.11 where the induction generator represents the wind farm generators.

It is generally reported in literature that all wind farms consume reactive power in one form or the other (even wind turbines that produce at unity power consume reactive power in other areas) and at the same time feed reactive power to the grid. These two factors reduce the power factor at the conventional power stations. At the primary side of wind farm substations, the wind farms affect the reactive power of:

- wind turbine themselves, especially wind turbines with directly grid connected induction generators;
- step up transformers between wind turbines and wind farms feeders;
- wind farm feeders;
- substation transformers

The influence of voltage and frequency deviations can be understood in the analysis of an induction generator embedded within a weak power system using the equivalent circuit of Figure 6.11.

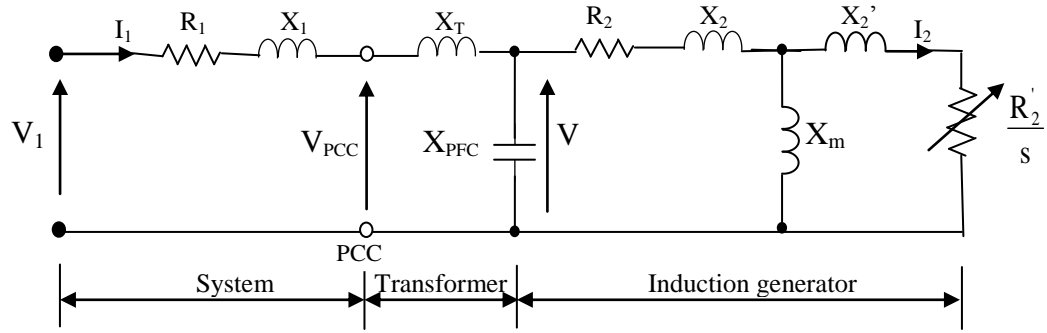


Figure 6.11. Induction generator connected to power system

where:

R_1 = power system resistance

X_1 = power system reactance

R_2 = Stator resistance

X_2 = Stator leakage reactance

R_2' = Rotor resistance referred to stator side

X_2' = Rotor leakage reactance referred to stator side

X_m = Magnetizing reactance (main reactance)

Kano is the nearest bus to the Katsina wind farm, reactive power injection would save the cost of longer lines to connect to other buses further away. The power factor for the Nigeria transmission system is 0.85 lagging and 0.95 leading [140]. The reactive power required to maintain a specific voltage in a weak grid is given in equation (2.88). The normalised reactive power feed-in for maintaining the voltage is Q/S_w [80].

For the 330kV network integrated with wind power at Kano:

$$P = 0.10175\text{pu}, R = 0.0247, X = 0.0742, V_0 = 1.0\text{pu}, V = 0.95$$

$$\text{Let } |Z|^2 = (R^2 + X^2) = 0.0247^2 + 0.0742^2$$

Then using equation (2.88), reactive power requirements is obtained as:

$$Q = 11.5470.$$

The reactive power was injected at bus 30 and the effect on the voltage profile is illustrated in Figure 6.12 where there is a general improvement in the voltage profile. The blue line is the voltage profile when 2.1018MW wind energy is injected at bus 30 without reactive compensation and the red line is when the computed reactive power is injected at bus 30. Integration of wind energy into weak grids raises the voltage level as seen. But at buses 30, 31 and 32 where the voltages were unacceptable low, reactive power compensation greatly improves the voltage that was near collapse but it is still below acceptable limit.

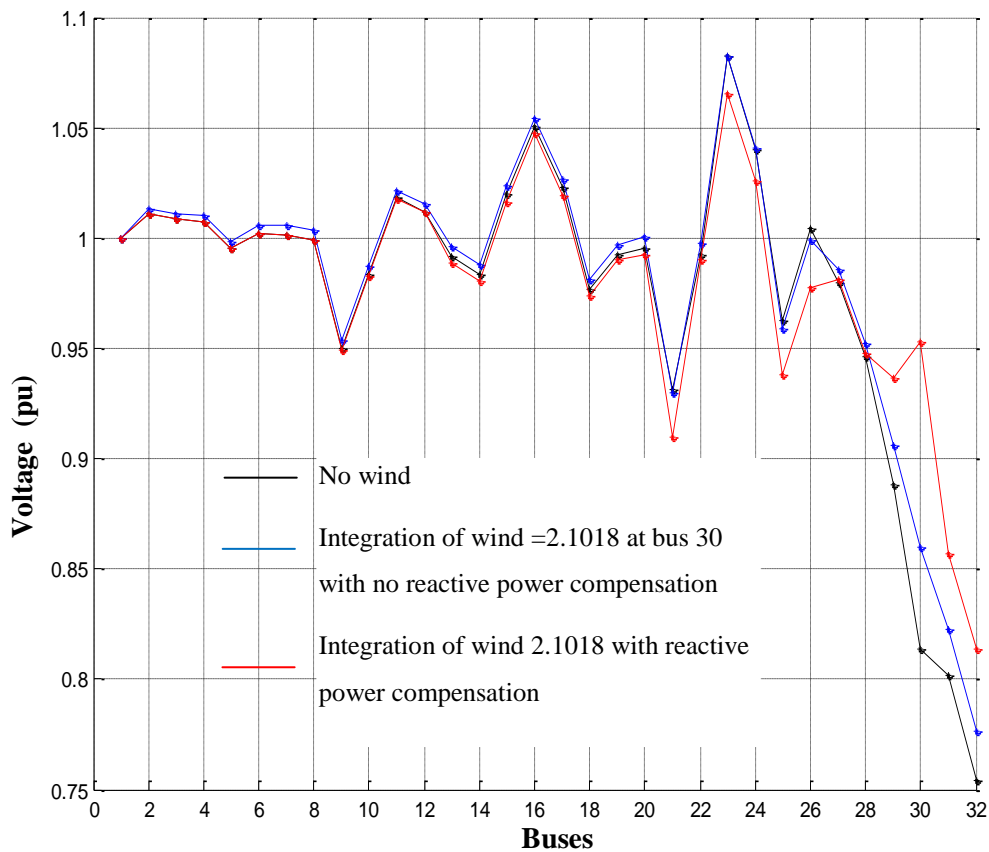


Figure 6.12. Wind integration without and with reactive power compensation at bus 30

Table 6.8 Increased levels of wind power

Bus no.	Voltages without wind	Voltage for wind P =0.1018	Voltage for wind P = 2.1018	Voltage for wind P = 4.1018
1	1.0000 - 0.0000i	1.0000 - 0.0000i	1.0000 - 0.0000i	1.0000 - 0.0000i
2	1.0037 - 0.1218i	1.0037 - 0.1218i	1.0061 - 0.1200i	1.0086 - 0.1188i
3	1.0009 - 0.1231i	1.0010 - 0.1230i	1.0040 - 0.1211i	1.0072 - 0.1197i
4	1.0004 - 0.1200i	1.0004 - 0.1199i	1.0037 - 0.1179i	1.0072 - 0.1165i
5	0.9927 - 0.0679i	0.9928 - 0.0678i	0.9962 - 0.0660i	0.9999 - 0.0648i
6	0.9886 - 0.1635i	0.9887 - 0.1633i	0.9932 - 0.1599i	0.9980 - 0.1576i
7	0.9798 - 0.2074i	0.9799 - 0.2073i	0.9847 - 0.2038i	0.9897 - 0.2014i
8	0.9747 - 0.2203i	0.9748 - 0.2201i	0.9796 - 0.2167i	0.9847 - 0.2142i
9	0.8986 - 0.3074i	0.8987 - 0.3073i	0.9040 - 0.3043i	0.9095 - 0.3022i
10	0.9456 - 0.2695i	0.9457 - 0.2693i	0.9506 - 0.2664i	0.9557 - 0.2642i
11	0.9897 - 0.2386i	0.9898 - 0.2385i	0.9939 - 0.2359i	0.9981 - 0.2341i
12	0.9929 - 0.1958i	0.9930 - 0.1956i	0.9967 - 0.1932i	1.0005 - 0.1915i
13	0.8975 - 0.4215i	0.8976 - 0.4213i	0.9049 - 0.4160i	0.9125 - 0.4124i
14	0.8862 - 0.4269i	0.8863 - 0.4266i	0.8937 - 0.4215i	0.9014 - 0.4179i
15	0.9350 - 0.4075i	0.9351 - 0.4073i	0.9420 - 0.4012i	0.9493 - 0.3970i
16	0.9808 - 0.3770i	0.9809 - 0.3768i	0.9872 - 0.3704i	0.9939 - 0.3660i
17	0.9392 - 0.4053i	0.9393 - 0.4050i	0.9461 - 0.3990i	0.9534 - 0.3948i
18	0.8686 - 0.4466i	0.8688 - 0.4464i	0.8766 - 0.4417i	0.8847 - 0.4383i
19	0.8989 - 0.4203i	0.8991 - 0.4201i	0.9065 - 0.4156i	0.9143 - 0.4124i
20	0.9040 - 0.4171i	0.9040 - 0.4171i	0.9092 - 0.4174i	0.9150 - 0.4187i
21	0.8771 - 0.3132i	0.8768 - 0.3130i	0.8770 - 0.3086i	0.8805 - 0.3068i
22	0.8989 - 0.4203i	0.8991 - 0.4201i	0.9067 - 0.4154i	0.9145 - 0.4121i
23	0.9517 - 0.5153i	0.9516 - 0.5149i	0.9565 - 0.5075i	0.9639 - 0.5028i
24	0.9513 - 0.4210i	0.9512 - 0.4207i	0.9554 - 0.4136i	0.9615 - 0.4090i
25	0.8944 - 0.3550i	0.8941 - 0.3546i	0.8939 - 0.3463i	0.8973 - 0.3414i
26	0.9256 - 0.3894i	0.9253 - 0.3887i	0.9255 - 0.3757i	0.9301 - 0.3664i
27	0.8817 - 0.4276i	0.8820 - 0.4273i	0.8923 - 0.4189i	0.9021 - 0.4118i
28	0.8316 - 0.4520i	0.8319 - 0.4516i	0.8428 - 0.4435i	0.8532 - 0.4367i
29	0.7480 - 0.4783i	0.7499 - 0.4770i	0.7868 - 0.4488i	0.8143 - 0.4189i
30	0.6530 - 0.4858i	0.6582 - 0.4829i	0.7514 - 0.4185i	0.8205 - 0.3436i
31	0.6384 - 0.4848i	0.6405 - 0.4838i	0.6810 - 0.4608i	0.7106 - 0.4352i
32	0.5784 - 0.4845i	0.5805 - 0.4836i	0.6227 - 0.4636i	0.6535 - 0.4405i

Table 6.9 Increased levels of wind power

Bus no.	Voltage for wind P =6.1018	Voltage for wind P =8.1018	Voltage for wind P =10.1018	Voltage for wind P = 2.1018 Q = 1.9634
1	1.0000 +0.0000i	1.0000 + 0.0000i	1.0000 + 0.0000i	1.0000 + 0.0000i
2	1.0115 - 0.1175i	1.0147 - 0.1164i	1.0181 - 0.1154i	1.0037 - 0.1200i
3	1.0109 - 0.1183i	1.0149 - 0.1172i	1.0191 - 0.1162i	1.0012 - 0.1209i
4	1.0111 - 0.1151i	1.0154 - 0.1139i	1.0200 - 0.1130i	1.0007 - 0.1177i
5	1.0040 - 0.0636i	1.0084 - 0.0627i	1.0131 - 0.0620i	0.9932 - 0.0656i
6	1.0034 - 0.1552i	1.0093 - 0.1534i	1.0156 - 0.1519i	0.9891 - 0.1594i
7	0.9954 - 0.1988i	1.0015 - 0.1969i	1.0081 - 0.1952i	0.9804 - 0.2034i
8	0.9905 - 0.2117i	0.9967 - 0.2097i	1.0033 - 0.2080i	0.9753 - 0.2163i
9	0.9160 - 0.2999i	0.9227 - 0.2981i	0.9301 - 0.2964i	0.8991 - 0.3043i
10	0.9616 - 0.2620i	0.9679 - 0.2602i	0.9746 - 0.2586i	0.9460 - 0.2663i
11	1.0031 - 0.2322i	1.0085 - 0.2307i	1.0142 - 0.2293i	0.9899 - 0.2359i
12	1.0051 - 0.1896i	1.0100 - 0.1882i	1.0153 - 0.1869i	0.9930 - 0.1931i
13	0.9217 - 0.4087i	0.9315 - 0.4058i	0.9423 - 0.4034i	0.8970 - 0.4154i
14	0.9106 - 0.4142i	0.9206 - 0.4113i	0.9315 - 0.4089i	0.8857 - 0.4208i
15	0.9581 - 0.3927i	0.9676 - 0.3895i	0.9781 - 0.3867i	0.9343 - 0.4004i
16	1.0021 - 0.3616i	1.0111 - 0.3582i	1.0209 - 0.3554i	0.9799 - 0.3695i
17	0.9621 - 0.3906i	0.9716 - 0.3874i	0.9820 - 0.3846i	0.9385 - 0.3982i
18	0.8945 - 0.4350i	0.9050 - 0.4323i	0.9164 - 0.4301i	0.8683 - 0.4410i
19	0.9235 - 0.4093i	0.9334 - 0.4066i	0.9441 - 0.4044i	0.8988 - 0.4151i
20	0.9225 - 0.4198i	0.9310 - 0.4212i	0.9406 - 0.4228i	0.9007 - 0.4165i
21	0.8878 - 0.3062i	0.8980 - 0.3070i	0.9115 - 0.3093i	0.8583 - 0.3020i
22	0.9239 - 0.4088i	0.9339 - 0.4059i	0.9446 - 0.4036i	0.8990 - 0.4149i
23	0.9748 - 0.4992i	0.9880 - 0.4970i	1.0040 - 0.4964i	0.9395 - 0.5022i
24	0.9705 - 0.4055i	0.9816 - 0.4033i	0.9949 - 0.4025i	0.9413 - 0.4088i
25	0.9047 - 0.3381i	0.9154 - 0.3367i	0.9295 - 0.3373i	0.8750 - 0.3387i
26	0.9393 - 0.3591i	0.9523 - 0.3539i	0.9693 - 0.3508i	0.9049 - 0.3688i
27	0.9127 - 0.4047i	0.9235 - 0.3982i	0.9345 - 0.3922i	0.8871 - 0.4196i
28	0.8645 - 0.4299i	0.8759 - 0.4236i	0.8876 - 0.4178i	0.8373 - 0.4441i
29	0.8354 - 0.3872i	0.8498 - 0.3542i	0.8571 - 0.3203i	0.8120 - 0.4662i
30	0.8710 - 0.2601i	0.9034 - 0.1694i	0.9161 - 0.0712i	0.8210 - 0.4837i
31	0.7332 - 0.4075i	0.7484 - 0.3782i	0.7557 - 0.3478i	0.7110 - 0.4784i
32	0.6768 - 0.4151i	0.6923 - 0.3877i	0.6993 - 0.3593i	0.6556 - 0.4816i

6.9 Effect of Increased Wind Power on the Voltage Level

Wind power level was increased gradually and the resulting voltages in Table 6.9 and the voltage profile in Figure 6.13 shows increased voltage change as the wind power increases. It is seen that the higher the level of wind power the higher the voltage generally. This validates the general researches done on wind energy integration that high wind power increases the voltage variation. The largest change in voltage, represented by the black line is when the highest wind power level is injected.

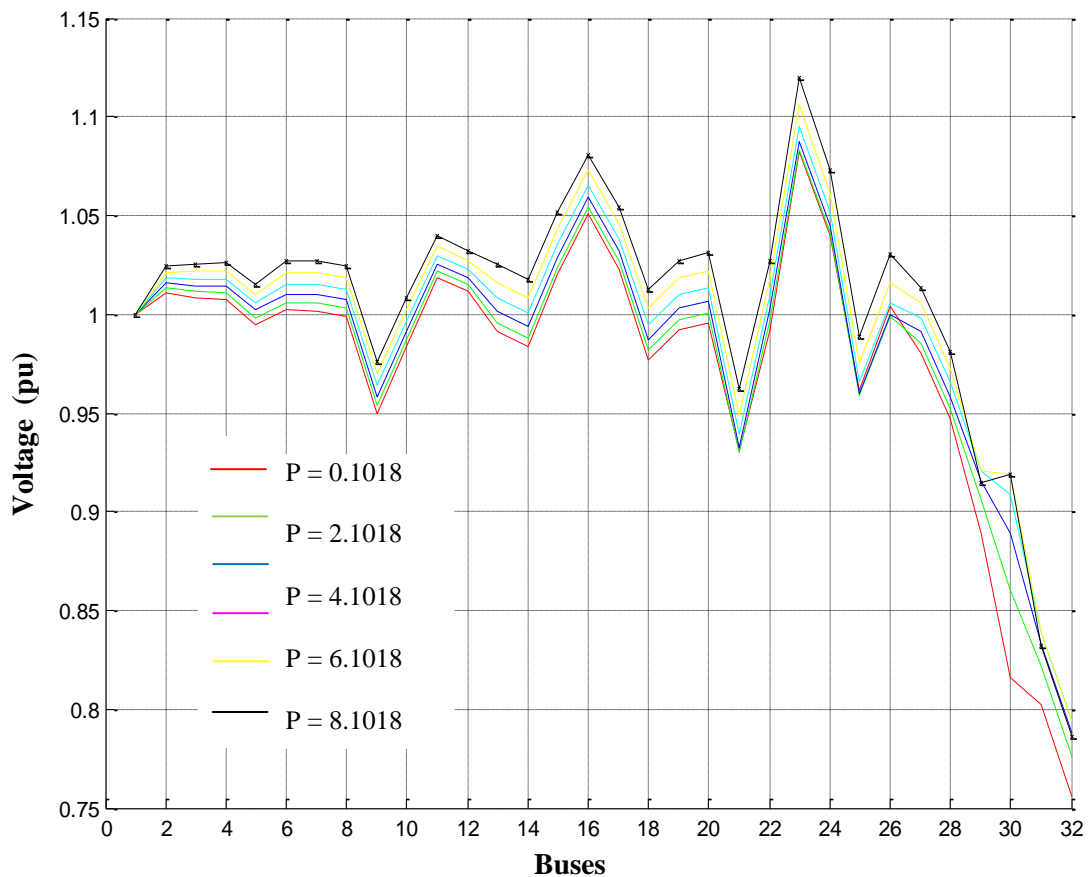


Figure 6.13. Increased levels of wind power at the PCC

The system is overloaded as shown in the next section; the lines around bus 30 are long and far from the nearest generating station. The wind farm which is an extra generating station, improves the voltage at the PCC and the buses close to it. Though wind power

affects voltage levels and power flows in the network, system-wide effects can be beneficial by supporting the voltage during low voltage situations [129]; this is true in the Nigeria case because injection of wind power raised the voltage levels that were very low. Comparison of voltage magnitudes at buses 31 and 32 when rated wind power was integrated shows rises of 0.12% at bus 31 and 0.15% at bus 32. Increase of wind power to 4.1018 pu shows rises of 3.9% at bus 31 and 4.5% at bus 32.

6.10 Analysis of the Stronger Grid

One of the characteristics of a strong grid is that the voltages are within acceptable limits. The grid was strengthened by reducing the load on the system and the voltage profile in Figure 6.14 shows a very improved profile with all voltages within acceptable limits except bus 21. This is a clear indication that the system in its original state is overloaded.

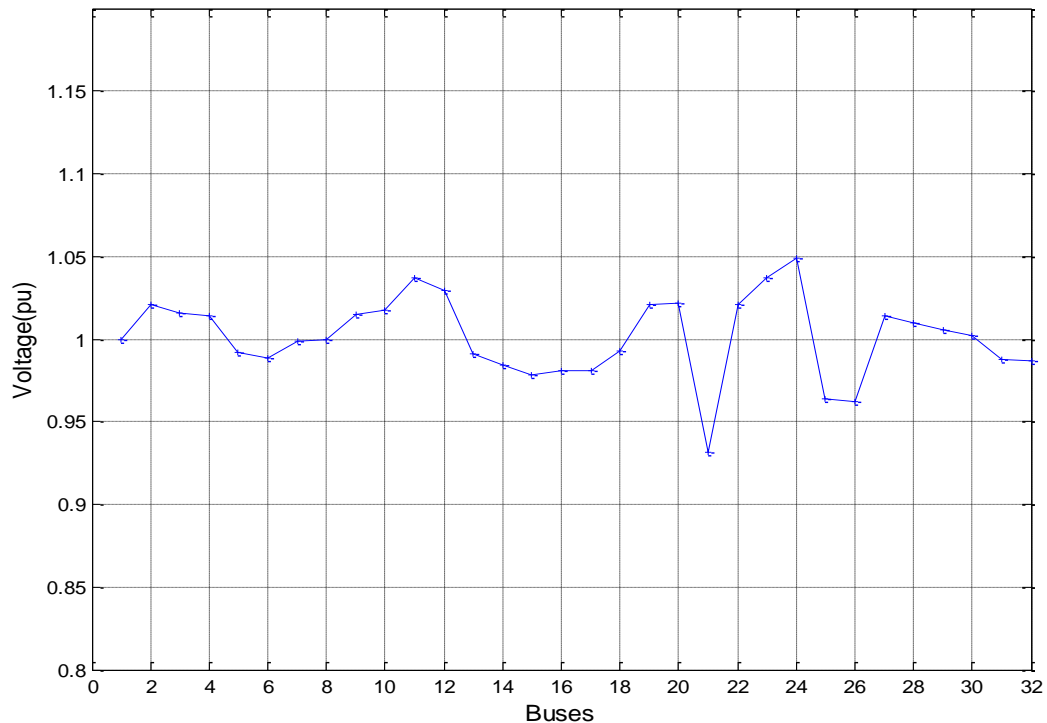


Figure 6.14. Voltage profile of strengthened grid

Rated wind power, $P = 10.1018\text{MW}$ was integrated to the strengthened grid. The voltage profile in Figure 6.15 reflects the review represented by Figure 2.14 where the voltage with wind energy is higher than the nominal voltage with some voltages that were originally within limits exceeding the higher limit as the blue line in Figure 2.15.

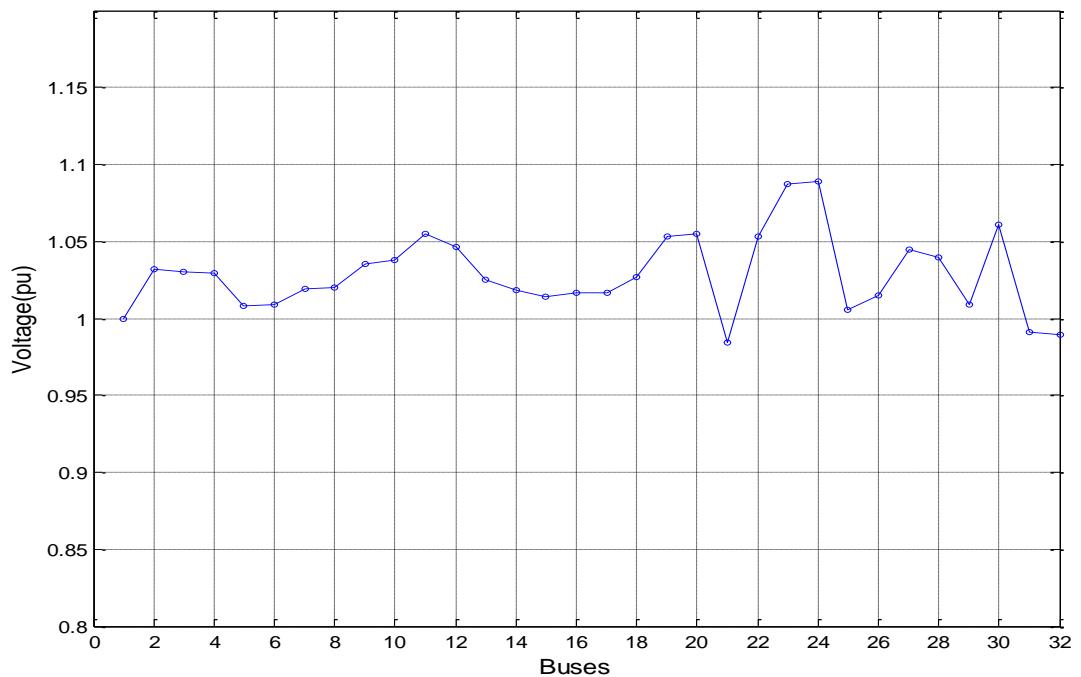


Figure 6.15. Voltage profile of strengthened grid with wind power ($P = 10.1018\text{MW}$)

6.11 Characterization of wind turbines

Configurations of wind turbines depend on manufacturers' specifications and point to the fact that power quality is likely to vary from one wind turbine to another. The following parameters are relevant for characterising the power quality of a wind turbine [141]:

- Wind turbine data (rated data)
- Flicker (Continuous operation, switching operations)
- Harmonics and Current distortions ($< 9\text{kHz}$)
- Response to voltage dips

- Active power characteristics (maximum output, ramp rate limitation and set-point control)
- Reactive power characteristics (reactive power capabilities and set-point control).
- Grid protection (tripping levels of over/under voltage magnitude and frequency)
- Reconnection time
- Induction generator coupled to the grid

6.12 Options to Enable More Wind Power in a Weak Grid

Literature generally agrees with the methods for increasing the capacity of a grid to absorb wind energy namely:

- Erecting new lines
- Curtailment or dissipation of the excess of wind energy,
- Use of energy storage systems to absorb the power unbalances.
- exporting the excess of wind to neighbour systems
- Introduction of load management.
- Voltage dependent disconnection of wind turbines
- Voltage dependent wind power production

Each of these methods has its challenges. Impedance is a single most important factor in determining whether a grid is weak or stiff. Reinforcing the grid by installing new lines in parallel with existing ones increases the cross section of the conductors which consequently reduces the impedance of the line. Low impedance means higher short circuit ratio S_k/S_w . But grid reinforcement is expensive compared to other methods. For the Nigerian case, this is not an option because grid reinforcement, even without wind energy, has been long overdue and steps are already being taken in this direction. Other methods of increasing its capacity to absorb wind power can only be effective after this.

Higher wind power is usually available in periods of lower demand and this creates constraints in the operation of a power system such as unbalances between generation and demand [142]. Power unbalance creates stability issues in normal power system operation and is therefore undesirable. Energy storage and control system is provided for wind energy to maintain the voltage level by absorbing extra wind energy. This reduces or evens out the power fluctuations and makes it possible to increase amount of wind energy integrated into the grid. Energy storage strategy reduces the wind energy curtailment and consequent waste of generated energy from wind. Curtailment of wind energy downplays the purpose of using green energy in the first place. Exporting excess wind energy has proved to be the best in reducing waste of electricity from wind energy [143]. Wind power forecast error can limit the exportation of excess wind power but forecast error becomes insignificant when compared to the benefits of international exchange [144].

6.13 Other Strategies for Increasing Wind Energy in the Grid and Application to Nigeria

Characteristics of wind power electricity in the grid are still being investigated for proper understanding and new strategies that could increase the capacity of a grid to absorb wind energy electricity are being developed. Some of the strategies proposed are discussed below.

6.13.1 *Getting Organized*

Research has shown that whole-systems approach in the integration of renewable into the existing system would deliver significant savings rather than the piecemeal methods currently being adopted [145]. Wind farms are just being installed in Nigeria and can be viewed as the right time because the whole system is being upgraded. The whole system can be organized to save cost and forestall some of the negative consequences of wind integration. In view of the level of generation and the number of transmission lines, any significant upgrade that can meet the present electrical power demand of the populace is

akin to installation of a new power system. Determination of the right PCC, the level of renewables to be integrated and at what levels they should be integrated (transmission or distribution levels) would greatly reduce cost and deliver a network that would run smoothly.

6.13.2 *Combining Wind Farm and Solar Energy*

According to research reported in [142], when wind farm and solar energy are combined in a grid, solar power smoothed the power over the year. The levels of solar power that would give this smoothing effect in a system may need to be determined in order to experience the benefits. Nigeria is blessed with abundant solar energy and could therefore benefit from such a combination.

6.13.3 *Application of Supernode to Nigeria power system*

A lot has changed in the production and utilization stages of the power system with new generation methods and loads being added to the contemporary power system. This has raised the need for the supernode method for harnessing power sources. A supernode is defined as “a hybrid system, which uses an islanded AC network to provide collection and routing of power on the supergrid.” [146]. A supernode acts as a pool for collecting abundant energy and from here the electrical power is transmitted to power systems outside the region or for transmission within the same network. It facilitates the sharing of energy among collaborating countries as is done between Britain and Germany [147].

The supernode concept is illustrated in Figure 6.16 where wind farms are connected radially to the main station containing multiple high voltage direct current (HVDC) converters [147, 148]. AC transmission is associated with high losses and so for the very long distances involved, transmission of the received power is done by HVDC technology.

Integrating many generating units with varied characteristics into an existing system raises the need for a robust system of control. For example, apart from the big wind

farms, distributed generation (DG) may comprise small wind farms, solar PV's, small hydro, etc. A central control point, (which Nigeria practiced), would have been the answer but this is difficult because of the varied nature of the generations being connected [149]. In the reference, the supernode is proffered as the solution to coordinate the functions of different power installations.

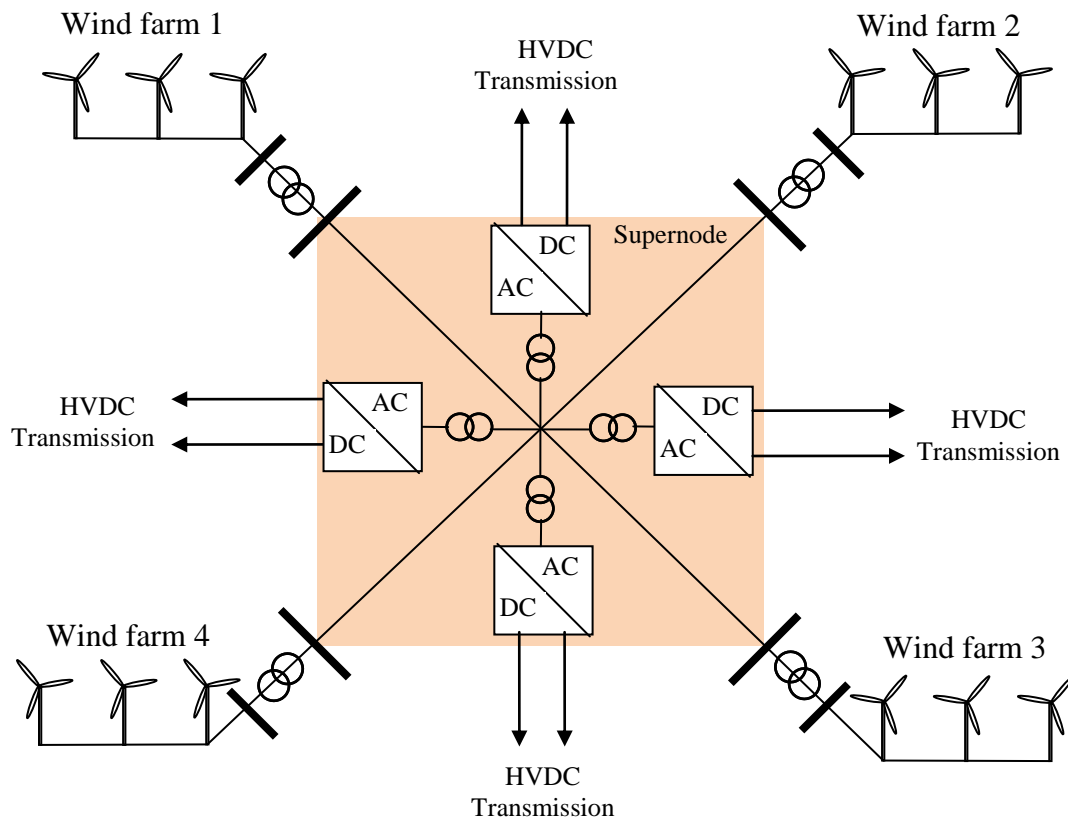


Figure 6.16. Supernode concept for wind farms

Though technical limits are often not an important factor in determining the level of wind energy to be integrated, the Nigeria power system is different because of the present state of the system which is overloaded and subject to voltage collapse. Transporting electricity from point of generation directly to point of utilization is inefficient and impacts on the reliability of the system [150]. Application of the concept to the Nigeria system would reduce the high losses associated with the present grid and consequently conserve the scarce energy. Also, because the supernode utilizes a web design with

integrated AC/DC systems, if there is a loss of a transmission line, the electricity it was supposed to transport can be re-routed to points of demand.

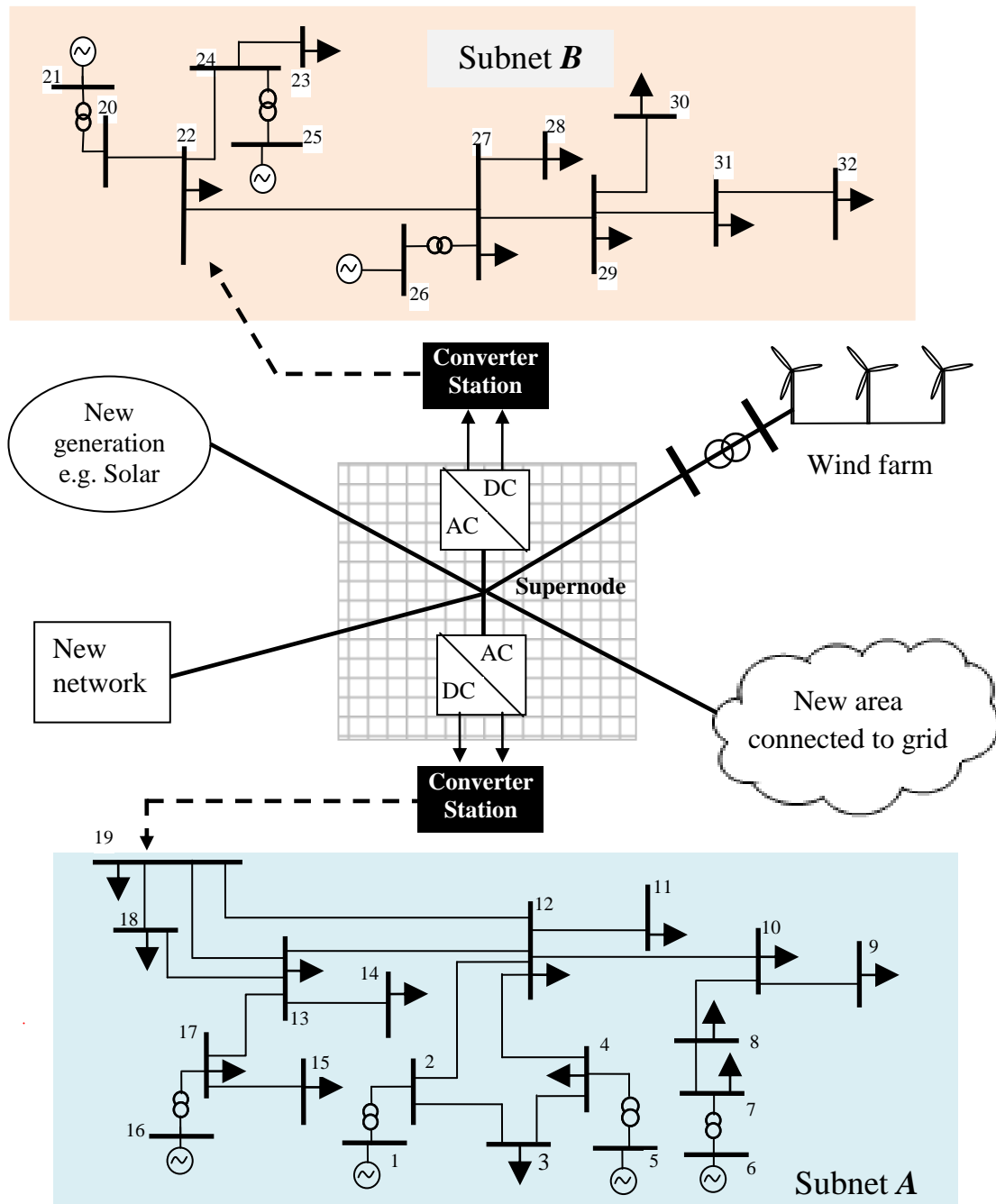


Figure 6.17. Application of supernode concept proposed for the Nigerian System

A supernode network on the grid takes voltage levels into consideration [149] and therefore fits into the transmission and distribution system arrangement which would be beneficial to Nigeria. Its utilization described in Figure 6.17 shows that other systems like wind farms, new network, etc, can also constitute subnetworks, apart from subnets *A* and *B* and all can be analysed using the SVUD.

6.14 Summary

This chapter has presented the analysis of the Nigeria 330kV network into which wind energy is integrated using the SVUD. The rated power of the Katsina wind farm was integrated before increased amounts were integrated. When rated wind power produced very little change in voltage, especially at the buses close to the PCC. The lack of appreciable difference in the voltage profile is due to the low level of wind power. Increased levels of wind energy increased voltage variation. The wind integration raised the voltages of the buses that were below acceptable limit thereby improving the voltage profile. This could be attributed to the fact that the generation capacity of the grid is insufficient and the wind farm serves as an extra generation capacity. An attempt was made to strengthen the present grid and the result was a much improved voltage profile. Integrating wind energy into this improved grid showed a characteristic associated with wind energy in strong grids which is voltage violating upper limits.

Various strategies for increasing wind power in a grid are discussed and reinforcement which is usually one of the last strategies due to the high cost involved is not an option for the Nigeria grid. Reinforcement of the grid is long overdue and other strategies can be effective after this.

The use of SVUD in the analysis is peculiar in that the effect of the wind power on the parts close to the PCC could be determined and at the same time with other parts as mentioned in chapter 5. The benefits provided by SVUD analysis could also help to plan the location of ancillary services in large systems because it does not only give information about the vicinity of the PCC but also the whole system.

A supernode concept is proffered in section 6.13 as a solution to the Nigerian power challenge. Instead of analysing individual systems in isolation, the supernode here forms a natural point of tear where SVUD can be used to determine the effects of the different networks working together and at the same time provide solid control of the system.

7 CONCLUSIONS AND RECOMMENDATIONS

7.1 Introduction

The volume of work done on the research topic ‘diakoptics’ by past and present researchers have shown how important this tool is, with the potential to provide the answers needed for less tasking analysis of the ever expanding power system. While load flow technique has remained the most used and probably the most important tool in the steady-state power system analysis, incorporating the virtues of diakoptics into the load flow analysis would further enhance its quality and this thesis work is presenting a contribution in this direction.

In diakoptics, a system is first torn into independent subnetworks which can be solved separately to obtain partial solutions of the network as demonstrated with the simple network in section 2.3. The partial solutions are then interconnected by a set of transformations to yield the solution of the whole system as if it were solved as a complete problem. It was discovered in the course of this work that, apart from a few good practices by other researchers, [5, 7, 13] methods of determining the best guidelines for tearing are actually heuristic. It is also important to note that the equal sizes of subnetworks do not always guarantee the best solution for whole nonlinear system analysis.

Various diakoptic methods proposed by other researchers were employed in the analysis of networks. A lot of methods were found to be applicable only for linear or linearized system analyses. For example, the linear *current-voltage* (IV) flow equations can be used instead of the traditional *power-voltage* (SV) flow equations which are the nonlinear quadratic type. In this work, two methods of power system analysis based on diakoptics have been proposed – the *Branch Voltage Multiplier technique* (BVMT) and the *Slack Bus Voltage Update Diakoptics* (SVUD) load flow tool.

Based on present study, the BVMT is found to be suitable for **IV** flow equation while SVUD is for **SV** flow equations. These two tools were employed in the analyses of a number of benchmark networks including IEEE 14-bus and 30-bus test systems. The accuracy and effectiveness of the algorithms were tested by comparing the results with those obtained from centralized load flow methods namely, conventional Gauss-Seidel and Newton-Raphson methods. Results were found to be the same as that of the linear system and also very close to the load flow iterative cases. Iterative procedures generally involve the solution of nonlinear systems which like many nonlinear problems do not give clear-cut-results [85, 86], and the SVUD is not an exception.

Since the major challenge in the wind power integration to weak grids is the change in steady-state voltage level, the SVUD provides an important tool for the determination of the voltage level of such grids and this method has been applied in the Nigeria 330kV transmission network with and without wind power input.

In view of the above, the main conclusions of this work are summarized in the contributions and possible further investigations below.

7.2 Contributions

The main contributions of this thesis are:

1. ***The Branch Voltage Multiplier Technique (BVMT) suitable for linear system analysis***

The BVMT proposes a simpler process of obtaining the equation of solution and the branch voltage e_b in diakoptics. When a branch or a line is removed to tear a network, an open circuit hypothetically exists and therefore current is not flowing in the removed branch. But this branch current is crucial in diakoptic analyses to obtain the complete solution of a network and is usually obtained from branch voltage in a long process.

Other works studied on diakoptic analysis of electrical power systems showed that the major difference in the methods is in the procedure for deriving the equation of solution.

These procedures are quite laborious. In the BVMT, the equation of solution is obtained directly by applying the technique of inversion of partitioned matrices to the BBD matrix of the network. Analysis of the inverted BBD matrix produced the complete solution of the network, even when the subnetworks are solved individually. This is much easier than the ones proposed in the original diakoptics and especially in references [3, 4, 7].

When BVMT was applied to AC power system analysis based on current injection formulation, the same results were obtained as the one piece solution. In the current injection formulation the flow equations are based on current (I) and voltage (V) with the resultant flow equation, $I=YV$ which is a linear system, rather than power (S) and voltage (V) flow equations.

2. Devising a method of obtaining removed branches voltages which is very simple and straightforward

The method of obtaining branch voltages was discovered experimentally and was later proved mathematically. The branch current, as explained above, is a key factor in diakoptic analysis and it is usually calculated from the branch voltage, e_b in complicated algebra. In this method, the load flow is first performed on the independent subnetworks without coupling with other subnetworks. The derived bus voltages are then utilized for direct computation of the branch voltage based on voltage difference between boundary buses. With this simple method of obtaining the branch voltage, the equation of e_b is suitable for IV load flow and is easy to incorporate directly into iterative load flow solutions. This was particularly advantageous in the SVUD load flow analysis and clarifies its application in reference [43].

3. Development of Slack Voltage Update Diakoptic (SVUD) load flow which is a novel analysis tool for power networks

A new algorithm SVUD has been proposed which is easy to incorporate in the existing load flow programmes. It involves the correction of computed voltages of the subsystems and updating of temporary slack bus voltages to reflect the solution of the whole nonlinear system as a piece.

Load flow analyses are usually based on power injections which are generally nonlinear and gives the nonlinear power flow equation, $F(x) = 0$. In the SVUD load flow, the diakoptic equations obtained in the BVMT formulation is more suitable for linear analysis but these equations were extended to suit nonlinear load flow applications. The developed equations were then embedded in Gauss-Seidel for iterative solutions.

The slack bus does not exist in real systems but plays a very important role in load flow analysis to supply or absorb transmission losses which are unknown until the final solution is obtained. For this reason the choice of a slack bus could affect the convergence of a load flow solution and this was obvious when choosing slack buses in subnetworks that do not contain the original slack bus. In centralized load flow analysis, a single slack bus with known voltage is required and this voltage is not evaluated during the load flow process but complex voltages of the generator and load buses vary during the iterative process. Slack buses of subnetworks that do not contain the main slack bus are selected from these generator and load buses. When conducting load flow of individual subnetworks the voltages of these temporary slack buses also remain constant. The novelty is to make these temporary slack buses behave as if they were in centralized analyses, their voltages are made to 'vary' during iteration by updating their values. This is done by using the mismatch between scheduled and calculated powers at those buses. This is a peculiar feature of this new tool hence it is called slack voltage updating diakoptic (SVUD) load flow.

4. Performing SVUD load flow analysis with an in-house computer programme developed to also update the slack buses voltages automatically

Sequential and parallel computing procedures for the SVUD load flow are presented in flow charts in section 3.6. Building on and extending the available MATLAB codes, a computer programme was produced to implement the tool. With this programme, all that was required was to plug in the data of any test system to be analysed. Lines of tear were chosen before load flow and these were input at the prompting of the computer programme. Slack bus or buses were chosen out of the displayed data for the subnetworks. If a subnetwork contains the original slack bus for the whole system this would be chosen for that subnetwork. Slack buses of other subnetworks were chosen by

discretion. After this, the bus voltages would be computed. Lines of tear could also be done automatically by the programme, but as the number of buses increased the computation time became very large as shown in section 4.7. Manually choosing lines of tear based on the topology of the system was a better option and was much faster.

4. Implementation of the SVUD load flow analysis on test systems for the determination of bus voltages

The proposed SVUD load flow method was employed in the solution of test networks including the IEEE 14-bus and 30-bus systems and the results were compared with results from centralized classical G-S analysis, and Newton-Raphson in certain instances. The numerical results, plots and the voltage mean square errors computed against the centralized analyses have shown the viability of the new tool.

The number of iterations that ensures convergence with the proposed algorithm was found to be less than those with classical G-S in all the test systems used. In one instance with the 14-bus network, iterations with SVUD were 5 while those of the classical G-S were 106. Another advantage of the SVUD is that of a likely saving in developing software for real time systems because it incorporates an established load flow analysis method. It is expected that the cost of designing and acquiring a commercial software would be quite lower than for a tool that does not have any element of existing software and need to be designed from scratch.

The major advantages of classical G-S load flow are its simplicity, small computer memory requirement and less computational time per iteration. These advantages faded mainly because of the need to analyse large systems for which G-S was found to be impracticable. This is because its rate of convergence depends largely on the number of buses in a network. The proposed SVUD ‘reduces’ the size of the network to solve by subdivision into independent parts and at the same time simulates a one-piece load flow analysis using only one slack bus. It is hoped that this work will bring G-S back to the forefront of load flow analysis tools.

5. *SVUD load flow determination of the voltage profile of the Nigeria 330kV transmission network using.*

The proposed SVUD load flow method was employed in the determination of the voltage profile of the Nigeria 330kV transmission network and this gave a snapshot of the state of the grid. The results show a number of violations of the voltage limits of the network by large margins especially in the north where the feeders are long. At bus 32, the voltage was so low that it could be termed a voltage collapse based on the definition of voltage collapse in section 5.7 and the grid can also be classified as a weak based on the general definition of a weak grid.

6. *Verifying the suitability of the Nigerian grid for wind energy integration based on voltage variation by applying the SVUD load flow method.*

Nigeria has just installed its first wind farm and higher levels of electricity from wind are expected in future. Searches conducted did not reveal any literature that applies diakoptic analysis to wind power integrated network. Diakoptics in form of the SVUD had been employed for the purpose of determining suitable points for connecting the new wind farm at Katsina to the grid and the level of wind power that the system can safely accommodate with the present state of the grid. Conclusions were based on voltage variations at the different PCC's tested and the surrounding buses when wind energy was integrated. Level of wind power was increased and voltage changes increased as the wind power increased. Different PCC's exhibited different changes in voltage. PCC's close to generating stations have lower voltage changes. Voltage change was observed at each PCC which is expected in a weak grid, but in this case the voltage profile improved because one of the major challenges of the Nigerian grid is insufficient generation capacity. The wind farm served to boost the generation capacity.

7.3 Recommendations and Further Work

The SVUD load flow has been proved to be an important tool in the analysis of power systems with the ability to handle more data and utilize less computer memory at a time. The SVUD retains the nonlinearity of the power flow equations, $F(x) = 0$ and therefore

could easily fit into the present load flow packages. The number of iterations of the G-S load flow has been successfully reduced in the SVUD load flow. However, there are areas pending to be investigated further in order to maximize the benefits of the SVUD such as:

1. *Reduction of communication between subnetworks and improved computer application during the SVUD load flow analysis*

In the SVUD analysis, significant communication goes on between subnetworks in transferring data to the central algorithm and then to the subnetworks during iterations. This causes latency and increases the overall solution time. Reducing communication between subnetworks will speed up the solution process and increase the overall efficiency of the tool.

A dual-core PC was used in the computations; computers with higher memories or parallel computers could also improve the solution time. Apart from MATLAB, other computer programming languages could be explored for the analysis.

2. *Tearing a network at the right points in order to obtain the best solution*

It was discovered in the course of this work that a system has to be torn in the right places for SVUD load flow to converge. Convergence of iterative solutions generally depends on the nature of the system and when a system is torn, one of the subnetworks may be ill-conditioned and this affects the overall convergence of the SVUD load flow. Also, even when convergence was achieved, it was discovered that certain points of tear gave results closer to centralized analyses than some other points. Though choosing points of tear a sensitive factor in diakoptics, further work is required to discover the likely causes and how to choose the points of tear.

Automatic tearing of the network could be the best if a number of factors are taken into consideration like the location of generator buses but computer programme developed in this work seeks to separate the network into equal parts or as close as possible in the case of odd number of buses. With this programme, as the number of buses increased

automatic tearing time increased considerably and with the 30-bus it was no longer feasible. A computer programme that can tear the network automatically within a short time would enhance the analysis and reduce the labour of manual selection of lines to remove.

3. Choice of slack buses in subnetworks without the original slack bus

It is generally known that the choice of a slack bus affects the convergence of load flow and even the results [151]. In this work, slack buses for subnetworks were chosen by discretion, and in some instances convergence was not achieved until the ‘right’ buses were chosen. Participation factors proposed in [152] is intended to reflect the important characteristics of a system which include network parameters, load, and generators locations and capacities. Choosing subnetworks slack buses based on participation factors and the principle of distributed slack could enhance the solution process and should be investigated.

4. Embedding the devised diakoptic algorithms in direct methods of load flow analysis instead of iterative procedures

The iterative procedure is a special form of ‘trial and error’ computation and therefore gives erroneous results in some instances. The traditional or familiar load flow methods are based on the general-purpose iterative procedures and usually have multiple solutions with only one of them corresponding to the real operative state of the electrical system. A reliable load flow method which does not involve iteration should be explored as it would maximize the merits of diakoptics. The proposed Holomorphic Embedding load flow method presented in [85] is a direct method of analysis and the devised diakoptic algorithm could be embedded in it. Since diakoptics is best suited to linear systems, a direct method of analysis of nonlinear systems may deliver better results.

5. SVUD Load flow analysis by Mesh current method

The connecting elements of an electrical network are composed of nodes, branches and meshes. In a network if B is the number of branches, N is the number of nodes, and M is

the number of meshes, the fundamental topological equation in network analysis [153] can be written as

$$M+N-1 = B \quad (7.1)$$

In power systems analysis two systems of equations are generally encountered - the nodal voltage equations and the mesh current equations; any of these systems can be solved, to determine the unknown values. The likely choice of solution should therefore be the system of equations with less number of variables. Equation (7.1) gives the clue for the choice. If $M > N-1$, then the nodal equations are less, if $M < N-1$, the mesh equations are less [153]. In most practical cases, the latter case is more common.

Iterative procedures are currently applied in the solution of nodal equations and the number of iterations usually runs into thousands to reach values with the desired precision. If mesh equations are solved in load flow analysis rather than nodal equations, a solution method could be devised which eliminates the need for large numbers of iterations. Diakoptics for mesh analysis has formulated in reference [154] been applied to small systems in [23, 155]. The performance of SVUD load flow analysis using mesh analysis could therefore be explored.

In addition to the areas for further investigations, the following are recommended for the Nigeria system.

6. *Strengthening the Nigeria power network for better delivery of power and ability to accommodate high electricity from wind.*

The voltage violations recorded in the analysis of the Nigeria 330kV network reflects the urgent need for appropriate measures to improve the grid. Also, a number of measures exist to increase the capacity of a grid to accommodate large wind power. Grid reinforcement is usually a last option because it is expensive, but in the Nigeria this is not an option. The grid has to be reinforced if the system is to deliver quality power with and without wind. Other measures would only be effective after this.

7. Application of supernode concept in the transmission of power in Nigeria.

Alternating current (AC) transmission is associated with high losses. High voltage direct current (HVDC) technology combined with AC reduces losses. This is realised in the supernode concept explained in section 6.13 and should be considered in the Nigeria system to reduce losses associated with the present grid.

With the deregulation of the Nigeria power system, generating power into a pool is to be done away with. However, the different energy providers can act like different countries, for example, Britain and Germany, and employ the supernode technology in harnessing wind energy resources and in the delivery of energy to consumers.

7.4 Summary

This research was carried out with the intent of contributing to analysis tools geared to reduce computation burden in power system analysis. The diakoptic tools devised in this research are based on well-proven electrical engineering and mathematical procedures. With computer-aided analyses the devised tools were tested on a number of benchmark networks and the results proved the validity of the tools.

The SVUD was used to analyse the Nigeria 330kV transmission network with and without wind integration. Since the steady-state voltage level is the key factor in weak grids, the focus was on the determination of bus voltages and how they change with varying levels of wind in the Nigeria network. In summary, this research has come up with analysis methods BVMT and especially, the SVUD load flow that could shape the future of power system analyses.

REFERENCES

- [1] M. R. Patel, *Wind and Solar Power Systems, Design, Analysis, and Operation*, Taylor & Francis Group, 2006.
- [2] T. Burton, N. Jenkins, D. Sharpe and E. Bossanyi,, *Wind Energy Handbook*, 2nd Edition, Wiley, 2011., Wiley, 2011.
- [3] G. Kron, “A method to solve very large physical systems in easy stages,” *Circuit Theory, IRE Transactions on*, vol. 2, no. 1, p. 71–90, 1953.
- [4] H. H. Happ, “Z Diakoptics – Torn Subdivision Radially Attached,” *IEEE Trans. Power Apparatus and Systems*, vol. 86, no. 6, pp. 751-769, 1967.
- [5] H. H. Happ, “Diakoptics and Piecewise Methods,” *IEEE Trans. Power Apparatus and Systems*, , vol. 86, no. 6, pp. 1373-1382, 1970..
- [6] H. H. Happ, “Diakoptics – The Solution of System Problems by Tearing,” *Proc. of IEEE*,, vol. 62, no. 7, pp. 930-940, 1974.
- [7] G. Kron, *Diakoptics: The Piecewise Solution of Large Scale Systems*, London: Macdonald & Co, 1963.
- [8] H. H. Happ, “Z-Diakoptics-torn subdivisions radially attached.,” *Power Apparatus and Systems, IEEE Transactions*, vol. 6, pp. 751-769, 1967.
- [9] S. Esmaili and S.M. Kouhsari , “A Distributed Simulation Based Approach for Detailed and Decentralized Power System Transient Stability Analysis,” *Electric Power Systems Research, Elsevier* , vol. 77, p. 673–684 , 2007.
- [10] J. R. Marti, L. R. Linares, J. A. Hollman and F. A. Moreir, “OVNI: Integrated Software/hardware Solution for Real-Time Simulation of Large Power Systems,” in *Conference Proc. of 14th Power Systems Computation Conference PSCC02*, Sevilla, Spain, 2002.

- [11] V. Lattarulo and F. Amoruso, "Diakoptic Approach to EMC Problems Involving the Human Body", *Electromagnetic Compatibility in Power Systems*, in *Electromagnetic Compatibility in Power Systems*, Oxford, Elsevier, 2007, pp. 133-164.
- [12] A. Klos, "What is Diakoptics?," *International Journal of Electrical Power and Energy Systems*, vol. 4, pp. 192-195, 1982.
- [13] A. Brameller, M. N. John and M. R. Scott, *Practical Diakoptics for Electrical Networks*, Chapman and Hall Ltd, 1969.
- [14] M. Ramamoorthy and B. J. Seshaprasad, "An Improved Method for Load Flow Studies of Large Power Systems," *IEE-IERE Proc*, vol. 9, no. 3, pp. 93-101, 1971.
- [15] G. N. Stenbakken. and J. A. Starzyk , "Diakoptics and Large Change Sensitivity Analysis," *IEEE Proc.* , vol. 139, no. 1, pp. 114-118, 1992.
- [16] A. Kalantari and S. M. Kouhsari, "An Exact Piecewise Method for Fault Studies in Interconnected Networks," *Electrical Power and Energy Systems*, vol. 30, p. 216–225, 2008.
- [17] R. Braae, *Matrix Algebra for Electrical Engineers*, I. Pitman, 1963.
- [18] N. Schorghofer, *The Third Branch of Physics-Essays on Scientific Computing*, 2005.
- [19] O. Tuncel, H. F. Bueckner and B. Koplik, "An Application of Diakoptics in the Determination of Turbine Bucket Frequencies by the Use of Perturbations," *Journal of Manufacturing Science and Engineering*, vol. 91, no. 4, pp. 1029-1034, 1969.
- [20] G.E. Howard and Y. L.Chow, "Diakoptic theory for microstripline structures," *In Antennas and Propagation Society International Symposium, AP-S. Merging Technologies for the 90's. Digest, IEEE*, pp. 1079-1082, 1990.

- [21] C. J. Sin and L. K. Goodman, "DC railway power network solutions by diakoptics," *In Railroad Conference, 1994., Proce ASME/IEEE Joint (in Conjunction with Area 1994 Annual Technical Conference), IEEE*, pp. 103-110, 1994.
- [22] S. H. Lui, "Domain decomposition methods for eigenvalue problems," *Journal of Computational and Applied Mathematics*, vol. 117, no. 1, pp. 17-34, 2000.
- [23] A. Brameller and K. L. Lo, "The application of diakoptics and the escalator method to the solution of very large eigenvalue problems," *International journal for Numerical Methods in Engineering*, vol. 2, no. 4, pp. 535-549, 1970.
- [24] S. Theja and H. Narayanan, "On the notion of generalized minor in topological network theory and matroids," *Linear Algebra and its Applications*, vol. 458, pp. 1-46, 2014.
- [25] K. C. Gupta, "Emerging trends in millimeter-wave CAD," *IEEE Transactions on Microwave Theory and Techniques*, vol. 46, no. 6, pp. 747-755, 1998.
- [26] K. Sung and Z. Chen, "A new SCN-based frequency-domain TLM node and its applications with the diakoptic method," *In Microwave Symposium, 2007. IEEE/MTT-S International. IEEE.*, pp. 277-280, 2007.
- [27] P. B. Johns, "Use of condensed and symmetrical TLM nodes in computer-aided electromagnetic design," *In IEE Proceedings H (Microwaves, Antennas and Propagation, IET Digital Library)*, vol. 133, no. 5, pp. 368-374, 1986.
- [28] K. Diao, Z. Wang, G. Burger, C. Chen, W. Rauch, and Y. Zhou, "Speedup of water distribution simulation by domain decomposition," *Environmental Modelling & Software*, vol. 52, pp. 253-263, 2014.
- [29] M. M. Chaabane, R. Plateaux, J. Choley, C. Karra, A. Rivière and M. Haddar, "Topological approach to solve frame structures using topological collections and transformations," *Comptes Rendus Mécanique*, vol. 342, no. 8, pp. 466-477, 2014.

- [30] S. Weng, Y. Xia, Y. Xu and H. Zhu, "An iterative substructuring approach to the calculation of eigensolution and eigensensitivity," *Journal of Sound and Vibration*, vol. 330, no. 14, pp. 3368-3380, 2011.
- [31] P. W. Aitchison, "Diakoptics as a General Approach in Engineering," *Journal of Engineering Mathematics*, vol. 21, p. 47 – 58, 1987.
- [32] A. Koochaki and S. M. Kouhsari, "Detailed Simulation of Transformer Internal Fault on Power System by Diakoptical Concept," *Advances in Electrical and Computer Engineering*, vol. 10, no. 3, 2010.
- [33] F. A. Moreira and L. C. Zanetta Jr, "Solution Method Based on the Theory of Diakoptics for an Efficient Time-Domain Transients Simulation of HVDC Converters," *IEEE/PES Transmission and Distribution Conference & Exposition: Latin America*, pp. 349-352, 2004..
- [34] M. El-Marsafawy, "Solution of Power Flow Outage Problems Using Diakoptics and Compensation," *JKAU: Eng. Science.*, vol. 8, pp. 3-20, 1996..
- [35] G. N. Korres, A. Tzavellas, E. Galinas, "A distributed implementation of multi-area power system state estimation on a cluster of computers," *Electric Power Systems Research*, vol. 102, pp. 20-32, 2013.
- [36] W. Jiang, V. Vittal, and G. T. Heydt, "Diakoptic State Estimation Using Phasor Measurement Units," *IEEE Transactions On Power Systems*, vol. 23, no. 4, pp. 1580-1589., 2008.
- [37] A. Gómez-Expósito, A. Jaén, C. Gómez-Quiles, P. Rousseaux, T. V. Cutsem, "A taxonomy of multi-area state estimation methods," *Electric Power Systems Research*, vol. 81, no. 4, pp. 1060-1069, 2011.
- [38] R. G. Andretich, H. E. Brown, H.H. Happ, and D. H. Hansen, "Piecewise Load Flow Solutions of Very Large Size Networks," *IEEE Summer Power Meeting and EHV Conference, Los Angeles, Calif.*, vol. 3, pp. 950-961, July 1970..
- [39] H. E. Brown, G. K. Carter, H.H. Happ and C. E. Person, "Power Flow Solution by

- Impedance Matrix Iterative Method,” *Power Apparatus and Systems, IEEE Transactions*, vol. 82, no. 65, pp. 1-10, 1963.
- [40] H. K. Kesavan, M. A. Pai, M. V. Bhat, “Piecewise Solution of The Load-Flow Problem,” *IEEE Transactions on Power Apparatus and Systems*, vol. 4, pp. 1382-1386, 1972.
- [41] J. Cai and N. Mitra, “Analytics for Steady State Operation of Autonomous Microgrids, p1-5,” *In Power and Energy Society General Meeting, 2012 IEEE*, pp. 1-5, 2012.
- [42] A. Kalantari, S. M. Kouhsari, and H. Rastegar, “Piecewise Fast Decoupled Load Flow Using Large Change Sensitivity,” *IEEE Power Engineering Society General Meeting*, vol. 2, p. 957– 961, 2003..
- [43] R. G. Andretich, H. E., Brown, H.H. Happ, and C. E. Person, “The Piecewise Solution of the Impedance Matrix Load Flow,” *IEEE Trans. on PAS*, vol. 87, no. 10, pp. 1877-1882, 1968.
- [44] L. Freris and D. Infield, , *Renewable Energy in Power Systems*, , Publication,, John Wiley & Sons, Ltd, 2008, p171-172..
- [45] H. Bindner, “Power Control for Wind Turbines in Weak Grids: Concepts Development,” Risø-R-1118(EN), Risø National Laboratory, Roskilde, 1999.
- [46] J. Soens, J. Driesen and R. Belmans, “Interaction between Electrical Grid Phenomena and the Wind Turbine's Behaviour,” *Proceedings of ISMA*, pp. 3969-3988, 2004.
- [47] G. O. Suvire and P. E. Mercado. ed: A. V., “Dynamic Modelling of a Wind Farm and Analysis of Its Impact on a Weak Power System,” in *Dynamic Modelling Book*, 2010, pp. 189-208..
- [48] R. A. Rohrer, “Circuit Partitioning Simplified,” *IEEE Trans. on Circuits and Systems*, vol. 35, no. 1, pp. 2-5, 1988.

- [49] L. Roy, "Piecewise Solution of Large Electrical Systems by Nodal Admittance Matrix," *Power Apparatus and Systems, IEEE Transactions*, vol. 4, pp. 1386-1396, 1972.
- [50] N. Sato and W. F. Tinney, "Techniques for Exploiting the Sparsity of the Network Admittance Matrix," *Power Apparatus and Systems, IEEE Trans.*, vol. 82, no. 69, pp. 944-950, 1963.
- [51] J. Black, "Utilizing HELM™ for Advanced Grid Management and Planning," 2012. [Online]. Available: http://energytech2012.org/wp-content/uploads/2012/05/W-S1-D-Battelle_EnergyTech2012_HELM_JBlack.pdf. [Accessed 15 January 2012].
- [52] S. Amari, "Information-theoretical foundations of diakoptics and codiakoptics,," *RAAG Memoirs*, vol. 3, pp. 351-371, 1962. .
- [53] T. Ohtsuki, Y. Ishizaki and H. Watanabe, "Topological degrees of freedom and mixed analysis of electrical networks," *IEEE Trans. on Circuit Theory*, Vols. CT-17, pp. 491-499, 1970. .
- [54] E. C. Ogbuobiri, W. F. Tinney, and J. E. Walker, "Sparsity-directed decomposition for Gaussian elimination on matrices," *IEEE Trans. on Power, Apparatus and Systems*, Vols. PAS-89, pp. 141-150, 1970.
- [55] J. Mitra and N. Cai, "Distributed Analytics for Steady State Operation of Autonomous Microgrids," *In Power and Energy Society General Meeting, IEEE*, pp. 1-5, 2012 IEEE.
- [56] R. B. Shipley, A. K. Ayoub, and D. W. Coleman, "Bus Admittance Tearing and the Partial Inverse," *Power Apparatus and Systems, IEEE Transactions* , vol. 5, pp. 2042-2048, 1972.
- [57] H. Elmqvist, and M. Otter, "Methods for tearing systems of equations in object-oriented modeling. In Proceedings ESM," vol. 94, pp. 1-3, 1994..
- [58] F. M. Uriarte, and Karen L. Butler-Purry., "Diakoptics in shipboard power system

- simulation,” *In Power Symposium, 2006. NAPS 2006. 38th North American*, pp. 201-210, 2006.
- [59] J. Vlach, K. Singhal, *Computer Methods for Circuit Analysis and Design*, New York: Van Nostrand Reinhold Company Inc., 1983.
- [60] M. A. Tomim, *Parallel Computation of Large Power System Networks Using the Multi-Area Thévenin Equivalents*, PhD Thesis , 2009.
- [61] M. A. Tomim, J. R. Marti, T. D. Rybel L. Wang and M. Yao,, “MATE Network Tearing Techniques for Multiprocessor Solution of Large Power System Networks,” *IEEE Power and Energy Society General Meeting*, pp. 1-6., 2010.
- [62] H. H. Happ, “Multicomputer Configurations and Diakoptics: Dispatch of Real Power in Power Pools,” *Power Apparatus and Systems, IEEE Transactions on*, vol. 5, pp. 764-772, 1969.
- [63] P. Sørensen, P. H. Madsen, A. Vikkelsø and K. K. Jensen, K.A. Fathima, A.K. Unnikrishnan and Z.V. Lakaparampil, “Power Quality and Integration of Wind Farms in Weak Grids in India,” Risø National Laboratory, Roskilde, 2000.
- [64] F. Santjer, G. J. Gerdes P. Christiansen and D. Milborrow, “Wind Turbine Grid Connection and Interaction,” ENERGIE, ENVIRONNEMENT ET DEVELOPEMENT DURABLE, Deutsches Windenergie-Institut GmbH Germany, Tech-wise A/S Denmark, DM Energy United Kingdom, Germany, 2001.
- [65] Z. Chen and F. Blaabjerg, “ Wind farm—A power source in future power systems,” *Renewable and Sustainable Energy Reviews*, vol. 13, no. 6, pp. 1288-1300., 2009.
- [66] R. Belhomme, S. White, N. Hatzargyriou, A. Tsikalakis, D. Lefebvre, T. Ranchin, F. fesquet, G. Arnold, S. Tselepis, A. Neris, T. Degner, and P. Tailor, “Distributed Generation on European islands and weak grids,” DISPOWER, Clamax Cedex, France, 2005.

- [67] E. T. Ackermann, *Wind Power in Power Systems*, Chichester, West Sussex , England: John Wiley & Sons, Ltd, 2005.
- [68] J. G. Slootweg, *Wind Power: Modelling and Impact on Power System Dynamics*, Ridderprint Offsetdrukkerij B.V: Ridderkerk, the Netherlands, 2003.
- [69] ENERGIE, “Wind Turbine Grid Connection and Interaction,” , ENVIRONNEMENT ET DEVELOPEMENT DURABLE, Deutsches Windenergie-Institut GmbH Germany, Tech-wise A/S Denmark, DM Energy United Kingdom, , United Kingdom, 2001.
- [70] N. G. Boulaxis, S. A. Papathanassiou, and M. P. Papadopoulos, “Wind turbine effect on the voltage profile of distribution networks,” *Renewable Energy*, vol. 25, no. 3, pp. 401-415., 2002.
- [71] R. Piwko, N. Miller, J. Sanchez-Gasca, X. Yuan, R. Dai, and J. Lyons, “Integrating Large Wind Farms into Weak Power Grids with Long Transmission Lines,” *IEEE/PES Transmission and Distribution Conference and Exhibition, Asia & Pacific, Dalion, China*, pp. 1-7, 2005.
- [72] IEEE Std 399-1990, *IEEE Recommended Practice for Industrial and Commercial Power Systems Analysis (ANSI)*, New York: Institute of Electrical and Electronics Engineers, Inc., 1990.
- [73] IEEE Std 399-1980, *IEEE Recommended Practice for Industrial and Commercial Power Systems Analysis (ANSI)*, Institute of Electrical and Electronics Engineers, Inc, 1980.
- [74] T. Gonen, *Electric Power Transmission System Engineering- Analysis and Design*, Canada: John Wiley and Sons, Inc., 1988.
- [75] J. J. Grainger, W. D. Stevenson, Jr., *Power System Analysis*, Singapore: McGraw-Hill, Inc, 1994.
- [76] P. Kundur, *Power system stability and Control* , p973, USA: McGraw-Hill, Inc, 1994.

- [77] IEEE, "IEEE Std. 519-1992. IEEE Recommended Practices and Requirements for Harmonic Control in Electrical Power Systems," 1992.
- [78] D. Hansen, "IEEE 519 Misapplications— Point of Common Coupling Issues," *IEEE PESGM Conversion and Delivery of Electrical Energy in the 21st Century*, pp. 1-3, 2008.
- [79] J. M. P. Pérez, F. P. G. Márquez, A. Tobias, M. Papaelias, "Wind turbine reliability analysis,," *Renewable and Sustainable Energy Reviews*, p. 463–472, 2013.
- [80] J. O. Tande, G. D. Marzio and K. Uhlen, "System Requirements for Wind Power Plants," SINTEF Energy Research, Trondheim, Norway, 2007..
- [81] B. Fox, D. Flynn, L. Bryans, N. Jenkins, D. Milborrow, M. O'Malley, R. Watson and O. Anaya-Lara, "Wind Power Integration Connection and System Operational Aspects," *IET Power Series 50, UK*,, vol. 50, pp. p56-75, 2007..
- [82] I. M. de Alegría, J. Andreu, J. L. Martín, P. Ibañez, J. L. Villate, and H. Camblong, "Connection requirements for wind farms: A survey on technical requierements and regulation.", *Renewable and Sustainable Energy Reviews*, vol. 11, no. 8, pp. 1858-1872, 2007.
- [83] X. Wang, Y. Song and M. Irving, *Modern Power Systems Analysis*, New York, USA: Springer Science+Business Media, LLC, 2008.
- [84] M. B. Cain, R. P. O'Neill, A. Castillo, "History of Optimal Power Flow and Formulations,Optimal Power Flow Paper 1," *FERC*, 2012.
- [85] A.Trias, "The Holomorphic Embedding Load Flow Method,," *IEEE PES General Meeting*, pp. 1-8., 2012.
- [86] M. Huneault and F. D. Galiana, "A Survey of the Optimal Power Flow Literature,," *IEEE Transactions on Power Systems*, vol. 6, no. 2, p. 762-770., 1991.

- [87] M. A. Laughton, "Decomposition techniques in power-system network load-flow analysis using the nodal-impedance matrix," *Proceedings of the Institution of Electrical Engineers*, vol. 115, no. 4, pp. 539-542, 1968.
- [88] B. H. Chowdhury, (Ed. Wayne Beaty), "Load Flow Analysis in Power Systems," in *Handbook of Electric Power Calculations*, McGraw-Hill, 2000, pp. 11.1-11.16,.
- [89] L. L. Freris and A. M. Sasson, "Investigation of the load-flow problem," *PROC.IEE*, vol. 115, no. 10, pp. 1459-1470, 1968.
- [90] Jaimes, A. M. Sasson and F. J., "Digital Methods Applied to Power Flow Studies," *IEEE TRANSACTIONS ON POWER APPARATUS AND SYSTEMS*, vol. 86, no. 7, pp. 860-867, 1967.
- [91] A. Hosseinzaman and A. Bargiela, "Parallel Simulation of Nonlinear Networks," *Proceedings PACTA*, vol. 92, pp. 1-11, 1992.
- [92] F. F. Wu, "Solution of Large-Scale Networks by Tearing," *IEEE Trans. Circuits Syst.*, , vol. 23, no. 12, pp. 706-713, 1976.
- [93] B. A. Carre, "Solution of Load-Flow Problems by Partitioning Systems into Trees," *IEEE TRANS. ON PAS*, vol. 87, no. 11, pp. 1931-1938., 1968.
- [94] A. M. Sasson, "Decomposition Techniques Applied to the Nonlinear Programming Load-Flow Method," *IEEE Trans on PAS*, vol. 89, no. 1, pp. 78-82, 1970.
- [95] F. Olobaniyi, H. Nouri and S. Ghauri, "Investigation of Diakoptics as a resourceful tool in power system analysis," *Universities Power Engineering Conference (UPEC), 2012, 47th International*, pp. 1-6, 2012.
- [96] Manitoba Research Centre Inc, PSCAD (Power Systems Computer Aided Design) 4.2.1 User's Guide, Manitoba, Canada : Manitoba HVDC Research Centre, 2010.

- [97] R. Kasturi and M.S. N. Potti, "Piecewise Newton –Raphson Load Flow – An Exact Method Using Ordered Elimination," *IEEE Transactions on Power Apparatus and Systems*, , vol. 95, no. 4, pp. 1244- 1253, 1976.
- [98] Sofer, S. G. Nash and A., *Linear and Non-linear Programming*, 546: McGraw-Hill International Editions, Industrial Engineering Series, 1996.
- [99] J. B. Ward and H. W. Hale, "Digital Computer Solution Of Power Flow Problems," *Power Apparatus and Systems, Part III. Trans. of the AIEE*, vol. 75, pp. 398-404, 1956.
- [100] Halder, A. Chakrabarti and S., *Power System Analysis Operation And Control*, New Delhi: 3rd edition, PHI Learning Private Limited, 2011.
- [101] M. Iordache and L. Dumitriu, "Efficient Decomposition Techniques for Symbolic Analysis of Large-Scale Analog," *Analog Integrated Circuits and Signal Processing*, vol. 40, no. 3, p. 235–253, 2004.
- [102] M. Central, MATLAB, [Online]. Available: http://www.mathworks.co.uk/matlabcentral/fileexchange/28954-ybus/content/ybus_final.m. [Accessed 20 August 2011].
- [103] E. Brown and E. Byrns, "combntns," MathWorks, 9 November 2007. [Online]. Available: <https://lost-contact.mit.edu/afs/cs.stanford.edu/package/matlab-r2009b/matlab/r2009b/toolbox/map/map/combntns.m>. [Accessed 12 July 2013].
- [104] A. E. Guile and W. Paterson, *Electrical Power Systems*, Vol. 1, Pergamon Press,, 1977.
- [105] "DATA SHEETS FOR IEEE 14 BUS SYSTEM," [Online]. Available: http://shodhganga.inflibnet.ac.in/bitstream/10603/5247/18/19_appendix.pdf. [Accessed 26 March 2013].
- [106] Pravi, "MATLAB CENTRAL," MATLAB, 8 May 2009. [Online]. Available: <http://uk.mathworks.com/matlabcentral/fileexchange/21059-newton-raphson-loadflow/content//nrlfppg/busdatas.m>. [Accessed 18 October 2012].

- [107] “Appendix-A, DATA FOR IEEE 30-BUS TEST SYSTEM,” 2010. [Online]. Available:
http://shodhganga.inflibnet.ac.in/bitstream/10603/1221/18/18_appendix.pdf .
[Accessed 20 August 2013].
- [108] O. O. Ajayi, R. O. Fagbenle, and J. Katende,, “Assessment of Wind Power Potential and Wind Electricity Generation Using WECS of Two Sites in South West, Nigeria,” *International Journal of Energy Science, World Academic Publishing* , vol. 1, no. 2, pp. 78-92, 2011.
- [109] J. F. Gutierrez, M. F. Bedrinana, C. A. Castro, “Critical comparison of robust load flow methods for ill-conditioned systems,” in *PowerTech, 2011 IEEE* , Trondheim, 2011.
- [110] R. Roebuck, C. Saylor and Y. Wallach, “Comparison Of Accuracy In Load-Flow,” *Circuits and Systems, Proceedings of the 33rd Midwest Symposium, IEEE*, vol. 1, p. 148 – 150, 1990.
- [111] R. Soremekun, A. A. Zin, A. Amoo, G. Bakare, U. Aliyu, “Optimal Economic Dispatch for the Nigerian Grid System Considering Voltage and Line Flow Constraints,” *The 5th International Power Engineering and Optimization Conference (PEOCO2011) IEEE, Malasia* , , pp. 341-345, 2011..
- [112] I. Samuel, J. Katende and F. Ibikunle, “Voltage Collapse and the Nigerian National Grid, EIECON,,” *EIE’s 2nd Intl’ Conf.Comp., Energy, Net., Robotics and Telecom./ eieCon2012*, pp. 128-131., 2012.
- [113] A. S. Sambo, B. Garba.I. H. Zarma and M. M. Gaji, “Electricity generation and the present challenges in the Nigerian power sector,” *Journal of Energy and Power Engineering*, vol. 6, no. 7, pp. 1050-1059., 2012.
- [114] A. O. Ibe, and E. K. Okedu, “A Critical Review of Grid Operations in Nigeria,” *Pacific Journal of Science and Technology*, vol. 10, pp. 486-490., 2009.
- [115] A. S. A. Bada, “Status and Opportunities in Transmission Company of Nigeria,,”

- Presidential Task Force on Power, Abuja, Nigeria, 2011.
- [116] Global Energy Network Institute (GENI), “National Electricity Transmission Grid of Nigeria,” National Energy Grid, [Online]. Available: http://www.geni.org/globalenergy/library/national_energy_grid/nigeria/nigeriannationalelectricitygrid.shtml. [Accessed 25 April 2011].
- [117] O. Anaya-Lara, N. Jenkins, J. Ekanayake, P. C. Hughes, WIND ENERGY GENERATION-Modelling and Control, ., Publication, 2009, p14-15], A John Wiley and Sons, Ltd, 2009, p14-15.
- [118] NERC, “The grid code for the Nigeria electricity transmission system, Grid Code-Version 01,” Nigerian Electricity Regulatory Commission, 2012.
- [119] A. Shahriari , A. H. A. Bakar , H. Mokhlis, “Comparative Studies on Non-Divergent Load Flow Methods in Well, III and Unsolvble Condition,” *In Power System Technology (POWERCON), 2010 International Conference on, IEEE.*, pp. 1-8, 2010.
- [120] G. A. Bakare, G. Krost, G. K. Venayagamoorthy, and U. O. Aliyu, “Differential Evolution Approach for Reactive Power Optimization of Nigerian Grid System,,” *IEEE, PESGM*, pp. 1-6., 2007.
- [121] M. S. Adaramola, S. S. Paul, S. O. Oyedepo, “Assessment of electricity generation and energy cost of wind energy conversion systems in north-central Nigeria,” *Elselvier, Energy Conversion and Management*, vol. 52, p. 3363–3368, 2011.
- [122] H. Gujba, Y. Mulugetta and A. Azapagic, “Environmental and economic appraisal of power generation capacity expansion plan in Nigeria,” *Elselvier: Energy Policy* , vol. 38, p. 5636–5652, 2010.
- [123] A. L. Amoo, D. M. Said, A. Yusuf and A. A. Mohd Zin, “Harmonic Power Flow in Nigerian Power System with PV Site,” in *IEEE 7th International Power Engineering and Optimization Conference (PEOCO2013)*, Langkawi, Malaysia,

- 2013.
- [124] O. J. Onojo, G. C. Onoiwu and S. O. Okozi , “Analysis of Power Flow Of Nigerian 330kv Grid System (Pre and Post) Using Matlab,” *EJNAS*, vol. 1, no. 2, pp. 59-66, 2013..
- [125] J. G. Abiola and T. M. Adekilekun, “Critical Clearing Time Evaluation of Nigerian 330kV,” *American Journal of Electrical Power and Energy Systems*, vol. 2, no. 6, pp. 123-128, 2013.
- [126] I. G. Adebayo, I. A. Adejumobi, G. A. Adepoju,, “Power Flow Analysis Using Load Tap–Changing Transformer (LTCT): A Case Study of Nigerian 330kv Transmission Grid System,” *International Journal of Engineering and Advanced Technology*, vol. 2, no. 3, pp. 230-237, 2013.
- [127] O. A. Komolafe, M. O. Omoigui, and A. Momoh, “Reliability Investigation of The Nigerian Electric Power Authority Transmission Network in a Deregulated Environment,,” *IEEE Industry Applications Conference, 38th IAS Annual Meeting*, ., pp. 1328-1331, 2003.
- [128] A. A. Maruf and K. U. Garba, “Determination of Bus Voltages, Power Losses and Load Flow in the Northern Nigeria 330kv Transmission Sub-Grid,” *International Journal of Advancements in Research & Technology*, vol. 2, no. 3, pp. 1-9, 2013.
- [129] European Wind Energy Association (EWEA), *Wind Energy - The Facts: A Guide to the Technology, Economics and Future of Wind Power*, Routledge, 2012.
- [130] A. S. Sambo, “Renewable Energy Electricity In Nigeria: The Way Forward,” in *Energy Commission of Nigeria Renewable Electricity Policy Conference*, 2006.
- [131] A. Evans, V. Strezov, and T. Evans, “Comparing the sustainability parameters of renewable, nuclear and fossil fuel electricity generation technologies,” *World Energy Council for Sustainable Energy, Congress Papers, Montréal* , vol. 27, 2010.
- [132] O. O. Ajayi, “The Potential for Wind Energy in Nigeria,” *Wind Engineering*,

- Multi-Science Publishing Company, UK*, vol. 34, no. 3, pp. 303-312, 2010.
- [133] S. Diaf and G. Notton, “Evaluation of electricity generation and energy cost of wind energy conversion systems in southern Algeria,” *Renewable and Sustainable Energy Reviews*, Elsevier, vol. 23, pp. 379-390. , 2013.
- [134] O. S. Ohunakin, “Wind resource evaluation in six selected high altitude locations in Nigeria,” *Renewable Energy*, Elsevier Ltd., vol. 36, pp. 3273-3281, 2011.
- [135] M. Guillermin, “Katsina 10MW Wind Farm Federal Ministry of Power Pilot Project in Wind Energy,” 2011. [Online]. Available: Source:<http://www.vergnet.com/pdf/fiches/en/nigeria-katsina.pdf>.. [Accessed 16 June 2014].
- [136] H. Holttinen and R. Hirvonen. Ed: T. Ackermann, “Power System Requirements for Wind Power,” in , *Wind Power in Power Systems*, , John Wiley & Sons, Ltd, 2005, pp. 143-167.
- [137] H. Langkowski, Trung Do Thanh, K-D. Dettmann, D. Schulz, “Grid Impedance Determination – Relevancy for Grid Integration of Renewable Energy Systems,” *Industrial Electronics, 35th Annual Conference (IECON) of IEEE*,, pp. 516-521, 2009.
- [138] M. J. Ghorbal W. Ghzaiely, I. Slama-Belkhodjaz and J. M. Guerrero, “Online Detection and Estimation of Grid Impedance Variation for Distributed Power Generation,” *Electrotechnical Conference (MELECON), 2012 16th IEEE Mediterranean*, , pp. 555 - 560, 2012 .
- [139] E. Muljadi and C.P. Butterfield, R. Yinger and H. Romanowitz, “Energy Storage and Reactive Power Compensator in a Large Wind Farm,” *42nd AIAA Aerospace Sciences, Meeting and Exhibit*,, pp. 1-13., 2008.
- [140] A. A. Sadiq, M. N. Nwohu, “Evaluation of Inter – Area Available Transfer Capability of Nigeria 330KV Network,” *IJET*, vol. 3, no. 2, pp. 148-158., 2013.
- [141] N.G. Boulaxis, S.A. Papathanassiou and M.P. Papadopoulos, “Slow Voltage

- Variation Assessment in Distribution Networks with Wind Penetration,” *Proc. EWEC’01*, , 2001..
- [142] C. McGee, “Exploring photoVoltaic technology for grid sustainability, Integrating Renewable Energy to the Grid, Optimising and Securing the network,” in *IET conference*,, London, UK , 2014..
- [143] B.C. Ummels E. Pelgrum M. Gibescu W.L. Kling, “Comparison of integration solutions for wind power in the Netherlands,” *IET Renewable Power Generation*, vol. 3, no. 3, pp. 2009, Vol. 3, Iss. 3, pp. 279–292., 2009.
- [144] S. Faias, J.Sousa, R. Castro, “Strategies for the Integration of Wind Energy into the Grid: An Application to the Portuguese Power System,” *IEEE, Energy Market (EEM), 7th International Conference on the European* , pp. 1-7, 2010.
- [145] G. Strbac, “Integrating Renewable Energy to the Grid, Optimising and Securing the network,” in *IET conference*,, London, UK, 2014.
- [146] F. Schettler, et al, “Roadmap to the Supergrid Technologies, Final Report,” Friends of the Supergrid (FOSG) WG 2 Technological, 2012.
- [147] J. Corbett, “Energy Bridge Ireland - UK Rationale and Technical Challenges,,” in *IET Conference* , London, UK, 2014.
- [148] J. L. Dominguez-Garcia, Analysis of the Contribution of Wind Power Plants to Damp Power System Oscillations, Universitat Politecnica de Catalunya, PhD Thesis, 2013.
- [149] R. Yokoyama and K. Nara, “New Concept of Energy Delivery Network for Practical Use of Distributed Generations and Customer Services-Committee Report of IEE Japan,” in *Power plants and power systems control 2003: a proceedings volume from the IFAC Symposium on Power Plants and Power Systems Control*, Oxford, UK., Elsevier Science, 2004, pp. 55-60.
- [150] W. B. e. al, “Highly Efficient Solutions for Smart and Bulk Power Transmission of “Green Energy”,,” in *21th World Energy Congress*, , September 2010,

Montreal.

- [151] D. P. Koester, S. Ranka and G. C. Fox, "A parallel Gauss-Seidel algorithm for sparse power system matrices.," *In Proceedings of the 1994 ACM/IEEE conference on Supercomputing.*, pp. 184-193, 1994.
- [152] S. Tong, and K. N. Miu., "Participation Factor Studies for Distributed Slack Bus Models in Three-Phase Distribution Power Flow Analysis," *In 2005/2006 IEEE/PES Transmission and Distribution Conference and Exhibition*, pp. 92-96, 2006.
- [153] J. V. Schmill, "New Scheme Applicable to Network Analysis Studies, Diakoptics, and Other Fields," *IEEE Transactions on PAS Vol. Pas-86, No. 11 November 1967*, p., vol. 86, no. 11, pp. 1437-1448, 1967.
- [154] F. M. Uriarte, "On Kron's diakoptics," *Electric Power Systems Research*, vol. 88, pp. 146-150, 2012.
- [155] K. Gregory, J. G. Kettleborough and I. R. Smith, "Diakoptic Mesh Analysis of Limited Size Power Supply Systems," *IEE PROCEEDINGS*, vol. 135, no. 2, pp. 124-130, 1988.
- [156] P. Praviraj, "MATLAB CENTRAL - Gauss Seidel Load Flow Analysis," MATLAB, 10 April 2008. [Online]. Available: <http://uk.mathworks.com/matlabcentral/fileexchange/14089-gauss-seidel-load-flow-analysis/content//ybusppg.m>. [Accessed 9 October 2012].
- [157] P. Praviraj, "MATLAB CENTRAL - Admittance Bus (Y-Bus) Formation," MATLAB, 2 April 2009. [Online]. Available: <http://uk.mathworks.com/matlabcentral/fileexchange/19512-admittance-bus--y-bus--formation/content//ybusppg/ybusppg.m>. [Accessed 2 November 2012].
- [158] A. Shashid, "MATLAB CENTRAL, Zbus Building Algorithm," MATLAB, 15 November 2009. [Online]. Available: <http://www.mathworks.co.uk/matlabcentral/fileexchange/25846-zbus-building->

- algorithm/content/ArslanZbus.m. [Accessed 8 November 2012].
- [159] A. A. Awan, "File Exchange - MATLAB Central," MATLAB, 17 October 2011. [Online]. Available: http://www.mathworks.com/matlabcentral/fileexchange/33304-z-bus-algorithm/content/Z_bus.m. [Accessed 8 November 2012].
- [160] J. Machowski, J. W. Bialek and J. R. Bumby, Power System Dynamics, West Sussex, UK: John Wiley and Sons, Ltd, 2008.

APPENDICES

APPENDIX A LOAD FLOW PROGRAMS

A.1 MATLAB Program For Gauss-Seidel Load Flow [102]

```

% Program for Gauss - Seidel Load Flow Analysis
% Case Study
% GSLF of complete System
% Assumption, Bus 1 is considered as Slack bus.
clc;
clear;

ybus = ybus14();           % Calling program "ybusEa.m" to get Y-Bus.
busdata = busd14();       % Calling "busdataCS2.m" for bus data.
bus = busdata(:,1);      % Bus number.
type = busdata(:,2);     % Type of Bus 1-Slack, 2-PV, 3-PQ.
V = busdata(:,3);        % Initial Bus Voltages.
th = busdata(:,4);       % Initial Bus Voltage Angles.
GenMW = busdata(:,5);    % PGi, Real Power injected into the buses.
GenMVAR = busdata(:,6);  % QGi, Reactive Power injected into the
buses.
LoadMW = busdata(:,7);   % PLi, Real Power Drawn from the buses.
LoadMVAR = busdata(:,8); % QLi, Reactive Power Drawn from the buses.
Qmin = busdata(:,9);     % Minimum Reactive Power Limit
Qmax = busdata(:,10);    % Maximum Reactive Power Limit
nbus = max(bus);         % To get no. of buses
P = GenMW - LoadMW;     % Pi = PGi - PLi, Real Power at the buses.
Q = GenMVAR - LoadMVAR; % Qi = QGi - QLi, Reactive Power at the
buses.
Vprev = V;
toler = 1;               % Tolerance.
iteration = 1;           % iteration starting
while (toler > 0.00001); % Start of while loop
    for i = 2:nbus
        sumyv = 0;
        for k = 1:nbus;
            if i ~= k
                sumyv = sumyv + ybus(i,k) * V(k); % Vk * Yik
            end
        end
        if type(i) == 2 % Computing Qi for PV bus
            Q(i) = -imag(conj(V(i)) * (sumyv + ybus(i,i) * V(i)));
            if (Q(i) > Qmax(i)) || (Q(i) < Qmin(i)) ; % Checking for Qi
Violation.
                if Q(i) < Qmin(i); % Whether violated the lower
limit.
                    Q(i) = Qmin(i);

```

```

        else % No, violated the upper limit.
            Q(i) = Qmax(i);
        end
        type(i) = 3; % If Violated, change PV bus to PQ bus.
    end
end
end
V(i) = (1/ybus(i,i))*((P(i)-j*Q(i))/conj(V(i)) - sumyv); %
Compute Bus Voltages.
if type(i) == 2 % For PV Buses, Voltage Magnitude remains same,
but Angle changes.
    V(i) = pol2rect(abs(Vprev(i)), angle(V(i)));
end
end
iteration = iteration+1; % Increment iteration count.
toler = max(abs(abs(V) - abs(Vprev))) % Calculate tolerance.
Vprev = V; % Vprev is required for next iteration, V(i) =
pol2rect(abs(Vprev(i)), angle(V(i)));
end % End of while loop / Iteration

iteration % Total iterations.
V % Bus Voltages in Complex form.
Vmag=abs(V);
theta=angle(V);
Vangle=theta*180/pi;

```

A.2 MATLAB Program For Newton Raphson Load Flow [102]

```

% Program for Newton-Raphson Load Flow Analysis.[.

nbus = 14; % IEEE-14
Y = ybusppg(); % Calling ybusppg.m to get Y-Bus Matrix..
busd = busdatas(14); % Calling busdatas..
BMva = 100; % Base MVA..
bus = busd(:,1); % Bus Number..
type = busd(:,2); % Type of Bus 1-Slack, 2-PV, 3-PQ..
V = busd(:,3); % Specified Voltage..
del = busd(:,4); % Voltage Angle..
Pg = busd(:,5)/BMva; % PGi..
Qg = busd(:,6)/BMva; % QGi..
Pl = busd(:,7)/BMva; % PLi..
Ql = busd(:,8)/BMva; % QLi..
Qmin = busd(:,9)/BMva; % Minimum Reactive Power Limit..
Qmax = busd(:,10)/BMva; % Maximum Reactive Power Limit..
P = Pg - Pl; % Pi = PGi - PLi..
Q = Qg - Ql; % Qi = QGi - QLi..
Psp = P; % P Specified..
Qsp = Q; % Q Specified..
G = real(Y); % Conductance matrix..
B = imag(Y); % Susceptance matrix..

```

```

pv = find(type == 2 | type == 1); % PV Buses..
pq = find(type == 3); % PQ Buses..
npv = length(pv); % No. of PV buses..
npq = length(pq); % No. of PQ buses..

Tol = 1;
Iter = 1;
while (Tol > 1e-5) % Iteration starting..

    P = zeros(nbus,1);
    Q = zeros(nbus,1);
    % Calculate P and Q
    for i = 1:nbus
        for k = 1:nbus
            P(i) = P(i) + V(i) * V(k) * (G(i,k) * cos(del(i)-del(k)) +
B(i,k) * sin(del(i)-del(k)));
            Q(i) = Q(i) + V(i) * V(k) * (G(i,k) * sin(del(i)-del(k)) -
B(i,k) * cos(del(i)-del(k)));
        end
    end

    % Checking Q-limit violations..
    if Iter <= 7 && Iter > 2 % Only checked up to 7th iterations..
        for n = 2:nbus
            if type(n) == 2
                QG = Q(n)+Ql(n);
                if QG < Qmin(n)
                    V(n) = V(n) + 0.01;
                elseif QG > Qmax(n)
                    V(n) = V(n) - 0.01;
                end
            end
        end
    end

    % Calculate change from specified value
    dPa = Psp-P;
    dQa = Qsp-Q;
    k = 1;
    dQ = zeros(npq,1);
    for i = 1:nbus
        if type(i) == 3
            dQ(k,1) = dQa(i);
            k = k+1;
        end
    end
    dP = dPa(2:nbus);
    M = [dP; dQ]; % Mismatch Vector

    % Jacobian
    % J1 - Derivative of Real Power Injections with Angles..
    J1 = zeros(nbus-1,nbus-1);
    for i = 1:(nbus-1)
        m = i+1;

```

```

    for k = 1:(nbus-1)
        n = k+1;
        if n == m
            for n = 1:nbus
                J1(i,k) = J1(i,k) + V(m) * V(n) * (-G(m,n) * sin(del(m) -
del(n)) + B(m,n) * cos(del(m) - del(n)));
            end
            J1(i,k) = J1(i,k) - V(m)^2 * B(m,m);
        else
            J1(i,k) = V(m) * V(n) * (G(m,n) * sin(del(m) - del(n)) -
B(m,n) * cos(del(m) - del(n)));
        end
    end
end

% J2 - Derivative of Real Power Injections with V..
J2 = zeros(nbus-1,npq);
for i = 1:(nbus-1)
    m = i+1;
    for k = 1:npq
        n = pq(k);
        if n == m
            for n = 1:nbus
                J2(i,k) = J2(i,k) + V(n) * (G(m,n) * cos(del(m) - del(n))
+ B(m,n) * sin(del(m) - del(n)));
            end
            J2(i,k) = J2(i,k) + V(m) * G(m,m);
        else
            J2(i,k) = V(m) * (G(m,n) * cos(del(m) - del(n)) +
B(m,n) * sin(del(m) - del(n)));
        end
    end
end

% J3 - Derivative of Reactive Power Injections with Angles..
J3 = zeros(npq,nbus-1);
for i = 1:npq
    m = pq(i);
    for k = 1:(nbus-1)
        n = k+1;
        if n == m
            for n = 1:nbus
                J3(i,k) = J3(i,k) + V(m) * V(n) * (G(m,n) * cos(del(m) -
del(n)) + B(m,n) * sin(del(m) - del(n)));
            end
            J3(i,k) = J3(i,k) - V(m)^2 * G(m,m);
        else
            J3(i,k) = V(m) * V(n) * (-G(m,n) * cos(del(m) - del(n)) -
B(m,n) * sin(del(m) - del(n)));
        end
    end
end

% J4 - Derivative of Reactive Power Injections with V..
J4 = zeros(npq,npq);
for i = 1:npq

```

```

    m = pq(i);
    for k = 1:npq
        n = pq(k);
        if n == m
            for n = 1:nbus
                J4(i,k) = J4(i,k) + V(n) * (G(m,n) * sin(del(m) - del(n))
- B(m,n) * cos(del(m) - del(n)));
            end
            J4(i,k) = J4(i,k) - V(m) * B(m,m);
        else
            J4(i,k) = V(m) * (G(m,n) * sin(del(m) - del(n)) -
B(m,n) * cos(del(m) - del(n)));
        end
    end
end

J = [J1 J2; J3 J4];           % Jacobian Matrix..

X = inv(J) * M;               % Correction Vector
dTh = X(1:nbus-1);           % Change in Voltage Angle..
dV = X(nbus:end);            % Change in Voltage Magnitude..

% Updating State Vectors..
del(2:nbus) = dTh + del(2:nbus); % Voltage Angle..
k = 1;
for i = 2:nbus
    if type(i) == 3
        V(i) = dV(k) + V(i); % Voltage Magnitude..
        k = k+1;
    end
end

Iter = Iter + 1;
Tol = max(abs(M));           % Tolerance..

end
loadflow(nbus,V,del,BMva); % Calling Loadflow.m..

```

A.3 Code for Finding Suitable Combinations

The code [103] below is used to find the right combinations of buses that form the boundary buses for line to be removed.

```

function out=combntns(choicevec,choose)
%COMBNTNS All possible combinations of a set of values
%
% c = COMBNTNS(choicevec,choose) returns all combinations of the
% values of the input choice vector. The size of the combinations
% are given by the second input. For example, if choicevec
% is [1 2 3 4 5], and choose is 2, the output is a matrix
% containing all distinct pairs of the choicevec set.

```

```

% The output matrix has "choose" columns and the combinatorial
% "length(choicevec)-choose-'choose'" rows. The function does not
% account for repeated values, treating each entry as distinct.
% As in all combinatorial counting, an entry is not paired with
% itself, and changed order does not constitute a new pairing.
% This function is recursive.
%
% See also NCHOOSEK.
% Copyright 1996-2007 The MathWorks, Inc.
% $Revision: 1.11.4.4 $ $Date: 2007/11/09 20:23:14 $
% Written by: E. Brown, E. Byrns

% Input dimension tests

if min(size(choicevec)) ~= 1 || ndims(choicevec) > 2
    error(['map:' mfilename ':mapError'], 'Input choices must be a
vector')

elseif max(size(choose)) ~= 1
    error(['map:' mfilename ':mapError'], 'Input choose must be a
scalar')

else
    choicevec = choicevec(:); % Enforce a column vector
end

% Ensure real inputs
choicevec = ignoreComplex(choicevec, mfilename, 'choicevec');
choose = ignoreComplex(choose, mfilename, 'choose');

% Cannot choose more than are available

choices=length(choicevec);
if choices<choose(1)
    error(['map:' mfilename ':mapError'], ...
        'Not enough choices to choose that many')
end

% Choose(1) ensures that a scalar is used. To test the
% size of choices upon input results in systems errors on
% the Macintosh. Maybe somehow related to recursive nature of
program.

% If the number of choices and the number to choose
% are the same, choicevec is the only output.

if choices==choose(1)
    out=choicevec';

% If being chosen one at a time, return each element of
% choicevec as its own row

elseif choose(1)==1
    out=choicevec;

```

```
% Otherwise, recur down to the level at which one such
% condition is met, and pack up the output as you come out of
% recursion.

else
    out = [];
    for i=1:choices-choose(1)+1
        tempout=combntns(choicevec(i+1:choices),choose(1)-1);
        out=[out; choicevec(i)*ones(size(tempout,1),1)
tempout];
    end
end
```

APPENDIX B PROGRAMMES FOR DIRECT COMPUTATION OF ADMITTANCE MATRICES

B.1 YBUS - program 1 [156]

```

% Program to form Admittance And Impedance Bus Formation....
% Praviraj P G, MTech I Year, EE Dept., IIT Roorkee, India, Email :
pravirajpg@gmail.com

function ybus = ybusppg(); % Returns ybus

linedata = linedata6(); % Calling "linedata6.m" for Line Data...
fb = linedata(:,1); % From bus number...
tb = linedata(:,2); % To bus number...
r = linedata(:,3); % Resistance, R...
x = linedata(:,4); % Reactance, X...
b = linedata(:,5); % Ground Admittance, B/2...
z = r + i*x; % Z matrix...
y = 1./z; % To get inverse of each element...
b = i*b; % Make B imaginary...

nbus = max(max(fb),max(tb)); % no. of buses...
nbranch = length(fb); % no. of branches...
ybus = zeros(nbus,nbus); % Initialise YBus...

% Formation of the Off Diagonal Elements...
for k=1:nbranch
    ybus(fb(k),tb(k)) = -y(k);
    ybus(tb(k),fb(k)) = ybus(fb(k),tb(k));
end

% Formation of Diagonal Elements....
for m=1:nbus
    for n=1:nbranch
        if fb(n) == m | tb(n) == m
            ybus(m,m) = ybus(m,m) + y(n) + b(n);
        end
    end
end
end
ybus; % Bus Admittance Matrix
zbus = inv(ybus); % Bus Impedance Matrix

```

B.2 YBUS - program 2 [157]

```

% Program to form Admittance Bus Formation with Transformer Tap setting..

num = 14; % IEEE-14, IEEE-30, IEEE-57 bus systems..
linedata = linedatas(num); % Calling "linedata6.m" for Line Data...
fb = linedata(:,1); % From bus number...

```

```

tb = linedata(:,2);      % To bus number...
r = linedata(:,3);      % Resistance, R...
x = linedata(:,4);      % Reactance, X...
b = linedata(:,5);      % Ground Admittance, B/2...
a = linedata(:,6);      % Tap setting value..
z = r + i*x;            % Z matrix...
y = 1./z;               % To get inverse of each element...
b = i*b;                % Make B imaginary...

nbus = max(max(fb),max(tb)); % no. of buses...
nbranch = length(fb);      % no. of branches...
Y = zeros(nbus,nbus);     % Initialise YBus...

% Formation of the Off Diagonal Elements...
for k=1:nbranch
    Y(fb(k),tb(k)) = Y(fb(k),tb(k))-y(k)/a(k);
    Y(tb(k),fb(k)) = Y(fb(k),tb(k));
end

% Formation of Diagonal Elements....
for m =1:nbus
    for n =1:nbranch
        if fb(n) == m
            Y(m,m) = Y(m,m) + y(n)/(a(n)^2) + b(n);
        elseif tb(n) == m
            Y(m,m) = Y(m,m) + y(n) + b(n);
        end
    end
end
Y % Bus Admittance Matrix..

```

APPENDIX C PROGRAMMES FOR DIRECT COMPUTATION OF IMPEDANCE MATRICES

C.1 ZBUS – Program 1 [158]

<http://www.mathworks.co.uk/matlabcentral/fileexchange/25846-zbus-building-algorithm/content/ArslanZbus.m>

Copyright 2009 Arslan Shahid, UET, Lahore, PAKISTAN.

```
clear all
clc
disp('Zbus Building Algorithm')
data=dlmread('data');

num_bus=max(max(data(:,1),data(:,2)));

sz=size(data);
size=sz(1,1);
buses_added=1;
bus_status=zeros(1,num_bus+1);

for n=1:size
    if(data(n,1)==0)
        temp=data(n,1);
        data(n,1)=data(n,2);
        data(n,2)=temp;
    end
    if(data(n,1)>data(n,2) && data(n,2)~=0)
        temp=data(n,1);
        data(n,1)=data(n,2);
        data(n,2)=temp;
    end
end

for n=1:size
    if(data(n,1)==1 && data(n,2)==0)
        temp1=data(1,:);
        data(1,:)=data(n,:);
        data(n,:)=temp1;
    end
end

for n=1:size
    for m=1:size
        if(data(m,1)==n)
            bus1=data(m,1);
```

```

bus2=data(m,2);
p_bus1=0;
p_bus2=0;
for k=1:num_bus
    if(bus_status(1,k)== bus1 && bus1~=0)
        p_bus1=1;
    end
    if(bus_status(1,k)== bus2 && bus2~=0)
        p_bus2=1;
    end
end
if(bus_status(1,buses_added)==0 && bus2==0 && p_bus1==0)
    disp('Adding Z=')
    disp(data(m,3)+ i*data(m,4))
    disp('between buses:')
    disp(bus1)
    disp(bus2)
    disp('This impedance is added between a new bus and
reference')

    buses_added=buses_added+1;
    bus_status(1,buses_added-1)=bus1;
    if(bus1==1)
        Zbus(bus1,bus1)=data(m,3)+i*data(m,4)
    else
        ssz=length(Zbus);
        Zbus(ssz+1,ssz+1)=data(m,3)+i*data(m,4)
    end

    disp(' ')
    disp(' ')
elseif(p_bus1==1 && p_bus2==0 && bus2~=0)
    disp('Adding Z=')
    disp(data(m,3)+ i*data(m,4))
    disp('between buses:')
    disp(bus1)
    disp(bus2)
    disp('This impedance is added between a new bus and an
existing bus')

    buses_added=buses_added+1;
    bus_status(1,buses_added-1)=bus2;
    size_zbus=length(Zbus);
    for var=1:size_zbus
        Zbus(size_zbus+1,var)=Zbus(bus1,var);
        Zbus(var,size_zbus+1)=Zbus(var,bus1);
    end
    Zbus(size_zbus+1,size_zbus+1)=Zbus(bus1,bus1)+
data(m,3)+ i*data(m,4);
    Zbus
    disp(' ')
    disp(' ')
elseif(p_bus1==1 && p_bus2==0 && bus2==0)
    disp('Adding Z=')
    disp(data(m,3)+ i*data(m,4))
    disp('between buses:')
    disp(bus1)
    disp(bus2)

```

```

disp('This impedance is added between an existing bus
and reference')
    size_zbus=length(Zbus);
    Zbus1=Zbus;
    for var=1:size_zbus
        Zbus1(size_zbus+1,var)=Zbus1(bus1,var);
        Zbus1(var,size_zbus+1)=Zbus1(var,bus1);
    end
    Zbus1(size_zbus+1,size_zbus+1)=Zbus1(bus1,bus1)+
data(m,3)+ i*data(m,4);
    for var1=1:size_zbus
        for var2=1:size_zbus
            Zbus(var1,var2)=Zbus1(var1,var2)-
Zbus1(var1,size_zbus+1)*Zbus1(size_zbus+1,var2)/Zbus1(size_zbus+1,size_
zbus+1);
        end
    end
    Zbus
    disp(' ')
    disp(' ')
    elseif(p_bus1==1 && p_bus2==1 && bus2~=0)
disp('Adding Z=')
disp(data(m,3)+ i*data(m,4))
disp('between buses:')
disp(bus1)
disp(bus2)
disp('This impedance is added between two existing
buses')
    size_zbus=length(Zbus);
    Zbus1=Zbus;
    for var=1:size_zbus
        Zbus1(size_zbus+1,var)=Zbus1(bus1,var)-
Zbus1(bus2,var);
        Zbus1(var,size_zbus+1)=Zbus1(var,bus1)-
Zbus1(var,bus2);
    end
    Zbus1(size_zbus+1,size_zbus+1)=Zbus1(bus1,bus1)+Zbus1(bus2,bus2)-
2*Zbus1(bus1,bus2) + data(m,3)+ i*data(m,4);
    for var1=1:size_zbus
        for var2=1:size_zbus
            Zbus(var1,var2)=Zbus1(var1,var2)-
Zbus1(var1,size_zbus+1)*Zbus1(size_zbus+1,var2)/Zbus1(size_zbus+1,size_
zbus+1);
        end
    end
    Zbus
    disp(' ')
    disp(' ')
end
end
end
bus_status

```

```

for var1=1:num_bus
    for var2=1:num_bus
        if(bus_status(1,var2)==var1)
            zvar1=Zbus(var2,:);
            Zbus(var2,:)=Zbus(var1,:);
            Zbus(var1,:)=zvar1;

            zvar2=Zbus(:,var2);
            Zbus(:,var2)=Zbus(:,var1);
            Zbus(:,var1)=zvar2;

            z_s=bus_status(1,var1);
            bus_status(1,var1)=bus_status(1,var2);
            bus_status(1,var2)=z_s;
        end
    end
end
Zbus

```

C.2 ZBUS - Program 2 [159]

```

Zbus = [0];
Quit = 0;
i = 0;
while Quit== 0

    Case = input('Which case is to be implemented = ');
    if Case == 1
        if i == 0
            Zb = input('Enter the value of impedance = ');
            Zbus = [Zb]
        end
        if i>0
            Zb = input('Enter the value of impedance = ');
            ord = length(Zb1);
            for d = 1:ord+1
                for e = i:ord+1
                    if d<=ord && e<=ord
                        Zbus1(d,e) = Zb1(d,e);
                    end
                    if d==ord+1 && e==ord+1
                        Zbus1(d,e)=Zb;
                    end
                    if d==ord+1 && d~=e || e==ord+1 && d~=e
                        Zbus1(d,e)= 0;
                    end
                end
            end
        end
        i=i+1;
    end
    Quit = input('Do you want to continue (y/n) = ');
end

```

```

        end
    end

    Zbus = [Zbus1]
end
end
if Case == 2
    Z_new = input('Enter the value of impedance for new bus = ');
    m = length(Zbus);
    for a=1:m
        for b=1:m
            Z_temp(a,b) = Zbus(a,b);
        end
    end
    for c = 1:m
        Z_temp(c,m+1) = Zbus(c,m);
        Z_temp(m+1,c) = Zbus(c,m);
        Z_temp(m+1,m+1) = Zbus(m,m)+Z_new;
    end
    Zbus = [Z_temp]
    i = i+1;
end
if Case == 3
    Z_new = input('Enter the value of impedance for new bus = ');
    m = length(Zbus);
    for a=1:m
        for b=1:m
            Z_temp(a,b) = Zbus(a,b);
        end
    end
    for c = 1:m
        Z_temp(c,m+1) = Zbus(c,m);
        Z_temp(m+1,c) = Zbus(c,m);
        Z_temp(m+1,m+1) = Zbus(m,m)+Z_new;
    end
    fprintf('Zbus before Kron Reduction:\n')
    Zbus = [Z_temp]
    m = length(Zbus);
    for i=1:m-1
        for k = 1:m-1
            Z(i,k) = Zbus(i,k) - ((Zbus(i,m)*Zbus(m,k))/Zbus(m,m));
        end
    end
    fprintf('Zbus after Kron Reduction:\n')
    Zbus = [Z]
end
if Case == 4
    Z1 = input('Enter the value of impedance = ');
    j = input('Enter the value of bus j = ');
    k = input('Enter the value of bus k = ');
    m = length(Zbus);
    for a=1:m
        for b=1:m
            Z_temp(a,b) = Zbus(a,b);
        end
    end
    for c = 1:m

```

```

        Z_temp(c,m+1) = Zbus(c,j)-Zbus(c,k);
        Z_temp(m+1,c) = Z_temp(c,m+1);
    end
    Z_temp(m+1,m+1) = Z1+Zbus(j,j)+Zbus(k,k)-2*Zbus(j,k);
    fprintf('Zbus before Kron Reduction:\n')
    Zbus = [Z_temp]
    m = length(Zbus);
    for i=1:m-1
        for k = 1:m-1
            Z(i,k) = Zbus(i,k) - ((Zbus(i,m)*Zbus(m,k))/Zbus(m,m));
        end
    end
    fprintf('Zbus after Kron Reduction:\n')
    Zbus = [Z]
end
    Quit = input('Do u want to quit = ');
    Zb1 = [Zbus];
end

```

APPENDIX D WIND ENERGY AND THE GRID

Wind energy is presently the dominant renewable energy source for electricity generation, extracted by means of wind turbine generators. Wind turbine generators commonly employ induction machines. Integration of large amounts of wind generation usually changes the system dynamics due to the intermittent nature of wind energy and characteristics of the induction generator. The induction generator plays a major role and therefore its and its influence on power system operation is briefly discussed in this section.

D.1.1 Power Available for Extraction

The power available in the air, P_{air} , is given by equation (D1) [58, 160].

$$P_{\text{air}} = \frac{1}{2} \rho A v^3 \quad (\text{D1})$$

where ρ = air density $\approx 1.225 \text{ kg/m}^3$

A = swept area of rotor

v = free wind speed

The full power available in the wind at any particular time cannot all be extracted by the wind turbine, so a power coefficient (C_p) is defined as

$$C_p = \frac{P_{\text{wt}}}{P_{\text{air}}} \quad (\text{D2})$$

$$P_{\text{wt}} = C_p \cdot P_{\text{air}} = C_p \cdot \frac{1}{2} \rho A v^3 \quad (\text{D3})$$

The maximum power that can be extracted from the wind, known as Beltz limit is given by $C_{p\text{max}} = 16/27 = 0.593$ [58, 143]. Also the tip speed ratio of a turbine may be defined as

$$\lambda = \frac{\omega R}{v} \quad (\text{D4})$$

where P_{wt} = power transferred to wind turbine

ω = rotational speed of wind turbine rotor

R = radius to tip of rotor and

v = free wind speed

C_{pmax} can only be achieved at a single tip speed ratio, and for a fixed rotational speed of the turbine this only occurs at a single wind speed. This is the basis of operating a wind turbine at variable rotational speed since it is possible to operate at maximum C_p over a range of wind speeds.

The overall performance of the wind turbine is described by its power curve (Figure. D.1). It relates the steady-state output power developed by the turbine to the free wind speed. Below the cut-in speed of about 5m/s, the turbine remains shut down as the power in the wind is too low for useful energy production. Then once operating, the power output increases following a broadly cubic relationship with wind speed (although modified by the variations in C_p) until rated wind speed is reached. Above rated wind speed the aerodynamic rotor is arranged to limit the mechanical loads on the drive train so that at very high wind speeds the turbine shuts down.

The choice of cut-in, rated and shutdown wind speed is made by the wind turbine designer who, for typical wind conditions will try to balance maximum energy extraction with controlling the mechanical loads (and hence the capital cost) of the turbine.

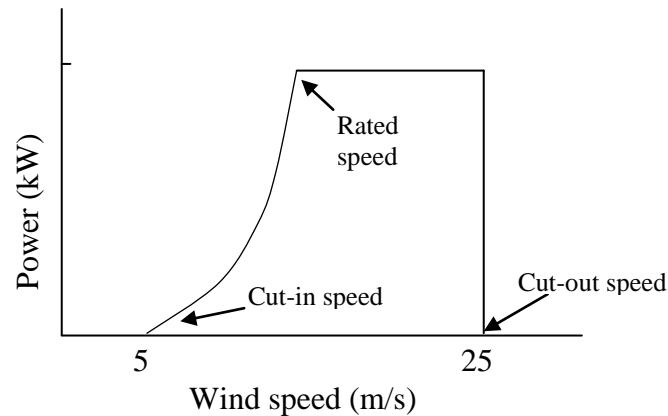


Figure D.1. Power curve of a wind turbine

D.2 Wind Energy Systems

Wind power from the wind is extracted by means of wind turbine generators. There are a few classifications of wind turbine generators but in terms of speed there are two types – the fixed wind turbines and the variable speed turbines.

D.2.1 Fixed-speed wind turbine

Fixed-speed wind turbine use induction generators. It is electrically simple and from the grid point of view is probably the most desirable because it can be viewed as a large fan drive where torque is applied to the shaft by wind. The generators directly connected to the network, limit the power when wind speed exceeds the rated value by applying any of the following methods:

- Pitch regulation: The blades rotate longitudinally axis.
- Stall regulation: The turbine blades stall when wind speeds exceed the limit.
- Assisted-stall regulation: The blades are rotated slowly about their longitudinal axis but the control is basically through stalling.

- Yaw control: When the wind speed exceeds the required limit, the rotor axis is moved out of the wind directions. This method is rarely used.

The components and characteristics of these turbines can be understood by the basic characteristics of an induction machine. Substantial pulsating torque is produced in the wind turbine rotors at the frequency of its blades due to tower shadow and wind shear effects. These torques pulsations are usually close to the natural frequency of the synchronous generator in the network [46]. Therefore direct connection of synchronous generators to the grid with simple mechanical drive train in fixed-speed wind turbines is not practicable. Modern fixed wind turbines generally use induction machines.

Advantages

- It is based on well-known technology and more reliable.
- It has fewer parts and is comparatively cheap.
- There is no need to electrically connect the rotor and the fixed system; the electrical system is therefore simple. Power is transferred from rotor to the stator magnetically.
- Frequency conversion is not required and so current harmonics do not exist in the electrical system.

Disadvantages

- The fixed-speed operation impacts on the system in the following ways:
 - Wind speed fluctuations are converted directly into electromechanical torque variations instead of rotational speed variations. This introduces high mechanical and fatigue stresses in the system. Secondly, the drop in torque due to tower and shear effects are not damped by speed variations, causing in high flicker levels.
 - The turbine speed cannot be synchronized with the wind speed to maximize the aerodynamic efficiency.

- A gear system used in the drive train requires frequent maintenance.
- The reactive power requirement of the machine cannot be controlled and the fixed relation between reactive and active power makes it very difficult to support grid voltage control.

D.2.2 Variable-speed wind turbines

Variable-speed wind turbines generally employ pitch control at high wind speeds, although stall control has also been used. The variable speed operation is accomplished by controlling the rotor resistance of the induction generator, that is, slip control or by using power electronics employed to connect the generator to the network.

Key advantages of the variable-speed wind turbines are stated below [81]

- ✓ They are cheap and provide simple pitch control is easy
- ✓ They reduce mechanical stresses; gusts of wind can be absorbed, i.e., energy is stored in the mechanical inertia of the turbine, creating an ‘elasticity’ that reduces torque pulsation.
- ✓ They dynamically compensate for torque and power pulsations caused by back pressure of the tower.
- ✓ The elasticity of the wind turbine system facilitates the damping of torque pulsations thereby improving the electrical power quality by reducing flicker.
- ✓ Adjusting turbine speed enhances higher energy capture and increases efficiency of the rotor.
- ✓ It does not have synchronisation problems and firm electrical controls can be used to reduce grid voltage sags.

D.2.2.1 Variable speed wind turbine configurations

There are three main types of variable-speed wind turbines:

Type I

Speed control is by the varying the rotor resistance of the induction generator, that is, slip control. Electronic power converter is not used and therefore behaves like fixed speed wind turbine in relation to its reactive capabilities.

Type II

Power electronic converter is employed with doubly-fed induction generator (DFIG). The standard practice is use converters rated at about 30% of the generator and provides dynamic reactive power control.

Type III

A synchronous generator with 3-phase stator winding may be used. Excitation may be supplied the rotor windings by a dc current from a separate circuit or permanent magnets attached to the rotor. Control is the same as Type II above but offers full control.

The most common configurations are the doubly-fed induction generator (DFIG) and the direct drive synchronous generator.

D.2.2.1 Doubly-fed induction generator (DFIG)

The general configuration of a DFIG is shown in Figure D2(b). It has a wound rotor but is constructed like the rotor of squirrel cage induction generator and connected to the grid through a power electronic converter. The converter separates the network electrical frequency from the rotor mechanical frequency, allowing for variable-speed operation of the wind turbine by injecting controllable voltage into the rotor at slip frequency. Protection of the generator and converters are by voltage limiters and over-current devices.

A DFIG system can transmit power to the grid through both the stator and rotor, while the rotor can also absorb power. When the generator is operating in the super-synchronous mode, that is rotational speed of the generator, ω_r , is higher than synchronous speed, ω_s , power flows from the rotor through the converters to the grid. If it is in the sub-synchronous mode where the generator speed is less than the synchronous speed, the rotor receives power from the grid through the converters. Its rating is mostly around 30% of the total generator rated power.

Advantages

The advantages from [46, 67, 80] of a DFIG are:

- ✓ The speed is variable within a sufficient range, with limited converter costs;
- ✓ The reactive power can be controlled by controlling the rotor currents with the converter; this allows the supply of voltage support towards the grid.

Disadvantages:

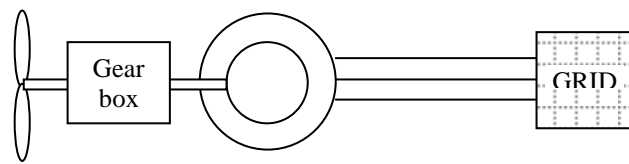
- A gear box is still necessary in the drive system and the speed range is well below what is required to obtain a generator speed of 10-25 rpm.
- Power transfer to and from the rotor is done with the help of slip rings and carbon brushes which require regular maintenance. They are a likely source of machine failure and increase the electrical losses.
- If a crowbar provides overcurrent protection to the converter (Figure D.1b), the crowbar switching is accompanied with the shut-down of the entire turbine.
- Grid disturbances caused by the dynamic behaviour of the turbine generator is complicated, especially in case of crowbar switching.

D.2.2.2 Direct Drive Synchronous Generator

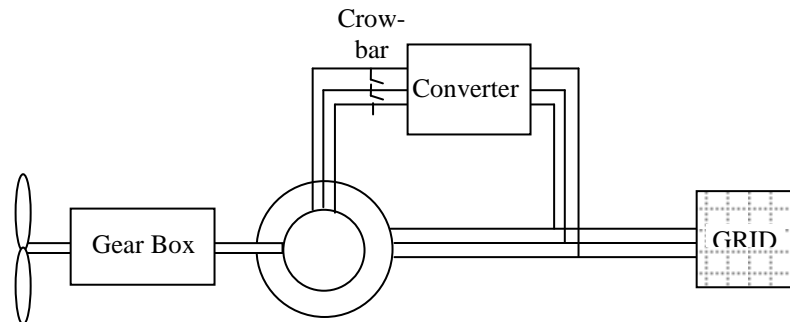
In the direct-drive synchronous generator, is directly driven by the wind turbine and therefore eliminates the need for a gearbox in the drive train. The rotor may be

electrically excited from a separate circuit or through permanent magnets attached to the rotor.

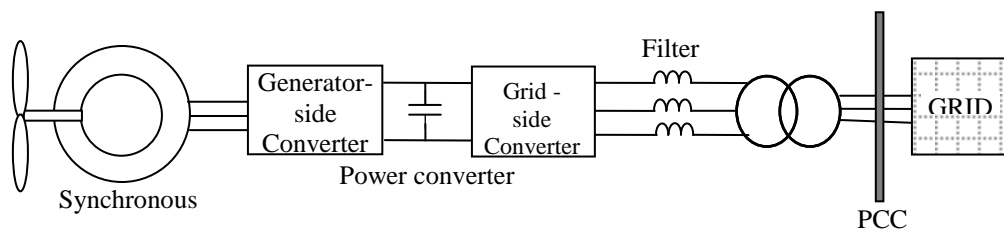
The grid connection is shown in Figure D.1c. All the power of the generator is processed through the converter. The amplitude and the frequency of the voltage can be fully controlled by the converter at the generator side, without the grid characteristics. This results in a generator speed that can be fully controlled over a wide range, even for very low speeds.



(a) Fixed speed, squirrel cage induction generator directly connected to grid



(b) Doubly-fed induction generator (DFIG)



(c) Direct drive synchronous generator

Figure D.2. Wind turbine configurations

Advantages are thus:

- ✓ The gearbox is eliminated with its attendant increase in manufacturing maintenance cost, producing of acoustic noise. Mechanical failure generally traced to the gear system is also eliminated.
- ✓ The converter permits full control of speed, active and reactive power in normal and disturbed grid conditions. The generator, though, still needs to be disconnected for safety reasons in highly disturbed grid conditions.

Main drawbacks are:

- All the generator power is processed by the converter and this requires expensive power electronic components with a very effective cooling system.
- To supply the high electrical torque required at low speeds, a large rotor diameter is needed.

D.3 Characterization of wind turbines

The different configurations of wind turbines indicate varying power quality levels from one wind turbine to another depending on the manufacturer's specifications.

The general parameters for characterising the power quality of a wind turbine are [81]:

- Rated data of the wind turbine
- Flicker produced during continuous or switching operations
- Harmonics and current distortions (< 9kHz)
- Response to voltage dips
- Active power characteristics based on maximum output, ramp rate limitation and set-point control.
- Reactive power capabilities and set-point control)
- Type of grid protection considering tripping levels of over/under voltage magnitude and frequency.
- Reconnection time of the turbine to the grid.

D.4 Induction Generator Coupled to the Grid

The simplicity of the induction machine makes it the favoured machine in many applications. It is commonly used as motors and therefore viewed as loads by the power system. However, induction machines are also often used as generators in wind farms and following analysis of its performance is based on [24, 58, 160].

The operation of an induction machine as a generator can be understood by considering its equivalent circuit of Figure D.3 which defines the power flow through the machine.

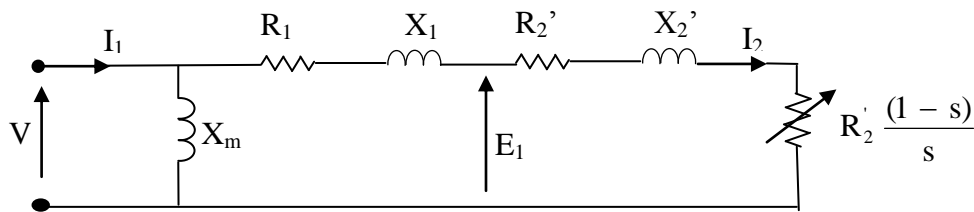


Figure D.3. Approximate equivalent circuit of the induction

Analysis of the simplified circuit gives

$$I_2 = \frac{V}{\sqrt{\left(R_1 + \frac{R_2'}{s}\right)^2 + (X_1 + X_2')^2}} \quad (D5)$$

If the losses in the stator resistance and the iron core are neglected, then the power supplied to the machine from the grid is the same as the power supplied to the rotor and is given by

$$P_{\text{grid}} \approx P_{\text{rot}} = 3I_2^2 \frac{R_2'}{s} = T_m \omega_{\text{sm}} \quad (D6)$$

The power loss in the rotor resistance and the mechanical power delivered are

$$\Delta P_{\text{rot}} = 3I_2^2 R_2' = sP_{\text{grid}} \quad (D7)$$

$$P_m = 3I_2^2 \frac{R(1-s)}{s} = P_{\text{grid}}(1-s) = T_m \omega_m \quad (\text{D8})$$

$$s = \frac{(\omega_{\text{sm}} - \omega_m)}{\omega_{\text{sm}}} = \frac{(\omega_s - \omega_r)}{\omega_s} \quad (\text{D9})$$

The power supplied to the rotor can be written in terms of the torque and angular synchronous speed ω_{sm} as $P_s \approx P_{\text{rot}} = T_m \omega_{\text{sm}}$.

Equations (D6) and (D8) allow the efficiency of the machine to be expressed as

$$\eta_{\text{motor}} = \frac{P_m}{P_{\text{grid}}} = (1-s), \quad \eta_{\text{gen}} = \frac{P_{\text{grid}}}{P_m} \frac{1}{(1-s)} \quad (\text{D10})$$

The shaft torque produced by the machine is obtained from (D8) as

$$T_m = \frac{P_m}{\omega_m} = \frac{P_m}{\omega_{\text{sm}}(1-s)} = \frac{3}{\omega_{\text{sm}}} \frac{V^2}{\left[\left(R_1 + R_2' / s \right)^2 + \left(X_1 + X_2' \right)^2 \right]} \frac{R_2'}{s} \quad (\text{D11})$$

The behaviour of a synchronous generator connected to the grid may be likened to a The mechanical mass/spring/damper system is used to depict the behaviour or where the effective spring stiffness is equivalent to the synchronizing power coefficient K_E (Figure D.4a) [160]. A synchronous generator is stiffly coupled to the grid which produces adverse effects when used as a wind turbine generator. Large stresses can be experienced in the drive shaft and gearbox due to the way the system responds to the dynamic torques produced by wind turbulence. An induction generator provides a ‘softer’ coupling to the system and allows a degree of movement at the generator which helps to reduce these shock torques. For a very small slip, the induction machine torque given by (D11) can be approximated as

$$T_m = \frac{3}{\omega_{sm}} \frac{V^2}{\left[\left(R_1 + \frac{R_2'}{s} \right)^2 + (X_1 + X_2')^2 \right]} \frac{R_2'}{s} \approx \frac{3V^2}{\omega_{sm}} \frac{1}{R_2} s = D_c \Delta\omega \quad (D12)$$

$s = \text{slip}$

R_1 and X_1 are the resistance and leakage reactance of a stator phase winding (the network reactance and transformer reactance are both incorporated into X_1).

R_2 and L_2 are the rotor resistance and leakage inductance per phase.

X_m is the magnetizing reactance

and I_m is the current flowing through X_m and sets up the rotating magnetic field.

ω_{sm} is the synchronous speed

ω_{rm} is the rotor speed

$\omega_s = 2\pi f = \omega_{sm} p$ is the angular electrical synchronous frequency,

$\omega_r = \omega_{rm} p$ is the rotor electrical angular frequency and

p is the number of pole pairs.

$\omega_{slip} = \omega_s - \omega_r = s\omega_s$, is the slip electrical frequency ($\omega_{slip} = \omega_s - \omega_r = s\omega_s$)

I_2 is the rotor current referred to the stator

R_2' and L_2' are the rotor resistance and leakage inductance referred to the stator

$\Delta\omega = \omega_s - \omega_r$ is the rotor speed deviation with respect to the synchronous speed

D_c is an equivalent 'damper constant'.

R_s is the network resistance incorporated into R_1 ,

V_s is the stator voltage and also the system supply voltage

P_s is power supplied to the machine

P_{rot} power supplied to the rotor ($P_s \approx P_{rot}$)

$P_{grid} = \text{supply power}$

ΔP_{rot} is power loss in rotor

P_m is the mechanical power

It can be seen from (D12) that the torque varies with speed, an indication that the coupling of the induction machine to the grid is analogous to a mechanical damper. The soft coupling, especially as large wind turbines, helps to reduce stress in the drive shaft due to the dynamic torques produced by wind gusting and wind turbulence. It can also be seen from (D12) that the 'damper constant' D_c determines the effective compliance and that this can be controlled by changing the rotor resistance.



Figure D.4. Wind turbine generator coupling to grid [160]

The system impedance impacts on the operation of an induction generator embedded within the power system and modify the equivalent circuit (Figure. D.5). Where V_{PCC} is the voltage at the point of common coupling and X_{PFC} is the power factor correction capacitance.

The torque-speed characteristics and the effect of supply voltage and rotor resistance are described in Figures D.6 which show that the generator speed follows directly from the

given mechanical load or generating torque. The only stable operating region is the narrow zone around the synchronous speed, between the highest value for motor and generator torque respectively. The supply voltage is determined by the grid and cannot be regulated. A large grid voltage dip may decrease the torque leading to instability. The variation of torque causes very little change in speed varies. Generator operation only occurs for speeds higher than ω_{m} .

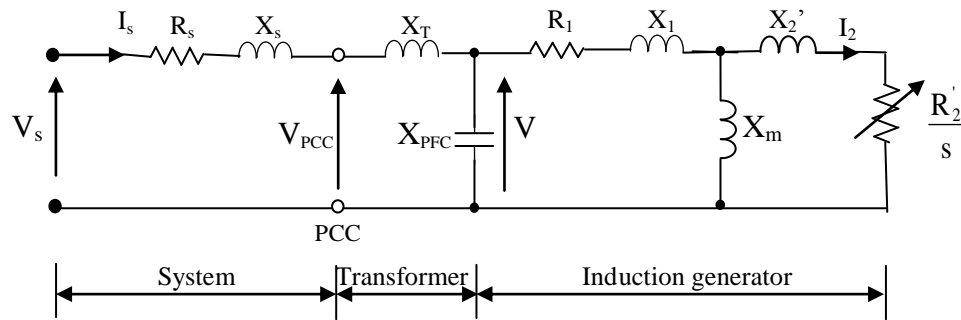


Figure D.5. Equivalent circuit of induction machine connected to power

Turbines equipped with this generator type are often called fixed-speed systems, although the speed varies over a narrow range. The peak of the torque/slip curve determines the pull-out torque and the system steady-state stability limit.

Equation (D11) shows how system reactance modifies the torque/slip characteristic. If the equivalent circuit is modified to a very approximate one as in Figure D.3 with the network resistance R_s incorporated into R_1 , the network reactance X_s and transformer reactance X_T incorporated into X_1 , and the stator voltage becoming the system supply voltage V_s .

Peak torque occurs when dT_m/ds is a maximum and occurs when

$$s_{\text{max}} = \frac{R_2'}{\sqrt{R_1^2 + (X_1 + X_2')^2}} \approx \frac{R_2'}{(X_1 + X_2')} \quad (\text{D13})$$

giving the pull-out torque

$$T_{m \max} = \frac{3}{2\omega_{sm}} \frac{V_s^2}{\left[R_1 + \sqrt{R_1^2 + (X_1 + X_2')^2} \right]} \quad (\text{D14})$$

consequently reduces the generator steady state stability. This will be most apparent on a weak system where system reactance is greatest (Figure D.6c). The pull-out torque is independent of the rotor resistance, but varies with the system reactance, X_1 . Increase in X_1 reduces the pull-out torque reduces and



Figure D.6. Effect of system reactance and voltage on pull-out torque [160]

Also, the pull-out torque will reduce if the system voltage is reduced (Figure D.6a), but has no influence on the slip at which the pull-out torque occurs. In contrast, the slip at

which the maximum torque occurs is determined by the rotor resistance (D.13); increasing the rotor resistance increases the maximum slip. This effect is illustrated in Figure D.6b. Increased rotor resistance makes the system connection more compliant, as described by (D12), and increases the speed at which the pull-out torque occurs; this can have implications on the transient stability of induction machines. As this is a relatively small speed range, turbines using this type of induction generator are often referred to as fixed-speed machines. Other types of inductions are those with slightly increased speed range, with significantly increased speed range (DFIG), and wide speed control generators.

APPENDIX E CODE FOR SVUD LOAD FLOW ANALYSIS

```

clear all
close all
clc;
clear;

busdata = busNigeria;

linedata = lineNigeria;

% new data - reverse columns 7 & 8
%busdata(:,7:8) = -1 * busdata(:,7:8);
%%

C=zeros(max(max(linedata(:,1:2)))); %connection matrix
L=zeros(max(max(linedata(:,1:2)))); %line index for connection matrix
for i=1:size(linedata,1)
    num2str([linedata(i,1),linedata(i,2)]);
    C(linedata(i,1),linedata(i,2))=1;
    L(linedata(i,1),linedata(i,2))=i; % line
end

D=C+C';

P=D; % potential lines to cut

count=0;

%return

scanning=1;

% aim for cluster sizes to be an integer factor of the total number of
% nodes in the network:
nNodes=size(busdata,1);
cntarget=factor(nNodes);
if exist('matlabpool')==2
    cntarget(cntarget>4)=[];
    cntarget=max(cntarget);
else
    cntarget=2;
end

%% ask user if they want to manually cut the network
manualflag = input('would you like to manually cut network (1 = yes,0 =
no): ');

if manualflag==1

```

```

manualworked=0; % boolean for if manual cut successfully split the
network

while manualworked==0

    % new
    clear manualslacks
    drawnet(linedata,'b')

    disp(' ')
    disp(' ')
    disp('Linedata: ')
    disp(' ')
    disp(' ')
    disp('line      node1      node2')
    for nn=1:size(linedata,1)
        disp([num2str(nn) '          ' num2str(linedata(nn,1)) '
' num2str(linedata(nn,2))])
    end

    disp(' ')
    disp(' ')

    disp('Please enter the line numbers you would like to cut in
square brackets.')
    cuts = input('For example, to cut lines 1, 4 & 6, enter [1,4,6]
: ');

    count=1;
    i=1;

    [CN{count},clustersize{count},nclusters{count},passfail{count}]=analyse
_clusters4(linedata,cuts(i,:),C);

    suitablecut=passfail{1}

    manualworked = manualworked
    %% check all subnets have slack buses available
    for ijk = 1:nclusters{count}
        snG{ijk}=find(CN{count}==ijk); % same as subnodesG used
later. Changed name so it doesn't conflict ( this could happen if an
old unsuitable network has more subnets than a newer suitable one with
fewer subnets )
        slacksuitable = zeros(numel(snG{ijk}),1);
        check1 = busdata(snG{ijk},2)==1;
        check2 =
(busdata(snG{ijk},2)==3) .* (busdata(snG{ijk},5)==0) .* (busdata(snG{ijk},6)
)==0);
        %check2 = check2 .*
(busdata(snG{ijk},9)==0) .* (busdata(snG{ijk},10)==0);
        slacksuitable = check1 + check2;
        if sum(slacksuitable)==0

```

```

        manualworked = 0;
        disp(['No slack buses available in subnet '
num2str(ijk)])
    end
    %%
end
%%

if suitablecut==1
    manualworked=1;
    %% new 30/11/2013
    %% manual selection of slack buses:
    manualslack = input('Would you like to manually select
slack buses for subnets? (1=yes, 0=no) : ');
    if manualslack == 1
        figure(1)
        clf
        drawnet(linedata, 'r--')
        linedata_cut = linedata;
        linedata_cut(cuts, :) = [];
        drawnet(linedata_cut, 'b')
        %title({'Network Map.', 'red = cut lines. blue = intact
lines'})

        for ijk = 1:nclusters(count)
            % display subnet nodes
            subnetbusdata = busdata(CN{1}==ijk, :);
            disp('Bus      Type      Vsp      theta
PGi      QGi      PLi      QLi      Qmin      Qmax ')
            disp(num2str(subnetbusdata))
            % input slack bus(global node or local node)?
            global is
            network is
            % probably the best for clarity, especially when the
            % shown in a figure window
            slackselected = 0;
            while slackselected == 0
                slackID = input('Enter slack bus node number:
');
                if isempty(find(subnetbusdata(:,1)==slackID))
                    slackselected = 0;
                    disp('Node number entered is not in subnet.
Please try again. ')
                else
                    slackselected = 1;
                    manualslacks(ijk)=slackID;
                end
            end
        end
    end
end
end
else
    disp(' ')
    disp(' ')
end

```

```

        disp('Cut configuration was not suitable for splitting the
network...')
        disp(' ')
        disp(' ')
    end

end

else

n=0;
n=ceil(size(linedata,1)/4)-1;%4;%round((size(linedata,1)+1)/2);
while scanning==1

    clear manualslacks
    %%
    cuts=combntns(1:size(linedata,1),n); % list of lines to cut

    % then calculate how many clusters are formed, and how many
nodes
    % belong to each cluster

    %analyse_clusters(..., ...)

    for i=1:size(cuts,1)

        count=count+1;
        disp(['Cutting lines [' num2str(cuts(i,:)) ']'])

        [CN{count},clustersize{count},nclusters{count},passfail{count}]=analyse
_clusters4(linedata,cuts(i,:),C);

        cuthistory{count}=cuts(i,:);

        cs=clustersize{count};

        if isempty(cs)==0 && nclusters{count}>1 &&
sum(cs==cs(1))==numel(cs)
            n=n+1;

            if nclusters{count}==cntarget
                scanning=0;
                break
            end
        end

    end

    if isempty(nclusters{count}) || sum(cs<=1)>0
        count=count-1;
        CN(end)=[];
        clustersize(end)=[];
        nclusters(end)=[];%=nclusters{1:count};
    end
end

```

```

passfail(end)=[];%=passfail{1:count};
cuthistory(end)=[];%=cuthistory{1:count};
continue
end

%% CHECKING ALL SUBNETS HAVE SLCK BUSES AVAILABLE
slacksavailable = 1 ;

for ijk = 1:nclusters(count)
    snG{ijk}=find(CN{count}==ijk);
    slacksuitable = zeros(numel(snG{ijk}),1);
    check1 = busdata(snG{ijk},2)==1;
    check2 =
(busdata(snG{ijk},2)==3) .* (busdata(snG{ijk},5)==0) .* (busdata(snG{ijk},6)
)==0);
    %check2 = check2 .*
(busdata(snG{ijk},9)==0) .* (busdata(snG{ijk},5)==10);
    slacksuitable = check1 + check2;
    if sum(slacksuitable)==0
        slacksavailable = 0;
    end
    %% PUT THIS IN THE "ANALYSE_CLUSTERS" FUNCTION
end

if n>0.5*size(linedata,1) && slacksavailable==1
    scanning=0;
    break
else
    n=n+1;
end

end

%%

end

%% manual selection of slack buses:
%if suitablecut==1
manualworked=1;
%% new 30/11/2013
%% manual selection of slack buses:
manualslack = input('Would you like to manually select slack buses
for subnets? (1=yes, 0=no) : ');
if manualslack == 1
    figure(1)
    clf
    drawnet(linedata,'r--')
    linedata_cut = linedata;
    linedata_cut(cuts(i,:),:) = [];
    drawnet(linedata_cut,'b')
    title({'Network Map.', 'red = cut lines. blue = intact lines'})

```

```

for ijk = 1:nclusters(count)
    % displly subnet nodes
    subnetbusdata = busdata(CN{1}==ijk,:);
    disp('Bus      Type      Vsp      theta      PGi
QGi      PLi      QLi      Qmin      Qmax ')
    disp(num2str(subnetbusdata))
    % input slack bus (global node or local node)? global is
    % probably the best for clarity,
    slackselected = 0;
    while slackselected == 0
        slackID = input('Enter slack bus node number: ');
        if isempty(find(subnetbusdata(:,1)==slackID))
            slackselected = 0;
            disp('Node number entered is not in subnet. Pls try
again. ' )
        else
            slackselected = 1;
            manualslacks(ijk)=slackID;
        end
    end
end
end
end

end

if manualflag==0
    disp('-----')
    disp(' ')
    disp(' ')
    disp([num2str(numel(nclusters)) ' cut configurations found:'])

    for i=1:numel(nclusters)

        disp(' ')
        disp(' ')

        disp([num2str(nclusters{i}) ' subnets are made by cutting links
[' num2str(cuthistory{i}) ']]')
        disp(['cuts between nodes:'])
        c=cuthistory{i};
        for j=1:numel(c)
            disp([num2str(linedata(c(j),1:2))])
        end
        disp(['number of nodes in each subnet are ['
num2str(clustersize{i}) ']]')

    end

    disp(' ')
    disp(' ')

```

```

disp('-----')
disp(' ')
disp(' ')

if exist('matlabpool')==2
    disp('Initialising multithread setup...')
    %matlabpool close force
    ncores=matlabpool('size');
    if ncores==0
        matlabpool open
    end
end

disp(' ')
disp(' ')

disp('Evaluating most suitable subnet configuration...')

nclust=cell2mat(nclusters);
configidx=1:numel(nclust);

for i=1:numel(nclust)

    cs=clustersize{i};
    uniformness(i)=max(abs(mean(cs)./cs)); % 0 if all clusters are
same size. The larger "uniformness" is, the less unifrom the cluster
sizes are.

    % don't pick any configurations where there are more clusters
than
    % cores!

    minclust(i)=min(cs);
    maxclust(i)=max(cs);

end

%% ideal config will have same or less subnets than cores, will be
very
%% uniform and have minimum number of cuts

a=[configidx; abs(1-uniformness); nclust; minclust]'; % ist some
statistics on each valid cut configuration

% filter by number of clusters
if exist('matlabpool')==2
    a(a(:,3)>ncores,:)=[]; % don't pick configurations with more
clusters than you have cores to multithread with
end

```

```

    % best configuration will have an equal number of nodes in each
cluster
    mostuniform=min(a(:,2));
    a(a(:,2)>mostuniform,:)=[];

    % larger clusters are likely to be more stable. Pick the solution
with
    % largest number of nodes in it'
    if size(a,1)>1
        maxclust=max(a(:,4));
        a(a(:,4)<maxclust)=[];
    end
    %%
    bestconfig=a(1,1); % this combination of cut wires in the network
is mst suitable
else
    if exist('matlabpool')==2
        disp('Initialising multithread setup...')
        %matlabpool close force
        ncores=matlabpool('size');
        if ncores==0
            matlabpool open
        end
    end
    bestconfig=1;
    cuthistory{1}=cuts;
    i=1;
    nclust=nclusters{i};
end
%bestconfig=5;

%% plot the cut config

% line data for plotting
figure(1)
clf
drawnet(linedata,'r--')

linedatap=linedata;
linedatap(cuthistory{i},:)=[];

drawnet(linedatap,'b')

title({'Network Map.', 'red = cut lines. blue = intact lines'})

clear linedatap % save some memory!

%%
%%%%%%%%%%%%%%%%%%%%%%%%%%%%%%%%%%%%%%%%%%%%%%%%%%%%%%%%%%%%%%%%%%%%%%%%
%
%%
%%%%%%%%%%%%%%%%%%%%%%%%%%%%%%%%%%%%%%%%%%%%%%%%%%%%%%%%%%%%%%%%%%%%%%%%
%

% setup 'linedata' for cuts:

```

```

cutlinedata=linedata(cuthistory{bestconfig},:);

linedata2=linedata;
linedata2(cuthistory{bestconfig},:)=[];

% setup "linedata" and "busdata" for subnets:
CN2=CN{bestconfig};
for i=1:nclust(bestconfig)

    subnodesG{i}=find(CN2==i); % global index of nodes in subnet

    %% new
    %%%%%%%%%%%%%%%%%%%%%%%%%%%%%%%%%%%%%%%%%%%%%%%%%%%%%%%%%%%%%

    %if type = 1
    % or if type =3 and PGi = 0 and QGi = 0
    if exist('manualslacks')==0
        % checking which nodes can be used as a slack bus...
        disp('checking slack buses are available...') % see if this
line runs when manually selecting line cuts - YES IT DOES ! GOOD!
        slacksuitable = zeros(numel(subnodesG{i}),1);
        check1 = busdata(subnodesG{i},2)==1;
        check2 =
(busdata(subnodesG{i},2)==3) .* (busdata(subnodesG{i},5)==0) .* (busdata(su
bnodesG{i},6)==0);
        %check2 = check2 .*
(busdata(subnodesG{i},9)==0) .* (busdata(subnodesG{i},10)==0);
        slacksuitable = check1 + check2;

        % if not, need to re-arrange so that subnet nodes are listed
with a
        % suitable slack bus as node 1
        if sum(slacksuitable)==0
            disp(['Subnet ' num2str(i) ' has no slack buses available.
Network cut configuration is invalid.'])
            return
            %% CODE SHOULD ACTUALLY RE-LOOP HERE AND ASK USER FOR
ANOTHER CONFIGURATION
        end

        if sum(check1)>0

            firstavailable = find(check1==1,1,'first');
            oldsubnodelist = subnodesG{i};
            newsubnodelist = subnodesG{i};
            newsubnodelist(1) = oldsubnodelist(firstavailable);
            newsubnodelist(firstavailable) = oldsubnodelist(1);
            subnodesG{i}=newsubnodelist;
        else%if slacksuitable(1)==0
            firstavailable = find(slacksuitable==1,1,'last');
            oldsubnodelist = subnodesG{i};
            newsubnodelist = subnodesG{i};
            newsubnodelist(1) = oldsubnodelist(firstavailable);

```

```

        newsubnodelist(firstavailable) = oldsubnodelist(1);
        subnodesG{i}=newsubnodelist;
    end
    if 0% slacksuitable(1)==0
        firstavailable = find(slacksuitable==1,1,'last');%'first');
        oldsubnodelist = subnodesG{i};
        newsubnodelist = subnodesG{i};
        %newsubnodelist(1) = firstavailable;
        newsubnodelist(1) = oldsubnodelist(firstavailable);
        newsubnodelist(firstavailable) = oldsubnodelist(1);
        subnodesG{i}=newsubnodelist;
        %return
    end

else
    firstavailable = find(subnodesG{i}==manualslacks(i));

    oldsubnodelist = subnodesG{i};
    newsubnodelist = subnodesG{i};
    newsubnodelist(1) = oldsubnodelist(firstavailable);
    newsubnodelist(firstavailable) = oldsubnodelist(1);
    subnodesG{i}=newsubnodelist;

end

%%
%%%%%%%%%%%%%%%%%%%%%%%%%%%%%%%%%%%%%%%%%%%%%%%%%%%%%%%%%%%%%%%%%%%%%%%%
subnodesL{i}=1:numel(subnodesG{i}); % local index of nodes in
subnet

subbusdataG{i}=busdata(subnodesG{i},:); % globally indexed subnet
bus data

lineInSubnet=[];
sn=subnodesG{i};
R=[];
for j=1:numel(sn)

    [r c]=find(linedata2(:,1:2)==sn(j));
    R=[R; r];

    %lineInSubnet=
    %sublinedata{i}=linedata
end

sublinedataG{i}=linedata2(unique(R),:); % globally indexed subnet
line data

% put local indexes in sublinedataL:
sublinedataL{i}=sublinedataG{i};
sld=sublinedataG{i};
%sldl=sld % debug variable

% key to convert global(row 1) node indexes to local(row2) node indexes

```

```

key=[subnodesG{i}; subnodesL{i}];      for j=1:size(sld,1)
    for k=1:2
        a=find(key(1, :)==sld(j,k));
        sld(j,k)=key(2,a);
    end
end
sublinedataL{i}=sld;

% put local indexes in subbusdataL:
sbd=subbusdataG{i};

% sbd1=sbd
for j=1:size(sbd,1)
    % sbd(j,1)
    a=find(key(1, :)==sbd(j,1));
    sbd(j,1)=key(2,a);
end
subbusdataL{i}=sbd;

Y{i}=ybusNigeria(sublinedataL{i});

%%

%L{i}=... %f connected to first node of line, say current is +ve

GLkey{i}=key;

end

assignin('base','Y',Y)

for j=1:i
    disp(' ')
    disp(' ')
    disp(['Y' num2str(j) ' = '])
    disp(num2str(Y{j}))
end
disp(' ')
disp(' ')

%%
% build L{1} (La) :

linkNodes=cutlinedata(:,1:2);

% look at left hand cut ends, assume current leaving these nodes
clear L

Z=diag(cutlinedata(:,3))+diag(cutlinedata(:,4))*1i; % link impedances

```

```

%% new
Dee = -Z;
%%
for i=1:numel(subnodesG)

    LL=zeros(numel(subnodesG{i}),size(linkNodes,1)); % find way to
detect size (row = number of nodes in subnet, col = number of links
touching subnet)

    for j=1:size(linkNodes,1)

        a=find(subnodesG{i}==(cutlinedata(j,1)));
        if isempty(a)==0
            LL(a,j)=1;
        end

        b=find(subnodesG{i}==(cutlinedata(j,2)));
        if isempty(b)==0
            LL(b,j)=-1;
        end

    end

    L{i}=LL;

    % if any bus in the subnet is a slack bus,
    bustype=subbusdataL{i};
    bustype=bustype(:,2);
    a=find(bustype==1);
    if isempty(a)==0 % if there is a slack bus in the subnet, delete
slack bus rows and columns from Y and rows from L

        Ytemp=Y{i}; % temporary variable (to get it out of cell array
type)
        Ytemp(:,a)=[];
        Ytemp(a,:)=[];
        Ltemp=L{i};
        Ltemp(a,:)=[];

        Ym{i}=Ltemp'*inv(Ytemp)*Ltemp;

        Y2{i}=Ytemp;
        L2{i}=Ltemp;

        b=find(bustype~=1);
        coridx{i}=b; % index of subnet voltages to target in the
update procedure (ignores slack bus)

    else
        Ym{i}=LL'*inv(Y{i})*LL;
        Y2{i}=Y{i};
        L2{i}=L{i};
    end
end

```

```

        coridx{i}=(1:size(subbusdataL{i},1))';

    end
    %% new
    slackidx{i}=(bustype==1);

    Dee = Dee - Ym{i};

    disp(' ')
    disp(' ')
    disp(['L' num2str(i) ' = '])
    disp(num2str(L{i}))

    disp(' ')
    disp(' ')
    disp(['Ym' num2str(i) ' = '])
    disp(num2str(Ym{i}))

end

disp(' ')
disp(' ')
disp(['Z = '])
disp(num2str(Z))

for i=1:numel(subnodesG)
    %% new
    gamma{i} = inv(Y2{i}) * L2{i} * inv(Dee);
    %%
end
assignin('base','gamma',gamma)

Vhist = cell(numel(subnodesG));
Vmodhist = Vhist;

Vold=ones(size(busdata,1),1)*inf;
tol=1e-4; % convergene tolerance

iter=0;
difference=inf;

dd=2; % difference between iterations
ddold=inf;
mintol=inf;
mintolloc=0; % iteration number at which point minimum tolerance change
was recorded

tolhist=[];

while dd>tol;
    iter=iter+1;

    % 1 iteration of gauss-seidel on individual subnets:

```

```

    if exist('matlabpool')==2 % if parallel cores available, they will be
used:

        parfor i=1:numel(subnodesG)

            %out=gaussfunNig(sublinedataL{i},subbusdataL{i},Y{i});
            out=gaussfunNig(sublinedataL{i},subbusdataL{i},Y{i});

            % update global busdata array:
            idx=subbusdataG{i};
            idx=idx(:,1);

            idxpar{i}=idx;
            Vsub{i}=out(:,1);
            %%

            %% new
            Vktemp = subbusdataL{i}; %V_k
            Vk{i} = Vktemp(:,3);
            Vkp1{i} = Vsub{i}; % V_k+1
            %%
        end

    else

        for i=1:numel(subnodesG)

            out=gaussfunNig(sublinedataL{i},subbusdataL{i},Y{i});

            disp(['Voltage after gauss-seidel for subnet ' num2str(i)
])
            V=out(:,1);

            % update global busdata array:
            idx=subbusdataG{i};
            idx=idx(:,1);
            busdata(idx,3)=V;

            Vsub{i}=V;
            %% new
            Vktemp = subbusdataL{i}; %V_k
            Vk{i} = Vktemp(:,3);
            Vkp1{i} = Vsub{i}; % V_k+1

            %%
        end

    end

    %calculate node voltages of subnets
    e=zeros(size(Z,1),1);
    for i=1:numel(subnodesG)
        Vkp_ws=Vkp1{i};
        Vkp_ws(slackidx{i}==1)=[]; % ws - without slack bus
    end

```

```

eL{i} = L2{i}'*Vkp_ws; % "e" local to subnet
e = e + eL{i};

%Vw{i} = Vkp_ws

end

if exist('matlabpool')==2 % if parallel cores available, they will be
used:
parfor i=1:numel(subnodesG)
% runs for all subnets:
Vkp=Vkp1{i};
%Vkpms = ; % ms - minus the slack bus
%Vkpms(slackidx{i}==1)=[];S
Vkp(slackidx{i}==0) = Vkp(slackidx{i}==0) + gamma{i}*e;
Vkup{i} = Vkp;%1{i};

I{i} = Y{i} * Vkp1{i};

% runs only if subnest needs a temporary slack bus:

% if original uncut network's slack but is not n subnet,
need to
% update the "temporary slack bus"
if sum(slackidx{i})==0
Vktemp=Vkp1{i};
Vslack_old = Vktemp(1);

Ytemp = Y{i};
Vkptemp = Vkp1{i};
conjsumYV = conj( Ytemp(1,1) * Vslack_old) ;
for ii=2:size(Vktemp,1)
conjsumYV = conjsumYV + conj( Ytemp(1,ii) *
Vkptemp(ii));
end
Sc=Vslack_old*conjsumYV % complex power

localbusdata = subbusdataL{i};
Sb = localbusdata(1,7) + 1i * localbusdata(1,8); %
schedules power

Sb = - Sb;
%%
dS = Sb-Sc;
dP=real(dS);
dQ = -imag(dS);

%Ib = Y{i}*Vktemp
Ib=I{i};

ab = real(Ib(1));
bb = imag(Ib(1));
Vb1 = Vktemp(1);
eb = real(Vb1);

```

```

fb = imag(Vb1);
gb = real(Ytemp(1,1)); %G11
hb = imag(Ytemp(1,1)); %B11

d1 = eb*gb + fb*bb + ab;
d2 = -eb*hb + fb*gb + bb;
m1 = -eb*hb +fb*gb -bb;
m2 = -eb*gb + fb*bb +ab;

Cb = d1*m2 - m1*d2;

mub = (m2*dP - d2*dQ)/Cb;
lambdab = (d1*dQ - m1*dP)/Cb;

dVkp1 = mub + 1i * lambdab;

% update temporary slack bus voltage:

Vkuptemp = Vkup{i};%Vkp1{i};%%
Vkup{i};%Vktemp;%Vkup{i};

Vkp(1) = Vkuptemp(1) - dVkp1;
Vkpmod = Vkuptemp(1) - dVkp1;

%if iter==2 && i==2
%   IBadam=I{i}
%   return
%end

sub_bus_table = subbusdataL{i};
sub_bus_table(:,3) = Vkp;
subbusdataL{i}=sub_bus_table;

SBDL{iter,i}=sub_bus_table;

Vhisttemp=Vhist{i};
Vhisttemp = [Vhisttemp sub_bus_table(:,3)];
Vhist{i}=Vhisttemp;

Vmdhisttemp = Vmdhist{i};
Vmdhisttemp = [Vmdhisttemp Vkpmod] ;
Vmdhist{i} = Vmdhisttemp;

DD{i} = abs(diff(Vk{i}-sub_bus_table(:,3)));

else

% Vkp=Vkp1{i};
% sub_bus_table = subbusdataL{i};
% sub_bus_table(:,3) = Vkp;
% subbusdata{i}=sub_bus_table
sub_bus_table = subbusdataL{i};

```

```

sub_bus_table(:,3) = Vkup{i};

subbusdataL{i}=sub_bus_table;
SBDL{iter,i}=sub_bus_table;

Vhisttemp=Vhist{i};
Vhisttemp = [Vhisttemp sub_bus_table(:,3)];
Vhist{i}=Vhisttemp;

DD{i} = abs(diff(Vk{i}-sub_bus_table(:,3)));
end

end

%%
else

% runs for all subnets:
Vkp=Vkp1{i};

Vkp(slackidx{i}==0) = Vkp(slackidx{i}==0) + gamma{i}*e;
Vkup{i} = Vkp;%1{i};

I{i} = Y{i} * Vkp1{i};

% runs only if subnet needs a temporary slack bus:

% if original uncut network's slack but is not n subnet, need
to
% update the "temptorary slack bus"
if sum(slackidx{i})==0
    Vktemp=Vkp1{i};

% assume t is always the 1st bus listed in the subnet for now,
% consider selection critria later

    Vslack_old = Vktemp(1);
    Ytemp = Y{i};
    Vkptemp = Vkp1{i};
    conjsumYV = conj( Ytemp(1,1) * Vslack_old) ;
    for ii=2:size(Vktemp,1)
        conjsumYV = conjsumYV + conj( Ytemp(1,ii) *
Vkptemp(ii));
    end
    Sc=Vslack_old*conjsumYV % complex power

% call the current subnet "subnet b" for clarity in
variables below...
    localbusdata = subbusdataL{i};
    Sb = localbusdata(1,7) + 1i * localbusdata(1,8); % schedule
power

    %% strange

```

```

Sb = - Sb; %to match Flo's version
%%
dS = Sb-Sc;
dP=real(dS);
dQ = -imag(dS);

Ib=I{i};
ab = real(Ib(1));
bb = imag(Ib(1));
Vb1 = Vktemp(1);
eb = real(Vb1);
fb = imag(Vb1);
gb = real(Ytemp(1,1)); %G11
hb = imag(Ytemp(1,1)); %B11

d1 = eb*gb + fb*bb + ab;
d2 = -eb*hb + fb*gb + bb;
m1 = -eb*hb +fb*gb -bb;
m2 = -eb*gb + fb*bb +ab;

Cb = d1*m2 - m1*d2;

mub = (m2*dP - d2*dQ)/Cb;
lambdab = (d1*dQ - m1*dP)/Cb;

dVkp1 = mub + 1i * lambdab;

Vkuptemp = Vkup{i};%Vkup{i};%Vkp1{i};%%
Vkup{i};%Vktemp;%Vkup{i};

Vkp(1) = Vkuptemp(1) - dVkp1;
Vkpmod = Vkuptemp(1) - dVkp1;

%if iter==2 && i==2
%   IBadam=I{i}
%   return
%end

sub_bus_table = subbusdataL{i};
sub_bus_table(:,3) = Vkp;
subbusdataL{i}=sub_bus_table;

SBDL{iter,i}=sub_bus_table;

Vhisttemp=Vhist{i};
Vhisttemp = [Vhisttemp sub_bus_table(:,3)];
Vhist{i}=Vhisttemp;

Vmdhisttemp = Vmdhist{i};
Vmdhisttemp = [Vmdhisttemp Vkpmod] ;
Vmdhist{i} = Vmdhisttemp;

DD{i} = abs(diff(Vk{i}-sub_bus_table(:,3)));

```

```

else

    % Vkp=Vkp1{i};
    % sub_bus_table = subbusdataL{i};
    % sub_bus_table(:,3) = Vkp;
    % subbusdata{i}=sub_bus_table
    sub_bus_table = subbusdataL{i};
    sub_bus_table(:,3) = Vkup{i};

    subbusdataL{i}=sub_bus_table;
    SBDL{iter,i}=sub_bus_table;

    Vhisttemp=Vhist{i};
    Vhisttemp = [Vhisttemp sub_bus_table(:,3)];
    Vhist{i}=Vhisttemp;

    DD{i} = abs(diff(Vk{i}-sub_bus_table(:,3)));
end

end

%%
dd=[];
for i=1: numel(subnodesG)

    dd = [dd; DD{i}];

end

dd=max(dd);

disp(['Max. voltage change for iteration ' num2str(iter) ' = '
num2str(dd)])
%% now update slack bus on all networks but the one with the uncut
network's
%% slack bus !
tolhist = [tolhist dd];
figure(10)
plot(tolhist)

exit if not converging any more
if iter == 200

    break
end

end

%%
% update the "busdata" table:
for i=1: numel(subnodesG)
    tempsubbus = subbusdataL{i};
    busdata(subnodesG{i},3) = tempsubbus(:,3);
end

```

```

disp(' ')
disp(' ')
disp(' ')
disp(' ')
%disp(['Solution converged to nearest ' num2str(tol)])
disp(['Solution converged to within ' num2str(dd) ' Volts.'])
disp(['Bus voltages are:'])
for i=1:nNodes
    disp(['Bus ' num2str(i) ' ' num2str(busdata(i,3))])

end
disp(' ')
disp(' ')
for i = 1:numel(subnodesG)

    disp(['subnet ' num2str(i) ':'])
    for j = 1:size(subbusdataL{i},1)
        globalnode = subnodesG{i};
        globalnode = globalnode(j);
        disp(['Bus ' num2str(globalnode) ' '
num2str(busdata(globalnode,3))])
    end
    disp(' ')

    figure(100+i)
    clear legendcell
    legendcell = cell(1,j); % j dshould be equal to number of subnodes
now
    for j = 1:size(subbusdataL{i},1)
        subplot(size(subbusdataL{i},1),1,j)
        plot(real(Vhist{i}'))
        globalnode = subnodesG{i};
        globalnode = globalnode(j);
        legendcell{j} = ['node ' num2str(globalnode)];
    end
    legend(legendcell)

end

%%

```

APPENDIX F PUBLICATION

Olobaniyi, F.; Nouri, H. ; Ghauri, S., “ Investigation of Diakoptics as a resourceful tool in power system analysis,” Universities Power Engineering Conference (UPEC), 2012, 47th International, pp. 1-6, 2012.

A copy of the paper is included below.

Investigation of Diakoptics as a Resourceful Tool in Power System Analysis

Abstract—The resourcefulness of Diakoptics as a tool with the potential ability to meet the challenges of modern power system analysis is outlined. The benefits include the generally accepted saving in computation time, but higher accuracy and the ability to use multicomputer configurations in analyses are highlighted. One of the reasons for the non-acceptance of Diakoptics as a universal tool is said to be the difficulty in understanding the concept. The concept is demonstrated using simple illustrative examples that are easy to understand and verify.

Index Terms—Conventional, Diakoptics, hypothetical, one-piece solution, intersection network, Sparsity technique, topology.

I. INTRODUCTION

Diakoptics was conceived and developed by DGabriel Kron, to solve Electrical Engineering problems precisely, power system problems, the original intent being the solution of problems in a less tasking manner with desired accuracy [1]. Diakoptics involves tearing of a large network into subsystems and had been proved to maintain the identity of the subsystems [1] thereby using and/or revealing some details of the system which would have been lost to oversimplification.

Due to its versatility, Diakoptics has since been developed and extended to other areas where large and/or complex systems are involved and is now viewed as basic a mathematical technique unconnected with specific applications [3]. Though present computers are much faster than when Diakoptics was conceived, speed is only one of the many benefits which include ability to apply to wider applications, avoiding unnecessary assumptions, applicability in symmetrical and non-symmetrical matrices. Also, from a computational point of view, it reduces the dimensions of matrices and is different from matrix partitioning in that the savings in number of computations in the case of Diakoptics is quite large [1].

The large number and heterogeneous nature of power system components make power system analysis tasking and time consuming. This is further heightened with the integration of wind energy and other renewable energy sources. Diakoptics, which is a piecewise solution, presents a useful tool which can reduce the complexity and burden of computation usually experienced.

Diakoptics has since been developed and extended to be seen as basic mathematical techniques unconnected with specific applications [3].

Diakoptics presents a very useful tool that can be explored in modern power system analysis and yet its use is very limited. Some reasons have been adduced as being responsible for lack of its full realization as a universal tool for power system analysis – the main one being the success of Sparsity Techniques. But Diakoptics has a very important advantage over Sparsity techniques, which is maintaining the individuality of the subsystems - an advantage exploited in computer analyses. Secondly, the Diakoptic solution procedure was difficult for an average engineer to understand [5]. This was corroborated by Roy, [6] which led to his proposal of another form of piecewise solution - the Nodal Matrix method. Discussants for the paper pointed out that his method is strongly connected to Diakoptics and yet lacked some important elements of nodal analysis.

In this paper, the Diakoptic concept will be demonstrated using simple illustrative examples that are easy to understand and verify. The resourcefulness of Diakoptics as a tool with the potential ability to meet the challenges of modern power system analysis will be highlighted.

II. THE VERSATILITY OF DIAKOPTICS

A. Benefits of Diakoptic Analysis

Its versatility is reflected in the diverse uses to which it has been put since conception. It may be argued that Diakoptics is no longer necessary since present computers are faster. But speed was only a by-product of the main intention - the facilitation of large system analysis. The method allows the most complex network problems to be solved in a detailed and orderly manner. [7].

Modern computers are much faster than when Diakoptics was conceived, yet their speeds and storages in most instances, cannot cope with the increased size and complexity of power systems, especially with the introduction of wind energy. In this regard Diakoptics appears to be a good tool with which to augment the computer performance.

Presently, computers/software that can handle very large power systems as a piece are not readily available and most researchers and engineers do not have access to such computers.

But if a network of say 1000 buses can be subdivided into a convenient number of subnetworks, much can be achieved in by researchers in finding solutions to many power system challenges.

Some of the inherent benefits of Diakoptics deduced from [1, 2, 4, 5, 7, 8 and 9] are summarized below.

- (i) It is based on well developed theory
- (ii) It permits wider applications
- (iii) It avoids unnecessary assumptions
- (iv) It is applicable in symmetrical and non-symmetrical matrices
- (v) From a computational point of view, reduces the dimensions of matrices. Partitioning of matrices if often used for this same purpose but the savings in number of computations in the case of Diakoptics is quite large [2].

The saving in computation time compared with one-piece solution is illustrated below. The amount of time, T , required to invert an $N \times N$ matrix is proportional to N^3 .

$$T = kN^3 \quad (1)$$

If the network matrix is divided into an $N/n \times N/n$ matrix, the total time required to solve the system diakoptically will be of the order of

$$T_d = 2kn(N/n)^3 = T/(\frac{1}{2}n^2) \quad (2)$$

where a safety factor of 2 has been included to take into account the additional labour required for the division into subsystems and the inversion of the tie impedance matrix, and for the computation of various additional products. [7].

From (2), even a division into two or three parts will yield an appreciable reduction in labour.

(vii) In the tearing method, any analytical difficulty in the original network will be repeated in the intersection network but that same difficulty is greatly reduced in complexity, extent and importance.

(viii) It was found to give good accuracy of results, restricted computation time and memory, and ease in application which could improve the cost/benefit ratio in emc problems.

(ix) Multicomputer configurations can be exploited to address information security, power processing and real-time constraints with minimum investments in the power network.

An important benefit of this decentralized approach is such that individual utilities will be responsible for modelling, analysis, and control of their own networks [8]. This 'division of labour' will greatly reduce the burden at the centre.

The method of decentralization by using multicomputer configuration is shown in Fig.1.

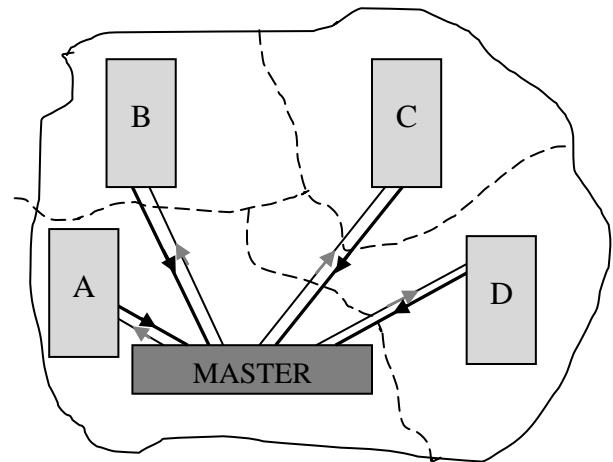


Fig 1: Multicomputer configuration

B. Applications

Since its conception, Diakoptics has been extended to and/or combined with other methods by a number of researchers to achieve desired results. The following are some of the applications

- Object Virtual Network Integrator using the Multi-area Thevenin Equivalent concept for simulating large power systems [5].
- Fault studies in large transformers and interconnected power systems [3, 10,].
- Combined with compensation methods for simulation of branch outages [12].
- Large change sensitivity for transient stability analysis [14].
- Modelling and Design of Complex Electromagnetic Systems which is ongoing. A number of publications have already been produced [14].
- Modelling of Brushless DC Generating Systems [15].
- Simulation of transients of HVDC Converters [16].

III. THE DIAKOPTIC CONCEPT

A. Basic Steps

Diakoptics is a combined theory of a pair of storehouses of information namely, equations+graph (or matrices+graph), associated with a given physical or economic system [2]. Diakoptics was coined from two Greek words, *dia* which means through, across or apart, and *kopto* which means tear or cut [5, 17].

In Diakoptics, a system is torn into a desired number of subsystems. The individual subsystems are solved separately, after which the solutions are combined and modified to yield the complete solution as if the system was not torn apart but solved as one piece [18].

Kron called the tearing process ‘a topological science on its own right’ [1]. In other words, there are important factors to consider when tearing a system and this is based on the nature of the problem. So the engineer needs to pick the point (s) of tear carefully. Also, there is usually a need to solve an additional system - the (n+1)th system.

The equations of solutions required are usually mesh or nodal equations, or special combinations of them.

A. Basic Solution Steps

Step 1

The system is torn into n parts taking the topology of the system and the nature of the problem into consideration.

Step 2

The n parts are solved separately to obtain partial solutions of the original network.

Step 3

The (n+1)th network which is the miniature form of the original network is constructed from the torn branches and solved. This is key to Diakoptics. In view of the important role played by this network, it has been called the intersection network, managerial system and the central brain [1].

Step 4

The (n+1) solutions are then combined with modifications to obtain the solution of the original system as if it was not torn.

Steps 2 and 3 can be interchanged.

B. Application in Nodal Analysis:

Nodal analysis plays a very important role in power system analysis. The concept of Diakoptics is demonstrated with the simple circuit of Fig 2 applying nodal analysis.

The nodal voltages, $V_p - V_t$ are the unknown quantities to be determined. The branches pt and rs in Fig. 2 are detached to yield the subnetworks in Fig. (3). Current directions in the branches to be removed are assigned arbitrarily before detaching from the original network. The detached branches

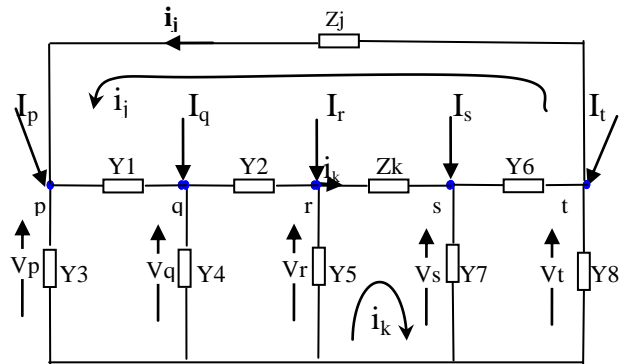


Fig. 2. Original Network [14]

are used to construct the intersection network in Fig (4).

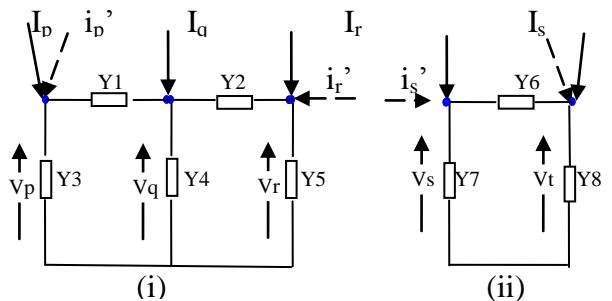


Fig. 3. Subnetworks

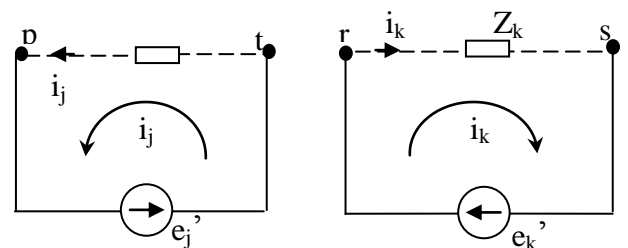


Fig. 4. Constructed network

The relationship between the hypothetical currents, i_a' and the assumed branch currents i_c in all detached branches are expressed in (3), and (4)

is the relationship between the voltages and currents.

$$\begin{bmatrix} i'_p \\ i'_q \\ i'_r \\ i'_s \\ i'_t \end{bmatrix} = \begin{bmatrix} 1 & \cdot \\ \cdot & \cdot \\ \cdot & -1 \\ \cdot & 1 \\ -1 & \cdot \end{bmatrix} \begin{bmatrix} i_j \\ i_k \end{bmatrix} \Rightarrow i'_a = C_{ac} i_c \quad (3)$$

$$\begin{bmatrix} Z_j & \cdot \\ \cdot & Z_k \end{bmatrix} \begin{bmatrix} i_j \\ i_k \end{bmatrix} = \begin{bmatrix} e'_j \\ e'_k \end{bmatrix} \Rightarrow Z_{cc} i_c = e'_c \quad (4)$$

The subnetworks are described by the nodal voltage equations:

$$\begin{bmatrix} (Y_1 - Y_3) & -Y_1 & 0 \\ -Y_1 & (Y_1 + Y_2 + Y_4) & -Y_2 \\ 0 & -Y_2 & (Y_2 + Y_5) \end{bmatrix} \begin{bmatrix} v_p \\ v_q \\ v_r \end{bmatrix} = \begin{bmatrix} I_p + i'_p \\ I_q + 0 \\ I_r + i'_r \end{bmatrix} \quad (5)$$

and

$$\begin{bmatrix} (Y_6 + Y_7) & -Y_6 \\ -Y_6 & (Y_6 + Y_8) \end{bmatrix} \begin{bmatrix} v_s \\ v_t \end{bmatrix} = \begin{bmatrix} I_s + i'_s \\ I_t + i'_t \end{bmatrix} \quad (6)$$

Equations (5) and (6) are combined to obtain the compound form in (7).

$$\begin{bmatrix} Y'_{11} & \cdot \\ \cdot & Y'_{22} \end{bmatrix} \begin{bmatrix} v_1 \\ v_2 \end{bmatrix} = \begin{bmatrix} I_1 + i'_1 \\ I_2 + i'_2 \end{bmatrix} \Rightarrow Y'_{aa} v_a = I_a + i'_a \quad (7)$$

Y'_{aa} is a block diagonal matrix (BDM). The corresponding Y_{aa} of the original network is of the same order but it is not a BDM.

After some algebra, the final equation of solution for nodal analysis is obtained as

$$v_a = Y'_{aa}{}^{-1} I_a - Y'_{aa}{}^{-1} C_{ac} Z'_{cc}{}^{-1} C'_{ca} Y'_{aa}{}^{-1} I_a \quad (8)$$

where $Z'_{cc} = Z_{cc} + C'_{ca} Y'_{aa}{}^{-1} C_{ac}$

Equation (8) eliminates the need to invert the full true matrix, Y_{aa} , of the original network (which is

not a BDM) thereby saving storage space and computation time.

IV. ILLUSTRATIVE EXAMPLES

A. Solution 1

Figure 5 is a three-phase 4-bus system. The per unit admittances are $y_{G1} = -j5$, $y_{G4} = -j4$, $y_{L1} = (0.145 - j0.109)$, $y_{L2} = (9.59 - j7.15)$, $y_{L3} = (1.16 - j1.55)$, $y_{L4} = (0.39 - j0.51)$, $y_{12} = -j6.25$, $y_{23} = -j1.85$, $y_{34} = -j5$. The currents injected into buses 1 and 4 are $I_1 = 5/\underline{-90^\circ}$ and $I_4 = 3.8/\underline{-60^\circ}$.

Nodal voltages at 1, 2, 3 and 4 are to be determined.

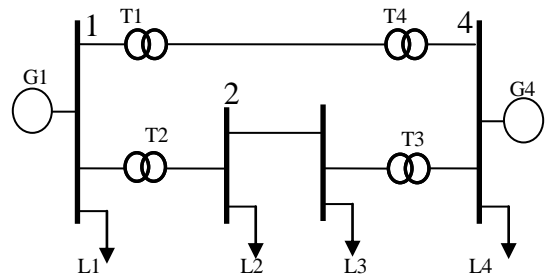


Fig. 5. [20]

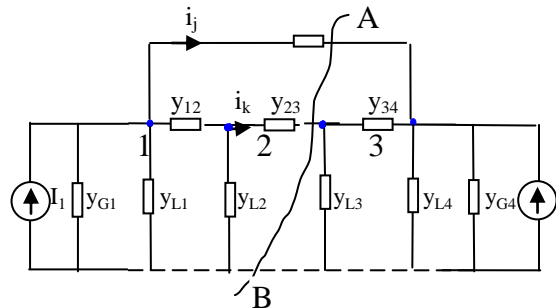


Fig. 6. Per unit admittance diagram (AB)

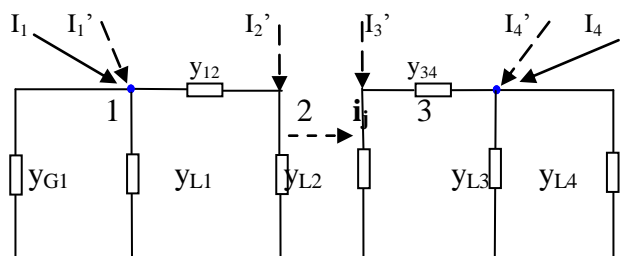


Fig. 7. Subnetworks

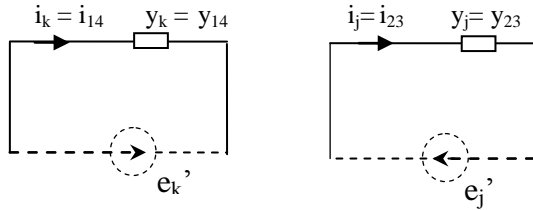


Fig. 8. Intersection network

$$\begin{bmatrix} (0.145 - j11.359) & j6.25 \\ j6.25 & (9.59 - j13.40) \end{bmatrix} \begin{bmatrix} V_1 \\ V_2 \end{bmatrix} = \begin{bmatrix} I_1 + i_1 \\ I_2 + i_2 \end{bmatrix}$$

$$\begin{bmatrix} (1.16 - j6.55) & j5 \\ j5 & (0.39 - j9.51) \end{bmatrix} \begin{bmatrix} V_3 \\ V_4 \end{bmatrix} = \begin{bmatrix} I_3 + i_3 \\ I_4 + i_4 \end{bmatrix}$$

$$Z_{ccic} = e'_c \Rightarrow \begin{bmatrix} j0.54 & \cdot \\ \cdot & j0.45 \end{bmatrix} \begin{bmatrix} i_j \\ i_k \end{bmatrix} = \begin{bmatrix} e'_j \\ e'_k \end{bmatrix}$$

$$C_{ac} = \begin{bmatrix} \cdot & -1 \\ -1 & \cdot \\ 1 & \cdot \\ \cdot & 1 \end{bmatrix}$$

$$\begin{bmatrix} I_1 \\ I_2 \\ I_3 \\ I_4 \end{bmatrix} = \begin{bmatrix} -j5.000 \\ 0 \\ 0 \\ 1.900 - j3.291 \end{bmatrix} = I_a$$

The matrices were substituted in (8), the *final equation of solution*.

MATLAB evaluation of the equation yielded the following results:

Diakoptics

$$V_1 = 0.5402 - j 0.0444, V_2 = 0.1821 - j0.1325$$

$$V_3 = 0.3630 + j0.0018, V_4 = 0.5420 + j0.1363$$

The relationships between the currents and nodal voltages in the equivalent networks in Fig. 7 are

$$Y'_{aa} = \begin{bmatrix} Y_{11} & \cdot \\ \cdot & Y_{22} \end{bmatrix}$$

where

$$Y_{11} = \begin{bmatrix} (0.145 - j11.359) & j6.25 \\ j6.25 & (9.59 - j13.40) \end{bmatrix}$$

and

$$Y_{22} = \begin{bmatrix} 1.16 - j6.55 & j5 \\ j5 & (0.39 - j9.51) \end{bmatrix}$$

$$\begin{bmatrix} Y_{11} & \cdot \\ \cdot & Y_{22} \end{bmatrix} \begin{bmatrix} V_1 \\ V_2 \end{bmatrix} = \begin{bmatrix} I_1 + i_1 \\ I_2 + i_2 \end{bmatrix} \quad (5a)$$

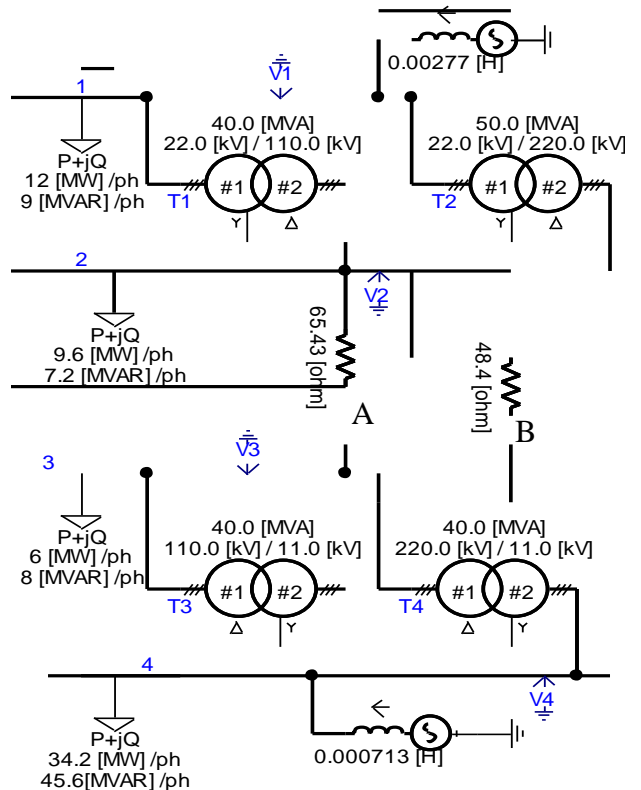


Fig. 9. Original network

Other methods (one-piece solutions) used to solve the same system gave the following results:

Conventional ZI method:

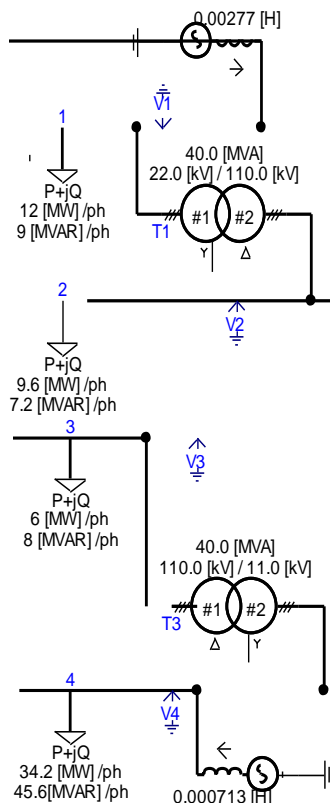
$$V_1 = 0.5408 - j0.0493, V_2 = 0.1848 - j0.1333, \\ V_3 = 0.3536 - j0.0003, V_4 = 0.5382 + j0.1406.$$

Partitioning

$$V_1 = 0.5408 - j0.0493, V_2 = 0.1848 - j0.1333, \\ V_3 = 0.3536 - j0.0003, V_4 = 0.5382 + j0.1406.$$

B. Solution 2

The network of Fig. 9 was torn into two subnetworks of Fig. 10. The voltages V1, V2, and V3, V4 were obtained with the aid of PSCAD (Power System Computer Aided Design). Each subnetwork was solved independently. Circuit breakers were then connected at points A and B. The breakers were opened to split the network into two and the analyses of the subnetworks were performed in parallel. Fig. 11 is the PSCAD result of the four voltages, showing one phase each for clarity.



(a) (b)

Fig.10. Subnetworks

The results showed that the nodal voltages in each method of tearing were the same. Large systems can therefore be torn using ideal circuit breakers [13] at the chosen points of tear.

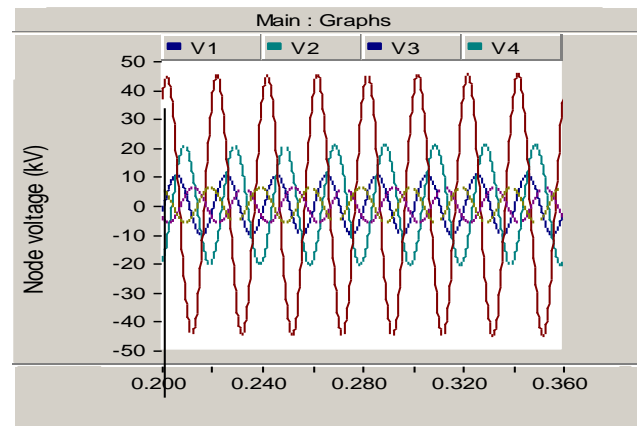


Fig.11. Voltages obtained in PSCAD operation

V. COMPARISON OF DIAKOPTIC ANALYSIS AND ONE-PIECE SOLUTIONS

The example proves one of the basic concepts of Diakoptics - the solution is obtained as if it was solved as one piece.

Obtaining the same solution as if the system was untorn is an important quality of diakoptics. But it has been discovered that when large and complex systems are overly approximated in order to simplify the process of one-piece solution, the quality of the analysis results tend to be reduced - another advantage Diakoptics has over the one-piece solution [5, 12]. Complex systems may give slightly different results based on the level of accuracy.

A glance at the two methods of solution in the illustrative examples may suggest that the conventional method is less cumbersome, easier and faster. The potentials of Diakoptics cannot be appreciated in circuits of these sizes, which when combined is much smaller than a subcircuit of a torn large system for which it was established. As stated above, the primary purpose of Diakoptics was not to save computation time but to facilitate the solution of complex system problems which for various reasons cannot be solved in one piece.

The piecewise solution provides a means of solving a problem in a routine manner and ensures that a large system is easily handled even by the desktop computers available to most researchers.

VI. CONCLUSION

The resourcefulness of Diakoptics as a tool with the potential ability to meet the challenges of modern power system analysis is demonstrated by tearing of a large network into subsystems and at the same time the identity of the subsystems is maintained. The concept is demonstrated using simple illustrative examples that are easy to understand and verify.

Versatility of Diakoptics suggests its application in almost every area of engineering and other fields where large and/or complex systems are involved. However, it is not proposed as an alternative to other methods of solution but as a means of augmentation when these methods become inadequate. Analysis of this investigation concludes that the extra pieces of information used in Diakoptic will facilitate important technical decisions in modern power systems where wind energy systems or renewable energy sources are integrated.

REFERENCES

- [1] H. H. Happ, "Z Diakoptics – Torn Subdivision Radially Attached, IEEE Trans. Power Apparatus and Systems, PAS-86, No. 6, pp751-769, June 1967.
- [2] G. Kron, Diakoptics – *The Piecewise Solution of Large Scale Systems*, vol. 2, London: Macdonald, 1963.
- [3] P. W. Aitchison, Diakoptics as a General Approach in Engineering. *Journal of Engineering Mathematics*, p21, 47–58, 1987.
- [4] Jose R. Marti, et al, OVNI: Integrated Software/hardware Solution for Real-Time Simulation of Large Power Systems, Conference Proc. of 1⁴th Power Systems Computation Conference PSCC02, Sevilla, Spain, 2002.
- [5] L. Roy, Piecewise Solution of Large Electrical Systems by Nodal Admittance Matrix, *IEEE Trans., Power App. & Syst. vol. PAS 91, 1386-1396, 1972.*
- [6] R. Braae, *Matrix Algebra for Electrical Engineers*, I. Pitman, 1963, p135-138.
- [7] V. Amoruso and F. Lattarulo, Diakoptic Approach to EMC Problems Involving the Human Body, *Electromagnetic Compatibility in Power Systems*, edited by Francesco Lattarulo, p133-164, 2007.
- [8] A. Kalantari and S. M. Kouhsari, An Exact Piecewise Method for Fault Studies in Interconnected Networks, *Electrical Power and Energy Systems* 30, p216–225, 2008.
- [9] A. Klos, What is Diakoptics? *International Journal of Electrical Power and Energy Systems*, vol. 4, p192-195, 1982.
- [10] A. Koochaki and S. M. Kouhsari, Detailed Simulation of Transformer Internal Fault on Power System by Diakoptical Concept, *Advances in Electrical and Computer Engineering*, Vol 10, No.3, 2010.
- [11] F. M. Uriarte and K. L. Butler-Purpy, Diakoptics in Shipboard Power System Simulation. In: *Power Symposium. NAPS. North American*. p201-210, 2006.
- [12] M. El-Marsafawy, Solution of Power Flow Outage Problems Using Diakoptics and Compensation, *JKAU: Eng. Science.*, vol. 8, p3-20, 1996.
- [13] S. Esmaili and S.M. Kouhsari, A Distributed Simulation Based Approach for

- Detailed and Decentralized Power System Transient Stability Analysis, *Electric Power Systems Research* 77 p673–684, 2007.
- [14] V. Vanher, K. Gregory, J. G. Klitorough and I. R. Smith, Modelling of Brushless DC Generating Systems, *IEEE Trans. on Aerospace and Electronic Systems* Vol. 29, No.1993.
- [15] A. Brameller, M. N. John and M. R. Scott, *Practical Diakoptics for Electrical Networks*, Chapman and Hall Ltd., 1969, p138-144.

